



Exotic decays of the 125 GeV Higgs boson

David Curtin,^{1,a} Rouven Essig,^{1,b} Stefania Gori,^{2,3,4,c} Prerit Jaiswal,^{5,d} Andrey Katz,^{6,e} Tao Liu,^{7,f} Zhen Liu,^{8,g} David McKeen,^{9,10,h} Jessie Shelton,^{6,i} Matthew Strassler,^{6,j} Ze'ev Surujon,^{1,k} Brock Tweedie,^{8,11,l} and Yi-Ming Zhong^{1,m}

¹*C.N. Yang Institute for Theoretical Physics, Stony Brook University, Stony Brook, New York 11794, USA*

²*Enrico Fermi Institute and Department of Physics, University of Chicago, Chicago, Illinois 60637, USA*

³*HEP Division, Argonne National Laboratory, 9700 Cass Avenue, Argonne, Illinois 60439, USA*

⁴*Perimeter Institute for Theoretical Physics, Waterloo, Ontario, Canada*

⁵*Department of Physics, Florida State University, Tallahassee, Florida 32306, USA*

⁶*Center for the Fundamental Laws of Nature, Harvard University, Cambridge, Massachusetts 02138, USA*

⁷*Department of Physics, The Hong Kong University of Science and Technology, Clear Water Bay, Kowloon, Hong Kong*

⁸*PITT PACC, Department of Physics and Astronomy, University of Pittsburgh, 3941 O'Hara Street, Pittsburgh, Pennsylvania 15260, USA*

⁹*Department of Physics and Astronomy, University of Victoria, Victoria, British Columbia V8P 5C2, Canada*

¹⁰*Department of Physics, University of Washington, Seattle, Washington 98195, USA*

¹¹*Physics Department, Boston University, Boston, Massachusetts 02215, USA*

(Received 17 March 2014; published 13 October 2014)

We perform an extensive survey of nonstandard Higgs decays that are consistent with the 125 GeV Higgs-like resonance. Our aim is to motivate a large set of new experimental analyses on the existing and forthcoming data from the Large Hadron Collider (LHC). The explicit search for exotic Higgs decays presents a largely untapped discovery opportunity for the LHC collaborations, as such decays may be easily missed by other searches. We emphasize that the Higgs is uniquely sensitive to the potential existence of new weakly coupled particles and provide a unified discussion of a large class of both simplified and complete models that give rise to characteristic patterns of exotic Higgs decays. We assess the status of exotic Higgs decays after LHC run I. In many cases we are able to set new nontrivial constraints by reinterpreting existing experimental analyses. We point out that improvements are possible with dedicated analyses and perform some preliminary collider studies. We prioritize the analyses according to their theoretical motivation and their experimental feasibility. This document is accompanied by a Web site that will be continuously updated with further information [<http://exotichiggs.physics.sunysb.edu>].

DOI: 10.1103/PhysRevD.90.075004

PACS numbers: 12.60.Fr, 14.80.Bn, 14.80.Da, 14.80.Ec

I. INTRODUCTION AND OVERVIEW

The discovery at the Large Hadron Collider (LHC) of a Higgs-like particle near 125 GeV [1,2] (referred to as “the Higgs” h for simplicity in this paper) is a triumph for theoretical [3–11] and experimental particle physics and

marks the culmination of several decades of experimental search. However, the experimental investigation of this new state has only just begun. The Higgs plays an essential role in the Standard Model (SM) of particle physics and impacts a wide range of new physics beyond the SM (BSM). The discovery of this new state presents us with a rich experimental program that includes the precise measurement of its couplings to SM particles, the search for additional Higgs-like states, and the focus of this paper: the search for “exotic” decays, i.e., decays that involve new light states beyond the SM.

The aim of this document is to provide a summary and overview of the theoretical motivation and basis for a large set of new analyses that could be done by the LHC experimentalists. In the course of doing so we provide a thorough and unified description of a large class of models that generate exotic Higgs decays and perform numerous original collider studies to assess the current status and discovery potential of different modes.

^adavid.curtin@stonybrook.edu

^brouven.essig@stonybrook.edu

^csgori@perimeterinstitute.ca

^dprerit.jaiswal@hep.fsu.edu

^eandrey@physics.harvard.edu

^ftaoliu@ust.hk

^gzh161@pitt.edu

^hdmckeen@uw.edu

ⁱjshelton@physics.harvard.edu

^jstrassler@physics.harvard.edu

^kzeev.surujon@stonybrook.edu

^lbat42@pitt.edu

^myiming.zhong@stonybrook.edu

Nonstandard Higgs decays have always been a well-motivated possibility as evidenced by an extensive existing, and growing, literature. They *remain* a well-motivated possibility even with the discovery of a Higgs particle that is consistent with the simplest SM expectations. Indeed, they may provide our *only* window into BSM physics at the LHC and must be searched for explicitly as they are often unconstrained by other analyses. The search for nonstandard Higgs decays should form an important component of the experimental program of the LHC and future colliders.

Our focus here will be on the existing LHC data at 7 and 8 TeV (“LHC7” and “LHC8”). However, many signatures will remain unconstrained by this data set and should be searched for during future runs of the LHC and at other colliders. While this document may be periodically updated, we note that it is accompanied by the Web site [12], which will serve as a centralized repository of information about new collider studies and experimental analyses.

This document is structured as follows. In Sec. IA, we provide a general motivation for nonstandard Higgs decays. In Sec. IB, we then detail the decay modes considered in the subsequent sections. We then summarize several simplified and complete models in Sec. IC that illustrate the ease with which nonstandard Higgs decays arise without being in conflict with the current LHC data. (Two Appendixes contain some additional details.) The remaining sections, Secs. II–XIX, each treat one exotic Higgs decay in detail and contain additional comments on theory motivation, existing (theoretical) collider studies, limits from existing collider searches (including our own reinterpretations of studies not aimed at Higgs decays), and in some cases our own preliminary collider studies outlining new search proposals at the LHC. A summary in Sec. XX considers the relative sensitivity of possible analyses and concludes with a suggested priority list for future analyses of both run I and run II data, a brief discussion of run II triggering issues, and a short catalog of research areas deserving further investigation in the short term.

A. General motivation to search for exotic Higgs decays

In this subsection, we review the reasons why searches for exotic Higgs decays are a particularly rich and fruitful way to search for new physics.

The data collected at LHC7 and LHC8 may easily contain $\mathcal{O}(50,000)$ exotic Higgs decays per experiment, presenting us with a large discovery potential for new physics, of a kind which is mostly unconstrained by existing analyses. Indeed, as we will explain in more detail in the following, the current data allow the branching ratio (Br) of the 125 GeV Higgs boson into BSM states to be as large as $\mathcal{O}(20\%–50\%)$, which includes constraints from observing the Higgs boson in various SM channels. Table I lists the number of exotic Higgs decays that could be contained in the LHC7 and LHC8 data, assuming $\text{Br}(h \rightarrow \text{BSM}) = 10\%$; we list these numbers separately for each Higgs production channel. Of course these are only the number of events *produced*; the trigger efficiency depends strongly on the final states that appear in the exotic decay. Nevertheless, the table makes it clear that, for exotic final states where triggering is not disastrously inefficient, a dedicated search has the potential for a spectacular discovery.

Several theoretical and experimental studies have constrained the possible Br into an invisible or an (as yet) undetected final state by fitting for the couplings of the Higgs to SM states. These “coupling fits” constrain $\text{Br}(h \rightarrow \text{BSM}) \lesssim 20\%$ at 95% C.L. if the Higgs is produced with SM strength; a larger BSM branching fraction, $\text{Br}(h \rightarrow \text{BSM}) \lesssim 30\%$, is possible if new physics is allowed to modify the loop-induced Higgs couplings to both gg and $\gamma\gamma$ (see for example [14–17] for some more recent fits). Fits that take more conservative approaches for the theoretical uncertainty on the SM Higgs production cross sections can leave room for larger ($\lesssim 60\%$) BSM branching fractions [18]. This result is similar to the one obtained by the ATLAS and CMS Collaborations [19,20]. Bounds can be further relaxed for models with Higgs couplings to gauge bosons larger than in the SM [21].

TABLE I. The number of exotic Higgs decays in existing LHC data, per experiment, at 7 TeV (5 fb^{-1}) and 8 TeV (20 fb^{-1}), and at a future 14 TeV run (300 fb^{-1}), assuming the Standard Model production cross section of a 125 GeV Higgs boson [13] and a branching ratio of $\text{Br}(h \rightarrow \text{BSM}) = 10\%$ for various production channels: gluon-gluon fusion (ggF), vector-boson fusion (VBF), associated production (hW^\pm and hZ , with and without branching ratios $W^\pm \rightarrow \ell^\pm\nu$ or $Z \rightarrow \ell^+\ell^-$, where $\ell = e, \mu$, included), and through radiation off the top quark ($t\bar{t}h$).

Production	$\sigma_{7 \text{ TeV}}$ (pb)	$N_{\text{ev}}^{10\%}, 5 \text{ fb}^{-1}$	$\sigma_{8 \text{ TeV}}$ (pb)	$N_{\text{ev}}^{10\%}, 20 \text{ fb}^{-1}$	$\sigma_{14 \text{ TeV}}$ (pb)	$N_{\text{ev}}^{10\%}, 300 \text{ fb}^{-1}$
ggF	15.13	7,600	19.27	38,500	49.85	1.5×10^6
VBF	1.22	610	1.58	3,200	4.18	125,000
hW^\pm	0.58	290	0.70	1,400	1.5	45,000
$hW^\pm(\ell^\pm\nu)$	0.58-0.21	62	0.70-0.21	300	1.5-0.21	9,600
hZ	0.34	170	0.42	830	0.88	26,500
$hZ(\ell^+\ell^-)$	0.34-0.067	11	0.42-0.067	56	0.88-0.067	1,800
$t\bar{t}h$	0.086	43	0.13	260	0.61	18,300

Future projections for the LHC suggest an ultimate precision on this indirect measurement of $\text{Br}(h \rightarrow \text{BSM})$ of $\mathcal{O}(5\text{--}10\%)$; see, e.g., [22–24]. Branching fractions of $\mathcal{O}(10\%)$ into exotic-decay modes are therefore not only still allowed by existing data but *will remain reasonable targets for the duration of the physics program of the LHC*.

In the right columns of Table I we show the possible number of exotic Higgs decays in the anticipated LHC14 data set with 300 fb^{-1} , again assuming $\text{Br}(h \rightarrow \text{BSM}) = 10\%$. The large rates for producing these exotic states suggest that branching fractions as small as $\mathcal{O}(10^{-6})$ could be detected, if the decay signature is both visible and clean.

As for any newly discovered particle, a detailed experimental characterization of the Higgs is imperative. Such an experimental characterization must necessarily include an exhaustive study of its decay modes. These programs have been established for other particles, such as the top quark, the Z boson, B -hadrons, etc., as rare decay modes of SM particles are prime places for new physics to appear. However, it is worth emphasizing that the Higgs boson is a special case. The tiny natural width of the SM Higgs boson, together with the ease with which the Higgs can mediate interactions with new physics, make exotic Higgs decays a natural and expected signature of a very broad class of theories beyond the SM.

A SM-like Higgs boson with a mass of $m_h = 125 \text{ GeV}$ has an extremely narrow width, $\Gamma_h \approx 4.07 \text{ MeV}$, so that $\Gamma_h/m_h \approx 3.3 \times 10^{-5}$. The reason is that tree-level decays to SM fermions are suppressed by the small Yukawa couplings, e.g., $y_{b,\tau} \lesssim \mathcal{O}(10^{-2})$, decays to two photons ($\gamma\gamma$), two gluons (gg), and $Z\gamma$ are suppressed by loop factors, and decays to WW^* and ZZ^* are suppressed by multibody phase space. Since the dominant decay, to two b quarks, is controlled by a coupling with a size of only ~ 0.017 [this assumes a running b -quark mass $m_b(125 \text{ GeV}) = 2.91 \text{ GeV}$ evaluated in the $\overline{\text{MS}}$ scheme], even a small coupling to another light state can easily open up additional sizable decay modes [25–28].

In fact, we have very good reasons to expect that new physics may couple preferentially to the Higgs boson. The brief survey in Sec. IC of simplified models and theories that produce exotic Higgs decays will provide ample examples that corroborate this statement. More generally, the Higgs provides one of only a few “portals” that allow SM matter to interact with hidden-sector matter that is not charged under the SM forces (e.g., [29–33]) and where the leading interaction can be (super)renormalizable.¹ Since the

¹The other two portals are the “vector portal” at mass dimension 2, namely the hypercharge field strength $B^{\mu\nu}$, and the “neutrino portal,” given by the product of the Higgs and a lepton doublet, HL , with mass dimension 5/2. The vector portal can mediate, e.g., kinetic mixing between hypercharge and a new $U(1)$ gauge field with the renormalizable interaction $F'_{\mu\nu} B^{\mu\nu}$; the neutrino portal operator can mediate the renormalizable coupling HLN , with N a sterile neutrino.

operator $|H|^2$ is a SM singlet, we can couple it to a singlet scalar field s through the Higgs portal as

$$\Delta\mathcal{L} = \frac{\zeta}{2} s^2 |H|^2, \quad (1)$$

where we have assumed for simplicity that s has a conserved Z_2 parity. This kind of interaction is a very common building block in models of extended Higgs sectors. If $m_s < m_h/2$, this interaction allows $h \rightarrow ss$ after electroweak symmetry breaking (EWSB), and *even a coupling as small as $\zeta = 10^{-2}$ yields $\text{Br}(h \rightarrow \text{BSM}) = 10\%$* . In Fig. 1 (left), we plot $\text{Br}(h \rightarrow ss)$ for various couplings ζ as a function of the singlet mass m_s . [The orange line shows the expected branching fraction if the interaction in Eq. (1) generates the s mass. Achieving larger branching fractions requires a cancellation between the Higgs contribution and another contribution to the s mass.] Even very small couplings of the Higgs boson to new states beyond the SM can lead to potential signals at the LHC.

There are many possible interactions through the Higgs portal. One striking and generic feature of these interactions is that searches for exotic Higgs decays can easily be sensitive to new physics scales $\gtrsim 1 \text{ TeV}$. As one example, consider the (effective) dimension-six Higgs-portal interaction

$$\Delta\mathcal{L} = \frac{\mu}{\Lambda^2} |H|^2 \bar{\psi}\psi, \quad (2)$$

where ψ is some new singlet fermion and μ is a chiral symmetry breaking parameter with dimensions of mass. Taking $\mu \sim m_\psi$ for simplicity, we show the resulting $\text{Br}(h \rightarrow \bar{\psi}\psi)$ versus m_ψ for various Λ in Fig. 1 (right). Even $\text{Br}(h \rightarrow \bar{\psi}\psi) \sim \mathcal{O}(10^{-2})$ induced by the higher-dimensional operator of Eq. (2) is sensitive to scales $\Lambda \gtrsim 1 \text{ TeV}$. The scaling $\mu \sim m_\psi$ is conservative—some models can yield $\mu \sim v$ or greater, allowing even further reach (see, e.g., Fig. 11). Thus exotic Higgs decays can indirectly probe new physics scales beyond the kinematic reach of the LHC and may provide the *only* evidence of a new sector that is accessible to the LHC.

Given the large Higgs sample that is being collected, it may at first glance seem surprising that the majority of possible exotic Higgs decay modes are poorly constrained, if at all, by existing searches. A major reason for this is that the dominant Higgs production process, gluon fusion, creates Higgs bosons largely at rest, without any associated objects. In a four-body exotic cascade decay of such a Higgs boson, for example, the characteristic transverse momenta of the daughter particles is not large, $p_T \lesssim 30 \text{ GeV}$. Typical exotica searches at the LHC place much higher analysis cuts on object energies, leaving such decays largely unconstrained. In addition, the SM backgrounds are larger at lower energies, so that dedicated analyses are required to find a new physics signal. In many

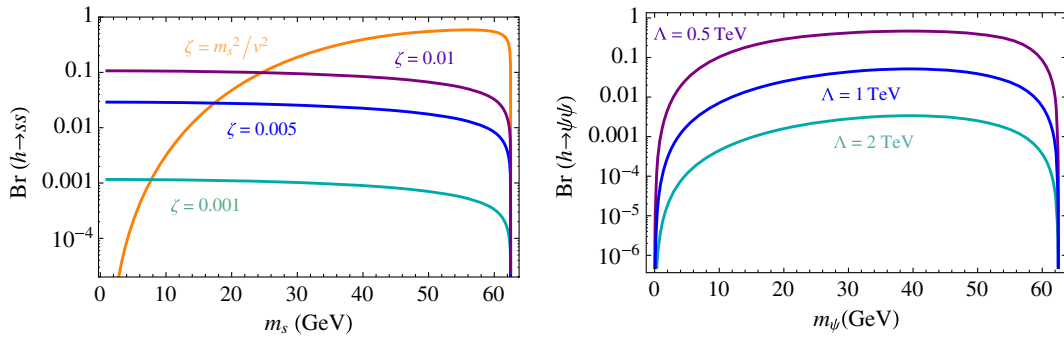


FIG. 1 (color online). Sensitivity of a 125 GeV Higgs to light weakly coupled particles. Left: Exotic Higgs branching fraction to a singlet scalar s versus the singlet’s mass m_s , assuming the interaction Eq. (1) is solely responsible for the $h \rightarrow ss$ decay. If the interaction in Eq. (1) generates the s mass, the result is the orange curve; the other curves are for fixed and independent values of ζ and m_s . Right: Exotic Higgs branching fraction to a new fermion ψ interacting with the Higgs as in Eq. (2) to illustrate the sensitivity of exotic Higgs decay searches to high scales, here Λ . We take here $\mu = m_\psi$.

cases, exotic Higgs decay signals are thus *not* seen or constrained by existing nontargeted analyses. It is necessary to perform *dedicated* searches for exotic Higgs decays. Since there are dozens of possible exotic-decay modes, dozens of new searches are needed to discover or constrain a broad and generic class of theories beyond the SM.

In some cases, particularly if the exotic decay produces only jets with or without E_T , it may be difficult to trigger on Higgs events produced in the (dominant) gluon-gluon-fusion channel. However, even under these pessimistic assumptions, a few hundred events should still be on tape in the existing 7 and 8 TeV data sets, since the associated production of the Higgs boson with a leptonically decaying Z or W boson will usually be recorded due to the presence of one or two leptons. Moreover, additional events may have triggered in the vector boson fusion (VBF) channel due to the rapidity gap of two of the jets in these events (see next paragraph). In some cases, more sophisticated triggers on combinations of objects, possibly with low thresholds, may be required to write a larger fraction of events to tape.

In addition to the “standard” LHC7 and LHC8 data sets, an additional 300–500 Hz of data were collected and “parked” during the LHC8 running. This parked data set was not reconstructed immediately but may present additional opportunities for exotic Higgs analyses. For example, at CMS, it included a trigger on Higgs VBF production ($M_{jj} > 650$ GeV and $|\Delta\eta_{jj}| > 3.5$) [34]. In ATLAS [35], the applications for Higgs physics are less direct but the lowered object p_T thresholds in the ATLAS delayed data stream may present opportunities. More generally, it is important for the LHC14 run to be aware of cases in which simple changes in the trigger could appreciably increase or decrease the number of recorded exotic decays.

The subject of exotic Higgs decays is not a new one. There is an extensive literature on exotic Higgs decays, much of it driven by the past desire to hide a light Higgs from LEP searches, both to preserve electroweak naturalness and to maximize agreement with precision

electroweak fits that yielded a best-fit Higgs mass below the LEP bound of ~ 114 GeV (see, e.g., [36] for a review). Now that the Higgs boson has been discovered, however, the questions have changed. We know the mass of (at least one) Higgs boson, and we also know that its branching fraction into exotic states cannot exceed $\approx 60\%$. The relevant question is now: *for various exotic final states, what branching fractions can be probed at the LHC, and how can the sensitivity to these final states be maximized?*

The search for exotic Higgs decays is a program which deserves to be pursued in a systematic fashion. Our aim in this work is to make such a physics program easier by providing a centralized assessment of models, signatures, and limits.

B. Exotic-decay modes of the 125 GeV Higgs boson

In this section, we list the exotic-decay modes that are the focus of this paper. We organize them by decay topology. While this is not the only possible way to make a systematic list of possible exotic decays, it has the advantage that it is well adapted to a large number of specific models in the literature, allowing a relatively simple mapping between these models and our list; however, since any number of final-state particles can be invisible, different topologies can yield the same experimental signature. We also focus on topologies that arise in models commonly found in the literature, many of which we review in Sec. IC.

In our discussion of exotic decays we will make *three simplifying assumptions*.

- (i) *The observed Higgs at 125 GeV is principally responsible for breaking the electroweak symmetry.*—This means that in models with additional physical scalars, the theory is usually close to a decoupling limit in which the 125 GeV state is SM-like. The production cross sections for this particle are then close to those predicted for the SM Higgs. The decay modes are also SM-like, but modifications of

$\mathcal{O}(10\%–50\%)$ are theoretically easily obtained and consistent with current data (see discussion in Sec. IA). We note that this is not the only scenario allowed by current LHC data, as some nondecoupling limits are still viable for BSM models (see, e.g., [37–40]), but the assumption of a decoupling-like limit is generic and minimal. We emphasize that any exotic-decay search that targets a 125 GeV Higgs should also scan over a much wider Higgs mass range, looking for additional Higgs bosons that may appear in a more complex Higgs sector and may often decay to a final state not found for an SM Higgs.

- (ii) *The observed Higgs at 125 GeV decays to new particles beyond the SM.*—We consider scenarios in which the newly discovered Higgs boson enables the discovery of new, weakly coupled particles, which in many cases have exotic Higgs decays as their primary or only production mode at the LHC. We do not consider rare Higgs decays to SM particles, which can be very sensitive to new physics, whether through its effects in loops (such as in $\gamma\gamma$ or $Z\gamma$), through its modifications of the $V-V-H$ couplings [41] or its nonstandard flavor structures (as in lepton family number-violating decays $h \rightarrow \tau\mu$; see [42,43], and references therein).
- (iii) *The initial exotic 125 GeV Higgs decay is to two neutral BSM particles.*—Generally, to compete with the SM decay modes, the Higgs decay to exotic particles needs to begin as a two-body decay, and LEP limits place stringent constraints on light charged particles [44,45]. Three-body or higher-body exotic decays typically require new states with masses $m \lesssim m_h$ that have substantial couplings to the Higgs boson, in order to induce any appreciable BSM branching fraction after the phase space suppression [46]. In some cases, these light particles can appear in loops and change the Higgs decay rates to $\gamma\gamma$ and/or

$Z\gamma$ final states. While this is certainly worthy of further study we will not do so here.

Our focus is thus on decays that begin via the two-body process $h \rightarrow X_1 X_2$, where $X_{1,2}$ are BSM states (possibly identical). Depending on the properties of X_1 and X_2 , a large number of distinct exotic Higgs decay modes are possible. The topologies we consider are shown in Fig. 2. Our choice is guided by existing models in the literature, but of course there are other possibilities as well. The specific modes we consider (as well as some modes that fall into the same category but that we do not discuss further) are listed below. In parentheses we list the section numbers where a particular decay mode will be discussed in more detail. A pair of particles in parentheses denotes that they form a resonance.

- (i) $h \rightarrow 2$.—This topology occurs for Higgs decays into BSM particles with a lifetime longer than detector scales. It includes $h \rightarrow$ invisible decays [25,47–49] and, in principle, $h \rightarrow R$ -hadrons, although the latter scenario is strongly constrained. In this paper, we consider only
- (1) $h \rightarrow$ invisible (E_T) (Sec. II).
- (ii) $h \rightarrow 2 \rightarrow 3$.—Here the Higgs decays to one final-state particle that is detector stable and another one that decays promptly or with a displaced vertex. Possibilities include
- (1) $h \rightarrow \gamma + E_T$ (Sec. XII);
 - (2) $h \rightarrow (bb) + E_T$ (Sec. XVIII);
 - (3) $h \rightarrow (\tau\tau) + E_T$ (Sec. XIX);
 - (4) $h \rightarrow (\gamma\gamma) + E_T$ (Sec. XIII);
 - (5) $h \rightarrow (\ell\ell) + E_T$ (collimated leptons, Sec. XVI).
- One might also consider $h \rightarrow \gamma + Z$ or $\gamma + Z'$, where the Z' decays to two SM particles and may have different decay modes than the Z ; for instance, the Z' could be leptophilic. In the SM, $\text{Br}(h \rightarrow \gamma Z) \sim 10^{-3}$, but this can be enhanced in BSM models, e.g., [50]. The *semi-invisible* $h \rightarrow \gamma + E_T$ signature arises in

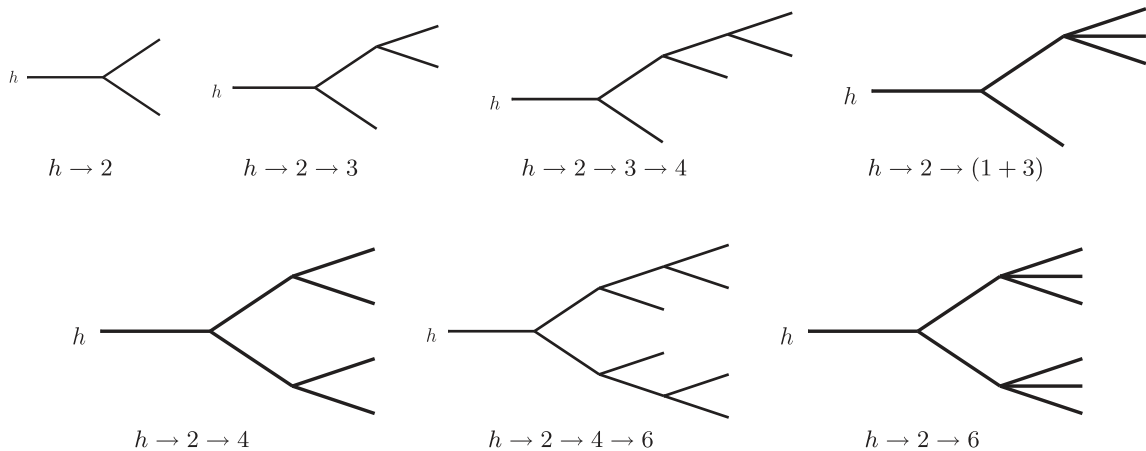


FIG. 2. The exotic Higgs decay topologies we consider in this document, along with the labels we use to refer to them. Every intermediate line in these diagrams represents an *on-shell, neutral* particle, which is either a Z boson or a BSM particle.

the SM ($h \rightarrow \gamma Z \rightarrow \gamma \nu \bar{\nu}$) but can also be enhanced in BSM theories, e.g., $h \rightarrow \tilde{B} \tilde{G} \rightarrow \gamma + 2\tilde{G}$, where \tilde{B} and \tilde{G} are a bino and gravitino, respectively [51].

- (iii) $h \rightarrow 2 \rightarrow 3 \rightarrow 4$.—For this topology, we only consider signatures that contain E_T . In particular, we consider Higgs decays to neutral fermions $h \rightarrow \chi_1 \chi_2$, where $\chi_2 \rightarrow a \chi_1$ or $\chi_2 \rightarrow V \chi_1$ and χ_1 is invisible. Similar decays can occur in more general hidden sectors where the roles of $\chi_{1,2}$ may be played either by fermionic or bosonic fields [32,52]. Such single-resonance topologies give rise to semi-invisible decays and appear in (for example) the PQ -symmetry limit of the next-to-minimal supersymmetric Standard Model (NMSSM) [53,54], where the resonance is exotic, or the SM extended with a neutrino sector like the ν SM [55–57], where the resonance is the W or Z . Discussion in a simplified model context can be found in [58].

We consider in more detail

- (1) $(b\bar{b}) + E_T$ (Sec. XVIII);
- (2) $(\tau\tau) + E_T$ (Sec. XIX);
- (3) $(\gamma\gamma) + E_T$ (Sec. XIII);
- (4) $(\ell^+ \ell^-) + E_T$ (isolated, Sec. XV; collimated, Sec. XVI).

- (iv) $h \rightarrow 2 \rightarrow (1+3)$.—This topology occurs when the resonant cascade decays of the $h \rightarrow 2 \rightarrow 3 \rightarrow 4$ topology go off shell. Here again we only consider semi-invisible signatures and focus on leptonic signatures.

- (1) $\ell^+ \ell^- + E_T$ (isolated, Sec. XV).

- (v) $h \rightarrow 2 \rightarrow 4$.—In this topology the Higgs decays as $h \rightarrow aa', ss', V_1 V_2, a V_1 \rightarrow (xx)(yy)$, where a and a' (s and s' , V_1 and V_2) are not necessarily distinct pseudoscalars (scalars, vectors). In most cases we can reconstruct two resonances. The scalars and pseudoscalars can typically decay to $x, y =$ quarks, leptons, photons, or gluons, while the vectors can typically decay to $x, y =$ quarks or leptons. This topology occurs in well-known BSM theories like the R -symmetric limit of the NMSSM [59–62], Little Higgs models [63–65], or any theory that features additional SM singlet scalars, such as [32,66–72]. Also possible is the fermionic decay $h \rightarrow \chi_2 \chi_2 \rightarrow 2(\gamma \chi_1)$, which occurs in, e.g., the MSSM with gauge-mediated supersymmetry (SUSY)-breaking [73] (see also [74] for discussions of 1–3 light jets + E_T in simplified models with this topology). In this paper, we consider in more detail

- (1) $(b\bar{b})(b\bar{b})$ (Sec. III);
- (2) $(b\bar{b})(\tau^+ \tau^-)$ (Sec. IV);
- (3) $(b\bar{b})(\mu^+ \mu^-)$ (Sec. V);
- (4) $(\tau^+ \tau^-)(\tau^+ \tau^-)$ (Sec. VI);
- (5) $(\tau^+ \tau^-)(\mu^+ \mu^-)$ (Sec. VI);
- (6) $(jj)(jj)$ (Sec. VII);
- (7) $(jj)(\gamma\gamma)$ (Sec. VIII);

- (8) $(\ell^+ \ell^-)(\ell^+ \ell^-)$ (Sec. X for $h \rightarrow ZZ_D$, Sec. XI for $h \rightarrow Z_D Z_D$, Sec. XVII for collimated leptons);

- (9) $(\gamma\gamma)(\gamma\gamma)$ (Sec. IX);

- (10) $\gamma\gamma + E_T$ (no $\gamma\gamma$ resonance, Sec. XIII).

- (vi) $h \rightarrow 2 \rightarrow 4 \rightarrow 6$.—Here both the Higgs' daughters undergo on-shell cascade decays. As for the single-cascade topology $h \rightarrow 2 \rightarrow (1+3)$, examples of such cascades include NMSSM neutralinos, decaying via $\chi_2 \rightarrow \chi_1 a$, $a \rightarrow f\bar{f}$, or right-handed neutrinos, decaying via $N_R \rightarrow \nu Z, \ell W$. More elaborate hidden sectors allow for many possibilities, such as $\phi_2 \rightarrow a \phi_1$, $a \rightarrow gg(\gamma\gamma)$, or $\phi_1 \rightarrow Z_D \phi_2$, $Z_D \rightarrow \ell\ell, q\bar{q}$ (here $\phi_{1,2}$ are BSM states that may be either fermions or scalars).

We only consider final states with leptons for this topology:

- (1) $h \rightarrow 2(\ell\ell) + E_T$ (isolated, Sec. XIV; collimated, Sec. XVII);
- (2) $h \rightarrow (\ell\ell) + E_T + X$ (isolated, Sec. XV; collimated, Sec. XVI).

- (vii) $h \rightarrow 2 \rightarrow 6$.—There are various possibilities here. Examples include Higgs decays to R -parity-violating neutralinos, which can yield $h \rightarrow \chi_1 \chi_1 \rightarrow 6j, 4j + 2\ell, 4\ell + 2\nu$. In addition, any of the resonant cascade decays discussed above may become three-body. Another example is flavored dark matter, where the Higgs can decay to two heavy dark flavors first and then into light quarks and the dark matter candidate via higher-dimensional operator, resulting in $h \rightarrow 4j + E_T$ [75].

We only consider final states with isolated leptons for this topology:

- (1) $h \rightarrow 2\ell + E_T + X$ (Sec. XV);
- (2) $h \rightarrow 4\ell + E_T$ (Sec. XIV).

- (viii) $h \rightarrow 2 \rightarrow$ many, where “many” refers to many SM particles, including “weird jets.” This occurs [32] in Higgs decays to hidden-sector particles that undergo a long series of cascade decays or a hidden-sector parton shower to (many) SM particles and possibly detector-stable hidden-sector particles that appear as E_T . The SM particles produced could be dominated by leptons, photons, or hadrons, leading to *lepton-jets*, *photon jets*, or *weird high-multiplicity jets*. We do not consider any of these final states in more detail.

- (ix) Finally, in all of the decay topologies listed above, *displaced vertices are possible and should be considered in the LHC analyses*. A simple example [32,76] is $h \rightarrow 2 \rightarrow 4$, where the two particles produced in the Higgs decay are long lived and decay far out in the detector; a similar signature arises in R -parity-violating supersymmetry [77]. These signatures offer opportunities for LHCb [76,77] as well as ATLAS and CMS, but we

do not cover them here. A number of relevant experimental searches have already been performed [78–95].

In the following sections we examine most of the above decay modes in detail, outline their theoretical motivations, and review existing collider studies and relevant experimental searches. For some channels with significant discovery potential we also define benchmark models that can be used to design future searches, obtain limits from already performed searches, and/or perform collider studies to demonstrate how much exclusion can be achieved with the extant LHC data set.

C. Theoretical models for exotic Higgs decays

In this section, we describe and review theoretical models that give rise to exotic Higgs decays. We begin with several “simplified models” (in the spirit of, e.g., [96]), which capture the essential ingredients that are involved in more complicated BSM models. It often makes sense to present experimental results in a simplified model framework, as only a few parameters are needed to capture the relevant details; for example, non-SM four-body decays of the Higgs of the form $h \rightarrow \phi\phi \rightarrow (f\bar{f})(f'f')$ (where ϕ is a singlet particle and f, f' are SM fermions) can be parametrized merely by $m_h = 125$ GeV, m_ϕ , $\text{Br}(h \rightarrow \phi\phi)$, and $\text{Br}(\phi \rightarrow f\bar{f})$. More parameters can be added if the decays are displaced or involve multistep cascades.

We discuss adding to the SM a scalar, one or two fermions, or a vector. We also describe various two-Higgs-doublet (2HDM) models with the addition of a scalar. We then turn our attention to more complicated models that have ingredients similar to the simplified models, namely the MSSM, NMSSM, and Little Higgs models. Finally, we summarize the rich phenomenology possible in hidden-valley models.

I. SM + scalar

A particularly simple extension of the SM is to add to it one real scalar singlet S . This model can easily produce nontrivial exotic Higgs decays, since (i) the Higgs can decay to pair of singlets and (ii) the singlet decays to SM particles (by virtue of mixing with the Higgs). Singlet scalars coupled to the Higgs also provide a well-known avenue for enhancing the electroweak phase transition in the early Universe, which is a necessary ingredient for electroweak baryogenesis (see, e.g., [97]). We describe this simple model below, as well as two small variations (one with more symmetry, one with a complex scalar), but all three models, as well as other variations, can yield essentially identical phenomenology. In Sec. IC 2, this will be generalized to two-Higgs-doublet models with a singlet.

Three examples.—At the renormalizable level, gauge invariance allows the singlet S to couple only to itself and to $H^\dagger H \equiv |H|^2$. The resulting potential is given by

$$V(H, S) = V(H) + \hat{V}(S) + kS|H|^2 + \frac{1}{2}\zeta S^2|H|^2, \quad (3)$$

where $\hat{V}(S)$ is a general quartic polynomial that may give S a vacuum expectation value. The couplings k and ζ generate mixings between H and S . Assuming those mixings are small, we identify the uneaten doublet degree of freedom to be the SM-like Higgs with $m_h = 125$ GeV and take the singlet field to have a mass below $m_h/2$. The small mixings give mass eigenstates h and s , which are mostly doublet- and singlet-like, respectively. The decays $h \rightarrow ss$ are generated by an effective cubic term, and s decays to SM particles via its doublet admixture.

Imposing a Z_2 symmetry $S \rightarrow -S$, we can obtain a simpler version of this model with similar phenomenology. In this case, $\hat{V}(S)$ contains only quadratic and quartic terms and $k = 0$, e.g.,

$$V(H, S) = -\mu^2|H|^2 - \frac{1}{2}\mu'^2 S^2 + \lambda|H|^4 + \frac{1}{4}\kappa S^4 + \frac{1}{2}\zeta S^2|H|^2. \quad (4)$$

Depending on the choice of couplings, the potential may have a minimum at $S = 0$, in which case the Z_2 is unbroken, there is no mixing between H and S , and the S does not decay; the coupling ζ induces the invisible decay $h \rightarrow ss$. If the minimum instead has $S \neq 0$, then the Z_2 is broken, and the coupling ζ now not only produces a cubic term but also a quadratic term that allows H and S to mix. In this case, the phenomenology is just as described in the previous paragraph, i.e., $h \rightarrow ss$ for $m_s < m_h/2$, with s decaying to SM particles.

A third model, with essentially identical phenomenology, involves a theory with a *complex* scalar and an *approximate* $U(1)$ global symmetry.² Here the scalar potential is as above, with S now complex, and with a small $U(1)$ breaking part:

$$V(H, S) = V_0(|H|^2, |S|^2) + V_1(|H|^2, S, S^\dagger), \quad (5)$$

$$V_0 = -\mu^2|H|^2 - \mu'^2|S|^2 + \lambda|H|^4 + \kappa|S|^4 + \zeta|S|^2|H|^2, \quad (6)$$

$$V_1 = (\rho + \xi_S|S|^2 + \xi_H|H|^2)S + \text{Hermitean conjugate} + \text{other terms}, \quad (7)$$

²An exact $U(1)$ symmetry leads to invisible decays, while a spontaneously broken $U(1)$ gives rise to an unacceptable massless Nambu-Goldstone boson; a gauged $U(1)$ will be discussed in Sec. IC 2.

where we have chosen not to consider the most general V_1 for illustration purposes. If the potential is such that S develops a nonzero vacuum expectation value, the spectrum consists of a massive scalar S and a light pseudo-Nambu-Goldstone boson a with mass m_a . If $m_s > \frac{1}{2}m_h > m_a$, then $h \rightarrow aa$ is possible, which is an invisible decay unless the $U(1)$ -violating terms also violate charge conjugation. In that case, a can mix with the massive state s , which in turn mixes with H as in previous examples, allowing the a to decay to SM particles, with couplings inherited from H .

Phenomenology.—After electroweak symmetry breaking there are two relevant *mass eigenstates*: the SM-like scalar h at 125 GeV containing a small admixture of S , and the mostly singlet scalar s containing a small admixture of H . The phenomenology of all three variants above is the same, as far as decays of the form $h \rightarrow ss \rightarrow \text{SM}$ are concerned. It can be captured in terms of three parameters:

- (1) The effective Lagrangian contains a term of the form $\mu_v h s s$, which gives $h \rightarrow ss$ with $\text{Br}(h \rightarrow \text{exotic})$ determined by μ_v .
- (2) The singlet's mass m_s affects $\text{Br}(h \rightarrow \text{exotic})$ and the type of SM final states available for $s \rightarrow \text{SM}$.
- (3) The mixing angle between S and H , denoted here by θ_S , determines the overall width of $s \rightarrow \text{SM}$. If s cannot decay to other non-SM fields, θ_S controls its lifetime.

Apart from these continuous parameters, the parity of s also affects the partial widths to different final states, mostly near thresholds. Note that the total width of s is usually not important for phenomenology if it decays promptly. However, the lifetime of s is macroscopic ($c\tau \sim \text{meters}$) if $\theta \lesssim 10^{-6}$. This possibility is technically natural and thus the experimental search for displaced vertices deserves serious consideration [76]; however, we do not discuss this further here. Therefore, for a large part of parameter space, only μ_v and m_s are relevant for collider phenomenology as this fixes $\text{Br}(h \rightarrow ss)$ and $\text{Br}(s \rightarrow \text{SM})$.

The partial width for exotic Higgs decays is given by

$$\Gamma(h \rightarrow ss) = \frac{1}{32\pi} \frac{\mu_v^2}{m_h} \sqrt{1 - \frac{4m_s^2}{m_h^2}} \approx \left(\frac{\mu_v/v}{0.03}\right)^2 \Gamma(h \rightarrow \text{SM}), \quad (8)$$

where the last step assumes $m_s \ll m_h/2$. Therefore, the new branching ratio is $\mathcal{O}(1)$ even for small values of μ_v/v . This is not surprising, if we recall that in the SM the bottom quark takes up almost 60% of the total width although its Yukawa coupling is only ~ 0.017 . In Fig. 3, we show contours of μ_v/v in the $\text{Br}(h \rightarrow ss)$ versus m_s plane.

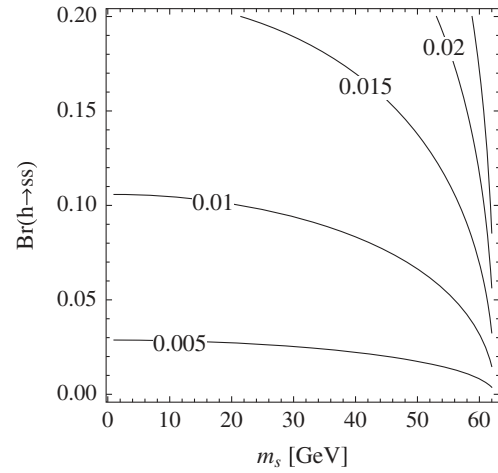


FIG. 3. Size of the cubic coupling μ_v in units of Higgs expectation value v to yield the indicated $h \rightarrow ss$ branching fraction as a function of singlet mass, as given by Eq. (8).

The individual partial widths of the singlet s to SM particles are readily computed using existing calculations for Higgs decays, e.g., [98,99]. Decays into W^*W^* and Z^*Z^* are negligible for $m_s < m_h/2$. At lowest order, the partial decay width to fermions is given by

$$\Gamma(s \rightarrow f\bar{f}) = \sin^2\theta_S \frac{N_c}{8\pi} \frac{m_s m_f^2}{v^2} \beta_f^3, \quad (9)$$

where $\beta_f = \sqrt{1 - 4m_f^2/m_s^2}$ and N_c is the number of colors, equaling 3(1) for quarks (leptons). For the pseudoscalar singlet state a , β_f^3 is replaced by β_f . The mixing suppression $\sin^2\theta_S$ is common to all partial widths, including those to gluons and photons and thus does not affect branching ratios if s only decays to SM particles. $\text{Br}(s \rightarrow \text{SM})$ and $\text{Br}(h \rightarrow ss \rightarrow \text{SM})$ are shown for $m_s > 1$ GeV in Fig. 4 on the left and right, respectively. It is clear that a simple singlet extension of the SM generically implies significant branching ratios of exotic Higgs decays to four SM objects. The indicated branching ratios include $\mathcal{O}(\alpha_s^2, \alpha_s^3)$ radiative corrections for decays to quarks, as well as next-to-leading-order (NLO) corrections to the loop-induced decays to photons and gluons [98].

The theoretical calculations become increasingly inaccurate as m_s is lowered to ~ 1 GeV, where perturbative QCD breaks down, or when m_s is close to a hadronic resonance, which can enhance the decay rates [41]. Decays to quarkonium states are suppressed for s but may be important for a . For $m_s < 1$ GeV and above the pion threshold, partial widths have to be computed within a low energy effective theory of QCD, such as soft-pion theory or the chiral Lagrangian method. Nevertheless, it is clear that the dominant decay of the singlet is to some combination of hadrons, which are boosted due to the

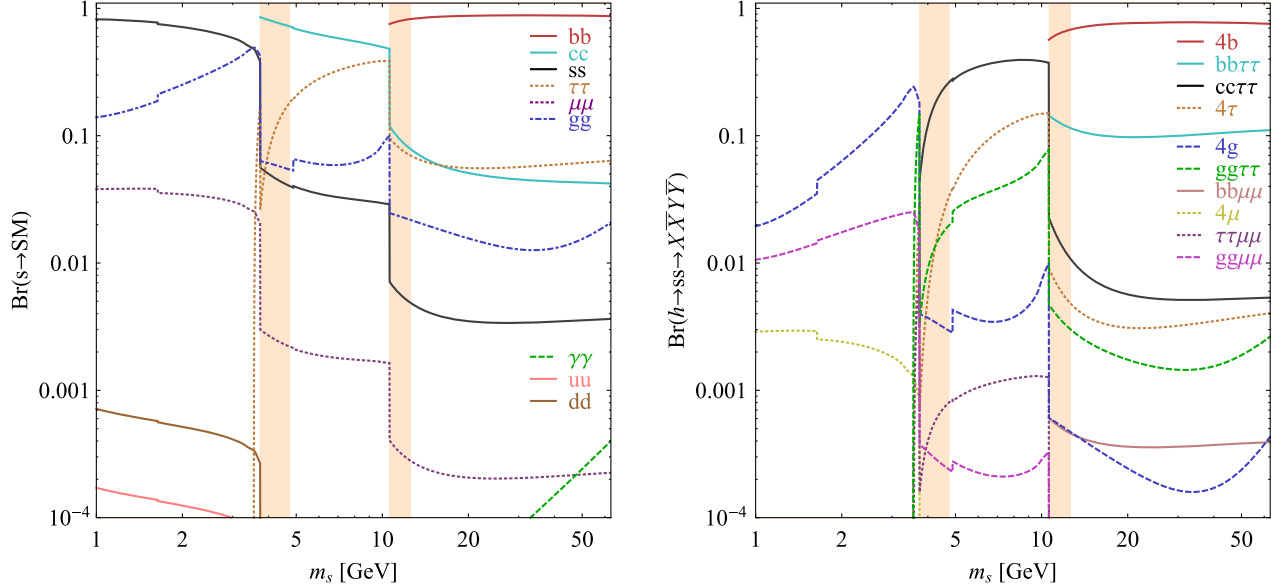


FIG. 4 (color online). Left: Branching ratios of a CP -even scalar singlet to SM particles, as a function of m_s . Right: Branching ratios of exotic decays of the 125 GeV Higgs boson as a function of m_s , in the SM + scalar model described in the text, scaled to $\text{Br}(h \rightarrow ss) = 1$. Hadronization effects likely invalidate our simple calculation in the shaded regions.

large mass difference between the singlet and h . The resulting two-track jet may look like a low-quality hadronic τ decay. Between the muon and pion thresholds ($210 \text{ MeV} \lesssim m_s \lesssim 270 \text{ MeV}$), the dominant decay is to $\mu^+\mu^-$, while for $m_s \lesssim 210 \text{ MeV}$, the dominant decay is to e^+e^- . Photons are the only possible final state for $m_s < 2m_e$, in which case the scalar is detector stable.

Further details of the branching ratio calculation can be found in Sec. IC 2 and Appendix A, which also includes a more detailed discussion of pseudoscalar decays.

For $m_s \lesssim 2m_b$, the $s\bar{b}b$ coupling can in principle be probed by bottomonium decay [100,101]. The strongest limits are $\text{Br}(\Upsilon(1S) \rightarrow \gamma\tau^+\tau^-) \lesssim 10^{-5}$ by BABAR [102], which constrains the Yukawa coupling to satisfy $y_{sbb} \lesssim 0.4$ for $\text{Br}(s \rightarrow \tau^+\tau^-) = 1$ [103,104]. In the SM+S scenario, $y_{sbb} = \sin\theta_S y_{hbb}$ with $y_{hbb} \approx 0.02$ in the SM. Clearly the Upsilon decay measurement provides no meaningful bounds on singlet extensions. Similar arguments apply to pseudoscalars, and hence the 2HDM + S and NMSSM in the next sections.

2. 2HDM (+scalar)

The SM Higgs sector is made up of a single $SU(2)_L$ doublet H with hypercharge $Y = +\frac{1}{2}$, denoted by $H \sim 2_{+1/2}$. Adding a doublet to this minimal picture is one of the simplest extensions of the Higgs sector compatible with a ρ parameter close to 1. Such extensions are found in several well-motivated theories, such as supersymmetry [105] and axion models [106,107], where holomorphy and the Peccei-Quinn symmetry, respectively, necessitate an additional doublet; theories of electroweak baryogenesis, which might be made viable with additional doublets [108]; and grand unified models [41]. For this reason, it makes sense to define the most general 2HDM and study it in detail (for a comprehensive review, see, e.g., [109]; for a discussion on the impact of recent SM-like Higgs boson discovery, see, e.g., [110]). Below we will then add a light scalar to the 2HDM to obtain a rich set of exotic Higgs decays.

The most general 2HDM Higgs potential is given by [41]

$$\begin{aligned}
 V = & m_1^2 |H_1|^2 + m_2^2 |H_2|^2 + \frac{\lambda_1}{2} |H_1|^4 + \frac{\lambda_2}{2} |H_2|^4 + \lambda_3 |H_1|^2 |H_2|^2 + \lambda_4 |H_1^\dagger H_2|^2 \\
 & + \frac{\lambda_5}{2} [(H_1 H_2)^2 + \text{c.c.}] + m_{12}^2 (H_1 H_2 + \text{c.c.}) \\
 & + [\lambda_6 |H_1|^2 (H_1 H_2) + \text{c.c.}] + [\lambda_7 |H_2|^2 (H_1 H_2) + \text{c.c.}].
 \end{aligned} \tag{10}$$

TABLE II. Couplings of the neutral scalar and pseudoscalar mass eigenstates in the four types of 2HDM with a \mathbb{Z}_2 symmetry, following the notation of [113]. The couplings are normalized to those of the SM Higgs.

	Couplings	I	II	III (lepton specific)	IV (flipped)
h	g_{hVV}	$\sin(\beta - \alpha)$	$\sin(\beta - \alpha)$	$\sin(\beta - \alpha)$	$\sin(\beta - \alpha)$
	$g_{h\bar{t}t}$	$\cos \alpha / \sin \beta$	$\cos \alpha / \sin \beta$	$\cos \alpha / \sin \beta$	$\cos \alpha / \sin \beta$
	$g_{hb\bar{b}}$	$\cos \alpha / \sin \beta$	$-\sin \alpha / \cos \beta$	$\cos \alpha / \sin \beta$	$-\sin \alpha / \cos \beta$
	$g_{h\tau\bar{\tau}}$	$\cos \alpha / \sin \beta$	$-\sin \alpha / \cos \beta$	$-\sin \alpha / \cos \beta$	$\cos \alpha / \sin \beta$
H^0	g_{H^0VV}	$\cos(\beta - \alpha)$	$\cos(\beta - \alpha)$	$\cos(\beta - \alpha)$	$\cos(\beta - \alpha)$
	$g_{H^0\bar{t}t}$	$\sin \alpha / \sin \beta$	$\sin \alpha / \sin \beta$	$\sin \alpha / \sin \beta$	$\sin \alpha / \sin \beta$
	$g_{H^0b\bar{b}}$	$\sin \alpha / \sin \beta$	$\cos \alpha / \cos \beta$	$\sin \alpha / \sin \beta$	$\cos \alpha / \cos \beta$
	$g_{H^0\tau\bar{\tau}}$	$\sin \alpha / \sin \beta$	$\cos \alpha / \cos \beta$	$\cos \alpha / \cos \beta$	$\sin \alpha / \sin \beta$
A	g_{AVV}	0	0	0	0
	$g_{A\bar{t}t}$	$\cot \beta$	$\cot \beta$	$\cot \beta$	$\cot \beta$
	$g_{Ab\bar{b}}$	$-\cot \beta$	$\tan \beta$	$-\cot \beta$	$\tan \beta$
	$g_{A\tau\bar{\tau}}$	$-\cot \beta$	$\tan \beta$	$\tan \beta$	$-\cot \beta$

We choose the charges of the Higgs fields such that $H_1 \sim 2_{-1/2}$ and $H_2 \sim 2_{+1/2}$. Note that we choose conventions that differ slightly from the ‘‘standard’’ conventions of [41,109]; this will simplify the transition to supersymmetry models below.³ The scalar doublets $H_{1,2}$ acquire vacuum expectation values $v_{1,2}$, which we assume here are real and aligned. Expanding around the minima yields two complex and four real degrees of freedom:

$$\begin{aligned}
 H_1 &= \frac{1}{\sqrt{2}} \begin{pmatrix} v_1 + H_{1,R}^0 + iH_{1,I}^0 \\ H_{1,R}^- + iH_{1,I}^- \end{pmatrix}, \\
 H_2 &= \frac{1}{\sqrt{2}} \begin{pmatrix} H_{2,R}^+ + iH_{2,I}^+ \\ v_2 + H_{2,R}^0 + iH_{2,I}^0 \end{pmatrix}.
 \end{aligned} \quad (11)$$

The charged scalar and pseudoscalar mass matrices are diagonalized by a rotation angle β , defined as $\tan \beta = v_2/v_1$. One charged (complex) field and one neutral pseudoscalar combination of $H_{1,2,I}^0$ are eaten by the SM gauge bosons after electroweak symmetry breaking. The other complex field yields two charged mass eigenstates H^\pm , which we assume are heavy and will thus play no further role in our discussions. The surviving three real degrees of freedom yield one neutral pseudoscalar mass eigenstate,

$$A = H_{1,I}^0 \sin \beta - H_{2,I}^0 \cos \beta, \quad (12)$$

and two neutral scalar mass eigenstates,

$$\begin{pmatrix} h \\ H^0 \end{pmatrix} = \begin{pmatrix} -\sin \alpha & \cos \alpha \\ \cos \alpha & \sin \alpha \end{pmatrix} \begin{pmatrix} H_{1,R}^0 \\ H_{2,R}^0 \end{pmatrix}, \quad (13)$$

³To recover the conventions of [41] set $\Phi_2 = H_2$, $\Phi_1 = i\sigma^2 H_1^*$.

where⁴ $-\pi/2 \leq \alpha \leq \pi/2$. Our notation anticipates the assumption below that the model is in a decoupling limit, so that h is the SM-like Higgs and H^0 is the other, heavier, scalar.

Allowing the most general Yukawa couplings to fermions would result in large flavor-changing neutral currents. This can be avoided by imposing \mathbb{Z}_2 symmetries to ensure that fermions with the same quantum numbers all couple to only one Higgs field. This results in four types of fermion couplings commonly discussed in the literature: type I (all fermions couple to H_2), type II (MSSM-like, d_R and e_R couple to H_1 , u_R to H_2), type III (lepton-specific, leptons and quarks couple to H_1 and H_2 , respectively) and type IV (flipped, with u_R, e_R coupling to H_2 and d_R to H_1). The couplings of the h, H^0 , and A mass eigenstates to fermions and gauge fields relative to the SM Higgs couplings are summarized in Table II.⁵

In general, 2HDMs could allow for exotic decays of the 125 GeV state of the form $h \rightarrow AA, H^0 \rightarrow hh, AA$ or $h \rightarrow ZA$ (where we temporarily identified the 125 GeV state with either h or H^0), where the daughter (pseudo)scalars decay to SM fermions or gauge bosons. However, while this possibility can be realized in certain corners of parameter space, 2HDMs are by now too constrained from existing data [114,115] to allow for a wide variety of exotic Higgs decay phenomenology.

These restrictions are easily avoided as follows. First, we assume the 2HDM is near or in the decoupling limit,

$$\alpha \rightarrow \pi/2 - \beta, \quad (14)$$

⁴Contrast this to the MSSM Higgs potential, where $-\pi/2 \leq \alpha \leq 0$.

⁵More general fermion couplings are possible within the framework of minimal flavor violation (MFV) [111,112]. We do not discuss this case here since we use the 2HDM to illustrate a range of possible exotic Higgs decay signatures, which would not be qualitatively different in the MFV scenarios.

where the lightest state in the 2HDM is h , which we identify with the observed 125 GeV state. In this limit, the fermion couplings of h also become identical to the SM Higgs, while the gauge boson couplings are very close to SM-like for $\tan\beta \gtrsim 5$. All of the properties of h are determined by just two parameters, $\tan\beta$ and α , and the type of fermion couplings. The remaining parameters, which control the rest of the Higgs spectrum and its phenomenology, are in general constrained by the measured production and decays of h [21,113,116–123], but plenty of viable parameter space exists in the decoupling limit.

Second, we add to the 2HDM one complex scalar singlet,

$$S = \frac{1}{\sqrt{2}}(S_R + iS_I),$$

which may attain a vacuum expectation value that we implicitly expand around. This singlet only couples to $H_{1,2}$ in the potential and has no direct Yukawa couplings, acquiring all of its couplings to SM fermions through its mixing with $H_{1,2}$. This mixing needs to be small to avoid spoiling the SM-like nature of h .

Under these two simple assumptions, exotic Higgs decays of the form

$$h \rightarrow ss \rightarrow X\bar{X}Y\bar{Y} \quad \text{or} \quad h \rightarrow aa \rightarrow X\bar{X}Y\bar{Y} \quad (15)$$

as well as

$$h \rightarrow aZ \rightarrow X\bar{X}Y\bar{Y} \quad (16)$$

are possible, where $s(a)$ is a (pseudo)scalar mass eigenstate mostly composed of $S_R(S_I)$ and X, Y are SM fermions or gauge bosons. We refer to this setup as the 2HDM + S. For type-II 2HDM + S, a light a corresponds roughly to the R -symmetry limit of the NMSSM (see Sec. IC 7). However,

the more general 2HDM framework allows for exotic Higgs decay phenomenologies that are much more diverse than those usually considered in a NMSSM-type setup.

To incorporate the already analyzed constraints on 2HDMs into the 2HDM + S (e.g., [123]), one can imagine adding a decoupled singlet sector to a 2HDM with α, β chosen so as to not yet be excluded.⁶ The real and imaginary components of S can be given separate masses, and small mixings to the 2HDM sector can then be introduced as a perturbation. Approximately the same constraints on α, β apply to this 2HDM + S, as long as $\text{Br}(h \rightarrow ss/aa/Za) \lesssim 10\%$. This allows for a wide range of possible exotic Higgs decays. There are some important differences depending on whether the lightest singlet state with a mass below $m_h/2$ is scalar or pseudoscalar. We will discuss them in turn.

*Light pseudoscalar (a).—*There are two pseudoscalar states in the 2HDM + S, one that is mostly A and one that is mostly S_I . One can choose the mostly singletlike pseudoscalar

$$a = \cos\theta_a S_I + \sin\theta_a A, \quad \theta_a \ll 1, \quad (17)$$

to be lighter than the SM-like Higgs. There are two possible exotic Higgs decays: $h \rightarrow Za$ for $m_a < m_h - m_Z \approx 35$ GeV and $h \rightarrow aa$ for $m_a < m_h/2 \approx 63$ GeV.

The partial width $\Gamma(h \rightarrow Za)$ is entirely fixed by the 2HDM parameters α, β and the mixing angle θ_a . The relevant interaction term in the effective Lagrangian is

$$\mathcal{L}_{\text{eff}} \supset g_{\text{eff}}(a\partial^\mu h - h\partial^\mu a)Z_\mu, \quad (18)$$

where $g_{\text{eff}} = \sqrt{\frac{g^2 + g'^2}{2}} \sin(\alpha - \beta) \sin\theta_a,$

which gives

$$\Gamma(h \rightarrow Za) = \frac{g_{\text{eff}}^2 [(m_h + m_Z + m_a)(m_h - m_Z + m_a)(m_h + m_Z - m_a)(m_h - m_Z - m_a)]^{3/2}}{16\pi m_h^3 m_Z^2}. \quad (19)$$

Figure 5 shows that $\theta_a \sim 0.1$ gives $\text{Br}(h \rightarrow Za) \sim 10\%$ in the absence of other exotic decays.

Two terms in the effective Lagrangian give rise to $h \rightarrow aa$ decays:

$$\mathcal{L}_{\text{eff}} \supset g_{hAA} hAA + \lambda_S |S|^2. \quad (20)$$

In terms of mass eigenstates, this contains

$$\mathcal{L}_{\text{eff}} \supset g_{hAA} \sin^2\theta_a haa + 4\lambda_S v_s \sin\zeta_1 \cos^2\theta_a haa, \quad (21)$$

where $\langle S \rangle = v_s$ is the singlet vacuum expectation value, and the (presumably small) mixing angle ζ_1 determines the

⁶As we have pointed out in Sec. IC 1, bottomonium decays provide no meaningful constraint on the 2HDM + S scenario.

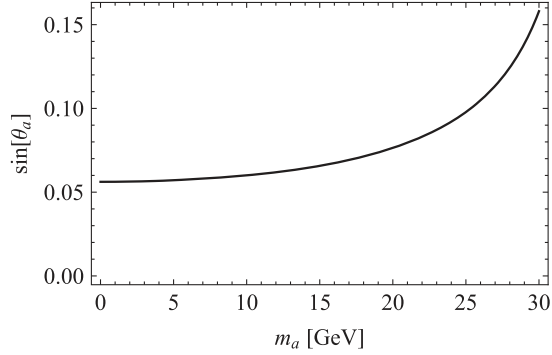


FIG. 5. Required mixing angle between the doublet and singlet-sector pseudoscalar for $\text{Br}(h \rightarrow aZ) = 10\%$, assuming no other exotic Higgs decays and $\alpha = \pi/2 - \beta$ (decoupling limit).

singlet scalar content of the SM-like Higgs; see Eq. (22). The first term by itself can easily give rise to $\text{Br}(h \rightarrow aa) \sim 10\%$ if $g_{hAA} \sim v$ and $\theta_s \sim 0.1$; see Fig. 3. (Figure 3 shows the results for Higgs partial widths to scalars, but these are almost identical to pseudoscalars, except near threshold.) The additional contribution from the second term (even without a singlet scalar below the Higgs mass) means that $\text{Br}(h \rightarrow aa)$ and $\text{Br}(h \rightarrow Za)$ can be independently adjusted.

The decay of a to SM fermions proceeds via the A couplings in Table II, multiplied by $\sin\theta_a$. Therefore, once the type of 2HDM model has been specified, the exotic Higgs decay phenomenology is entirely dictated by the two exotic branching ratios $\text{Br}(h \rightarrow aa)$ and $\text{Br}(h \rightarrow Za)$, as well as $\tan\beta$, which determines a 's fermion couplings. Perturbative unitarity of the Yukawa couplings sets a lower bound of $\tan\beta > 0.28$ [123]; we will show results for $\tan\beta$ as low as ~ 0.5 .

In Figs. 7–9, we show $\text{Br}(a \rightarrow X\bar{X})$, where X is a SM particle. These include $\mathcal{O}(\alpha_s^2, \alpha_s^3)$ radiative corrections for decays to quarks, which can be readily computed [98,99] (for details see Appendix A). As mentioned in Sec. IC 1, perturbative QCD can be used for pseudoscalar masses above ~ 1 GeV, though the calculation breaks down near quarkonium states [124]. A detailed investigation of this is beyond the scope of this paper. The results can be summarized as follows:

- (i) Type I (Fig. 6).—Since all fermions couple only to H_2 , the branching ratios are independent of $\tan\beta$. The pseudoscalar couplings to all fermions are proportional to those of the SM Higgs, all with the same proportionality constant, and the branching ratios are thus very similar to those of the SM + S model with a complex S and a light pseudoscalar a (i.e., for example, proportional to the mass of the final-state fermions).
- (ii) Type II (Fig. 7).—The exotic-decay branching ratios are those of NMSSM models. Unlike type-I models, they now depend on $\tan\beta$, with decays to down-type

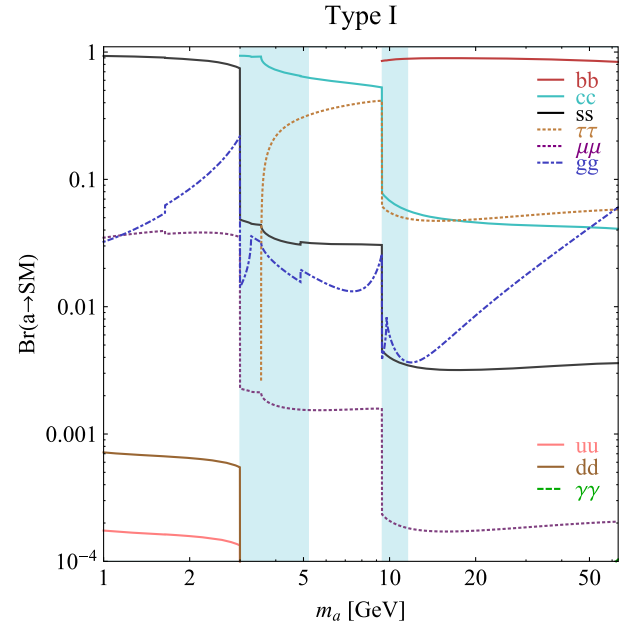


FIG. 6 (color online). Branching ratios of a singletlike pseudoscalar in the 2HDM + S for type-I Yukawa couplings. Decays to quarkonia likely invalidate our simple calculations in the shaded regions.

fermions suppressed (enhanced) for down-type fermions for $\tan\beta < 1$ ($\tan\beta > 1$).

- (iii) Type III (Fig. 8).—The branching ratios are $\tan\beta$ dependent. For $\tan\beta > 1$, pseudoscalar decays to leptons are enhanced over decays to quarks. For example, unlike the NMSSM above the $b\bar{b}$ threshold, decays to $\tau^+\tau^-$ can dominate over decays to $b\bar{b}$; similarly, above the $\mu^+\mu^-$ threshold, decays to $\mu^+\mu^-$ can dominate over decays to heavier, kinematically accessible quark pairs. This justifies extending, for example, NMSSM-driven 4τ searches over the entire mass range above the $b\bar{b}$ threshold. For $\tan\beta < 1$, decays to quarks are enhanced over decays to leptons.
- (iv) Type IV (Fig. 9).—The branching ratios are $\tan\beta$ dependent. For $\tan\beta < 1$ and compared to the NMSSM, the pseudoscalar decays to up-type quarks and leptons can be enhanced with respect to down-type quarks, so that branching ratios to $b\bar{b}$, $c\bar{c}$ and $\tau^+\tau^-$ can be similar. This opens up the possibility of detecting this model in the $2b2\tau$ or $2c2\tau$ final state.

Note that the branching ratios are only independent of $\tan\beta$ for type I, and all types reduce to type I for $\tan\beta = 1$.

A sizable $\text{Br}(h \rightarrow Za)$ would open up additional exciting search channels with leptons that reconstruct the Z boson. This is discussed in Sec. X.

For $3m_\pi < m_a < 1$ GeV the decay rate calculations suffer large theoretical uncertainties but the dominant decay channels will likely be muons and hadrons. Below the pion,

$\tan \beta=0.5$, TYPE II

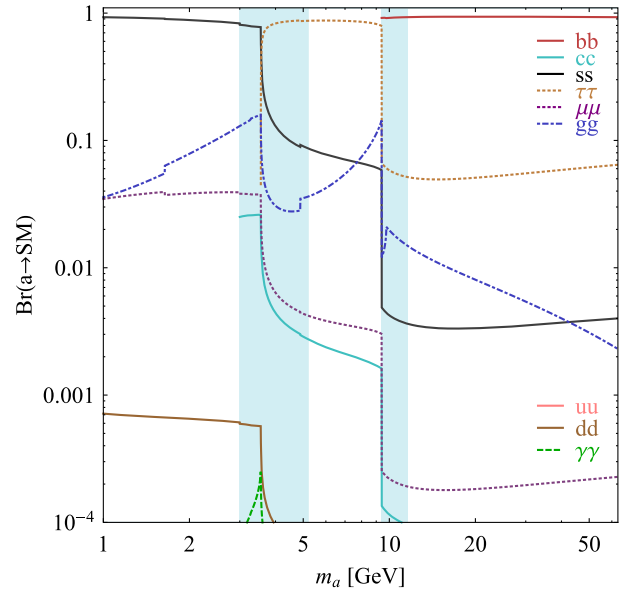
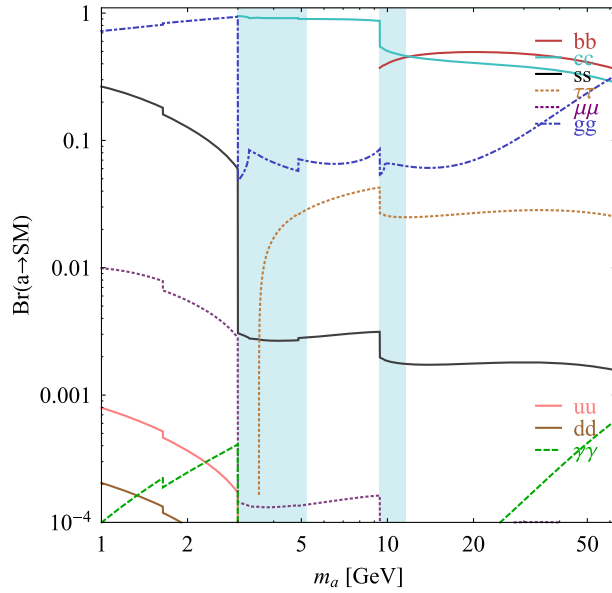
 $\tan \beta=5$, TYPE II


FIG. 7 (color online). Branching ratios of a singletlike pseudoscalar in the 2HDM + S for type-II Yukawa couplings. Decays to quarkonia likely invalidate our simple calculations in the shaded regions.

muon, and electron thresholds, the pseudoscalar decays dominantly to muons, electrons, and photons, respectively, except for $\tan \beta < 1$ in type II, III and $\tan \beta > 1$ in type IV, where the suppressed lepton couplings can also cause decays to photons to dominate below the pion threshold. If the pseudoscalar couples to both quarks and leptons, then requiring its mixing angle to be small enough to not conflict with constraints from, e.g., meson decays and the muon anomalous magnetic moment implies that any allowed

decay to two muons (for $2m_\mu < m_a < 3m_\pi$) is likely to have at least a displaced vertex (or be detector stable), while any allowed decay to two electrons (for $2m_e < m_a < 2m_\mu$) will be detector stable [125]. For pseudoscalars that couple preferentially to leptons, the meson-decay constraints are absent and prompt decays to muons are allowed; however, allowed decays to electrons will likely have at least a displaced vertex and need to be detector stable as m_a is decreased well below the muon threshold [125].

 $\tan \beta=0.5$, TYPE III

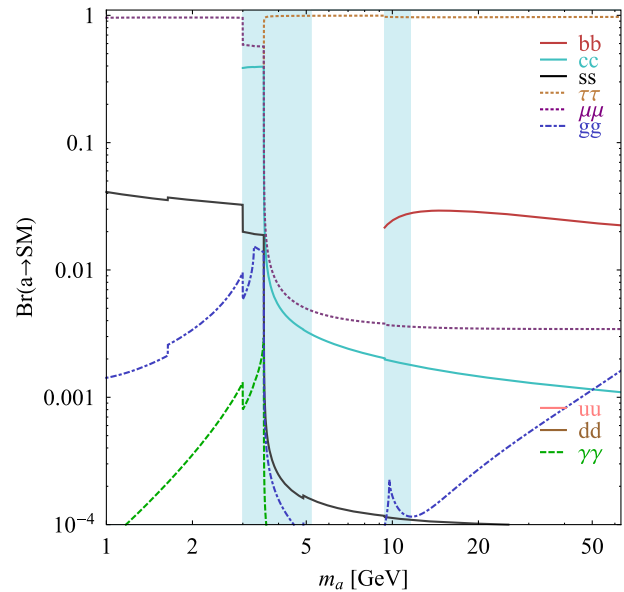
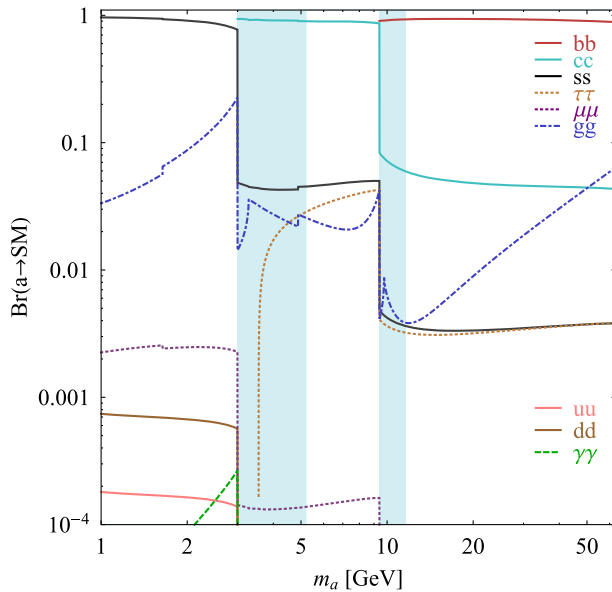
 $\tan \beta=5$, TYPE III


FIG. 8 (color online). Branching ratios of a singletlike pseudoscalar in the 2HDM + S for type-III Yukawa couplings. Decays to quarkonia likely invalidate our simple calculations in the shaded regions.

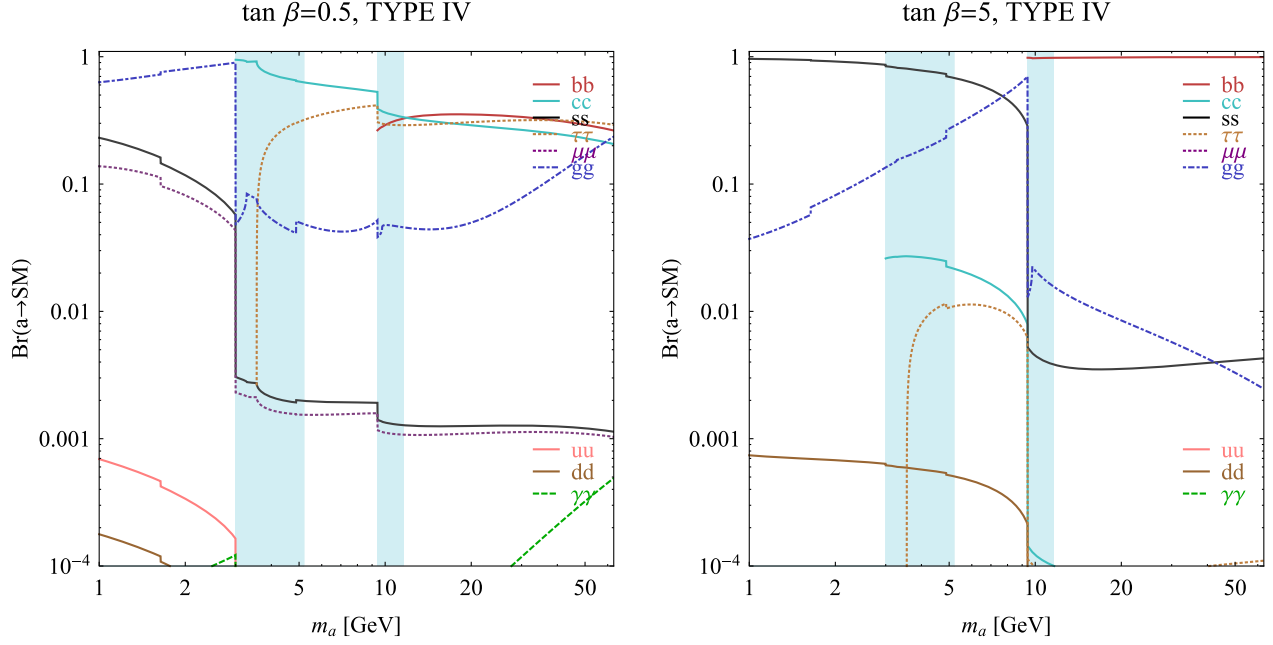


FIG. 9 (color online). Branching ratios of a singletlike pseudoscalar in the 2HDM + S for type-IV Yukawa couplings. Decays to quarkonia likely invalidate our simple calculations in the shaded regions.

Light scalar (s).—We now assume that the mass of the real singlet S_R is below $m_h/2$. The scalar Higgs spectrum, Eq. (13), gets extended by the additional real singlet, which mixes with the doublet sector

$$\begin{pmatrix} h \\ H^0 \\ s \end{pmatrix} = \begin{pmatrix} 1 & 0 & 0 \\ 0 & \cos \zeta_2 & \sin \zeta_2 \\ 0 & -\sin \zeta_2 & \cos \zeta_2 \end{pmatrix} \begin{pmatrix} \cos \zeta_1 & 0 & \sin \zeta_1 \\ 0 & 1 & 0 \\ -\sin \zeta_1 & 0 & \cos \zeta_1 \end{pmatrix} \begin{pmatrix} -\sin \alpha & \cos \alpha & 0 \\ \cos \alpha & \sin \alpha & 0 \\ 0 & 0 & 1 \end{pmatrix} \begin{pmatrix} H_{1,R}^0 \\ H_{2,R}^0 \\ S_R \end{pmatrix}.$$

If we assume that the mixing angles $\zeta_{1,2}$ are small, this simplifies to

$$\begin{pmatrix} h \\ H^0 \\ s \end{pmatrix} = \begin{pmatrix} -\sin \alpha & \cos \alpha & \zeta_1 \\ \cos \alpha & \sin \alpha & \zeta_2 \\ (-\zeta_2 \cos \alpha + \zeta_1 \sin \alpha) & (-\zeta_1 \cos \alpha - \zeta_2 \sin \alpha) & 1 \end{pmatrix} \begin{pmatrix} H_{1,R}^0 \\ H_{2,R}^0 \\ S_R \end{pmatrix}. \quad (22)$$

In this approximation, h and H have the same Yukawa couplings as in the regular 2HDM but now contain a small S_R component that allows the decay $h \rightarrow ss$. The mostly singlet state s on the other hand mixes with some admixture of $H_{1,R}^0$ and $H_{2,R}^0$. This can be expressed in more familiar notation by adopting the following parameterization for the small singlet-doublet mixing angles:

$$\zeta_1 = -\zeta \cos(\alpha - \alpha'), \quad \zeta_2 = -\zeta \sin(\alpha - \alpha'), \quad (23)$$

$$\Rightarrow \begin{pmatrix} h \\ H^0 \\ s \end{pmatrix} = \begin{pmatrix} -\sin \alpha & \cos \alpha & -\zeta \cos(\alpha - \alpha') \\ \cos \alpha & \sin \alpha & -\zeta \sin(\alpha - \alpha') \\ -\zeta \sin \alpha' & \zeta \cos \alpha' & 1 \end{pmatrix} \begin{pmatrix} H_{1,R}^0 \\ H_{2,R}^0 \\ S_R \end{pmatrix}. \quad (24)$$

The *arbitrary* angle α' determines the $H_{1R,2R}^0$ admixture contained within s , while the *small* mixing parameter ζ gives its overall normalization. The couplings of s to SM fields are now identical to those of the SM-like Higgs h in

Table II, scaled down by ζ and with the replacement $\alpha \rightarrow \alpha'$. Since α and α' can be independently chosen, s can have an even broader range of branching fractions than a and mirrors the range of possible h decays in the regular

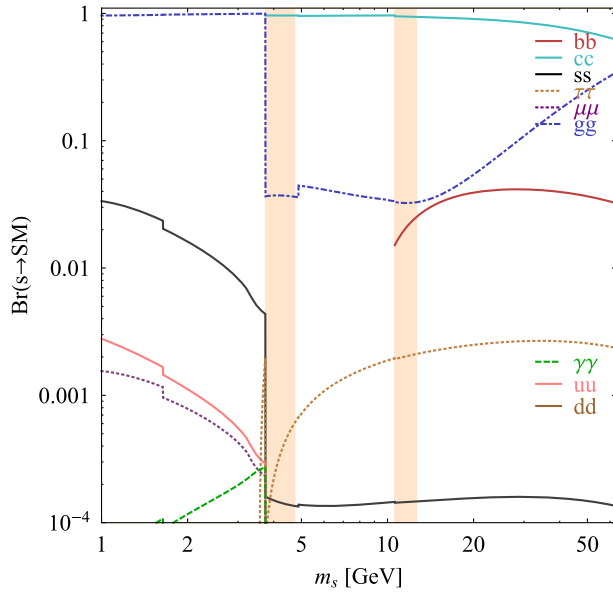
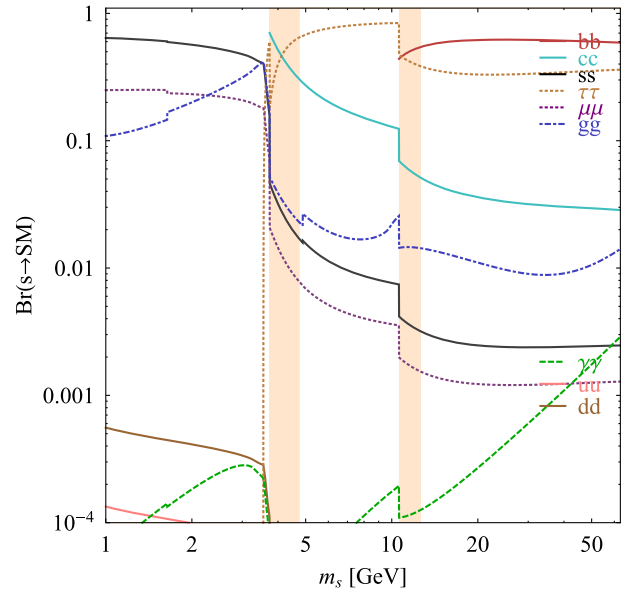
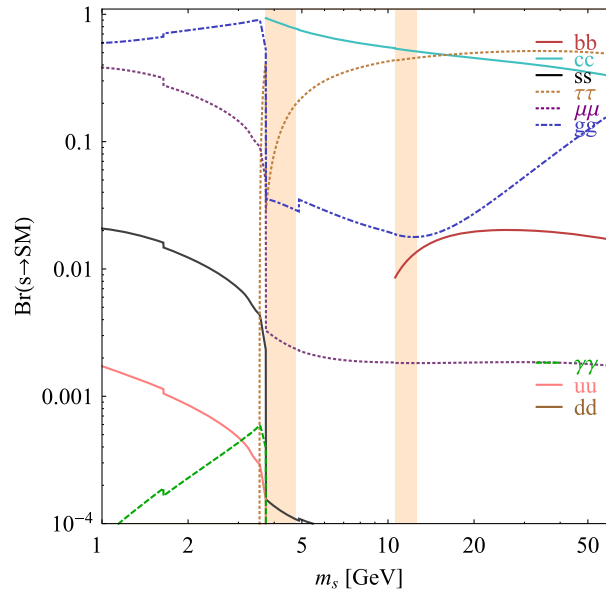
$\alpha = 0.1, \tan \beta = 0.5, \text{TYPE II}$

 $\alpha = -1.4, \tan \beta = 0.5, \text{TYPE III}$

 $\alpha = 0.1, \tan \beta = 0.5, \text{TYPE IV}$


FIG. 10 (color online). Singlet scalar branching ratios in the 2HDM + S for different $\tan \beta, \alpha'$ and Yukawa coupling type. These examples illustrate the possible qualitative differences to the pseudoscalar case, such as dominance of $s \rightarrow c\bar{c}$ decay above $b\bar{b}$ threshold; democratic decay to $b\bar{b}$ and $\tau^+\tau^-$; and democratic decay to $c\bar{c}$ and $\tau^+\tau^-$. Hadronization effects likely invalidate our simple calculations in the shaded regions.

2HDM, but without a mass restriction beyond $m_s < m_h/2$. Just as for h , choosing $\alpha' \rightarrow \frac{\pi}{2} - \beta$ amounts to giving s fermion couplings that are SM-Higgs-like (up to the overall mixing factor ζ). In this limit, the 2HDM + S theory reduces to the SM + S case discussed in Sec. IC 1. On the other hand, choosing $\alpha' = \beta$ gives the same couplings as the pseudoscalar case.

The $s \rightarrow X\bar{X}$ branching ratios are computed analogously to the pseudoscalar case, with further details again given in

Appendix A. There is a large range of possible decay phenomenologies. Figure 10 illustrates some examples that have qualitatively new features compared to the pseudoscalar case, namely the possible dominance of $s \rightarrow c\bar{c}$ decays above the $b\bar{b}$ threshold; similar decay rates to $b\bar{b}$ and $\tau^+\tau^-$; and similar decay rates to $c\bar{c}$ and $\tau^+\tau^-$.

Summary.—The 2HDM + S allows for a large variety of Higgs decay phenomenologies $h \rightarrow aa \rightarrow X\bar{X}Y\bar{Y}$,

$h \rightarrow ss \rightarrow X\bar{X}Y\bar{Y}$, and $h \rightarrow aZ \rightarrow X\bar{X}Y\bar{Y}$ by coupling the SM-like Higgs h to a singletlike scalar s or pseudoscalar a . While the singlet's couplings within each fermion “family” (down-type quarks, up-type quarks, or leptons) are ranked by their Yukawa couplings, the relative coupling strength to each family can be adjusted, and arbitrarily so in the scalar case.

A simple illustration of the rich decay phenomenology is to consider, for example, the dominant decay mode(s) above the $b\bar{b}$ threshold. With the three largest Yukawa couplings in each family being to the bottom, charm, or tau, we demonstrated every possible combination of dominant decays: similar decays widths to $b\bar{b}$, $c\bar{c}$, and $\tau^+\tau^-$, dominant decay widths to any two out of those three, or just one dominant mode. This motivates searches for a large variety of nonstandard four-body final states of exotic Higgs decays.

In Sec. IC 5, we motivate additional four-body Higgs decay channels, ranked by gauge coupling instead of Yukawa coupling. We will see that even decays to $\mu^+\mu^-$ and e^+e^- can dominate above the $b\bar{b}$ threshold.

3. SM + fermion

We here discuss exotic Higgs decays that can arise by the addition of a light fermion to the SM. We focus on two possibilities, *neutrino portal-mediated* and *Higgs portal-mediated* Higgs decays.

The leading interaction of a single Majorana fermion χ with the SM fields is given by the renormalizable but lepton-number-violating “neutrino portal” operator:

$$\mathcal{L}_N = y\chi HL. \quad (25)$$

If this lepton-number-violating coupling is forbidden, the leading coupling between χ and the SM is through the dimension-five Higgs portal operator⁷

$$\mathcal{L}_{\chi H} = \frac{\kappa}{2M}(\chi\chi + \chi^\dagger\chi^\dagger)|H|^2. \quad (26)$$

This kind of coupling occurs, for instance, in the MSSM when all BSM degrees of freedom except a binolike neutralino are integrated out at a high scale. In the MSSM, the states integrated out to generate this operator are fermionic, with electroweak quantum numbers. In UV completions where the state being integrated out is bosonic, the operator of Eq. (26) has effective coupling $\frac{\mu}{2M^2}$, where μ is some hidden sector mass scale. This is a consequence of chiral symmetry, and, as we frequently may have $\mu \ll M$, may result in the Higgs portal interaction becoming effective dimension six. As an example of this kind of

⁷The dipole operator $\chi^\dagger \sigma^{\mu\nu} \chi F_{\mu\nu}$ is also dimension five but vanishes for a Majorana χ .

UV completion, consider a simple hidden sector consisting of a singlet scalar S together with the fermion χ ,

$$\mathcal{L} = (cS + m_0)(\chi\chi + \chi^\dagger\chi^\dagger) + V(S) + \zeta S^2|H|^2, \quad (27)$$

and let $V(S)$ allow S to develop a vacuum expectation value, $\langle S \rangle \equiv \mu$.⁸ Then integrating out the excitations of S around this $\langle S \rangle$, with mass m_s , we obtain the operator

$$\mathcal{L}_{\chi H} = \frac{c\zeta\mu}{m_s^2}(\chi\chi + \chi^\dagger\chi^\dagger)|H|^2. \quad (28)$$

The mass of the fermion is $m_\chi = m_0 + c\mu$, so either there are large cancellations or $c\mu \sim m_0 \sim m_\chi \ll m_s$, and the operator is effective dimension six.

Neutrino portal-mediated Higgs decays.—We first consider exotic Higgs decays mediated by the neutrino portal operator, Eq. (25). The renormalizable neutrino portal coupling occurs in the so-called ν SM, the minimal model that can give mass to the SM neutrinos. Here the SM is extended by sterile neutrinos, allowing the SM neutrinos to get a mass from a seesaw-type mechanism triggered by a Majorana mass term $(M/2)\chi\chi$. The operator of Eq. (25) mixes the sterile neutrino χ with the active SM neutrino ν arising from the $SU(2)$ doublet L . In the absence of large cancellations in the neutrino mass matrix, sterile neutrinos must be extremely heavy, $M \gg v$, or extremely decoupled, $y \ll y_e \ll 1$. In this limit, the decay $h \rightarrow \nu\chi$ is negligible, even if kinematically allowed. However, the authors of [55,126] show that active-sterile mixing angles as large as several percent are possible, with (accidental) cancellations among the Yukawa couplings still allowing for small active neutrino masses. Mixing angles of the order of a few percent may imply a sizable partial width for $h \rightarrow \nu\chi$:

$$\Gamma(h \rightarrow \nu\chi) = \frac{|y|^2}{8\pi} m_h \left(1 - \frac{m_\chi^2}{m_h^2}\right)^{3/2}, \quad (29)$$

where m_χ is the mass of the sterile neutrino χ . For $m_h < 130$ GeV, neutrino data and pion decay constraints on W -lepton coupling universality still allow the partial width into $h \rightarrow \nu\chi$ to exceed that into $h \rightarrow b\bar{b}$; see [55] for a detailed discussion (see also [58]).

The mass mixing between sterile [right-handed (RH)] neutrinos and active [left-handed (LH)] neutrinos introduces couplings of the RH neutrinos to W and Z gauge

⁸For simplicity, we do not consider the possible interaction $S|H|^2$. This operator could be forbidden in the presence of a global symmetry taking $S \rightarrow -S$, $\chi \rightarrow i\chi$, which would also forbid the mass term $m_0(\chi\chi + \chi^\dagger\chi^\dagger)$.

bosons. Therefore, in the region of parameter space for which the active-sterile mixing angle Θ is close to its phenomenological upper bound, the RH neutrinos decay promptly into $\chi \rightarrow \ell W^* \rightarrow \ell f f'$ and $\chi \rightarrow \nu Z^* \rightarrow \nu f f'$, where f and f' are either a lepton or a quark of the SM, and with all branching ratios fixed by the electroweak quantum numbers of the SM fermions. In general χ may have nonzero mixings with one, two, or all three SM neutrinos.

Higgs portal-mediated Higgs decays.—We next turn to the higher-dimension decays, mediated by the higher-dimension operator of Eq. (26). After electroweak symmetry breaking, this operator yields a coupling $\lambda h(\chi\chi + \chi^\dagger\chi^\dagger)$, with effective Yukawa coupling given by $\lambda = \kappa v/2M$. The resulting partial width into χ is then

$$\Gamma(h \rightarrow \chi\chi) = \frac{m_h}{8\pi} \left(\frac{\kappa v}{M}\right)^2 \left(1 - \frac{4m_\chi^2}{m_h^2}\right)^{3/2}. \quad (30)$$

As the effective Yukawa coupling λ is only competing with the small b -quark Yukawa, substantial branching fractions $\text{Br}(h \rightarrow \chi\chi)$ can be obtained even for Higgs portal scales M significantly above a TeV, as shown in Fig. 11, where we fix $\kappa = 1$ for simplicity.

The kinds of signatures that are realized depends on how χ decays. If the Higgs portal coupling of Eq. (26) is the only interaction that the new fermion χ possesses, then χ is absolutely stable, and the resulting Higgs decay is invisible. In general, however, χ will possess additional interactions. If these interactions preserve the \mathbb{Z}_2 symmetry taking $\chi \rightarrow -\chi$, then χ will remain stable. On the other hand, if the \mathbb{Z}_2 is violated by a dimension-six operator of the form

$$\mathcal{L}_f = \frac{1}{\Lambda^2} \chi f_1 f_2 f_3, \quad (31)$$

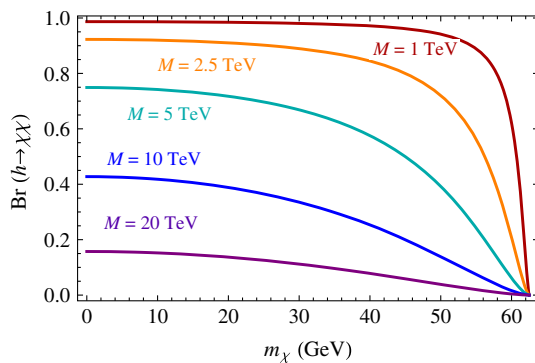


FIG. 11 (color online). Higgs branching fraction into Majorana fermions χ resulting from the partial width of Eq. (30), as a function of the Higgs portal scale M and the mass of the fermion m_χ . We fix the coupling κ to be equal to 1.

where $f_1 f_2 f_3$ is a gauge-invariant combination of quarks and leptons, then χ will undergo the three-body decay $\chi \rightarrow f_1 f_2 f_3$. Some of these decays are familiar from previous study of R -parity-violating neutralino decays in the MSSM, namely those involving holomorphic combinations of SM fermion fields (we suppress spinor structures for simplicity):

$$\lambda_{ijk} L_i L_j e_k^c, \quad \lambda'_{ijk} L_i Q_j d_k^c, \quad \lambda''_{ijk} u_i^c d_j^c d_k^c. \quad (32)$$

One may also consider the nonholomorphic operators [127]

$$\kappa_{ijk} Q_i Q_j d_k^{c\dagger}, \quad \kappa'_{ijk} L_i^\dagger Q_j u_k^c, \quad \kappa''_{ijk} u_i d_j^{c\dagger} e_k^c. \quad (33)$$

Another flavor-violating possibility appearing at dimension six is the radiative decay $\chi \rightarrow \gamma\nu$, mediated by

$$\mathcal{O}_{\gamma\nu} = \chi H L_i \sigma^{\mu\nu} B_{\mu\nu}. \quad (34)$$

While this operator can yield two-body final states, it naturally scales with a loop factor. All of these lepton and/or baryon-number-violating decays necessarily have non-trivial flavor structure, and the combinations of operators that appear depends on the flavor structure of the UV theory. Unlike the SM plus scalar interactions considered in Secs. IC 1 and IC 2 or the neutrino-portal decays discussed earlier, the possible decays of χ are not determined by the Higgs coupling to the fermion but require additional interactions, involving the flavor structure of the theory.

To summarize, the exotic Higgs signatures from a single additional (Majorana) fermion species are then Higgs decays to either invisible particles, or to one or more four- or six-body final states, where the six bodies form two three-body resonances of equal mass. When neutrinos are among the final-state partons, the final states will include missing energy, and the resonances will not be reconstructable. This is always the case in the possible four-body final states where neutrinos are always involved and is sometimes the case in the six-body final states.

4. SM + 2 fermions

It is worth generalizing the previous discussion to the case with two new singlet fermions χ_1 and χ_2 . The Majorana mass matrix for these two fermions has three parameters, and the dimension-five Higgs portal operators form a matrix

$$\mathcal{L}_\chi = \frac{c_{ij}}{\Lambda} \chi_i \chi_j |H|^2. \quad (35)$$

After electroweak symmetry breaking, the BSM fermions form two mass eigenstates χ_1 and χ_2 , with mass $m_2 > m_1$. If we take relatively light fermions $m_h > 2m_2$, the decays

$h \rightarrow \chi_2\chi_2$, $h \rightarrow \chi_1\chi_2$ and $h \rightarrow \chi_1\chi_1$ are all possible. This kind of interaction appears in, for instance, the NMSSM (see Sec. IC 8.), where χ_2 and χ_1 are mostly bino- and singlinolike, respectively, and the higher-dimension Higgs portal coupling of Eq. (35) results after integrating out the charged Higgsinos. It can also arise in (possibly supersymmetric) hidden valleys; see Sec. IC 10.

Let us first consider the case where there is a \mathbb{Z}_2 symmetry which takes $\chi_i \rightarrow -\chi_i$. In this case, χ_1 is stable, but the heavier new state decays as $\chi_2 \rightarrow \chi_1 + X$. If the Higgs portal coupling of Eq. (35) is the only coupling of the χ_i , then the decay will proceed through an off-shell Higgs, $\chi_2 \rightarrow h^*\chi_1 \rightarrow (f\bar{f}, g\bar{g}, \gamma\gamma)\chi_1$. In this case, branching fractions into different SM partons will be determined by the Higgs couplings and will typically result in Higgs decays to E_T plus one or two nonresonant quark-antiquark, lepton-antilepton, or gluon pairs, depending on the available phase space.

If the χ_i have additional interactions besides their coupling to the Higgs, such as a dipole coupling to the hypercharge field strength,

$$\mathcal{L}_\chi = \frac{1}{\mu}\chi_1^\dagger\sigma_{\mu\nu}\chi_2 B^{\mu\nu}, \quad (36)$$

or a coupling to the Z boson induced by mixing with states transforming under $SU(2)_L$,

$$\mathcal{L}_\chi = h_{ij}\chi_i^\dagger\sigma^\mu\chi_j Z_\mu, \quad (37)$$

then other decay patterns are possible. The dipole operator allows the decays $\chi_2 \rightarrow \gamma\chi_1$, as well as $\chi_2 \rightarrow \chi_1 Z$ if $m_2 - m_1 > m_Z$ (phase space suppression renders decays through an off-shell Z largely irrelevant when $m_2 - m_1 < m_Z$). The operator of Eq. (37) also yields $\chi_2 \rightarrow \chi_1 Z$ when phase space allows, or if $m_2 - m_1 < m_Z$, will mediate the three-body decays $\chi_2 \rightarrow f\bar{f}\chi_1$ with branching ratios set by the Z branching fractions.

Note that a common feature of all these decays is that the pairs of SM partons have a kinematic end point at $m_{f\bar{f},g\bar{g},\gamma\gamma} < m_2 - m_1$, and that the transverse mass of the visible partons and the E_T is bounded from above.

The Z boson coupling can arise in NMSSM-like models (see, e.g., Sec. IC 7) or in models with additional RH neutrinos [56,57] that mix with the SM neutrinos. In the latter case, the couplings h_{ij} in (37) are sufficiently small that the neutrino decay lengths are macroscopic. In the former case, the couplings can instead be larger, and the Majorana fermions can have a prompt decay into SM fermions. Additional examples are models with a fourth generation of fermions where the two fourth-generation neutrinos do not mix with the SM neutrinos [128–130]. In these models, the mass range $M_1 \gtrsim 30$ GeV, $M_2 - M_1 \lesssim 20$ GeV is allowed by LEP measurements of the Z width

and LEP bounds on $e^+e^- \rightarrow \chi_1\chi_2, \chi_2\chi_2$ [128]. In this region of parameter space, $h \rightarrow \chi_2\chi_2$, as well as $h \rightarrow \chi_1\chi_1$, can have a sizable branching ratio [129]. Furthermore, the heavier neutrino χ_2 can decay promptly via $\chi_2 \rightarrow Z^*\chi_1$, while the lighter neutrino χ_1 is long lived.

If the \mathbb{Z}_2 parity is violated, allowing χ_1 to decay, Higgs decays to as many as ten partons may result. We will not consider such complex decays in this work, but one should bear in mind that they can occur.

Many models with new fermion species also contain new bosonic degrees of freedom, which, if light, open new possibilities for the decays of the χ_i . We will see examples of this in Sec. IC 8.

5. SM + vector

Preliminaries.—An additional $U(1)_D$ gauge symmetry added to the SM is theoretically well motivated and occurs in many top-down and bottom-up extensions of the SM. The $U(1)_D$ vector boson (the “dark photon” or the “dark Z ”) is usually referred to as A' , Z' , γ_D , or Z_D in the literature and various possibilities exist to connect the additional $U(1)_D$ to the SM (see, e.g., [131–134] for reviews). In Sec. IC 10, we will discuss more complicated hidden-valley phenomenology, involving non-Abelian gauge symmetries and/or composite states [32,135]. Here we focus on Higgs decays that involve an A' , with the A' mass between \sim MeV and 63 GeV. A sub-GeV A' has generated a lot of interest in the last few years due to anomalies related to dark matter [136–139] and as an explanation of the discrepancy between the calculated and measured muon anomalous magnetic moment [140].

The $U(1)_D$ can couple to the SM sector via a small gauge kinetic mixing term $\frac{1}{2}\epsilon F'_{\mu\nu}B^{\mu\nu}$ [141–143] between the dark photon and the hypercharge gauge boson. This renormalizable interaction can be generated at a high scale in a grand unified theory or in the context of string theory with a wide range of $\epsilon \sim 10^{-17}$ – 10^{-2} [141,144–151]. This term effectively gives SM matter a dark millicharge, made more obvious by a $GL(2, R)$ field redefinition $B_\mu \rightarrow B_\mu - \epsilon A'_\mu$ which yields canonical kinetic terms, and allows for dark photon decay to SM particles and possible experimental detection. To avoid the tight constraints on new long-range forces, a “dark Higgs” S with a nonzero vacuum expectation value can give a nonzero mass to the A' . An A' with a sub-GeV mass can be probed at beam dumps and colliders, and with measurements of the muon anomalous magnetic moment, supernova cooling, and rare meson decays [140,151–166]; see Fig. 12 and, e.g., [134] for a recent review.

A broken $U(1)_D$ can also lead to exotic Higgs decays, especially if there is mixing between the two Higgs sectors. In this context we refer to the corresponding vector field as Z_D .

The possibility of $h \rightarrow Z_D Z_D$ through Higgs-to-dark-Higgs mixing or $h \rightarrow ZZ_D$ through Z - Z_D mass mixing (which is also induced by the above-mentioned kinetic mixing) was discussed in [177] and [165,166], respectively, with both occurring, for example, in hidden-valley models [32,135].

To examine the range of possible exotic Higgs phenomena due to a $U(1)_D$ sector we examine the model of [177], but with m_h set to 125 GeV and allowing for the full range of dark-Higgs and dark- Z masses relevant to exotic Higgs decay phenomenology.⁹ This includes Higgs-to-dark-Higgs mixing and kinetic mixing between the B boson and the dark vector Z_D , but no explicit mass mixing between the Z and Z_D .¹⁰ We will assume prompt Z_D decays, which requires $m_{Z_D} \gtrsim 10$ MeV given the current constraints shown in Fig. 12.

For $m_{Z_D} > 10$ GeV, the most stringent constraints come from precision electroweak measurements; we have verified the results in [167]. These constraints are largely driven by the tree-level shift to the Z mass¹¹ and limit $\epsilon \lesssim 0.02$ for $m_{Z_D} < m_h/2$.

Also shown in Fig. 12 is a new constraint we derived by recasting the CMS $20 + 5 \text{ fb}^{-1} h \rightarrow ZZ^*$ analysis [175], as described in Sec. X. (We obtain a similar bound from the corresponding ATLAS analysis [176].) This new bound is already almost competitive with the electroweak precision measurement bounds (green region labeled EWPM) for some masses and can be optimized further with a dedicated search. We expect LHC14 with 300 fb^{-1} to be sensitive to $\text{Br}(h \rightarrow ZZ_D)$ as low as $\sim 10^{-4}$ or 10^{-5} . This would make the LHC the best probe of dark vector kinetic mixing for $10 \text{ GeV} \lesssim m_{Z_D} \lesssim m_h/2$ in the foreseeable future.

Model details.—The model is defined by a $U(1)_D$ gauge sector and a SM singlet S that has unit charge under the $U(1)_D$. The kinetic terms of the hypercharge and $U(1)_D$ gauge bosons (adopting mostly the notation of [165]) are

⁹Reference [178] appeared while this work was being completed, performing a similar analysis with a different focus on constraining the couplings of the extended Higgs potential for relatively low $m_{Z_D} < 5$ GeV.

¹⁰The constraints shown in Fig. 12 are altered in the presence of such pure mass mixing, which requires additional Higgs doublets that also carry dark charge. The resulting $Z_D \rightarrow \text{SM}$ decays would be more Z -like and lead to additional constraints from rare meson decays as well as new parity-violating interactions [165]. However, we stress that the exotic Higgs phenomenology would not be qualitatively different.

¹¹Additional and more model-dependent constraints arise when m_{Z_D} is approximately equal to the center-of-mass energy of e^+e^- experiments [167].

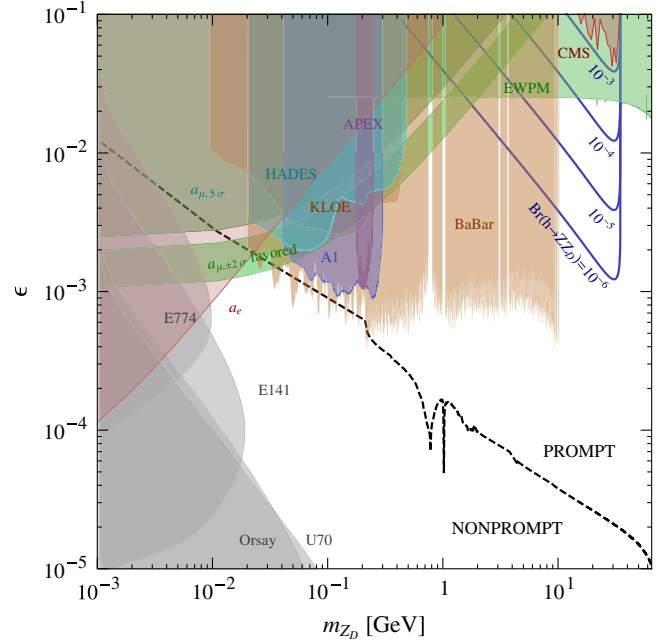


FIG. 12 (color online). Constraints on ϵ, m_{Z_D} for pure kinetic mixing (no additional source of Z - Z_D mass mixing) for $m_{Z_D} \sim \text{MeV}–10 \text{ GeV}$. The black dashed line separates prompt ($c\tau < 1 \mu\text{m}$) from nonprompt Z_D decays. The three blue lines are contours of $\text{Br}(h \rightarrow ZZ_D)$ of 10^{-4} , 10^{-5} , and 10^{-6} , respectively. Shaded regions are existing experimental constraints [140,152–164,167–174]; see, e.g., [134] for a recent review. The red shaded region “CMS” is a new limit we derived by recasting the CMS $20 + 5 \text{ fb}^{-1} h \rightarrow ZZ^*$ analysis [175], as described in Sec. X. (We obtain a similar bound from the corresponding ATLAS analysis [176].) This new bound can be optimized with a dedicated LHC measurement, likely improving upon the electroweak precision measurement bounds (green region labeled “EWPM” [167]) for some masses.

$$\mathcal{L}_{\text{gauge}} = -\frac{1}{4} \hat{B}_{\mu\nu} \hat{B}^{\mu\nu} - \frac{1}{4} \hat{Z}_{D\mu\nu} \hat{Z}_D^{\mu\nu} + \frac{1}{2} \frac{\epsilon}{\cos \theta_W} \hat{B}_{\mu\nu} \hat{Z}_D^{\mu\nu}, \quad (38)$$

with $\hat{B}_{\mu\nu} = \partial_\mu \hat{B}_\nu - \partial_\nu \hat{B}_\mu$, $\hat{Z}_{D\mu\nu} = \partial_\mu \hat{Z}_{D\nu} - \partial_\nu \hat{Z}_{D\mu}$, and $\cos \theta_W = g/\sqrt{g^2 + g'^2}$ is the usual Weinberg mixing angle. The hatted quantities are fields before diagonalizing the kinetic term. The Higgs potential is

$$V_0 = -\mu^2 |H|^2 + \lambda |H|^4 - \mu_D^2 |S|^2 + \lambda_D |S|^4 + \zeta |S|^2 |H|^2. \quad (39)$$

The dark Higgs S acquires a vacuum expectation value and gives Z_D , which “eats” the pseudoscalar component of S , some mass m_{Z_D} . There are two connections between the dark and the SM sectors: the gauge kinetic mixing ϵ and the Higgs mixing ζ . The phenomenology depends on which one dominates.

The gauge kinetic term is diagonalized by transforming the gauge fields

$$\begin{pmatrix} Z_D \\ B \end{pmatrix} = \begin{pmatrix} 1 & 0 \\ -\frac{\epsilon}{\cos\theta_W} & 1 \end{pmatrix} \begin{pmatrix} \hat{Z}_D \\ \hat{B} \end{pmatrix}, \quad (40)$$

where we always work to lowest order in the small ϵ . \hat{B} therefore gets replaced by $B + \frac{\epsilon}{\cos\theta_W} Z_D$, giving all SM fermions a dark millicharge proportional to their hypercharge, while particle couplings to \hat{B} remain unchanged when transforming to B .

The Z_D and Z gauge boson mass terms are

$$\mathcal{L}_{\text{mass}} = \frac{1}{8} w^2 g_D^2 (\hat{Z}_{D\mu})^2 + \frac{1}{8} v^2 (-g \hat{W}_\mu^3 + g' \hat{B}_\mu)^2, \quad (41)$$

where g_D is the gauge coupling of $U(1)_D$ and w is the vacuum expectation value of S . Writing in terms of canonically normalized gauge fields this becomes

$$\begin{aligned} \mathcal{L}_{\text{mass}} &= \frac{1}{8} w^2 g_D^2 (Z_{D\mu})^2 \\ &+ \frac{1}{8} v^2 \left(-g W_\mu^3 + g' B_\mu + g' \frac{\epsilon}{\cos\theta_W} Z_{D\mu} \right)^2. \end{aligned} \quad (42)$$

The SM gauge boson $Z_\mu = -\sin\theta_W B_\mu + \cos\theta_W W_\mu^3$ is no longer a mass eigenstate:

$$\mathcal{L}_{\text{mass}} = \frac{1}{2} m_{Z_D}^2 (Z_{D\mu})^2 + \frac{1}{2} m_Z^2 (Z_\mu - \epsilon \tan\theta_W Z_{D\mu})^2. \quad (43)$$

To leading order in ϵ the mass eigenstates with masses $m_Z, m_{Z_D} + \mathcal{O}(\epsilon^2)$ are

$$\begin{aligned} \tilde{Z} &= Z + \epsilon_Z Z_D, \\ \tilde{Z}_D &= Z_D - \epsilon_Z Z, \quad \text{where } \epsilon_Z = \frac{\epsilon \tan\theta_W m_Z^2}{m_Z^2 - m_{Z_D}^2}. \end{aligned} \quad (44)$$

(Henceforth, we omit the tildes and will refer to the mass eigenstates unless otherwise noted.) Therefore, there are interaction terms of the form $2\epsilon_Z \frac{m_{Z_D}^2}{v} h Z_\mu Z_{D\mu}^2$ and $\epsilon_Z^2 \frac{m_{Z_D}^4}{m_Z^2 v} h Z_{D\mu} Z_{D\mu}^2$ which lead to $h \rightarrow Z_D Z$ and $h \rightarrow Z_D Z_D$ decays (though the latter is strongly suppressed); see Fig. 14.

If Z_D is the lightest state in the dark sector, it will decay to SM particles. This is entirely due to the kinetic mixing in Eq. (38), but in the basis of Eq. (44) it is due to the dark millicharge of SM fermions and the accompanying mass mixing with the Z . Explicitly, the coupling of Z_D to SM fermions is

$$\mathcal{L} \supset g_{Z_D f f} Z_D^\mu \bar{f} \gamma_\mu f, \quad (45)$$

where

$$\begin{aligned} g_{Z_D f f} &= -g' \frac{\epsilon}{\cos\theta_W} Y \\ &- \epsilon \tan\theta_W \frac{m_Z^2}{m_Z^2 - m_{Z_D}^2} \frac{1}{\sqrt{g^2 + g'^2}} (g^2 T_3 - g'^2 Y). \end{aligned} \quad (46)$$

The first and second terms come from dark millicharge and Z - Z_D mass mixing, respectively. This coupling is dominantly photon-like, up to deviations $\sim \mathcal{O}(m_{Z_D}^2/m_Z^2)$:

$$\begin{aligned} g_{Z_D f f} &= \epsilon g' \left\{ -(T_3 + Y) \cos\theta_W \left(1 + \frac{m_{Z_D}^2}{m_Z^2} \right) + \frac{Y}{\cos\theta_W} \frac{m_{Z_D}^2}{m_Z^2} \right. \\ &\left. + \mathcal{O}\left(\frac{m_{Z_D}^4}{m_Z^4}\right) \right\}. \end{aligned} \quad (47)$$

For $m_{Z_D} \gtrsim \text{GeV}$ the Z_D branching ratios are easily computed to lowest order and without QCD corrections and are shown in Fig. 13(a). For $m_{Z_D} \lesssim \text{GeV}$, nonperturbative QCD effects are important. They can be computed from the QCD contribution to the imaginary part of the electromagnetic two-point function, which in turn is determined from cross-section measurements of $e^+e^- \rightarrow \text{hadrons}$ [179]. The resulting branching ratios are shown in Fig. 13(b).

The most important qualitative difference to the scalar decays considered in Secs. IC 1 and IC 2 is that branching ratios are ordered by gauge coupling instead of Yukawa coupling, meaning decays to e^+e^- and $\mu^+\mu^-$ remain large above the τ thresholds. Prompt Z_D decay requires $\epsilon \gtrsim 10^{-5} - 10^{-3}$, as indicated in Fig. 12, which summarizes the constraints on Z_D kinetic mixing for our regime of interest.

The Higgs potential is minimized by vacuum expectation values of H^0 and S :

$$H^0 = \frac{1}{\sqrt{2}}(h + v), \quad S = \frac{1}{\sqrt{2}}(s + w), \quad (48)$$

where to leading order in the small Higgs mixing ζ ,

$$\begin{aligned} v &= \frac{\mu}{\sqrt{\lambda}} - \zeta \frac{\mu_D^2}{4\lambda_D \sqrt{\lambda} \mu} \approx 246 \text{ GeV} \\ \text{and } w &= \frac{\mu_D}{\sqrt{\lambda_D}} - \zeta \frac{\mu^2}{4\lambda \sqrt{\lambda_D} \mu_D}. \end{aligned} \quad (49)$$

The mass eigenstates

$$\begin{aligned} \tilde{h} &= h - \epsilon_h s, \\ \tilde{s} &= s + \epsilon_h h, \quad \text{where } \epsilon_h = \zeta \frac{\mu \mu_D}{2\sqrt{\lambda \lambda_D} |\mu^2 - \mu_D^2|}, \end{aligned} \quad (50)$$

have masses

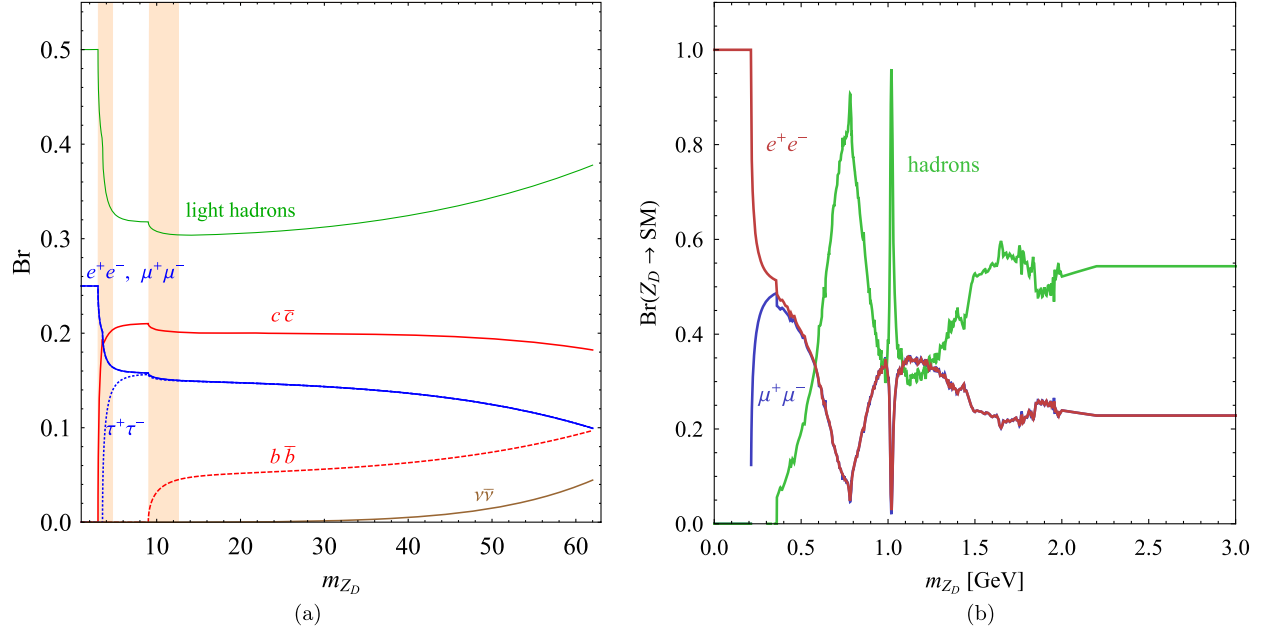


FIG. 13 (color online). (a) Branching ratios for Z_D decay, to lowest order and without QCD corrections, assuming decays to the dark sector are kinematically forbidden. Hadronization effects likely invalidate our simple calculation in the shaded region. (b) Branching ratios for Z_D decay for $m_{Z_D} \lesssim 3$ GeV, including nonperturbative QCD effects.

$$m_h^2 = 2\mu^2 - \zeta \frac{\mu_D^2}{\lambda_D} \quad \text{and} \quad m_s^2 = 2\mu_D^2 - \zeta \frac{\mu^2}{\lambda}. \quad (51)$$

(Again we drop the tildes from now on and always refer to the mass eigenstates.) The effective Lagrangian contains terms of the form $\kappa h s s$, where $\kappa = \zeta(m_h^3 + 2m_h m_s^2) / (\sqrt{16\lambda}(m_h^2 - m_s^2))$, and $2\epsilon_h \frac{m_{Z_D}^2}{w} h Z_D \mu Z_D^\mu$, which lead to exotic Higgs decays $h \rightarrow ss$ and $h \rightarrow Z_D Z_D$; see Fig. 14. The vertex $h s Z_D$ is present but is suppressed by both mixings.

We can now discuss the relevant limits of this theory for exotic Higgs phenomenology.

- (i) *Gauge mixing dominates.*—For $\epsilon \gg \zeta$ the dominant exotic Higgs decay is $h \rightarrow ZZ_D$. To leading order in $m_{Z_D}^2/m_Z^2$ the partial width is

$$\Gamma(h \rightarrow ZZ_D) = \frac{\epsilon^2 \tan^2 \theta_W m_{Z_D}^2 (m_h^2 - m_Z^2)^3}{16\pi m_h^3 m_Z^2 v^2}. \quad (52)$$

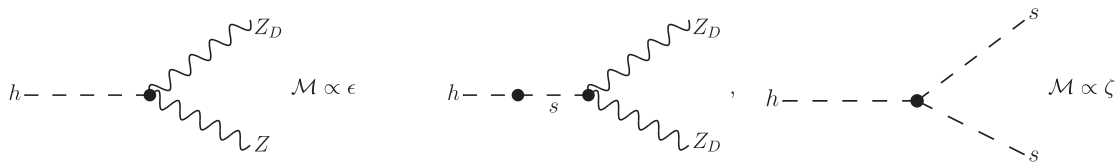


FIG. 14. The dominant exotic Higgs decays in the SM + V model. The $h \rightarrow ZZ_D$ matrix element is proportional to the gauge kinetic mixing ϵ , while $h \rightarrow Z_D Z_D$ and $h \rightarrow ss$ are controlled by the Higgs mixing parameter ζ . The vertex $h s Z_D$ is present but suppressed by both mixings.

This agrees with the full analytical expression to $\sim 10\%$ for $m_h - m_Z - m_{Z_D} > 1$ GeV. Figure 12 shows contours of $\text{Br}(h \rightarrow ZZ_D) = 10^{-4}, 10^{-5}, 10^{-6}$. The largest Br allowed by indirect electroweak precision constraints is $\sim 3 \times 10^{-4}$.

In this regime, the SM + V theory leads to the $f\bar{f} + Z$ exotic Higgs signatures discussed in Sec. X. As outlined above, dedicated LHC searches for this signal at run I and II can improve upon the electroweak precision limit. For very light Z_D above the electron threshold this would also lead to lepton-jets + Z signatures; see Sec. XVI [150].

Note that $\Gamma(h \rightarrow ZZ_D) \propto \epsilon^2$. In addition, the dark vector will also contribute at the same order to the $\Gamma(h \rightarrow Z\ell^+\ell^-)$ partial width (in the nonresonant region) via its interference with Z^* in $h \rightarrow ZZ^* \rightarrow Z\ell^+\ell^-$. Since kinetic mixing shows up in both Z_D production and decay, this will lead to $\mathcal{O}(\epsilon^2)$ deviations in the dilepton spectrum and may represent

a discovery opportunity, particularly for $m_{Z_D} > m_h - m_Z$. We leave this for future investigation.

- (ii) *Higgs mixing dominates.*—When $\zeta \gg \epsilon$ and Higgs mixing dominates then $h \rightarrow Z_D Z_D, ss$ are both

possible, depending on the spectrum of the dark sector. (We still assume that ϵ is large enough for Z_D to decay promptly.) The partial decay widths to leading order in ζ are

$$\begin{aligned}\Gamma(h \rightarrow Z_D Z_D) &= \frac{\zeta^2 v^2}{32\pi m_h} \sqrt{1 - \frac{4m_{Z_D}^2}{m_h^2} \frac{(m_h^2 + 2m_{Z_D}^2)^2 - 8(m_h^2 - m_{Z_D}^2)m_{Z_D}^2}{(m_h^2 - m_s^2)^2}}, \\ \Gamma(h \rightarrow ss) &= \frac{\zeta^2 v^2}{32\pi m_h} \sqrt{1 - \frac{4m_s^2}{m_h^2} \frac{(m_h^2 + 2m_s^2)^2}{(m_h^2 - m_s^2)^2}}.\end{aligned}\quad (53)$$

Different regions of the (m_{Z_D}, m_s) mass plane are shown in Fig. 15, along with the size of the Higgs mixing $\zeta \sim 10^{-3}$ – 10^{-2} required for $\text{Br}(h \rightarrow Z_D Z_D, ss) = 10\%$ and the relative rates of $h \rightarrow ss$ versus $h \rightarrow Z_D Z_D$ decays when both are allowed.

In region A ($m_s > m_h/2, m_{Z_D} < m_h/2$) the only relevant exotic Higgs decay is $h \rightarrow Z_D Z_D$. This allows for spectacular $h \rightarrow 2\ell 2\ell'$ decays ($\ell, \ell' = e$ or μ) with a reconstructed Z_D resonance above the τ or b thresholds.

Region B allows exotic Higgs decays both to $Z_D Z_D$ and ss . The presence of two resonances below half the Higgs mass gives a rich exotic-decay phenomenology. $h \rightarrow ss \rightarrow 4Z_D$ occurs with roughly equal probability as $h \rightarrow Z_D Z_D$ and can result in spectacular final states with as many as eight leptons. Note that, in this simplified model, there is no corresponding $Z_D \rightarrow ss$ decay in the lower right corner of that mass plane. However, a (pseudo)scalar pair could be produced from dark vector decay in, e.g., a 2HDM + V framework, resulting in final states with as many as eight b quarks.

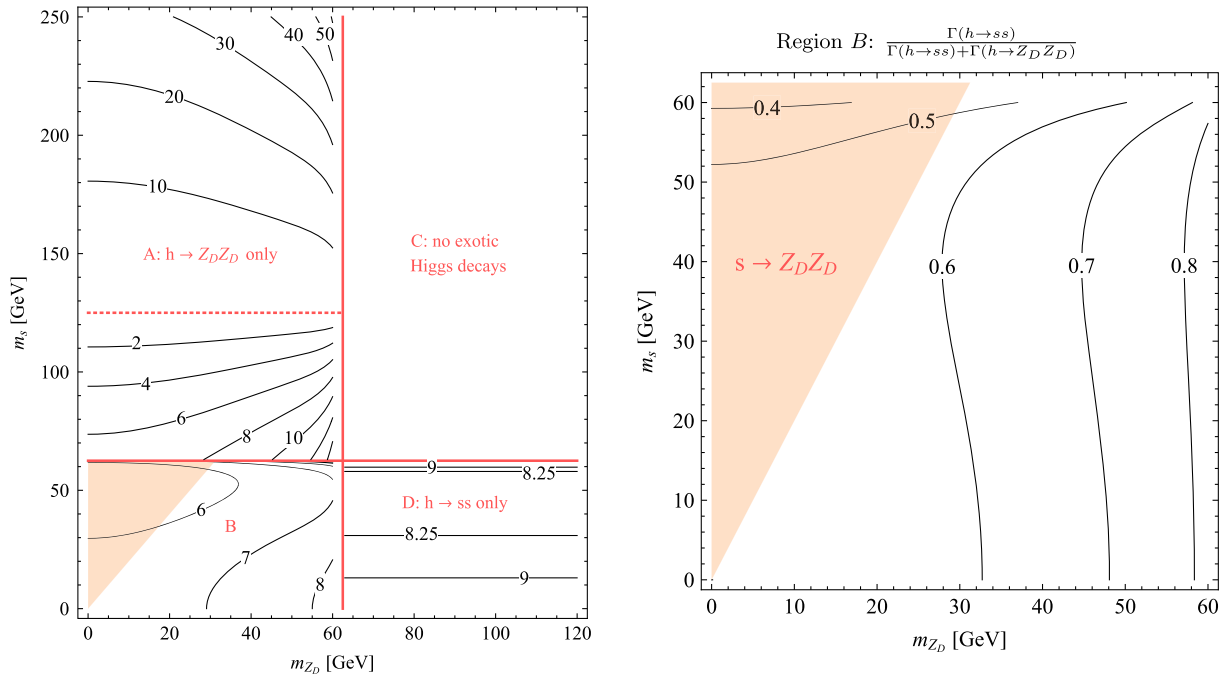


FIG. 15 (color online). Left: Mass plane in the SM + V model with different exotic Higgs decays for $\zeta \gg \epsilon$ (i.e., when the mixing between the Higgs and dark Higgs dominates over the kinetic mixing). The black contours are the values of $\zeta \times 10^3$ required for $\text{Br}(h \rightarrow Z_D Z_D, ss) = 10\%$. Region A is the case examined by [177] (the dotted red line indicates $m_h = m_s$). Region C has no exotic Higgs decays. Region D reproduces the SM + S model of Sec. IC 1. Region B has both $h \rightarrow ss$ and $h \rightarrow Z_D Z_D$ decays, with the $h \rightarrow ss$ fraction of exotic decays shown on the right. In the upper left shaded region, $s \rightarrow Z_D Z_D$ is the dominant decay mode of the dark scalar. This allows the Higgs to decay to up to eight SM fermions.

Already with current data, limits of $\text{Br}(h \rightarrow Z_D Z_D) \lesssim 10^{-4}$ can be achieved; see Sec. XI. Each of the above cases may, for suitable masses, also lead to interesting “lepton-jet” signatures; see Sec. XVI.

- (iii) *Intermediate regime*.—Here the decays induced by kinetic and Higgs mixing are comparable. For example, Fig. 12 shows that $\epsilon \sim 10^{-2}$ is not excluded for some values of m_{Z_D} , allowing $\text{Br}(h \rightarrow ZZ_D) \sim 10^{-4}$. The branching ratios for $h \rightarrow Z_D Z_D$, ss will be similar if $\zeta \sim 10^{-4}$.

Summary.—In summary, the SM + V setup allows for many different kinds of exotic Higgs decays, including $h \rightarrow ZZ_D$, $h \rightarrow Z_D Z_D$, and $h \rightarrow ss$, with $Z_D \rightarrow f\tilde{f}$, and $s \rightarrow f\tilde{f}$ or $s \rightarrow Z_D Z_D \rightarrow (f\tilde{f})(f\tilde{f})$. This leads to final states of $Z + (f\tilde{f})$, $(f\tilde{f})(f\tilde{f})$, and $((f\tilde{f})(f\tilde{f}))((f\tilde{f})(f\tilde{f}))$, where parentheses around a set of particles denotes a resonance (all final-state particles combined will form the Higgs resonance). Since the Z_D (although not the s) couples to the fermions’ gauge charges, final states with several light leptons have sizable branching fractions over the entire kinematically permitted mass range. Certain spectra can produce interesting lepton-jet signatures.

6. MSSM

In this section, we study the possible Higgs exotic decays in the framework of the MSSM with R symmetry.

The Higgs sector of the MSSM has been extensively studied in the light of the recent Higgs discovery. In particular a Higgs at around 125 GeV with SM-like properties can be realized in the decoupling limit where the additional scalars and pseudoscalars are heavy ($m_{a,H,H^\pm} \gtrsim 300$ GeV). In this regime, exotic decays of the type $h \rightarrow A^0 Z$, $h \rightarrow HH$, $h \rightarrow A^0 A^0$, $h \rightarrow H^\pm W$ are kinematically forbidden (here A^0 denotes the CP -odd scalar).¹² In general, the regime $m_A \leq m_h/2$ is highly constrained. This is due to the fact that the masses of the H , A^0 , and H^\pm scalars of the MSSM are closely tied to one another. In particular, at the tree level $m_{H^\pm}^2 = m_A^2 + m_W^2$, leading to a charged Higgs boson already excluded by LEP searches, for $m_A \lesssim 60$ GeV.

Additional Higgs exotic decays could be realized if some of the sparticles are lighter than the Higgs boson. This possibility is however very constrained by LEP and LHC searches. In particular, assuming a LEP bound at around 100 GeV for electrically charged sparticles, the only possible Higgs exotic decays, in the framework of the

¹²SM-like Higgs bosons can also be achieved in a corner of parameter space where the additional scalar and pseudoscalars are lighter than m_h (see, for example, [38,180,181]). Low energy flavor observables like $b \rightarrow s\gamma$, however, set important constraints on this region of parameter space [40,182]. Furthermore, the decays of the SM-like Higgs into lighter scalars are still not kinematically accessible.

MSSM, are to sneutrinos or to neutralinos.¹³ However, in view of the LEP lower bound on the masses of the left-handed sleptons, which are related through $SU(2)$ symmetry to the sneutrino masses, the decay to sneutrinos are generically kinematically closed.

The decay of the Higgs into neutralinos $h \rightarrow \chi_i \chi_j$ [183] is therefore typically the only accessible decay (here, as elsewhere, we suppress the superscript “0” on neutralinos to streamline notation). This decay mode is most easily realized in models with nonuniversal gaugino masses, for which the universality relation $M_1 \sim \frac{M_2}{2} \sim \frac{M_3}{7}$ at the electroweak scale is relaxed, allowing the lightest supersymmetric particle (LSP) to lie below half the higgs mass while still satisfying the LEP and LHC bounds on chargino and gluino masses. As neutralinos which couple to the Higgs boson also typically couple to the Z , the main constraint on Higgs decays to neutralinos comes from the precise LEP measurements of the invisible and total widths of the Z boson, for $m_{\chi_i} + m_{\chi_j} < m_Z$. However, as Fig. 16 shows, for mainly bino LSPs, it is possible to accommodate a sizable branching ratio for the decay $h \rightarrow \chi_1 \chi_1$ while still maintaining compatibility with the LEP Z measurements (see also [184–188] for recent studies). The parameter space for which $h \rightarrow \chi_1 \chi_2$ is open is strongly constrained by both LEP Z measurements (the yellow region in Fig. 16 is the region excluded by the LEP measurement of the Z invisible width) and chargino searches.

In summary, the MSSM generally can now only provide for Higgs decays into neutralinos. These neutralinos may either be detector stable, in which case the Higgs decay is invisible (as discussed in Sec. II), or, in models with gauge-mediated supersymmetry breaking, they may decay within the detector to photon-gravitino pairs [73] (as studied in Sec. XIII). Higgs decays to other sparticles or to other (pseudo)scalars in the extended MSSM Higgs sector are now strongly constrained by the LEP and LHC experiments.

In the following, we will investigate the possible Higgs exotic decays in the framework of the NMSSM. In this model, both the Higgs as well as the neutralino sectors are significantly richer, which provides us with a larger set of possibilities.

7. NMSSM with exotic Higgs decay to scalars

The field content of the NMSSM is very similar to the MSSM; it differs merely by the addition of a singlet superfield S , which is introduced to address the μ problem of the MSSM (for an exhaustive review of the NMSSM see, e.g., [189]). The superpotential and soft supersymmetry-breaking terms of the Higgs sector are given by

¹³Light sbottoms are another possibility, but this is now almost entirely ruled out [45].

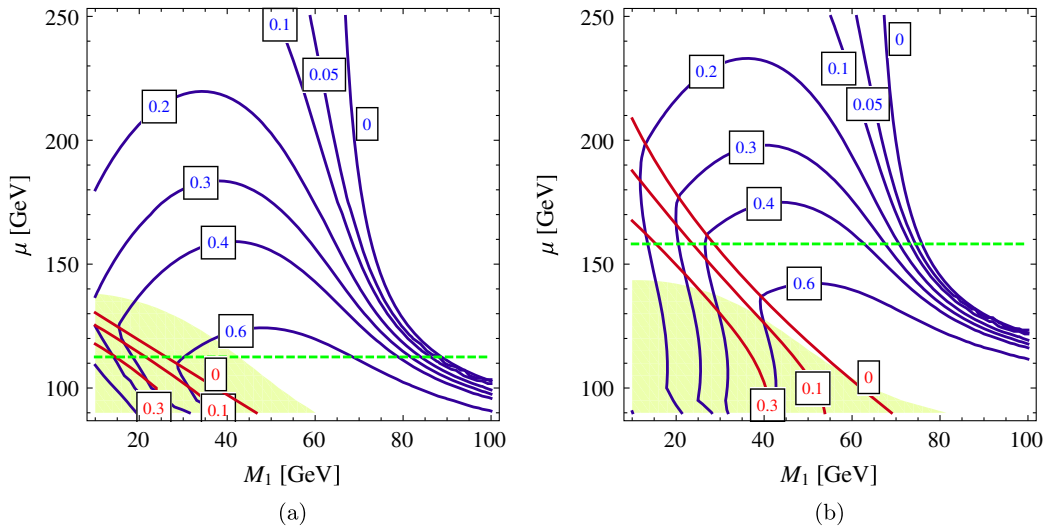


FIG. 16 (color online). Branching ratios of the Higgs into neutralinos: $\text{Br}(h \rightarrow \chi_1 \chi_1)$ and $\text{Br}(h \rightarrow \chi_1 \chi_2)$ are shown in blue and red, respectively. The yellow region is the region excluded by the LEP bound on the Z invisible width. The region below the dashed green line is the region with a lightest chargino below the LEP bound of ~ 100 GeV. The input parameters are $\tan \beta = 10$ and $M_2 = 300$ GeV (a), $M_2 = 150$ GeV (b).

$$W = \lambda S H_u H_d + \frac{\kappa}{3} S^3, \quad (54)$$

$$V_{\text{soft}} = m_{H_d}^2 |H_d|^2 + m_{H_u}^2 |H_u|^2 + m_S^2 |S|^2 + \left(-\lambda A_\lambda H_u H_d S + \frac{1}{3} A_\kappa \kappa S^3 + \text{H.c.} \right). \quad (55)$$

The phenomenology of this model can be easily connected to the simplified models that we have reviewed in previous sections. If we disregard the Higgsinos and singlino (which if heavy are largely irrelevant for Higgs phenomenology), the Higgs sector of the NMSSM is essentially that of a type-II “2HDM + scalar” model (see Sec. IC 2), where we can immediately identify H_d, H_u as H_1, H_2 .

The singlet scalar $S = \frac{1}{\sqrt{2}}(S_R + iS_I)$ can obtain a vacuum expectation value $\langle S \rangle = v_s$, generating an effective μ parameter $\mu_{\text{eff}} = \lambda v_s$. The presence of additional light singlet scalars, pseudoscalars, and fermions allows for exotic Higgs decays within the NMSSM. In this section we discuss decays to light CP -even scalars s or pseudoscalars a of the form

$$h \rightarrow ss, \quad h \rightarrow aa, \quad h \rightarrow aZ. \quad (56)$$

Decays to fermions are covered in the next section, Sec. IC 8.

There are three ways of realizing the above decays within the NMSSM. In each case, the exotic Higgs decay phenomenology is a subset of the type-II 2HDM + S discussed in Sec. IC 2, with some additional restrictions (like $-\pi/2 < \alpha < 0$).

The first is an accidental cancellation resulting in a light singletlike s or a . Recent examples of such models have been found in a parameter scan [190] [for recent studies on the constraint on $\text{Br}(h \rightarrow ss, aa)$, e.g., see [191]]. By choosing $\lambda, \kappa \sim 0.5$, $|A_\lambda| \lesssim 150$ GeV and $A_\kappa \sim 0$ the lightest pseudoscalar can satisfy $m_a < m_h/2$ for a SM-like Higgs h , with $\text{Br}(h \rightarrow aa)$ or $\text{Br}(h \rightarrow Za) \sim \mathcal{O}(0.1)$. On the other hand, $\lambda, \kappa \sim 0.5$, $A_\lambda \sim 0-200$ GeV and $A_\kappa \sim -500$ GeV can result in a singletlike light Higgs satisfying $m_s < m_h/2$ with $\text{Br}(h \rightarrow ss) \sim \mathcal{O}(0.1)$.

There are also two symmetry limits resulting in light pseudoscalars, namely the R limit and the PQ limit of the NMSSM. The R -symmetry limit is realized for $A_\lambda, A_\kappa \rightarrow 0$ [71,192,193], defined by the scalar field transformations

$$H_u \rightarrow H_u e^{i\varphi_R}, \quad H_d \rightarrow H_d e^{i\varphi_R}, \quad S \rightarrow S e^{i\varphi_R}. \quad (57)$$

This global symmetry is spontaneously broken by the Higgs vacuum expectation values v_u, v_d, v_s , which results in a massless Nambu-Goldstone boson (the R axion) appearing in the spectrum:

$$A_R \propto v \sin 2\beta A + v_s S_I, \quad (58)$$

where

$$A = \cos \beta H_{uI} + \sin \beta H_{dI}, \quad v = \sqrt{v_u^2 + v_d^2}.$$

In most of the parameter space $v_s = \frac{\mu_{\text{eff}}}{\lambda} \gg v \sin 2\beta$, making A_R mostly singletlike. To avoid cosmological constraints on a massless axion and to help stabilize the vacuum, the R symmetry is usually taken to be approximate. This leads to

a light, mostly singletlike pseudo-Goldstone boson and depending on the exact parameters chosen opens up the possibility of $h \rightarrow aa$ for $a = A_R$. Through its A component, a then decays to SM fermions, dominantly $b\bar{b}$ and $\tau^+\tau^-$ above the respective thresholds (see Fig. 7).

For $\kappa, A_\kappa \rightarrow 0$ [107,194–202], there is an approximate PQ symmetry:

$$H_u \rightarrow H_u e^{i\varphi_{PQ}}, \quad H_d \rightarrow H_d e^{i\varphi_{PQ}}, \quad S \rightarrow S e^{-2i\varphi_{PQ}}. \quad (59)$$

The PQ -symmetry limit is also shared by some other singlet extensions of the MSSM, including the nearly MSSM (nMSSM) [203] and the general NMSSM (e.g., see [189]). Analogously to the R limit there is a PQ axion,

$$A_{PQ} \propto v \sin 2\beta A - 2v_s S_I. \quad (60)$$

Exotic Higgs decays to this pseudoscalar, and even the singletlike scalar, are in principle possible. However, for $m_h = 125$ GeV, exotic Higgs decays to (pseudo)scalars are generically not dominant in the PQ limit. Instead, decays to binos and singlinos can dominate. This will be discussed in the next subsection.

8. NMSSM with exotic Higgs decay to fermions

While both the R and the PQ limits lead to a light pseudoscalar as discussed in Sec. IC 7, the PQ limit with $m_h = 125$ GeV typically leads to different exotic Higgs decay phenomenology, in which decays to fermions can be as or more important than decays to scalars [53,54].

When $v_s \gg v_u, v_d$, the dominant tree-level contributions to the masses of the singletlike scalars and singlinlike fermion \tilde{S} are [53,196,204]

$$m_s^2 \sim \kappa v_s (A_\kappa + 4\kappa v_s), \quad m_a^2 \sim -3\kappa v_s A_\kappa, \quad m_{\tilde{S}} \sim 2\kappa v_s. \quad (61)$$

The pseudoscalar a is light in both the R and PQ limits, but in the PQ limit s and \tilde{S} must be light as well. This cannot be realized in the R limit, since vacuum stability for small κ requires $A_\lambda \sim \mu \tan \beta$, strongly breaking R symmetry.

This abundance of possible light singletlike states opens up many different exotic Higgs decays, giving phenomenology that is qualitatively unlike the decays in the R limit. In the R limit, the coupling of the SM-like Higgs to the R -axion eigenstate is $g_{haa} \sim \mathcal{O}(m_h^2/v_s^2) \times v$ [71,192]. The trilinear coupling g_{haa} is equivalent to the mass parameter μ_v of Fig. 3, and as can be seen from that figure, v_s as large as $10m_h$ can still yield a sizable branching fraction $\text{Br}(h \rightarrow aa) \sim 0.1$.

The corresponding couplings in the PQ limit instead scale as [53,54]

$$g_{haa}, g_{hss} \sim \mathcal{O}(\lambda^2 \epsilon' v), \quad (62)$$

where

$$\epsilon' = \left| \frac{A_\lambda}{\mu_{\text{eff}} \tan \beta} - 1 \right| < \frac{m_Z}{\mu_{\text{eff}} \tan \beta} \quad (63)$$

is required by vacuum stability (avoiding a runaway in the S direction). For a given μ_{eff} , small λ corresponds to small singlet-doublet mixing and mostly SM-like Higgs phenomenology. Correspondingly, parameter scans using NMSSMTOOLS [205–208] indicate that $\lambda \lesssim 0.2$ dominates the surviving parameter space in the PQ limit ($\kappa \ll \lambda$) (see Appendix B). It is thus common in the PQ limit to obtain $g_{haa}, g_{hss} \ll v$, suppressing exotic Higgs decays to (pseudo)scalars. However, the PQ limit allows the SM-like Higgs boson to decay into a pair of light neutralinos $h \rightarrow \chi_i \chi_j$ [53,54,209]. The relevant vertex couplings for a singlinolike χ_1 and a binolike χ_2 are [53,54]

$$C_{h\chi_1\chi_2} \sim \mathcal{O}\left(\frac{g_1 v}{v_s}\right), \quad C_{h\chi_1\chi_1} \sim \mathcal{O}\left(\frac{\lambda v}{v_s \tan \beta}\right). \quad (64)$$

For $m_{\chi_2} \lesssim 100$ and $m_{\chi_1} \sim \mathcal{O}(1-10)$ GeV the off-diagonal decay $h \rightarrow \chi_1 \chi_2$ can be kinematically accessible with an $\mathcal{O}(0.1)$ branching fraction. The purely invisible decay $h \rightarrow \chi_1 \chi_1$ is suppressed by a factor of $\sim \lambda/(g_1 \tan \beta)$ relative to the off-diagonal decay, ignoring phase space factors. Meanwhile, Higgs decay to a pair of binolike χ_2 also scales as a single factor of the bino-Higgsino mixing angle, $C_{h\chi_2\chi_2} \sim \mathcal{O}(g_1/\lambda) C_{h\chi_1\chi_2}$, and if $h \rightarrow \chi_2 \chi_2$ is kinematically available, this branching fraction can be important.

For $m_{\chi_2} - m_{\chi_1} > \min\{m_s, m_a\}$, the heavier neutralino can decay via $\chi_2 \rightarrow \chi_1 a$ or $\chi_2 \rightarrow \chi_1 s$ [53,54]. This leads to a plethora of possible $h \rightarrow (xx) + E_T$ or $h \rightarrow (xx)(yy) + E_T$ decays, where x, y are SM partons (most likely b, τ , or light jets; see Sec. IC 2) that reconstruct the singlet boson mass a or s . If $m_{\chi_2} - m_{\chi_1} < \min\{m_s, m_a\}$, the principal decay mode of χ_2 is the three-body decay $\chi_2 \rightarrow (a, s)^* \chi_1 \rightarrow (xx)\chi_1$, while the radiative mode $\chi_2 \rightarrow \chi_1 \gamma$ may become significant, with $\text{Br}(h \rightarrow \chi_1 \chi_1 \gamma)$ as high as $\mathcal{O}(0.1)$. On-shell $\chi_2 \rightarrow \chi_1 Z$ does not occur until $m_{\chi_2} - m_{\chi_1} > m_Z$. Given that we require $m_{\chi_2} - m_{\chi_1} < m_h - 2m_{\chi_1}$, these points are sparse. Figure 17 shows the corresponding exotic-decay topologies. Further discussion can be found in Appendix B, together with some example model points which illustrate the main exotic Higgs decay modes in the PQ -symmetry limit of the NMSSM in Table XXI.

Summary.—The PQ limit of the NMSSM yields semi-invisible exotic Higgs decays into pairs of light neutralinos, most typically $h \rightarrow \chi_2 \chi_1$ or $h \rightarrow \chi_2 \chi_2$, with $\chi_2 \rightarrow \chi_1 a, \chi_1 s$, and $a, s \rightarrow (f\bar{f}, gg, \gamma\gamma)$ [53,54]. This yields final states of the form $(b\bar{b}) + E_T$, $(\tau\tau) + E_T$, $(b\bar{b})(b\bar{b}) + E_T$, $(\tau\tau)(\tau\tau) + E_T$, $(b\bar{b})(\tau\tau) + E_T$, and the rarer but cleaner $\gamma + E_T$, $(2, 4)\mu + E_T$, $(\mu\mu)(b\bar{b}) + E_T$. Depending on the

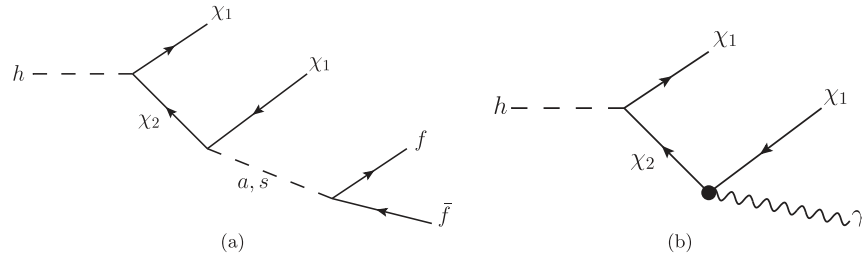


FIG. 17. Two significant fermionic decay topologies of the SM-like Higgs boson in the PQ -symmetry limit. (a) Depending on whether $\min\{m_s, m_a\}$ exceeds $m_{\chi_2} - m_{\chi_1}$, $a(s)$ may or may not be on shell. (b) To be non-negligible, the radiative χ_2 decay requires $\min\{m_s, m_a\} > m_{\chi_2} - m_{\chi_1}$.

spectrum, the visible particles may be collimated or isolated. Current experimental constraints and future prospects for a subset of these decays are discussed in Secs. XII ($\gamma + E_T$), XIII ($2\gamma + E_T$), XVI (collimated $2\ell + X$), XVII (collimated $4\ell + X$), XVIII ($bb + E_T$), and XIX ($\tau\tau + E_T$).

9. Little Higgs

Another class of models with additional potentially light spin-0 fields is Little Higgs [210–212]. In these models, the SM Higgs doublet serves as a pseudo-Nambu-Goldstone boson (PNGB) of multiple approximate global symmetries. Explicit breaking of this set of symmetries is *collective*, namely, apparent only in the presence of at least two terms in the Lagrangian. This ensures that quadratically divergent diagrams contributing to the Higgs mass parameter require two loops, thereby allowing one to push the cutoff scale to $\Lambda \sim (4\pi)^2 v \sim 10$ TeV instead of the usual $4\pi v \sim 1$ TeV.

In order to implement collective symmetry breaking, the electroweak gauge group is extended to a larger global symmetry, which is partially gauged. The partial gauging introduces the explicit breaking, which is crucial for having a nonzero Higgs mass as well as Yukawa couplings. In most Little Higgs models, all the spontaneously broken global generators are explicitly broken by the partial gauging, thereby giving mass to the associated Goldstone bosons. However, in some models, not all global generators are explicitly broken at leading order, either because they are collectively broken like the ones related to the Higgs doublet, or because that would interfere with collective symmetry breaking [65,213]. A consequence of this is the presence of light (pseudo)scalars a with direct couplings to the SM Higgs, which potentially leads to exotic Higgs decays [63,214].

If one imposes MFV [215–218] in order to avoid large flavor-changing neutral currents, the couplings of a to SM fermions are proportional to the SM Yukawas, and thus the coupling to the b quark is typically enhanced.

However, an enhanced decay rate of a to gluons is possible in some cases, as well as an enhanced rate to charm quarks—which arises for models with enhanced up-

Yukawa couplings compared to down-Yukawa. The former possibility results in a “buried Higgs” [219,220] scenario, with the Higgs decaying to four gluon-originated jets, while the latter implies $h \rightarrow 4c$ decays, also known as “charming Higgs” [221] (see also [222] for a more recent jet substructure study), where a may decay to $c\bar{c}$ even if $m_a > 2m_b$. Although the original version of the charming Higgs is excluded by the observed Higgs mass, other versions may exist (and in any case the same final state arises in other models, such as the type-IV 2HDM + scalar models mentioned in Sec. 1C.2.)

As a final comment, note that in models with multiple light particles, cascade decays among these particles, and more complex final states, such as $h \rightarrow a'd' \rightarrow (aaa)(aaa)$, could result.

10. Hidden valleys

In the hidden-valley scenario [32,52,76,135,223,224], a sector of SM-singlet particles, interacting among themselves, is appended to the SM. These are then coupled to the SM through irrelevant operators at the TeV scale, or through marginal operators with weak couplings. An important additional feature of a hidden valley, distinct from a general hidden sector, is that a mass gap (or a symmetry) forbids one or more of the valley particles from decaying entirely to hidden-sector particles; instead, these particles decay to SM particles. Interactions between the SM and hidden valley may also allow the 125 GeV Higgs to decay to valley particles, which in turn decay to SM particles.

The phenomenology of Higgs decays to hidden valleys can sometimes be captured by “simplified” models, including the ones studied earlier in this section, but much more complex patterns of decays may easily arise. This is especially true if hidden valleys have strong and perhaps confining interactions. For instance, if hidden-valley confinement generates hidden “hadrons,” then, just as QCD has a variety of hadrons that decay to nonhadronic final states, often with long lifetimes, and with masses that are spread widely around 1 GeV, the hidden valley may have multiple particles of comparable masses that decay to SM particles, sometimes with very long lifetimes.

More generally, common features that arise in hidden valleys, generally as a result of self-interactions of one sort or another, include the following.

- (i) Multiple types of neutral particles with narrow widths arise, decaying to the SM particles via very weak interactions.
- (ii) Because their decays are mediated by very weak interactions, their lifetimes may be long, though they are sensitive to unknown parameters; decays may occur promptly, at a displaced vertex, or far outside the detector, giving a E_T signal.
- (iii) As they interact so weakly with the SM, they are rarely produced directly; instead, they are dominantly produced in the decays of heavy particles, including the Higgs, neutralinos, etc.
- (iv) When created in the decays of heavy particles, the new particles, if sufficiently light, may commonly be highly boosted.
- (v) Because of their self-interactions, the new particles are often produced in clusters, just as QCD hadrons (and their parent gluons) are produced in the showering and hadronization that forms QCD jets.

Hidden valleys arise in several theoretical contexts. Dark matter may well be from a hidden sector; for instance, the Weakly Interacting Massive Particle “(WIMP) miracle” can apply to particles that are not WIMPs at all [225]. Many of the models that have attempted to explain recent hints of indirect and direct dark matter detection have involved hidden valleys, the most famous being [136,137]. Supersymmetry-breaking models typically have a hidden sector, within which some particles (often just a single spin-one or spin-zero particle) occasionally survive to low energy. And model building that attempts to generate the SM from string theory generally leads to additional non-SM gauge groups under which no SM particles are charged. Hidden valleys have also appeared in certain attempts to address the hierarchy problem (cf. twin Higgs [226], in which the top quark and W loops that correct the Higgs mass are canceled by particles in a hidden valley).

Entry to the hidden valley may occur through a wide variety of “portals”; any neutral particle, or particle-antiparticle pair, may couple to operators made from valley fields, and consequently may itself decay to such particles, and may mediate transitions between SM and valley fields. The Z boson can be a portal; rare Z decays, and rare Z -mediated processes, can be used to put significant bounds on certain types of hidden valleys. However, explicit calculation shows these bounds are not sufficient to rule out the possibility [32,76] that the Higgs itself has decays to a hidden valley that could be discovered in current or future LHC data. This is because of the Higgs’ narrow width, which makes it far more sensitive to very small couplings than is the Z , which is nearly 3 orders of magnitude wider.

Aside from direct limits from Z decays, rare B and other meson decays, and direct production limits, constraints on

hidden valleys can arise from precision tests of the SM. However, these are generally rather weak [32], since the hidden-valley sector is weakly coupled to the SM. Cosmological constraints are sometimes important, but very large classes of models evade them easily [32].

The hidden-valley scenario is relevant for our current purposes because new Higgs decays commonly arise in hidden-valley models. What makes hidden valleys an experimental challenge is that the range of theoretical possibilities is very large. None of the potential motivations—dark matter, supersymmetry breaking, naturalness, or string theory—point us toward any particular type of hidden valley, nor is there a strong reason for it to be minimal. The diversity of phenomena in quantum field theory in its various manifestations (e.g., extra dimensions) is enormous, and any of these phenomena might appear in a hidden sector. Fortunately, many models produce similar experimental signals. Indeed, in many hidden valleys, the dominant discoverable process is the same as one that occurs in one of the models that we have already discussed.

We first give a few examples of phenomena that can arise in hidden valleys that, though very different in their origin from theories we have already discussed, give signals that we have already discussed. We then give some examples of phenomena that we have not discussed that can arise in these models.

SM+scalar, 2HDM+scalar (*Secs. 1C1 and 1C2*).—Consider a confining hidden valley, with its own gauge group G and quarks Q_i , and a Higgs-like scalar S that gives mass to the Q_i via a $SQ_i\bar{Q}_i$ coupling, but does not break G . We imagine that S mixes with one of the SM Higgs doublets; for example, this model could be an extension of the NMSSM. If the gauge group confines and breaks chiral symmetry, with PNGBs K_v , then a SK_vK_v coupling and the mixing of S and the Higgs allow the decay $h \rightarrow K_vK_v$. The K_v may then decay to SM fermions, with the heaviest fermions available typically most common; this can occur for instance via mixing with a heavy Z' or with a SM pseudoscalar Higgs. An example (not at all unique) is given in the model of [32], which shows decays may be prompt for m_{K_v} above about 20 GeV.

SM + 2 fermions (*and similar*) (*Sec. 1C3*).—The same signal that arises in a simplified model with fermions may arise in hidden valleys, for much the same reasons. But it may arise even when there are no fermions at all. Consider the same model just mentioned, but with two flavors of PNGBs (as with pions and kaons in the SM), π_v and K_v . It may be that the π_v are stable or very long lived, and produce only E_T , while K_v cannot decay to two or more π_v . This could be due to kinematic constraints (like kaons in QCD if m_K were less than $2m_\pi$), or symmetries. In that case K_v may decay via a small coupling to a scalar field S that mixes with h , or via a spin-one vector V that mixes with Z . This opens up the possibility of $K_v \rightarrow \pi_v h^*$ or

$K_v \rightarrow \pi_v Z^*$, which would produce a nonresonant pair of SM fermions, or resonant decays such as $K_v \rightarrow \pi_v S$ or $K_v \rightarrow \pi_v V$.

In other hidden valleys, it can happen that there are two states, the heavier of which can only decay to the lighter via a loop of heavy particles, which allows for a radiative (i.e., photon emission) decay. If the lighter state is stable or decays invisibly, then the signal of two photons + E_T can arise.

The lesson here is that these signals can arise whenever we have two states, the lighter of which is invisible and the heavier of which can only decay to the lighter via emission of an on- or off-shell particle that decays to SM fermions or gauge bosons.

SM + vector (*Sec. IC 5*).—There are several ways for spin-one particles to arise naturally in a hidden valley, and for these to mix with the photon and/or Z to allow them to decay to SM fermions. There could be a broken $U(1)$ symmetry, giving what is often called a dark photon. Mixing with the hypercharge boson is through renormalizable kinetic mixing. There could be a broken non-Abelian gauge symmetry; in this case, there could be several spin-one particles, with the heavier ones decaying to the lighter ones via a cascade. Such a scenario only permits mixing with hypercharge through a dimension-five version of kinetic mixing. Finally, the spin-one particles could be stable bound states ρ_v , like a ρ meson in a theory with no chiral symmetry breaking and no pions. (An example with a stable vector and a stable pseudovector was given in [32].)

Decays of the Higgs to such particles can be induced using any of the mechanisms mentioned above or in the simplified model discussion. For instance, decay of a Higgs to two ρ_v (or, if there are two vectors ρ_1, ρ_2 , the decay $h \rightarrow \rho_1 \rho_2$) can occur along the same lines as the decay $h \rightarrow K_v K_v$ mentioned earlier.

A particularly well-known example of this type of hidden valley is [150], in which an elementary dark photon of low mass preferentially creates light leptons with very few photons or neutral pions. Dark matter annihilation can create these dark photons and thus provide leptonic final states potentially consistent with certain astrophysical observations. Because the dark photon must be lightweight, it tends to be produced with a high boost, giving the now-famous phenomenon of a lepton-jet. A simple lepton-jet contains two nearby leptons, isolated from other particles but not from one another. (More complex lepton jets will be addressed below.)

In this paper, we have limited ourselves to relatively simple final states to which the Higgs might decay. However, the complex final states that are common in hidden valleys are important to keep in mind, as they can pose considerable (though interesting) experimental challenges. For instance, even limited complexity can lead to

eight or more visible partons, from four hidden valley scalars, pseudoscalars, or vectors (possibly plus E_T) in a Higgs decay. The kinematics are then dependent on the hidden sector's mass spectrum and internal dynamics, giving rise to a wide array of signals.

This direction of research lies beyond our scope and should be returned to in the future. However, a couple of relatively simple experimental cases deserve note. First, any of the final states mentioned above may be accompanied by valley particles that are long lived on detector time scales and therefore invisible. This motivates searches for similar final states accompanied by E_T , which we address in Secs. XII–XIX.

Second, many models produce “complex” lepton-jets, in which multiple dark photons (or dark non-Abelian bosons or ρ mesons) are created near one another, clustered either by the kinematics of a cascade decay or by the physics of hidden-valley showering and hadronization. Some efforts have been made to find such objects [227]. Another interesting possibility would give several such dark photons created with low momentum along with E_T , leading to many unclustered very soft leptons. An attempt to search for such final states was made by CDF [228]. Unfortunately, in models where the vector bosons can decay also to pions, the leptons are fewer and hadrons often take their place, making the challenges much greater. One important signature, which is useful for particles of mass up to several GeV, is a dipion resonance with the same mass as a dilepton resonance. In models where the light particles are pseudoscalars, and often produce taus and rarely muons, it is not clear whether a good search strategy exists, unless rates are sufficient for a dimuon resonance search.

Another issue that commonly arises in hidden valleys is long-lived neutral particles [32]. Valley particles, by definition, are neutral under all SM gauge groups. The case of hadrons in QCD offers a useful analogy. Most hadrons in QCD are highly unstable, but a few are stable, and others are metastable, for a diversity of reasons (exact and approximate symmetries, weak forces, kinematic constraints, etc.). Their decays are often very slow on QCD time scales, and their lifetimes are spread across many orders of magnitude, from the neutron at 15 min to the π^0 at a hundredth of a femtosecond. The same could be true of a sector of hidden-valley particles. The particles that are stable on detector time scales will give us nothing but E_T . The shorter-lived particles will give us prompt decays, of the sort that we discuss in this article. But it is quite common, given a rich spectrum of particles with a variety of lifetimes, that one or more will decay typically with a displaced vertex. An example of a natural theory where such particles may arise in Higgs decays [76] is the twin Higgs [226], though the details are still to be worked out. This issue takes us beyond our current purposes, but this possibility has already received some amount of experimental study, as in [78–95, 229, 230]

II. $h \rightarrow E_T$

A. Theoretical motivation

Higgs decays into a new stable, neutral particle have a venerable history, going back to the pioneering work of Suzuki and Shrock [25]. Since the astrophysical evidence for particle dark matter strongly suggests the existence of new neutral degrees of freedom, potential Higgs decays to dark matter (DM) are a topic of particular interest [29,231,232]. While the most minimal models of Higgs-coupled DM with $2m_{\text{DM}} < 125$ GeV have been excluded by LHC observations of the Higgs boson alone (direct detection, particularly from XENON100, also constrains these models; see, e.g., [233]), nonminimal models can easily still allow for light thermal DM coupling to the SM predominantly through the Higgs [234–236]. Dark matter therefore constitutes one of the most robust motivations for the invisible decay mode.

The possibility that the Higgs might dominantly decay to neutralinos in models with weak-scale supersymmetry [183] has received comparatively less attention due to the difficulty of achieving this signature in traditional constrained Minimal Supersymmetric Standard Model-type models of supersymmetry breaking [237]. With less restricted spectra, or in nonminimal models such as the NMSSM, it is easier to realize Higgs decays to neutralinos [188,238–241] and/or Goldstinos [49,242].

Beyond supersymmetry and DM, many theoretical frameworks predict one or more new neutral particles, often naturally light, which can furnish an invisible BSM decay mode for the Higgs boson. Frequently considered examples are Majorons [25,27,243] as well as more general PNBGs [244]; hidden sectors [30–32,245,246]; fourth-generation neutrinos [247,248]; and right-handed neutrinos [249] and their Kaluza-Klein excitations [237] or superpartners [250].

B. Existing collider studies

The Higgs decay to missing energy is a difficult experimental signature due to the lack of kinematic information in the final state and the irreducible background from SM $Z \rightarrow \nu\bar{\nu}$ production. Nevertheless, the excellent theoretical motivation for this signal has made it a focus of study for many years. A Higgs decaying invisibly must be produced in association with another object in order to be observed. In order of production cross section, the reasonable candidates are then

- (i) $gg \rightarrow h + \text{jets}$;
- (ii) VBF production of $h + 2j$;
- (iii) $Wh, W \rightarrow \ell\nu$;
- (iv) $Zh, Z \rightarrow \ell^+\ell^-, (b\bar{b})$.

While $t\bar{t}h$ associated production initially appeared promising [251,252], the small cross section and complex final state make this mode challenging.

The monojet + E_T signal, sensitive to gluon fusion production with initial state radiation (ISR),¹⁴ has a large rate, but its reach is limited by the lack of kinematic handles to separate an invisible Higgs from the nearby background $Z + j$ [48]. Similarly, production in association with a leptonic W is not useful for an invisibly decaying Higgs boson, due to the lack of kinematic information in the final state that could separate the signal from the large Drell-Yan background $qq \rightarrow W^* \rightarrow \ell\nu$ [254–256].

The VBF production mode offers the best combination of cross-section and signal-to-background discrimination at the LHC, both for 14 TeV [47,257] and 7 and 8 TeV [48].¹⁵ Reference [48] estimates that 20 fb^{-1} at 8 TeV can allow limits to be placed for $\text{Br}(h \rightarrow E_T) \gtrsim 0.4$, while Ref. [258] estimates the sensitivity $\text{Br}(h \rightarrow E_T) \gtrsim 0.25$ with 300 fb^{-1} at 14 TeV. Meanwhile Ref. [256] estimates sensitivity for $\text{Br}(h \rightarrow E_T) \gtrsim 0.50$ with 30 fb^{-1} at 14 TeV. Assumptions about systematic errors are critical in obtaining these estimates.

Associated production with a leptonically decaying Z boson has a significantly smaller LHC cross section than any of the above production modes, but on the other hand the final state contains more kinematic information [254,255,259]. For a 125 GeV Higgs, $Zh, Z \rightarrow \ell\ell$ can nearly approach the reach of VBF at the 14 TeV LHC [256], though its utility at 7 and 8 TeV is more limited [48]. Including $Z \rightarrow b\bar{b}$ as well as $Z \rightarrow \ell^+\ell^-$ decays can incrementally improve the reach, at both the Tevatron [237] and the LHC [258].

C. Existing experimental searches and limits

The best existing constraints come from ATLAS measurements targeting Zh associated production with $Z \rightarrow \ell\ell$, which limit the invisible branching fraction to be

$$\text{Br}(h \rightarrow \text{invisible}) < 0.65 (0.84 \text{ expected}) \quad (65)$$

at 95% C.L. [260] with 47 fb^{-1} at 7 TeV and 13.0 fb^{-1} at 8 TeV. The measurement by CMS in the same channel with the full 7 and 8 TeV data sets places a 95% C.L. upper bound on the invisible branching fraction of $\text{Br}(h \rightarrow \text{invisible}) < 0.75 (0.91)$ [261]. CMS also has a measurement in the VBF channel, with a 95% C.L. upper limit [262]

$$\text{Br}(h \rightarrow \text{invisible}) < 0.69 \text{ observed} (0.53 \text{ expected}) \quad (66)$$

with 19.6 fb^{-1} of 8 TeV data. Much weaker limits come from reinterpretation of monojet + E_T measurements [253].

¹⁴There is a potentially significant contribution from VBF to monojet + E_T searches, depending on the jet criteria adopted in the search [253].

¹⁵Note that searches targeting the VBF production mode also see a secondary signal contribution from $gg \rightarrow h + 2j$, which is relatively more important at 7 and 8 TeV than at 14 TeV.

III. $h \rightarrow 4b$

One possible exotic Higgs decays is to four b quarks via a light resonance X : $h \rightarrow XX \rightarrow b\bar{b}b\bar{b}$. Below, we outline the theoretical motivation to consider such decays and discuss their LHC phenomenology.

A. Theoretical motivation

In the SM, a 125 GeV Higgs can decay to four b quarks via ZZ^* . This branching ratio is small: $\text{Br}(h \rightarrow ZZ^*) \times \text{Br}(Z \rightarrow b\bar{b})^2 \sim 10^{-4}$. The $b\bar{b}$ pair associated with the on-shell Z boson is relatively uncollimated because of the large Z mass, and the resulting signature has a large irreducible QCD background. A more experimentally viable situation occurs in models where the Higgs decays to new particles “ X ” which further decay to a pair of b quarks. Such a decay topology can arise in several new physics scenarios, such the general 2HDM + S (Sec. IC 2), extensions of the SM with hidden light gauge bosons (Sec. IC 5), the (R -symmetry limit of the) NMSSM (Sec. IC 7), the Little Higgs model (Sec. IC 9), and commonly in the hidden-valley scenario (Sec. IC 10). In all of these models, $X \rightarrow b\bar{b}$ can be the dominant decay mode in certain regions of parameter space, therefore strongly motivating the study of the $h \rightarrow 4b$ decay channel.

- (i) 2HDM + S.—In two-Higgs-doublet models with an additional light singlet, the decay $h \rightarrow ss$ or $h \rightarrow aa$, where s (a) is the mostly singlet (pseudo)scalar, is generic. Depending on $\tan\beta$, the decays $s \rightarrow b\bar{b}$ or $a \rightarrow b\bar{b}$ are also generic (although not guaranteed) in all four 2HDM types as long as $m_a, m_s > 2m_b$.
- (ii) R -symmetry limit in the NMSSM.—The additional two degrees of freedom in the NMSSM Higgs sector (which corresponds to a type-II 2HDM + S model) make a light pseudoscalar a with sizable coupling to the SM-like Higgs and SM fermions possible. In the case of an approximate R symmetry, the imaginary component of the new singlet is naturally light, since it serves as a pseudo-Goldstone boson of the spontaneously broken $U(1)_R$, once the singlet acquires a vacuum expectation value. For $m_a \leq m_h/2$, the decay $h \rightarrow aa$ opens up. (Note, however, that while a is light in the PQ limit of the NMSSM, the decay $h \rightarrow aa$ is generically suppressed compared to other decays; see [53] or Sec. IC 8.) The pseudoscalar a couples to fermions proportional to the Yukawa matrices, which are enhanced by $\sin\beta/\sin\alpha$. This makes large decay branching ratios for $a \rightarrow b\bar{b}$ natural in large regions of parameter space.
- (iii) *Little Higgs models*.—Another class of models with potentially light pseudoscalars is the Little Higgs model. The couplings of a to SM fermions are again proportional to the SM Yukawas if one imposes MFV [215–218] in order to get rid of large flavor

violation; thus the coupling to the b quark is typically enhanced.

B. Existing collider studies

Most of the existing collider studies are performed within the NMSSM framework (the Little Higgs model was considered in [263]) under the assumption that $\text{Br}(h \rightarrow aa) \simeq 1$. Those studies that have been performed at the LHC were done for $\sqrt{s} = 14$ TeV. The case with $\sqrt{s} = 8$ TeV has not explicitly been studied, but insight can still be gained from previous work.

1. LEP and Tevatron

Much of the earlier literature on exotic Higgs decays was framed in the context of trying to evade the LEP limit of $m_h > 114$ GeV for a Higgs produced with SM-like strength, allowing for a lighter and more natural Higgs. For example, [264] presented constraints from LEP on NMSSM cascade decays; for $h \rightarrow 4b$, the Higgs mass constraint is around 110 GeV, only slightly weaker than the LEP constraint on a SM Higgs. The 125 GeV Higgs is not constrained by LEP, as it is above LEP’s kinematic limit. The Tevatron also does not have any exclusion power for $h \rightarrow 4b$ with SM-strength production [202,263,265,266].

2. LHC

The literature contains several collider studies examining $h \rightarrow 4b$ decay at the 14 TeV LHC. References [59,60] considered the $4b$ final state in the context of VBF Higgs production, but this signature is very difficult to distinguish from QCD background. More recently the focus has been on the Wh production mode [191,263,266,267], where the tagged lepton greatly reduces backgrounds and enhances discovery potential.

Reference [191] is the most recent study demonstrating how a very simple $4b$ search could constrain $h \rightarrow aa \rightarrow b\bar{b}b\bar{b}$ at LHC14. It makes use of the known Higgs mass and utilizes full showering and fast detector simulation. The total signal cross section is parameterized in terms of the associated Higgs production cross section σ_{Wh} :

$$\sigma_{4b} = C_{4b}^2 \sigma_{Wh}, \quad (67)$$

where

$$C_{4b}^2 = \kappa_{hVV}^2 \text{Br}(h \rightarrow aa) \text{Br}(a \rightarrow b\bar{b}) \quad (68)$$

and κ_{hVV} is the WhV coupling strength relative to the SM. Within the assumptions we make in this survey, $C_{4b}^2 = \text{Br}(h \rightarrow 2a \rightarrow 4b)$. The selection requirements are exactly four b tags (with assumed 70%, 5%, and 1% efficiency for b , c , and light flavor jet, respectively), one isolated lepton, and a reconstructed m_{4b} in the Higgs mass window. This greatly reduces the main backgrounds

($t\bar{t}$ + jets and V + jets). At the 14 TeV LHC with 300 fb^{-1} of data, this gives signal significance $S/\sqrt{B} = 2$ for $\text{Br}(h \rightarrow 2a \rightarrow 4b) \approx 0.1$ if $m_a > 30 \text{ GeV}$.

Searching for $h \rightarrow 2a \rightarrow 4b$ decay if $m_a < 30 \text{ GeV}$ requires the use of jet substructure. This case was addressed by [267], which primarily deals with the much more difficult signature $h \rightarrow aa \rightarrow 4g$ (also considered in [220,268–270]), with $h \rightarrow 4b$ considered as a special case that can also make use of heavy flavor tagging. They focus on boosted Higgs production in association with a W or Z (with $C_{4b}^2 = 1$ in the above notation) by requiring a reconstructed vector boson to have $p_V^T > 200 \text{ GeV}$. A range of pseudoscalar masses is considered for a 120 GeV Higgs.

For $m_a \lesssim 30 \text{ GeV}$, a boosted Higgs decaying as $h \rightarrow aa \rightarrow 4j$ can produce a two-, three-, or four-pronged fat jet. Pseudoscalar candidates are constructed to minimize their mass difference, requiring the lighter pseudoscalar candidate to have at least 75% of the mass of the heavier one, and by selecting events with a fat jet mass close to the hypothesized Higgs mass and looking for a pseudoscalar mass resonance.

Assuming $\text{Br}(h \rightarrow 4b) = 1$, without heavy flavor tagging the $h \rightarrow 4j$ signature can be observed at 3σ with 100 fb^{-1} of LHC14 luminosity; adding one (two) b tags improves the $h \rightarrow 4b$ discovery signal to $\sim 6\sigma$ ($\gtrsim 10\sigma$). Naively scaling this sensitivity to 300 fb^{-1} we obtain a signal significance $S/\sqrt{B} \approx 2$ for $\text{Br}(h \rightarrow 2a \rightarrow 4b) \approx 0.1$. This is comparable to the result for $m_a > 30 \text{ GeV}$ by [191].

It therefore seems reasonable to expect the LHC14 to have 2σ sensitivity to $\text{Br}(h \rightarrow 2a \rightarrow 4b) = 0.1$ (0.2) with 300 fb^{-1} (100 fb^{-1}) of data across the kinematically allowed mass range for the pseudoscalar a .

C. Existing experimental searches and limits

Because of large QCD backgrounds to the $4b$ final state, the only realistic discovery mode for $h \rightarrow b\bar{b}b\bar{b}$ at the LHC is Wh associated production. The produced lepton allows for the event to be triggered on, which is difficult for the relatively soft all-hadronic final state resulting from gluon-fusion or vector-boson fusion Higgs production. Therefore, the relevant final state for experimental searches is $4b + \ell + \cancel{E}_T$ (or some variety with fewer b tags).

To the best of our knowledge, no such search has been performed. $V(h \rightarrow b\bar{b})$ searches [271,272] have not yet reached SM sensitivity and are even less likely to find the softer signal from four b 's. Searches for $b(h \rightarrow b\bar{b})$ production [273,274] do not look for an isolated lepton or large amounts of \cancel{E}_T , which results in large backgrounds, and SUSY searches for final states containing several b jets like [275] also typically do not require a lepton while requiring an amount of missing energy that is much too high for Vh production.

The $h \rightarrow aa \rightarrow 4b$ process will contribute to the signal region of SM $h \rightarrow 2b$ searches. The recent CMS analysis

[276] observes a 2σ excess consistent with a SM-like 125 GeV Higgs, constituting the first indication of $h \rightarrow \bar{b}b$ decay at the LHC. The signal strength corresponding to this excess is

$$\mu_{2b} \equiv \frac{\sigma_h \text{Br} h \rightarrow b\bar{b}}{[\sigma_h \text{Br} h \rightarrow b\bar{b}]_{\text{SM}}} = 1.0 \pm 0.5. \quad (69)$$

We can, in principle, use this to derive a limit on $\text{Br}(h \rightarrow 4b)$. Define the m_a -dependent efficiency ratio

$$r_{4b}(m_a) = \frac{\epsilon_{h \rightarrow 2a \rightarrow 4b}}{\epsilon_{h \rightarrow 2b}} \quad (70)$$

for a $h \rightarrow 2a \rightarrow 4b$ event to end up in the signal region of the $h \rightarrow 2b$ search, relative to a SM-like $h \rightarrow 2b$ event. Assuming a SM-like partial width $\Gamma_{h \rightarrow 2b}^{\text{SM}}$, as well as SM-like Higgs production, and defining the total Higgs width in the SM to be Γ_h^{SM} , the *expected* signal strength observed in a $h \rightarrow 2b$ search will be

$$\begin{aligned} \mu_{2b} &= \frac{\Gamma_{h \rightarrow 2b}^{\text{SM}} + r_{4b} \Gamma_{h \rightarrow 2a \rightarrow 4b}}{\Gamma_h^{\text{SM}} + \Gamma_{h \rightarrow 2a \rightarrow 4b}} \frac{\Gamma_h^{\text{SM}}}{\Gamma_{h \rightarrow 2b}^{\text{SM}}} \\ &= 1 + \text{Br}(h \rightarrow 2a \rightarrow 4b) \left[\frac{r_{4b}}{\text{Br}(h \rightarrow 2b)^{\text{SM}}} - 1 \right]. \end{aligned} \quad (71)$$

For $\text{Br}(h \rightarrow 2b)^{\text{SM}} \approx 0.6$, this expected signal strength is shown in Fig. 18.

To estimate r_{4b} for the analysis in [276] we simulated $h \rightarrow 2b$ and $h \rightarrow 2a \rightarrow 4b$ events in MADGRAPH and PYTHIA. Applying the analysis cuts from [276] we find that $0.5 \lesssim r_{4b} \lesssim 1.5$, with higher efficiency for lighter pseudoscalar masses $m_a \sim 15 \text{ GeV}$, since the resulting

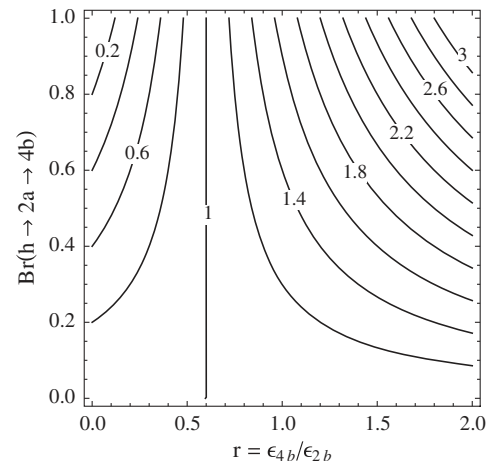


FIG. 18. Expected signal strength observed in a $h \rightarrow 2b$ search, assuming SM-like Higgs production and couplings with the exception of a new $h \rightarrow 2a \rightarrow 4b$ decay mode with selection efficiency r_{4b} relative to the efficiency of SM-like $h \rightarrow 2b$ events.

collimated $2b$ jets are tagged as single b jets from $h \rightarrow 2b$ decay. Given the 2σ limit of $\mu_{2b} < 1.9$ by [276] we can then read off a limit on $\text{Br}(h \rightarrow 2a \rightarrow 4b)$ from Fig. 18. For $m_a \sim 15$ GeV, the limit¹⁶ is $\text{Br}(h \rightarrow 2a \rightarrow 4b) \lesssim 0.7$, while no meaningful limits are derived for heavier pseudoscalars.

Clearly there exists motivation for a dedicated experimental search, which could easily be performed by triggering on leptons and missing energy from associated Higgs production, and performing a $4b$ search similar to the studies by [191,267].

D. Proposals for new searches at the LHC

The LHC14 studies [191,263,266,267] as well as the above-mentioned limit from the $h \rightarrow 2b$ search make it plausible that a 2σ sensitivity for the $\text{Br}(h \rightarrow 4b) \lesssim 0.5$ could be obtained using 25 fb^{-1} of LHC8 data (this is based on a naive scaling of cross sections and luminosity). More study would be needed to investigate the sensitivity in more detail. The boosted regime is also worth exploring at LHC8, either by looking for explicitly boosted pseudoscalars from Higgs decay giving two-pronged double- b jets (depending on m_a) or for fully boosted Higgses as in [267], or by looking indirectly via a diagonal cut in the $(p_{T,2b}, m_{2b})$ plane and requiring low ΔR_{2b} . These analyses can be easily parameterized in a simplified model with a single pseudoscalar a of mass m_a and a 125 GeV Higgs with SM-like production modes. The signature space then only has two parameters: m_a and C_{4b}^2 as defined in Eq. (68).

IV. $h \rightarrow 2b2\tau$

A. Theoretical motivation

This channel can become very important in the case that the Higgs decays into a pair of light (pseudo)scalars, $h \rightarrow aa$, with a further mostly decaying into the third-generation fermions $b\bar{b}$ or $\tau^+\tau^-$. In the mass range $2m_b < m_a < m_h/2$ the Higgs can have a relatively large branching ratio into aa , while both decays into $b\bar{b}$ and $\tau^+\tau^-$ are allowed by phase space. In many models, e.g., the NMSSM (see Sec. IC 7), Little Higgs models (see Sec. IC 9) and certain hidden-valley models (see Sec. IC 10), the couplings of a to SM fermions will be roughly proportional to the SM Yukawa couplings (with some corrections that depend on $\tan\beta$), leading to $\text{Br}(a \rightarrow b\bar{b}) \approx 94\%$ and $\text{Br}(a \rightarrow \tau^+\tau^-) \approx 6\%$. In this case $\sim 90\%$ of all the aa decays will end up in $b\bar{b}b\bar{b}$, $\sim 10\%$ in $b\bar{b}\tau^+\tau^-$ and less than 1% in $\tau^+\tau^-\tau^+\tau^-$. The first mode was discussed in Sec. III

¹⁶The assumption of SM-like $\Gamma_{h \rightarrow 2b}$ in our interpretation does not take into account the reduced $hb\bar{b}$ coupling when $\text{Br}(h \rightarrow 2a \rightarrow 4b)$ is high due to large Higgs-singlet mixing in a model like SM + S or 2HDM + S. In such a case, consistently taking the reduced $\Gamma_{h \rightarrow 2b}$ into account would make this limit slightly weaker.

and is very challenging, especially in the range of $m_a \lesssim 30$ GeV, where the b jets start merging. The last channel, $h \rightarrow 4\tau$, is discussed in Sec. VI for general models. However, in the class of models considered here, where $\text{Br}(a \rightarrow b\bar{b})/\text{Br}(a \rightarrow \tau^+\tau^-) \approx 3m_b^2/m_\tau^2$, the 4τ rate is likely too small to be exploited. In this case, $b\bar{b}\tau^+\tau^-$ can be a reasonable compromise between branching fraction and visibility of the signal. In particular, more than 50% of the ditau decays include at least one isolated lepton.

B. Existing collider studies

This channel has attracted the attention of several research groups both in the context of the Tevatron and of the LHC. Most of the studies assumed a $\mathcal{O}(1)$ branching fraction for the decay $h \rightarrow aa$.

(i) References [266,277] performed a feasibility study for this mode at the Tevatron. This study used associated production of the Higgs with a leptonic W . The study found very few sources of irreducible backgrounds, but also very small $\sigma(Wh) \times \text{Br}(h \rightarrow b\bar{b}\tau^+\tau^-)$. For example, for $\text{Br}(h \rightarrow aa) = 1$, which is bigger than what we can realistically assume today, effective production rates after the acceptance cuts $\sigma(Wh) \times \text{Br}(h \rightarrow b\bar{b}\tau^+\tau^-) = 0.55 \text{ fb}$ have been found for a Higgs with mass $m_h = 120$ GeV and with a very optimistic assumption on the branching ratios of the pseudo-scalar a : $\text{Br}(a \rightarrow b\bar{b}) = 0.7$ and $\text{Br}(a \rightarrow \tau^+\tau^-) = 0.3$ [277].¹⁷ This can probably be improved by $\sim 40\%$ if this channel is combined with $Z(\rightarrow \ell^+\ell^-)h$ associated production. But probably little more can be gained at the Tevatron, and one cannot hope for more than just a few signal events in the realistic case.

(ii) This study was performed in Ref. [278] for the LHC at 14 TeV. Motivated by the SM $h \rightarrow \tau^+\tau^-$ channel, the authors concentrated on the VBF Higgs production mode. This study largely relies on a precise reconstruction of $m_{b\bar{b}}$ for rejection of the dominant $t\bar{t}$ background, while $m_{\tau\tau}$ and $m_{b\bar{b}\tau\tau}$ are not considered. The study is rather preliminary, and it claims that with 100 fb^{-1} data, a significance of $S/\sqrt{B} \sim 2$ is possible after b tagging.

It is also worth noticing that this study only considered channels with both τ 's decaying leptonically (denoted τ_ℓ), and the situation can probably be significantly improved by including τ 's decaying hadronically (denoted τ_h), e.g., $\tau_\ell\tau_h$ and maybe even $\tau_h\tau_h$ final states. Unfortunately we have not found any other dedicated studies along these lines.

¹⁷Note that these branching ratios can only be obtained in a small region of parameter space of the NMSSM that predicts very large radiative corrections to the $a\tau^+\tau^-$ and $ab\bar{b}$ couplings.

TABLE III. Relative and cumulative efficiencies of the signal “ S ” ($h \rightarrow aa \rightarrow b\bar{b}\mu^+\mu^-$) and backgrounds for $m_a = 30$ GeV (without b tagging) at 8 TeV LHC. The labels bb , cc , and jj indicate SM Drell-Yan (Z/γ^*) productions with final states $b\bar{b}\mu^+\mu^-$, $c\bar{c}\mu^+\mu^-$, and $j\bar{j}\mu^+\mu^-$, respectively. For the signal normalization, we assume $\text{Br}(h \rightarrow aa) = 10\%$ and a 2HDM-type III (leptonic-specific) + S model with $\tan\beta = 2$. The latter assumption leads to $2 \times \text{Br}(a \rightarrow b\bar{b})\text{Br}(a \rightarrow \mu^+\mu^-) = 1.7 \times 10^{-3}$ (see Sec. IC 2).

Selection criteria	S (rel.)	S (cum.)	bb (rel.)	bb (cum.)	cc (rel.)	cc (cum.)	jj (rel.)	jj (cum.)
$N_{\text{ev,initial}}$ (25 fb $^{-1}$)		80.8		1.9×10^5		4.3×10^5		1.1×10^7
Two opposite sign μ 's	100%	100%	100%	100%	100%	100%	100%	100%
$ \eta(\mu_1) , \eta(\mu_2) < 2.5$								
$p_{T,\mu_1,\mu_2} > 17, 8$ GeV	58%	58%	69%	69%	41%	41%	63%	63%
At least two jets	100%	58%	100%	69%	100%	41%	100%	63%
$ \eta(j_1) , \eta(j_2) < 2.5$								
$p_T(j_1), p_T(j_2) > 25$ GeV	6.6%	3.8%	18%	12%	16%	6.4%	18%	11%
$\Delta R_{j_1, j_2, j\mu, \mu_1\mu_2} > 0.7, 0.4, 0.4$	100%	3.8%	96%	12%	97%	6.2%	95%	11%
$ m(j_1, j_2) - m_a < 15$ GeV	100%	3.8%	5.3%	6.4×10^{-3}	5.5%	3.4×10^{-3}	5.3%	5.7×10^{-3}
$ m(\mu_1, \mu_2, j_1, j_2) - m_h < 15$ GeV	100%	3.8%	2.7%	1.7×10^{-3}	8.6%	2.9×10^{-4}	4.3%	2.4×10^{-4}
$ m(\mu_1, \mu_2) - m_a < 1$ GeV	100%	3.8%	4.1%	7×10^{-6}	2.8%	8×10^{-6}	3.6%	8.7×10^{-6}
$N_{\text{ev,final}}$ (25 fb $^{-1}$, no b tag)		3.1		1.3		3.4		97.8
		$S = 3.1$		$B_{\text{total}} = 102.5$		$S/B_{\text{total}} = 0.03$		$S/\sqrt{B_{\text{total}}} = 0.31$

(iii) Reference [266] also very briefly discussed this search for 14 TeV LHC, considering only associated production with a W or Z , decaying leptonically. This study found this mode largely unfeasible at 100 fb $^{-1}$ due to very small S/B ratio.

C. Discussion of future searches at the LHC

We are not aware of any current experimental searches in this channel. Searches for $h + 2b$ with $h \rightarrow 2\tau$ [279,280] are not sensitive to the $2b2\tau$ decay mode, as they did not search for 2τ resonances below 90 GeV. Nonetheless, this channel might be a very important direction for studies of the LHC at 14 TeV. Probably, in order to have optimal reach, all three major production modes (gluon fusion, VBF, and W/Z associated production) should be combined together. Different production modes may be dominated by different backgrounds. While $t\bar{t}$ looks indeed like a formidable background for VBF, it is possible that $\gamma^*/Z^* +$ jets dominates the two other channels.

It is also worth noticing additional complications for very small values of m_a . First, as the mass of a is getting close to the Υ mass, the branching ratio $a \rightarrow b\bar{b}$ can be significantly reduced in favor of $a \rightarrow \eta + X$, leading effectively to a $\tau^+\tau^-j$ event topology and opening up additional possible backgrounds from bottomonium decays [281] (see [124] for a detailed discussion and calculation of the branching ratios). In addition, the τ 's tend to merge in this region of parameter space, failing isolated reconstruction criteria and yielding effectively a single τ -like jet instead of two. Finally, triggering on these events may be an issue. In particular, one can only be confident that associated production events are triggered with a reasonable efficiency. At LHC8, one can also probably

use parked data at CMS gathered via the (low-efficiency) VBF trigger. It is not clear, though, whether a search in this channel is feasible. At the 14 TeV LHC, the trigger thresholds may be too high for this type of decay, and therefore one probably has to focus on associated production.

We conclude that more dedicated feasibility studies for the LHC are needed in this particular channel.

V. $h \rightarrow 2b2\mu$

The possibility of the Higgs boson decaying to $(b\bar{b})(\mu^+\mu^-)$ is intriguing. In the context of NMSSM and 2HDM + S models it represents a compromise between the very difficult but often dominant $4b$ mode (see Sec. III) and the spectacular but rare 4μ signature. Below we present the theoretical motivation to consider this decay mode and demonstrate the reach of a dedicated search at both run I and II of the LHC. A detailed study will appear in [282].

A. Theoretical motivation

The $h \rightarrow (b\bar{b})(\mu^+\mu^-)$ decay mode occurs when the Higgs field couples to one or more bosons $a^{(i)}$ that couple to b quarks and muons, with at least one $a^{(i)}$ heavy enough to decay to $b\bar{b}$. As discussed in Sec. IC 1, the simplest realization of such a scenario is given by extending the SM to include an additional real singlet scalar. However, searching for this mode is motivated in any model with additional singlets that couple to quarks in proportion to their masses.¹⁸ This includes the 2HDM + S

¹⁸If the coupling is through gauge interactions, fully leptonic final states are generally the preferred discovery channel; see Secs. X and XI.

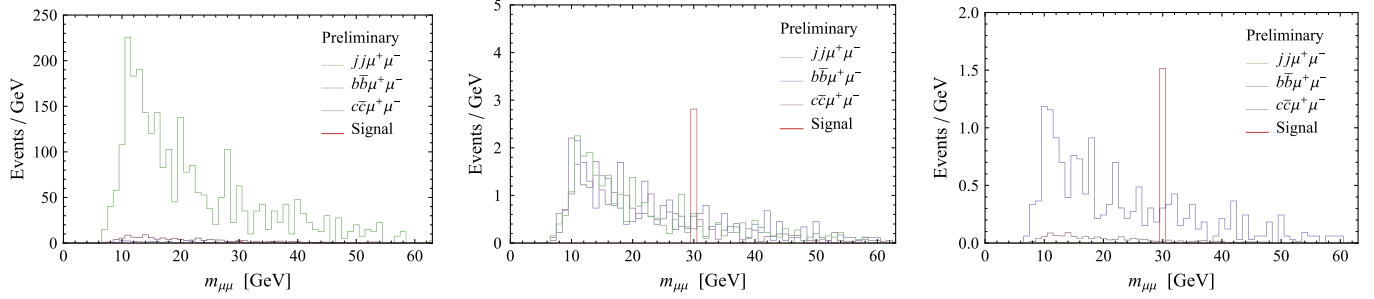


FIG. 19 (color online). Dimuon invariant mass spectrum, $m_{\mu\mu}$, for signal ($m_a = 30$ GeV) and backgrounds for 25 fb^{-1} at 8 TeV LHC after all kinematic cuts (except for $m_{\mu\mu}$ cuts) with (left) no b tag, (middle) at least one b tag, and (right) two b tags. For the signal normalization, we assume $\text{Br}(h \rightarrow aa) = 10\%$ and $2 \times \text{Br}(a \rightarrow b\bar{b})\text{Br}(a \rightarrow \mu^+\mu^-) = 1.7 \times 10^{-3}$ as in Table III.

(Sec. IC 2) and the well-known NMSSM (Sec. IC 7), as well as many hidden valleys (Sec. IC 10).

The small coupling to muons leads to very hierarchical branching ratios:

$$\text{Br}(h \rightarrow 4\mu) = \frac{\varepsilon}{2} \text{Br}(h \rightarrow 2b2\mu) = \varepsilon^2 \text{Br}(h \rightarrow 4b), \quad (72)$$

with $\varepsilon \equiv \text{Br}(a \rightarrow \mu^+\mu^-)/\text{Br}(a \rightarrow b\bar{b}) \sim m_\mu^2/3m_b^2 \approx 2 \times 10^{-4}$ in the SM + S. (Nonminimal scalar models can modify this ratio, but the ratio is in general very small.) Assuming SM Higgs production and $\text{Br}(h \rightarrow aa) = 10\%$ leads to zero $h \rightarrow 2a \rightarrow 4\mu$ events from gluon fusion at LHC run I, while about 20 $h \rightarrow 2a \rightarrow 2b2\mu$ events are expected to occur. Even though this is much less than the few hundred $h \rightarrow 2a \rightarrow 4b$ events expected from associated production, the backgrounds for the $4b$ search are so challenging (see Sec. III) that the $2b2\mu$ channel may provide much better sensitivity. This is even more attractive in nonminimal models, where, e.g., $\tan\beta$ can enhance the leptonic pseudoscalar branching fraction significantly. It is also possible that the Higgs decays to two pseudoscalars, $h \rightarrow a_1 a_2$, which have large branching fractions to $2b$ and 2μ , respectively. The presence of a clean dimuon resonance makes the $2b2\mu$ decay mode very attractive for discovering SM extensions with extra singlets.

B. Existing collider studies and experimental searches

To the best of our knowledge there have been no theoretical collider studies of this final state, and there are no limits on this decay channel from existing searches. A similar topology is searched for in $h \rightarrow b\bar{b}$ from associated production with a Z boson, where the Z decays to $\mu^+\mu^-$. However, this search is not relevant for $(2b)(2\mu)$, since the required $b\bar{b}$ invariant mass was $\mathcal{O}(125 \text{ GeV})$, and the two muons were required to reconstruct the Z boson. A dedicated search is therefore needed for this channel.

C. Proposals for new searches at the LHC

We estimate the discovery potential of a very simple search for $h \rightarrow 2a \rightarrow 2b2\mu$ with run I LHC data as well as

100 fb^{-1} at 14 TeV. This preliminary study is simulated at parton level for signal and backgrounds (see [282] for a more complete study).

1. LHC 7 and 8 TeV

We assume the Higgs is produced through gluon fusion and has a nonzero branching ratio as $h \rightarrow aa \rightarrow (b\bar{b})(\mu^+\mu^-)$. We do not include Higgs bosons produced through VBF in our analysis, although this would slightly increase the sensitivity to this channel. The final state consists of two opposite-sign muons and two b -tagged jets and is simulated for $m_h = 125 \text{ GeV}$ and $m_a \in (15, 60) \text{ GeV}$. (Lower masses involve complicated decays to quarkonia [124], which are beyond the scope of this study.) The main background is Drell-Yan (DY) production with associated jets, $Z/\gamma^* + 2j/2c/2b$, where the Z -decay/ γ^* produces two muons. In this preliminary estimate, we neglect backgrounds arising from lepton misidentification of jets, diboson production VV , and $t\bar{t}$ production, which are expected to be subdominant to DY. (The $t\bar{t}$ background has a total cross section comparable to DY + jets but does not contribute significantly in the low dimuon invariant mass region [283,284], and also typically

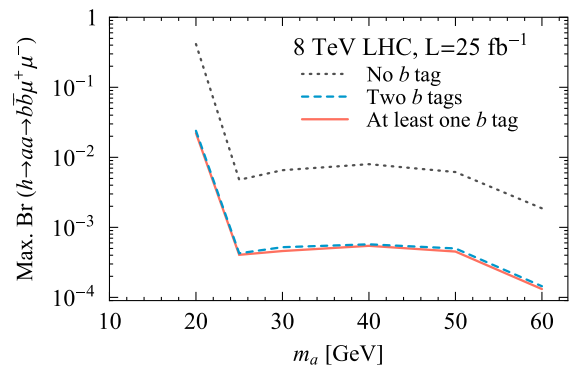


FIG. 20 (color online). Expected 95% C.L. sensitivity to $\text{Br}(h \rightarrow aa \rightarrow b\bar{b}\mu^+\mu^-)$ for 25 fb^{-1} data at 8 TeV LHC. The solid, dashed, and dotted lines show the limits for at least one b tag, two b tags, and no b tag, respectively.

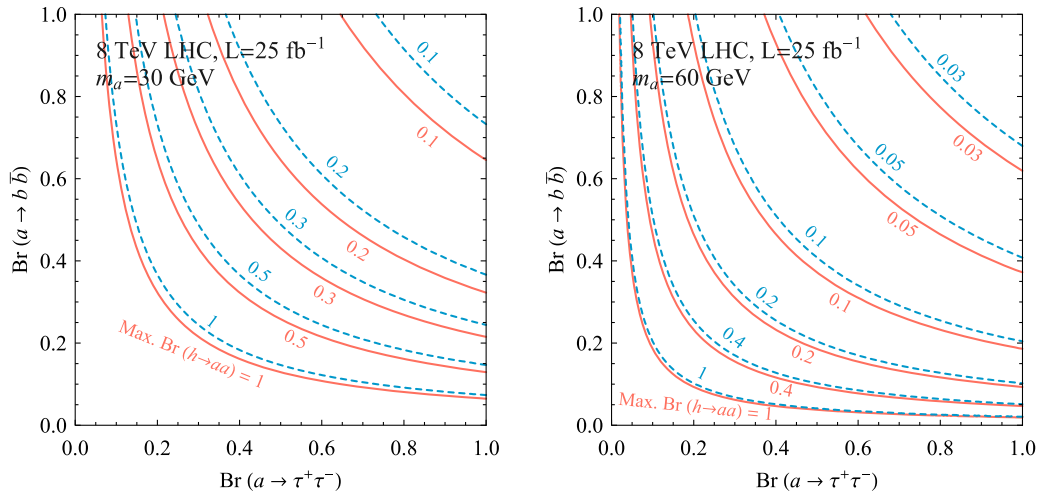


FIG. 21 (color online). Expected 95% C.L. sensitivity to $\text{Br}(h \rightarrow aa)$ from a $h \rightarrow b\bar{b}\mu^+\mu^-$ search as a function of $\text{Br}(a \rightarrow b\bar{b})$ and $\text{Br}(a \rightarrow \tau^+\tau^-)$, assuming that the pseudoscalar coupling to leptons is proportional to the lepton masses. We show $m_a = 30$ GeV (left) and $m_a = 60$ GeV (right) with 25 fb^{-1} of data at the 8 TeV LHC (see text for further details). The red solid lines and blue dashed lines present the limits for at least one b tag and two b tags, respectively. The corresponding sensitivities to $\text{Br}(h \rightarrow aa \rightarrow b\bar{b}\mu^+\mu^-)$ are given in Fig. 20.

produces a sizable amount of \cancel{E}_T that is not present for the signal.)

Both signal and background are simulated to lowest order at parton level in MADGRAPH 5 [285]. The signal is renormalized by the NLO gluon-fusion cross section $\sigma_{ggF} \approx 19.3 \text{ pb}$ [13]. The obtained leading-order cross sections for backgrounds¹⁹ are $\sigma_{b\bar{b}\mu^+\mu^-} \approx 3.7 \text{ pb}$, $\sigma_{c\bar{c}\mu^+\mu^-} \approx 8.6 \text{ pb}$, and $\sigma_{jj\mu^+\mu^-} \approx 226 \text{ pb}$. These samples are scaled up by a representative K factor of 2. We approximate the total run I data with 25 fb^{-1} at $\sqrt{s} = 8 \text{ TeV}$.

To approximate trigger threshold and detector reconstruction requirements, we impose the following preselection cuts: only use partons with $|\eta| < 2.5$; require ΔR between any two jets to be > 0.7 , and between two muons or between a muon and a jet > 0.4 ; two leading jets

with $p_{Tj_{1,2}} > 25 \text{ GeV}$; two muons with $p_{T\mu_{1,2}} > 17$ and 8 GeV , respectively. To roughly simulate b (mis)tagging we reweight events according to constant tagging probabilities of 65%, 10% and 0.5% for b , c , and light jets, respectively [286]. Following this preselection, we require either zero, one, or two b tags and use mass reconstruction cuts to focus in on the signal for each pseudoscalar mass:

$$\begin{aligned} |m_{\mu\mu} - m_a| < 1 \text{ GeV}, & \quad |m_{jj} - m_a| < 15 \text{ GeV}, \\ |m_{jj\mu\mu} - m_h| < 15 \text{ GeV}. & \end{aligned} \quad (73)$$

Table III shows the relative and cumulative efficiencies for the signal and backgrounds. Figure 19 shows an example of distributions of the signal with $m_a = 30 \text{ GeV}$ and backgrounds after applying the kinematic cuts and tagging probabilities above. As expected, Z/γ^* production clearly dominates the signal if no b tag is applied. The signal is visible only in the b -tagged cases.

We demonstrate 95% C.L. sensitivity of $\text{Br}(h \rightarrow aa \rightarrow b\bar{b}\mu^+\mu^-)$ with respect to m_a in Fig. 20. For $m_a \leq 25 \text{ GeV}$, the $b\bar{b}$ from a decay are collimated enough to fail our simple reconstruction cuts. A more sophisticated substructure analysis is required in this regime [282].

The upper limits on $\text{Br}(h \rightarrow aa \rightarrow b\bar{b}\mu^+\mu^-)$ can be further translated into upper bounds for $\text{Br}(h \rightarrow aa)$ for a fixed m_a by noticing

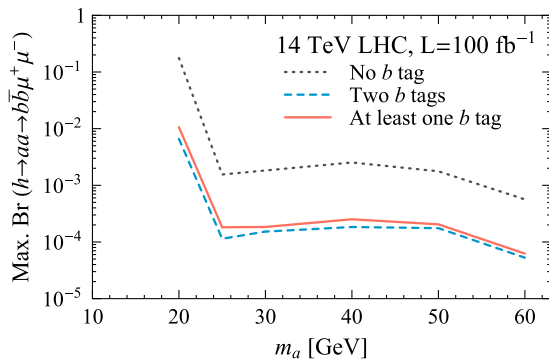


FIG. 22 (color online). Expected 95% C.L. sensitivity to $\text{Br}(h \rightarrow aa \rightarrow b\bar{b}\mu^+\mu^-)$ for 100 fb^{-1} of data at 14 TeV LHC. The solid, dashed, and dotted lines show the limits for at least one b tag, two b tags, and no b tag, respectively.

¹⁹We impose generator-level cuts $p_T(j) > 10 \text{ GeV}$, $p_T(l) > 5 \text{ GeV}$, $\eta(j) < 5$, $\eta(l) < 2.5$, $\Delta R_{jj,\mu\mu,j\mu} > 0.4$. Here j includes heavy flavor.

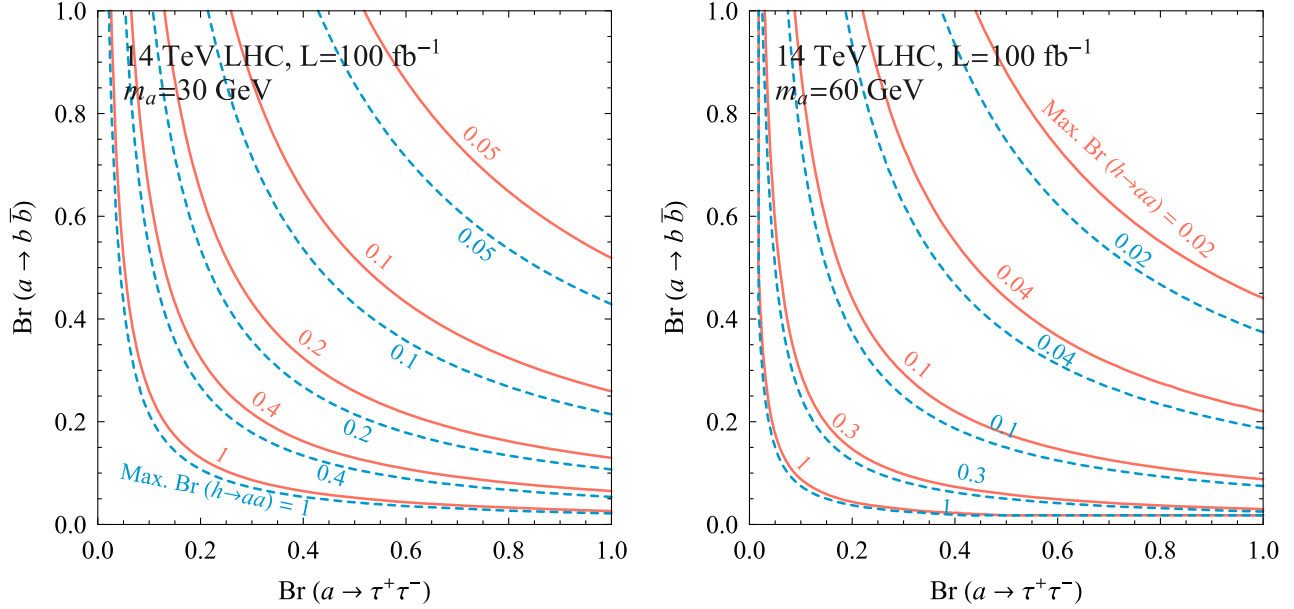


FIG. 23 (color online). Expected 95% C.L. sensitivity to $\text{Br}(h \rightarrow aa)$ from a $h \rightarrow b\bar{b}\mu^+\mu^-$ search as a function of $\text{Br}(a \rightarrow b\bar{b})$ and $\text{Br}(a \rightarrow \tau^+\tau^-)$, assuming that the pseudoscalar coupling to leptons is proportional to the lepton masses. We show $m_a = 30$ GeV (left) and $m_a = 60$ GeV (right) with 100 fb^{-1} of data at the 14 TeV LHC (see text for further details). The red solid lines and blue dashed lines present the limits for at least one b tag and two b tags, respectively. The corresponding expected sensitivities to $\text{Br}(h \rightarrow aa \rightarrow b\bar{b}\mu^+\mu^-)$ are given in Fig. 20.

$$\begin{aligned} \text{Br}(h \rightarrow aa) &= \frac{\text{Br}(h \rightarrow aa \rightarrow b\bar{b}\mu^+\mu^-)}{2\text{Br}(a \rightarrow b\bar{b})\text{Br}(a \rightarrow \mu^+\mu^-)} \\ &= \frac{\text{Br}(h \rightarrow aa \rightarrow b\bar{b}\mu^+\mu^-)}{2\text{Br}(a \rightarrow b\bar{b})\text{Br}(a \rightarrow \tau^+\tau^-)} \frac{m_\tau^2 \beta_\tau}{m_\mu^2 \beta_\mu}, \end{aligned} \quad (74)$$

where $\beta_f \equiv (1 - 4m_f^2/m_a^2)^{1/2}$. This allows us to show in Fig. 21 limits on $\text{Br}(h \rightarrow aa)$ in the plane of a branching ratios to $b\bar{b}$ and $\tau\tau$, which can be free parameters relative to each other (see, e.g., 2HDM + S, Sec. IC 2), while the ratio between $\tau\tau$ and $\mu\mu$ is fixed by their masses. From Fig. 20 the corresponding upper limits on $\text{Br}(h \rightarrow aa \rightarrow b\bar{b}\mu^+\mu^-)$ are 4.6×10^{-4} ($m_a = 30$ GeV, at least one b tag), 5.2×10^{-4} ($m_a = 30$ GeV, two b tags), 1.3×10^{-4} ($m_a = 60$ GeV, at least one b tag), and 1.4×10^{-4} ($m_a = 60$ GeV, two b tags).

2. LHC 14 TeV

We repeat the study with identical cuts for 100fb^{-1} of data at the 14 TeV LHC. The gluon fusion NLO Higgs production cross section is $\sigma_{ggF} = 49.85$ pb [13]. Drell-Yan background cross sections at LO from MADGRAPH with identical generator-level cuts are $\sigma_{b\bar{b}\mu^+\mu^-} = 9.68$ pb, $\sigma_{c\bar{c}\mu^+\mu^-} = 20.5$ pb, and $\sigma_{jj\mu^+\mu^-} = 452.5$ pb, again upscaled by a K factor of 2.

The expected 95% C.L. sensitivity of the 14 TeV LHC is shown in Fig. 22. We then translate this sensitivity to the expected 95% C.L. sensitivity to $\text{Br}(h \rightarrow aa)$ as a function of the branching ratios of a to $b\bar{b}$ and $\tau^+\tau^-$, assuming that

the pseudoscalar coupling to τ 's and μ 's is proportional to m_τ and m_μ , respectively. Figure 23 demonstrates the expected sensitivity to $m_a = 30$ GeV and $m_a = 60$ GeV. The corresponding expected sensitivities to $\text{Br}(h \rightarrow aa \rightarrow b\bar{b}\mu^+\mu^-)$ are 1.8×10^{-4} ($m_a = 30$ GeV, at least one b tag), 1.5×10^{-4} ($m_a = 30$ GeV, two b tags), 6.2×10^{-5} ($m_a = 60$ GeV, at least one b tag), and 5.3×10^{-5} ($m_a = 60$ GeV, two b tags).

3. Summary

Our simple parton-level study demonstrates that $\sim 10^{-4}$ – 10^{-3} sensitivity to $\text{Br}(h \rightarrow 2a \rightarrow 2b2\mu)$ is possible at the LHC. We will investigate this channel more closely in [282], but these preliminary results already strongly suggest conducting a corresponding search with available run I data.

VI. $h \rightarrow 4\tau, 2\tau 2\mu$

A. Theoretical motivation

In this section, we consider scenarios where the Higgs can decay into a pair of scalar or pseudoscalar bosons “ a ” with a mass between $2m_\tau$ and $m_h/2$, and with a sizable decay rate to tau pairs. As discussed in Sec. IC 2, such a state can arise in 2HDM models supplemented with a singlet scalar field, especially if m_a is below the bottomonium region. A well-known example is the NMSSM with an approximately conserved R symmetry (IC 7), which is a class of type-II models with a very light pseudo-Goldstone

TABLE IV. Approximate raw numbers of events for a selection of $h \rightarrow 2a \rightarrow 4\tau$ decay channels, assuming $\text{Br}(h \rightarrow 2a) = 10\%$ and $\text{Br}(a \rightarrow \tau^+\tau^-) \simeq 1$, with the 2012 LHC data set (8 TeV, 20 fb⁻¹). No trigger or reconstruction cuts have been applied. (Categories are not all mutually exclusive, and leptons from W/Z decay are not being counted.)

2012 4τ	Total	$\geq 1\mu$	$\geq 2\mu$	$\geq 3\mu$	$\geq 2\ell$	$\geq 3\ell$	4ℓ	$2 \times (\geq 1\mu)$	$(\mu\mu/\mu e) + (0\mu)$
ggF	38000	20200	10100	700	28600	4600	580	3800	4700
VBF	3200	1700	850	60	2400	400	50	320	400
$W(\rightarrow \ell\nu)h$	300	160	80	5	220	40	5	30	40
$Z(\rightarrow \nu\bar{\nu})h$	150	80	40	3	110	20	2	15	20
$Z(\rightarrow \ell^+\ell^-)h$	55	30	15	1	40	7	1	5	7

boson; see also hidden valleys, Sec. IC 10. Another simple example is the set of type-III (lepton specific) 2HDM models with modestly large $\tan\beta$, with or without extra singlet fields (Sec. IC 2). There, leptonic decays can dominate for new scalar or pseudoscalar states of almost any mass.

Besides focusing on the mass range $m_a = [2m_\tau, m_h/2]$, the main assumption that we will employ is that the couplings of a are in direct proportion to the lepton masses. For a above the tau pair threshold, this means that the branching fractions to lepton pairs are in proportion $\tau^+\tau^- : \mu^+\mu^- : e^+e^- \simeq m_\tau^2 : m_\mu^2 : m_e^2 \simeq 1 : 3.5 \times 10^{-3} : 8 \times 10^{-8}$. By far the dominant $2 \rightarrow 4$ fully leptonic branching fraction is then 4τ , though there is also a nearly 1% relative Br to $2\tau 2\mu$, which contains a tight 2μ resonance [104].²⁰ We do not need to make any explicit assumptions about the branching fractions to nonleptonic states, though here we will not consider possible signal contributions from decays with these states. For example, if a is above the b -quark pair threshold, $a \rightarrow 2b$ can dominate, and the $2a \rightarrow 4b$ and mixed $2b2\tau$ decay modes can be much larger than 4τ . We discuss these in detail in Secs. III and IV, respectively.

Taus can decay either leptonically (35%) or hadronically (65%). These further subdivide into electron or muon leptonic decays, and one- and three-prong (and very rarely five-prong) hadronic decays. In cases where $m_a \ll m_h$, the two taus or prompt muons from an individual a decay can merge according to standard isolation criteria. (Generally, $\Delta R \sim 4m_a/m_h$, e.g., roughly 0.3 for $m_a = 9$ GeV.) We therefore are presented with a large number of final-state channels containing various combinations of isolated or nonisolated leptons, in association with a number of tau-like jets. The number of options is further multiplied when we consider the various Higgs production modes. To get a sense of orientation, we show in Table IV the expected raw number of events in several nonexclusive 4τ final-state

²⁰Lighter states, between the muon and tau pair thresholds, can decay dominantly to muons and lead to a 4μ final state with multiple resonant features. For dedicated searches see [287,288]. Note that in this particular regime the leptons are highly collimated, such that searches for lepton-jets can also place nontrivial bounds (see, e.g., [289]).

channels for the 2012 LHC data set, taking as a benchmark $\text{Br}(h \rightarrow 2a) = 10\%$ and $\text{Br}(a \rightarrow 2\tau) \simeq 1$. We pay special attention to muons, which are easier to identify than electrons, especially with nearby hadrons or other electrons. In Table V we show an analogous set of numbers for the $2\tau 2\mu$ final-state channels.

While these raw numbers start at the tens of thousands, the various decay channels all have tradeoffs. One of the primary concerns is that the mass energy of the Higgs must be distributed between a large number of final-state particles, many of which are invisible neutrinos. A typical τ receives $\mathcal{O}(1/4)$ of the energy, suggesting $p_T(\tau) \sim 30$ GeV. However, when the τ decays, the visible p_T frequently falls below normal reconstruction thresholds. The leptonic decays, which are naively cleaner than the hadronic decays, have more neutrinos and less visible energy. Therefore, while we appear to be presented with many opportunities for clean leptonic tags, the leptons are often too soft to either trigger or reconstruct. The fact that these leptons can be nonisolated from each other or from a nearby hadronic tau further complicates matters. If nonisolated leptons and/or hadronic taus are considered, backgrounds from QCD must be carefully accounted for. In particular the signal can be faked by $\Upsilon(1S-3S)$ leptonic decays, for which the Br's are a few percent, and by events with γ^*/Z^* emissions.

Another handle is the kinematics of the decay. In principle, each event is triply resonant, reconstructing to two a 's and the 125 GeV Higgs. However, the neutrinos in the tau decays present a complication. In the 4τ mode,

TABLE V. Approximate raw numbers of events for a selection of 2τ decay channels within $h \rightarrow 2a \rightarrow 2\tau 2\mu$, assuming $\text{Br}(h \rightarrow 2a) = 10\%$, $\text{Br}(a \rightarrow \tau^+\tau^-) \simeq 1$, and $\text{Br}(a \rightarrow \mu^+\mu^-) = 0.35\%$, with the 2012 LHC data set (8 TeV, 20 fb⁻¹). No trigger or reconstruction cuts have been applied. (Categories are not all mutually exclusive, and leptons from W/Z and $a \rightarrow \mu^+\mu^-$ decay are not being counted.)

2012 $2\tau 2\mu$	Total	$\geq 1\mu$	$\geq 1\ell$	2ℓ
ggF	266	75	120	33
VBF	22	6.3	10	2.7
$W/Z(\rightarrow \ell\tau s/\nu\tau s)h$	3.5	1.0	1.6	0.4

assuming that every visible τ decay can even be identified, typically the best that we can do is to attempt to reconstruct the Higgs's visible mass or variants of its transverse mass folding in the E_T . There is therefore no sharp resonance peak. Reconstruction of the a mass further suffers from the fact that the E_T contributed by each individual a is *a priori* unknown. The a mass's utility as a discriminating variable against backgrounds is also highly reduced if m_a is at or below the bottomonium region. These difficulties highlight the major advantage of the $2\tau 2\mu$ mode. Though the overall rate is much smaller than 4τ , every event is tightly localized around the same value of $m(\mu^+\mu^-)$. The prompt muons also tend to be much more energetic than the leptons produced in tau decays, significantly enhancing the relative rate once realistic momentum cuts are applied.

The complications associated with $h \rightarrow 2a \rightarrow 4\tau$ and the low rates for $2\tau 2\mu$ means that at present these decays are difficult to constrain, and no significant limits exist from dedicated searches. Nonetheless, the signals are distinct enough that they can ultimately be observed or constrained, even for $\text{Br}(h \rightarrow 2a \rightarrow 4\tau) \lesssim 10\%$. This will especially be true over the lifetime of the LHC, as the higher statistics will allow better exploitation of the cleaner subleading final-state channels. In the following subsections, we discuss ways in which theorists and experimentalists have sought to construct viable search strategies, review existing dedicated and nondedicated searches, and quantify to what extent the nondedicated searches might place meaningful constraints. In particular, we estimate that a combination of recent CMS three-lepton and four-lepton searches at 8 TeV may already constrain $\text{Br}(h \rightarrow 2a \rightarrow 4\tau) \lesssim 20\%–40\%$ for $m_a \gtrsim 15$ GeV. We further estimate that a dedicated $\mu^+\mu^-$ resonance search in three- or four-lepton events could indirectly probe down to $\text{Br}(h \rightarrow 2a \rightarrow 4\tau) \lesssim 10\%$ with the 2012 data, even for $m_a < 10$ GeV.

B. Existing collider studies

Recent interest in $h \rightarrow 2a \rightarrow 4\tau$ searches was in part spurred by the observation [290] of a “blind spot” between the direct OPAL bound of 86 GeV [291] (limited only by an unfortunate choice of signal simulation range) and the LEP kinematic reach of approximately 115 GeV. In particular, this would have allowed a lighter SM-like Higgs, requiring a less fine-tuned NMSSM. However, as we now know, the SM-like Higgs was beyond LEP's reach.

Subsequent search proposals at the Tevatron and LHC have exploited the fact that the majority of the $2a$ decay channels contain one or more leptons. The chance of producing a fully hadronic final state is only about $(0.65)^4 = 18\%$. It has also been pointed out that close-by hadronic taus (or a hadronic tau and an electron) still constitute a jetlike object with unusually low track activity and a distinctive calorimeter pattern, leaving various options for tagging it as a “ditau jet.”

Below, we briefly review several recent proposals using a variety of strategies. Note that these all typically assume $\text{Br}(h \rightarrow 2a \rightarrow 4\tau) \approx 1$ and masses in the range $m_a \approx [2m_\tau, m_\Upsilon]$, so that the $a \rightarrow 2\tau$ decays are highly collimated.

1. Trilepton and collinear $e\mu$

In Ref. [292], the $h \rightarrow 2a \rightarrow 4\tau$ decay mode is studied in the context of the Tevatron. For ggF, they consider trilepton channels and channels where one of the tau pairs decayed to a roughly collinear $e\mu$ pair (to reduce γ^* and hadronic decay backgrounds). The starting efficiency for trilepton from its Br is roughly 10%, but after accounting for cuts on lepton p_T (3 GeV), η (2.0), and isolation, the final efficiency becomes only 0.5%. The estimated cross section times acceptance for ggF is then 4 fb, or $\mathcal{O}(40)$ events for run II. The collinear $e\mu$ case, assumed to recoil against a low-track ditau jet, could have higher efficiency but also faces higher backgrounds that are much more difficult to model. No attempt is made to estimate these. Utilizing the associated Wh and Zh production modes is also suggested, though the rates tend to be even smaller. While the rate limitations at the Tevatron make all of these searches unlikely to yield a signal, especially since recent LHC results imply that exotic Higgs decays cannot dominate, most of these ideas can readily be adapted to the LHC.

2. Two $\mu\tau_h$ jets

In [293], the 4τ decay is studied for VBF and Wh production at LHC14, exploiting a pair of decays $a \rightarrow \mu\tau_h$ (one-prong). For VBF, the events are assumed to be selected with a same-sign dimuon trigger allowing an off-line selection of $p_T > 7$ GeV, while the Wh channel is triggered with the leptonic W decay. The specific requirements of the two channels are not identical, but each demands two muons (same-sign for VBF) and two one-prong hadronic taus, forming two approximately collinear $\mu\tau$ systems. For LHC14 and $m_h = 125$ GeV, VBF is predicted to have $\sigma \times A \sim 20–70$ fb and Wh 4–10 fb, increasing for lighter pseudoscalars. Scaling to LHC8 with 20 fb^{-1} , and multiplying by a reference $\text{Br}(h \rightarrow 2a) = 10\%$, we estimate 15–55 events (VBF) and 3.7–9 events (Wh). The upper ranges of these numbers are close to the raw counts expected from Br alone, suggesting very high estimated reconstruction efficiency and/or other exclusive final states being picked up by the analysis. VBF is more promising in terms of raw event counts, but backgrounds are not assessed. The Wh search is expected to be “almost background free.” No search of this type has been performed yet.

3. Dimuon resonance

Reference [104] considers the subleading decay sequence $h \rightarrow 2a \rightarrow 2\tau 2\mu$, with a focus on identifying the sharp 2μ resonance at m_a . The taus are assumed to decay hadronically and are simply treated as a jet with aligned \vec{E}_T . The Higgs resonance is also shown to be approximately reconstructable, though this is not used for discrimination, as S/B is already $\gg 1$. For a 125 GeV Higgs and 7 GeV pseudoscalar a , 5 fb^{-1} at LHC14 is estimated to give 2σ sensitivity to $\text{Br}(h \rightarrow 2a) < 10\%$ via ggF production. Note that the statistics from the 2012 run corresponds to about 8 fb^{-1} of LHC14, so this strategy may already be capable of rather stringent limits. D0 has performed a search of this type, which we describe in the next subsection.

4. Ditau jets

In [294], a calorimeter based “ditau-jet tag” is assessed in the context of $Zh \rightarrow (\ell^+\ell^-)(4\tau)$. (See also [295] for tracker-based techniques tailored to boosted $h \rightarrow 2\tau$ “jets.”) For this purpose no lepton identification is used. The main ditau-jet discriminating variables considered are the N -subjettiness ratio τ_3/τ_1 operating on electromagnetic calorimeter (ECAL) cells and the m/p_T ratio. (A more powerful likelihood-based tag is also studied.) E_T and $p_T(Z)$ are also applied to purify the signal. For LHC14, $\sigma \times A \gtrsim 1 \text{ fb}$ is achieved with $S/B \approx 0.5$. Scaling $\text{Br}(h \rightarrow 2a) \rightarrow 10\%$, and σ and luminosity to a 2012-like data set, this would yield only $\mathcal{O}(1 \text{ event})$ with $S/B \ll 1$. However, the ditau-jet tag can also be considered for searches in channels with higher cross sections.

C. Existing experimental searches and limits

Dedicated searches for prompt 4τ and $2\tau 2\mu$ final states of the Higgs have been performed at LEP [291,296] and at the Tevatron [287], respectively, but no significant constraints have yet been established for $m_h = 125 \text{ GeV}$. No dedicated search has yet been performed at the LHC. We briefly discuss the Tevatron search and also some nondedicated searches at the LHC that may have sensitivity to our signal or can serve as starting points for new dedicated searches. We then recast a subset of the nondedicated searches to derive new, nontrivial limits.

1. Tevatron $2\tau 2\mu$

With 4 fb^{-1} , D0 searched for $2\tau 2\mu$ (and 4μ) in ggF events [287], based on the strategy presented in [104]. Most accepted events pass a 4–6 GeV dimuon trigger. Muon ID is relaxed for one of the muons in the $a \rightarrow 2\mu$ candidate, but its inner track can still be reconstructed. The search is a bump hunt in the muon-pair mass spectrum over the range $m_a = [3.6, 19] \text{ GeV}$. The $a \rightarrow 2\tau$ ditau jet is minimally identified by requiring significant E_T , possibly near a jet with low track multiplicity. Assuming unit branching fractions for a 125 GeV Higgs, the limit is approximately

a factor of 4 above the SM production cross section at the low range of m_a and steadily weakens for larger m_a .

2. LHC high-multiplicity leptons

A variety of high-multiplicity lepton ($\geq 3\ell$) searches have now been completed at the LHC, mainly motivated by supersymmetry, including scenarios with R -parity violation. Several searches are focused on tau signals. Typical SUSY multilepton searches demand large amounts of \vec{E}_T , hadronic activity, and/or one or more b tags, any one of which can very efficiently eliminate the 4τ and $2\tau 2\mu$ Higgs signals. Still, relatively more inclusive three- and four-lepton searches have been performed by CMS [297–300] (most recently 9.2 fb^{-1} three- and four-lepton and 19.5 fb^{-1} four-lepton at LHC8) and ATLAS [301] (4.7 fb^{-1} at LHC7). While these largely utilize standard lepton and tau isolation requirements, they use quite low p_T thresholds. The analysis of [300] uses particle-flow isolation and does not count nearby leptons against each other. The multilepton searches are especially interesting to consider for $m_a \gtrsim 15 \text{ GeV}$, where the isolation issues are less severe and experimental vetoes on low-mass dilepton pairs are avoided.

3. LHC same-sign dilepton

Same-sign dileptons are also a standard signal of supersymmetry, and we expect that the usual searches are similarly unconstraining. However, ATLAS has performed an inclusive search for new physics in same-sign dileptons using the full 2011 data set [302]. While this again relies on lepton isolation, it is nonetheless useful to understand what kind of limit might apply to our scenarios.

4. New LHC recast limits

While the existing dedicated searches are not constraining, we can explore the power of the nondedicated searches. We keep our study as model independent as possible by scanning across the full kinematic range $m_a = [2m_\tau, m_h/2]$ and leaving $\text{Br}(h \rightarrow 2a)$ and $\text{Br}(a \rightarrow \tau^+\tau^-)$ as free parameters. We express our results as a function of the limits on total branching fraction $\text{Br}(h \rightarrow 2a \rightarrow 4\tau) = \text{Br}(h \rightarrow 2a) \times \text{Br}(a \rightarrow \tau^+\tau^-)^2$ versus m_a . Note that while masses above m_τ are not usually considered in conjunction with an appreciable Br to leptons, we again emphasize that they can arise easily if a is mostly composed of (or mixed into) the leptonic Higgs field in the type-III 2HDM. Depending on the a 's coupling to b quarks, there can also be nontrivial effects from decays and mixings into the bottomonium sector when $m_a \approx m_\Upsilon$, which we neglect (see [124,281] for more details).

A remaining free parameter is the CP phase of the a 's Yukawa couplings. Assuming CP conservation, a may be a CP -odd pseudoscalar or a CP -even scalar. We fix a to be the former. There are two consequences of favoring CP -odd over CP -even. First, this choice can affect the relative

Br's to 2τ and 2μ , but only for m_a very close to $2m_\tau$ [e.g., for $m_a = 5$ GeV, the ratio $\text{Br}(a \rightarrow \mu^+\mu^-)/\text{Br}(a \rightarrow \tau^+\tau^-)$ is approximately twice as large in the CP -even case]. Second, there is an imprint of the a 's CP on the azimuthal decay angle correlations of the two taus in the a rest frame. We expect this to be a minor effect, but it can in principle affect isolation rates.

We simulate ggF, VBF, and $(W/Z)h$ production of a 125 GeV Higgs decaying to $2a$ in PYTHIA 8.176 [303], which includes a full treatment of tau spin correlations.²¹ We set the cross sections to the values recommended by the LHC Higgs Cross Section Working Group [304]. For ggF, we reweight the p_T spectrum after showering to the NLO + NLL predictions of HQT 2.0 [305,306].

We do not apply a detector model nor simulate pileup. For the leptons, particle level should still furnish an adequate zeroth-order approximation of the full detector, including isolation. However, lepton identification efficiencies can be important, especially for soft leptons. CMS provides a detailed discussion and parametrizations of these efficiencies in the appendix of [300], and we apply these for our CMS analyses. For ATLAS, which uses harder lepton p_T cuts for the analysis that we study, we coarsely assume flat efficiencies of 90% for muons and 75% for electrons. Lepton isolation requirements vary by analysis, and we have adjusted them on a case-by-case basis.

The hadronic taus are much more difficult to reliably model. For these, we take a minimalistic approach, simply “rebuilding” each hadronic tau out of its visible decay products and applying a flat 50% identification efficiency if its visible p_T exceeds 15 GeV. However, two hadronic taus within $\Delta R < 0.45$ (averaging between ATLAS and CMS radii) are assumed to be unidentifiable, as are hadronic taus with a lepton with $p_T > 2$ GeV within the same radius. This mimics the isolation failures that would occur in these cases.

For the jets and missing energy, we reconstruct the former with the anti- k_T algorithm with $R = 0.45$, and the latter from the two-vector sum of all neutrinos. Jets that overlap with identified hadronic taus are removed.

We consider constraints from three recent LHC multi-lepton analyses.²²

- (1) *CMS PAS SUS-12-026*.—Three and four leptons in many exclusive bins, 9.2 fb^{-1} at 8 TeV [298].
- (2) *CMS PAS SUS-13-010*.—Four leptons with at least one OSSF pair, 19.5 fb^{-1} at 8 TeV [300].

²¹We have also checked $t\bar{t}h$. This production channel is rare, but it gives many opportunities for lepton production. We estimate that this represents up to a 10% contribution to the signal in the four-lepton and same-sign dilepton searches below but do not explicitly incorporate it into the derivation of constraints.

²²We do not consider the related but superseded analyses [297,301]. We also do not consider [299], which is very closely related to (1) and uses the same data set, but divides the analysis bins by S_T instead of by E_T . This division tends to give lower S/B in the three-lepton bins.

- (3) *ATLAS 1210.4538*.—Same-sign dileptons, 4.7 fb^{-1} at 7 TeV [302].

As a first step, we use the reported background rates to verify our treatment of the reconstructions. We generate diboson events in PYTHIA, and $W^\pm W^\pm$ and $t\bar{t}(W/Z)$ in MADGRAPH, normalizing each to NLO. For (1) and (2), we compare four-lepton analysis channels to our ZZ simulation. For (1), we use the channel “OSSF2, on-Z, $H_T < 200$ GeV, $E_T < 50$ GeV, $0\tau, 0b$.” We predict 56 events, and CMS predicts 73 ± 16 . For (2), we compare to the bin “ $M_1 = [75, 110]$ GeV, $M_2 = [75, 110]$ GeV.” It is normalized to the central CMS ZZ cross section measurement, which is about 10% higher than the NLO prediction. Weighting our sample accordingly, we predict 130 events, and CMS predicts 150. For (3), we compare our simulations to the “prompt” same-sign dilepton background estimated by ATLAS. In the $(e^\pm e^\pm, e^\pm \mu^\pm, \mu^\pm \mu^\pm)$ channels we obtain (78, 275, 165) events, and ATLAS predicts $(101 \pm 13, 346 \pm 43, 205 \pm 26)$. In all of the comparisons there is a systematic tendency for our predictions to underestimate the experiments by about 20%. This may be related to our idealized treatment of isolation and suggests that our Higgs signal estimates may be slightly conservative.

We run the search using a number of preselected bins from the different analyses. From the CMS multilepton searches (1) and (2), we focused on bins with high S/B . The selected bins are listed in Table VI. From the ATLAS same-sign dilepton search (3), we have added positive-charge and negative-charge counts for the $m(\ell^\pm \ell^\pm) > 15$ GeV bins, but maintained the binning in flavor. In Table VII we display the expected number of signal events for two example mass points ($m_a = 12$ GeV and $m_a = 50$ GeV) and compare to the SM backgrounds predicted by CMS and ATLAS.

We estimate 95% confidence constraints on $\text{Br}(h \rightarrow 2a \rightarrow 4\tau)$ using a simple CL_S analysis. Signal rates in the various experimental analysis bins come from our simulations. Background rates, their systematic errors, and observed counts come from the experiments. We do not apply a systematic error to the signal, as we cannot fully quantify the reliability of our modeling of the detection and reconstruction steps. (It should be understood that our signal predictions are merely a guide.) For our test statistic, we use the Poisson likelihood ratio between $S + B$ and B hypotheses, constructed using the central B expectation values. Within each pseudoexperiment, we vary the bin-by-bin expectation values for B according to the reported systematic errors, treating them as independent and Gaussian distributed.²³

Figure 24 shows the limits that we obtain from the individual analyses, as well as from a combination of the

²³Negative expectation values are reset to zero when they arise in the pseudoexperiments.

TABLE VI. Analysis bins used in setting our $h \rightarrow 2a \rightarrow 4\tau$ limits.

CMS PAS SUS-12-026 (9.2 fb ⁻¹ , 8 TeV)	
1a)	Three-lepton, OSSF0, $H_T < 200$ GeV, $E_T < 50$ GeV, $0\tau, 0b$
1b)	Three-lepton, OSSF0, $H_T < 200$ GeV, $E_T = [50, 100]$ GeV, $0\tau, 0b$
1c)	Three-lepton, OSSF0, $H_T < 200$ GeV, $E_T > 100$ GeV, $0\tau, 0b$
1d)	Three-lepton, OSSF0, $H_T > 200$ GeV, $E_T > 100$ GeV, $0\tau, 0b$
1e)	Three-lepton, OSSF1, below-Z, $H_T < 200$ GeV, $E_T < 50$ GeV, $0\tau, 0b$
1f)	Three-lepton, OSSF1, below-Z, $H_T > 200$ GeV, $E_T = [50, 100]$ GeV, $0\tau, 0b$
1g)	Three-lepton, OSSF1, below-Z, $H_T > 200$ GeV, $E_T > 100$ GeV, $0\tau, 0b$
CMS PAS SUS-13-010 (19.5 fb ⁻¹ , 8 TeV)	
2a)	$M_1 < 75$ GeV, $M_2 < 75$ GeV
2b)	$M_1 = [75, 110]$ GeV, $M_2 < 75$ GeV
ATLAS 1210.4548 (4.7 fb ⁻¹ , 7 TeV)	
3a)	$e^\pm e^\pm, m(\ell^\pm \ell^\pm) > 15$ GeV
3b)	$e^\pm \mu^\pm, m(\ell^\pm \ell^\pm) > 15$ GeV
3c)	$\mu^\pm \mu^\pm, m(\ell^\pm \ell^\pm) > 15$ GeV

CMS analyses. It can be seen that $\text{Br}(h \rightarrow 2a \rightarrow 4\tau)$ can be excluded at the 20%–40% level provided $m_a \gtrsim 15$ GeV, and that these limits are dominated by the CMS three-lepton bins. Below 15 GeV, standard quarkonium vetoes begin to make all of the searches very inefficient. Below about 10 GeV, isolation cuts also begin to have a major impact, though less significantly for analysis (2). We conclude that tight limits can already be placed with existing data, provided that a is massive enough and has small couplings to quarks so that $a \rightarrow b\bar{b}$ does not compete. However, this leaves fully open the interesting NMSSM-motivated region with $m_a \lesssim m_\tau$.

D. Proposals for new searches at the LHC

We have focused on multilepton searches because they are relatively clean and because existing limits could be quickly estimated. These results can be considered an update and extension of some of the strategies proposed in [292]. The other strategies discussed in Sec. VI B can also have a significant role, and we might expect versions of these searches in the near future from the LHC experiments using the 2012 data set. It will be interesting to see how these extend the limits that we have estimated, especially for lighter m_a . However, looking ahead to possible future searches, we can concretely suggest a novel strategy: exploit the $2\tau 2\mu$ final state within three- and four-lepton events.²⁴ This would supplement the more inclusive $2\tau 2\mu$ search proposed in [104] and implemented in [287], representing an analysis channel with extra-low backgrounds. Given the shrinking range of viable Br, and the relatively high rate for

²⁴A similar strategy was also discussed for associated production of a with a heavy Higgs (via $q\bar{q} \rightarrow Z^* \rightarrow Ha$) in the lepton-specific 2HDM [307]. That study was aimed at $m_a, m_H \gtrsim 100$ GeV.

TABLE VII. Signal predictions and SM backgrounds in all of the analysis bins considered for exclusions in this subsection. See Table VI for descriptions. The signal prediction here is given fixing $\text{Br}(h \rightarrow 2a \rightarrow 4\tau) = 10\%$ for reference, though it is a free parameter in setting the exclusions.

Channel	$m_a = 12$ GeV	$m_a = 50$ GeV	Background	Observed
1a)	2.57	3.31	27 ± 6.7	23
1b)	0.19	1.1	17.75 ± 7.5	16
1c)	0.01	0.18	4.5 ± 2.3	3
1d)	0	0.3	1.9 ± 1.2	1
1e)	2.5	9.5	282 ± 29	258
1f)	0	0.29	4.5 ± 0.9	4
1g)	0.02	0.68	3.5 ± 0.8	2
2a)	1.48	0.2	10.4 ± 2	14
2b)	0.97	0.22	35 ± 8	30
3a)	2.8	3.7	346 ± 44	329
3b)	7.2	9.2	639 ± 71	658
3c)	3.7	5.5	247 ± 30	264

the 2τ side of the event to produce a lepton, this type of search should offer good long-term prospects.

We have observed in our own simulations that a surprisingly large fraction of three-lepton and four-lepton events passing experimental cuts come from the $2\tau 2\mu$ channel. For example, for the point $m_a = 60$ GeV within the bin “three-lepton, OSSF1, below-Z, $H_T < 200$ GeV, $E_T < 50$ GeV, $0\tau, 0b$ ” (1e), about 20% of the events contain $a \rightarrow 2\mu$. Since S/B will improve by far more than a factor of 5 by focusing in on a tight resonance peak, this suggests that a powerful search could be constructed by utilizing $m(\mu^+\mu^-)$ spectral information within high-multiplicity lepton events. The resonance also offers a much safer way to search within the $m_a \lesssim 10$ GeV region, where leptonic a decays are expected to dominate for a broader class of models.

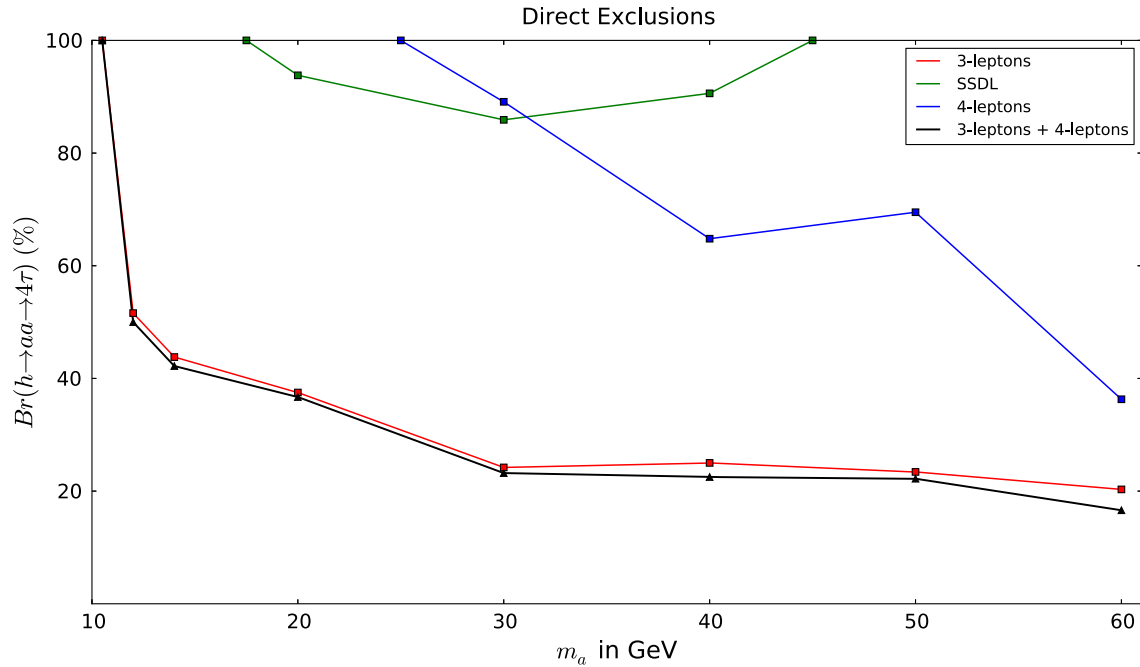


FIG. 24 (color online). Estimated exclusion of $\text{Br}(h \rightarrow 2a \rightarrow 4\tau)$ from LHC multilepton and same-sign dilepton searches: (1) CMS three-lepton from [298] in red, (2) CMS four-lepton from [300] in blue, (3) ATLAS same-sign dilepton from [302] in green. The black line shows a combination of the multilepton searches (1) and (2). [The combination of all channels, including (3), is less constraining by several percent.]

To construct an example of such a search, we can follow the reconstructions of the CMS four-lepton analysis [300] [search (2) above], but removing their restriction $m(\ell^+\ell^-) > 12$ GeV and allowing events with three or more leptons instead of exactly four. Crucially for the low-mass region, this search uses a full particle-flow form of isolation and does not count leptons towards each others' isolation cones. We include a Z veto to help reduce Z + jets and diboson backgrounds. We also focus on “below- Z ” events, where the $\ell^+\ell^-$ pair closest to the Z mass is below 75 GeV. These vetoes have little effect on the signal efficiencies.²⁵

In reconstructing the $\mu^+\mu^-$ resonance, there remains a combinatoric issue when more than one pairing of this type is possible. This ambiguity afflicts the majority of three-lepton and four-lepton events containing at least one $\mu^+\mu^-$ pair, since muons are reconstructed with higher efficiency than electrons. (For example, $\mu^+\mu^-\mu^\pm$ is found more often than $\mu^+\mu^-e^\pm$.) In practice, it is possible to pick the smallest-mass pairing for $m_a \ll m_h/2$ and the largest-mass

pairing for $m_a \approx m_h/2$. However, for $m_a \approx m_h/4$, neither of these options is ideal. Instead, we can construct a third option by using the fact that $m_h \approx 125$ GeV, that the Higgs decays isotropically, and that it is usually produced with little transverse boost: we pick the $\mu^+\mu^-$ pair whose trajectory would make the largest opening angle with the beam in the Higgs rest frame, assuming $p_T(h) = 0$. For each m_a , we use the pairing choice that gives the strongest resonance peak.²⁶

Estimating backgrounds to such a search can be difficult, as leptons from heavy flavor decays and from fakes can be significant contributions. We have simulated the contributions from electroweak three-lepton and four-lepton production, including taus and allowing for Z^*/γ^* down to $m \sim \text{GeV}$. Given a signal that lives inside of a resolution-limited mass window of approximately $(1 \pm 0.01)m_a$, these backgrounds are usually small, tallying to $\mathcal{O}(1)$ event for any m_a for 2012. The dominant $Z^*/\gamma^* + \text{jets}$ background can be coarsely estimated from the sum of below- Z bins of analysis (1) and would constitute approximately 800 events

²⁵It might also be possible to apply a E_T discriminator for this search, though we have not attempted this. The E_T in signal events tends to be below 50 GeV. An accurate understanding of the efficacy of a E_T cut would require a resolution model, as well as a model for the E_T distribution of backgrounds. An approximate reconstruction of the Higgs resonance might also be possible and usable either for further discrimination or for verification of the source of a possible signal.

²⁶The crossover between smallest-mass and largest-mass choices being the most effective is at $m_a \approx 40$ GeV, and in this region the largest-opening-angle choice keeps about 15% more events in the peak. For very low-mass resonances, this choice underperforms the smallest-mass choice by a comparable amount, and similarly for high-mass resonances (near $m_h/2$) relative to the largest-mass choice.

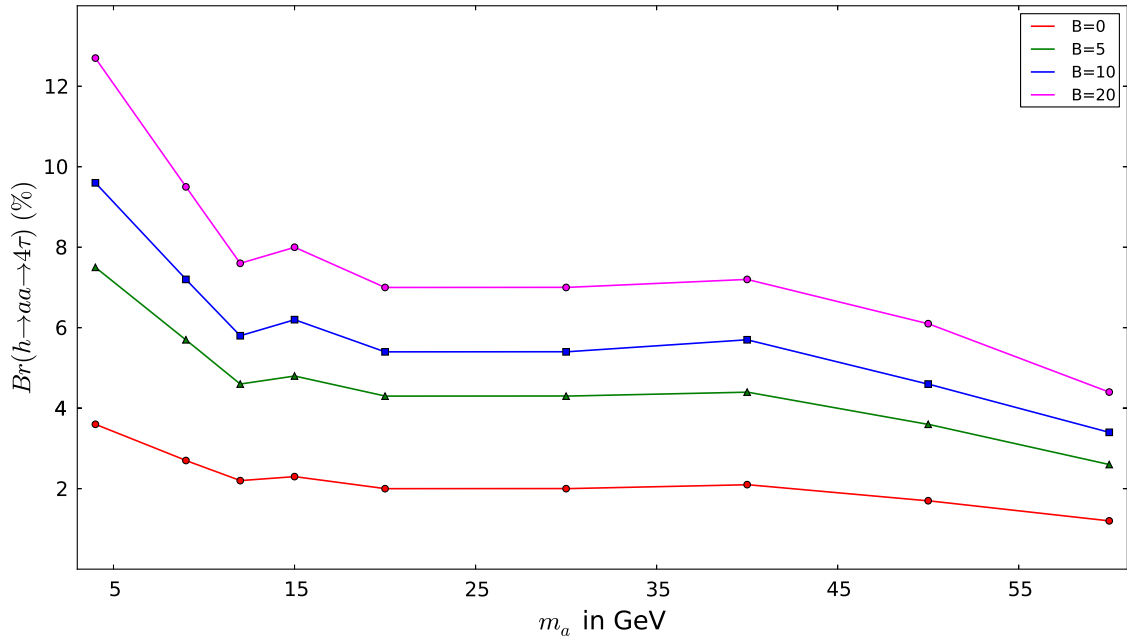
Expected exclusion with 2012 data from $\mu^+\mu^-$ resonances

FIG. 25 (color online). Median estimates of expected indirect exclusions on $\text{Br}(h \rightarrow 2a \rightarrow 4\tau)$ using the subdominant ($a \rightarrow 2\tau$) \times ($a \rightarrow 2\mu$) channel and exploiting that leptonic branching fractions of a are mass ordered. The results are based on a simulated $\mu^+\mu^-$ resonance search in $\geq 3\ell$ events, assuming the 2012 data set. Since we cannot reliably predict the background under the resonance peak, we show expected exclusions for $B = 0, 5, 10$ and 20 events, respectively. We neglect systematic uncertainties. (The lowest displayed mass is 4.0 GeV.)

for $m(\mu^+\mu^-) \gtrsim 10$ GeV with 20 fb^{-1} . (In this estimate, we conservatively do not attempt to remove the e^+e^- events.) We are not given a spectral shape for this background, but if we assume that it is not very strongly featured, then we can estimate $\mathcal{O}(10 \text{ events})$ per 1 GeV interval. We also do not know the spectrum for $m(\mu^+\mu^-) \lesssim 10$ GeV, though the shrinking absolute resolution on $m(\mu^+\mu^-)$ (down to less than 100 MeV at CMS) allows the differential background rate to grow by an order of magnitude without affecting S/B . Of course, extra care would need to be taken in the vicinity of known hadronic resonances such as the Υ 's.

To give a sense of what might be possible with the 2012 data set, we show in Fig. 25 the limits assuming a sequence of possible background levels with $m(\mu^+\mu^-)$ within $\pm 1\%$ of m_a , and neglecting systematics. Taking as reference $\text{Br}(h \rightarrow 2a \rightarrow 4\tau) = 10\%$, the signal rates inside the peak vary from eight events for $m_a = 4$ GeV to 25 events for $m_a = 60$ GeV. Depending on the background assumption and on m_a , the excluded $\text{Br}(h \rightarrow 2a \rightarrow 4\tau)$ varies from percent scale to just above 10%. This strong level of exclusion applies even down to $m_a \approx 2m_\tau$.²⁷ We imagine

²⁷Note that while isolation of a single lepton from the $a \rightarrow \tau^+\tau^-$ side of the event becomes progressively more difficult for low-mass points, $\text{Br}(a \rightarrow \mu^+\mu^-)$ is also increasing. At 4 GeV, the rate has doubled. This effect would be even more pronounced for CP -even scalars.

that these results will only improve as data from the next run of the LHC become available, provided that the multilepton triggers can be maintained at p_T thresholds comparable to their 2012 values.

VII. $h \rightarrow 4j$

Standard Model decays of the Higgs boson can lead to a four-jet final state via intermediate vector boson decays, $h \rightarrow WW^*/ZZ^* \rightarrow jjjj$. Only one of the jet pairs is produced on resonance in this process. In this section, we discuss the distinct possibility of exotic Higgs decays to $4j$ in a two-step decay process proceeding through a neutral (pseudo)scalar field a : $h \rightarrow aa \rightarrow jjjj$. There are then two jet-pair resonances. Below, we outline the theoretical motivations for considering $4j$ decays of the Higgs and discuss the LHC phenomenology and future discovery prospects of this channel.

A. Theoretical motivation

The $h \rightarrow jjjj$ channel has been extensively studied in the context of super Little Higgs models [308–310] (a brief description of the Little Higgs mechanism is given in Sec. I C 9). The intermediate decay product a is a PNCB and generally very light. In a large region of parameter space of these models, $h \rightarrow aa \rightarrow jjjj$ is the dominant decay mode.

Given that the Higgs mass of approximately 125 GeV requires fine-tuning of the simplest versions of these models, one may take a simplified model approach for the cascade decay in the presence of a light pseudoscalar (or scalar) a . Two possibilities allow for the decay of a to jets.

- (i) The pseudo(scalar) a can mix with another heavier pseudoscalar if a second Higgs doublet is present, for example in the NMSSM or, more generally, in the 2HDM + S models; see Secs. IC 2 and IC 6. This allows for the decay of a to SM fermions, often (depending on the 2HDM type) dominated by $a \rightarrow b\bar{b}$ for $m_a > 2m_b$ and $a \rightarrow \tau^-\tau^+$ for $2m_\tau < m_a < 2m_b$ for a large or moderate $\tan\beta$. This leads to $4b$, $2b2\tau$, $2b2\mu$, 4τ , and $2\tau2\mu$ signals as discussed in Secs. III–VI. However, if a is very light ($3m_\pi < m_a < 2m_\tau$), it predominantly decays to two (merged) light jets as the above channels are not kinematically viable.

If $\tan\beta$ is small ($\tan\beta \lesssim 0.5$), the couplings of a to the down-type quarks and charged leptons can be very suppressed. In this case, a dominantly decays to light (mostly charm) jets even if decays to b 's or τ 's are kinematically allowed. Thus, the parameter space of m_a up to $m_h/2$ is available for the exotic-decay mode. A similar situation also occurs in the “charming Higgs” scenario of the Little Higgs model [221].

- (ii) New heavy BSM vectorlike fermions can couple to a and, therefore, allow for its decay into gluons or photons through loop processes [202,264,311]. This scenario can be realized in Little Higgs models and extra dimensional models. For m_a above a few GeV up to $m_h/2$, $h \rightarrow aa \rightarrow gggg$ dominates over $h \rightarrow aa \rightarrow \gamma\gamma gg$ and $h \rightarrow aa \rightarrow \gamma\gamma\gamma\gamma$. In general, the signal is hard to find against combinatorial background. However, large masses of the new vectorlike fermions may lead to visibly displaced vertices of $a \rightarrow gg$, which can enhance the discovery potential of the channel [311]. Studies on related decay modes in this scenario, $h \rightarrow aa \rightarrow \gamma\gamma gg$ and $h \rightarrow aa \rightarrow \gamma\gamma\gamma\gamma$, can be found in Secs. VIII and IX, respectively.

B. Existing collider studies

Before the discovery of the 125 GeV Higgs boson, much of the phenomenology of the Higgs decaying to four jets was aimed at hiding the Higgs boson at LEP. One way to accomplish this was in the “buried Higgs” scenario, where the decay $h \rightarrow jjjj$ is “buried” in the large QCD background. Indeed, the LEP bounds for this scenario are much weaker than the bound on a SM Higgs. For $m_h > 90$ GeV [291], m_a was studied in a range where each pair of jets from the pseudoscalar decay would be highly collimated and appear as a single jet.

There are a few existing collider studies for the 14 TeV LHC run in the four-jet final state. In [222] the authors study the $h \rightarrow 4c$ decay mode in the context of charming Higgs. We mention this study here since it does not use b tagging and hence is useful for generic $4j$ decays. The study uses jet substructure to help identify the pseudoscalar as a boosted jet while reducing the otherwise overwhelming background.

Other relevant collider studies are [220,269], which we briefly summarize below. (There also exist collider studies that consider exotic Higgs production modes [268], but we do not consider them here.)

In [269], Higgs production in association with a W boson is considered as the production mode for $m_h = 120$ GeV followed by the Higgs decay, $h \rightarrow aa \rightarrow jjjj$. The pre-selection cuts in this analysis include isolated leptons with $p_T > 20$ GeV, at least two jets with $p_T > 40, 30$ GeV, reconstructed leptonic W transverse mass $m_T < m_W$, and a b -jet veto to reduce SM background. Further analysis is divided into categories depending on the mass of a .

- (i) $m_a = 4$ GeV.—In this case the gluons from a decay appear as a single jet to the hadronic calorimeter (HCAL). ECAL variables are imposed to distinguish these merged jets from single-pronged QCD jets. 7σ significance is possible at the LHC14 with 30 fb^{-1} data assuming $\text{Br}(h \rightarrow aa \rightarrow gggg) \sim 100\%$. However, assuming a more realistic branching ratio of $\text{Br}(h \rightarrow aa \rightarrow gggg) \sim 10\%$ in the post Higgs discovery era, 2σ exclusion (3σ evidence) is possible with 300 fb^{-1} (500 fb^{-1}) of data at LHC14.
- (ii) $m_a = 8$ GeV.—Simple jet substructure techniques can be used for discovery. The authors find that $\sim 3\sigma$ statistical significance can be reached with 30 fb^{-1} data assuming $\text{Br}(h \rightarrow aa \rightarrow gggg) \sim 100\%$. With $\text{Br}(h \rightarrow aa \rightarrow gggg) \sim 10\%$, however, 2σ exclusion (3σ evidence) requires 1000 fb^{-1} (3000 fb^{-1}) of data at LHC14.

A separate jet substructure analysis on $h \rightarrow aa \rightarrow jjjj$ is also presented in [220], with the inclusion of the $t\bar{t}h$ production channel besides the Vh channel, demonstrating similar discovery potential in both channels. Here variables sensitive to the soft radiation patterns of the color singlet $a \rightarrow gg$ jet are employed instead of ECAL-based observables. The authors reach a similar conclusion for discovery prospects as described above.

The above two analyses [220,269] have exploited the fact that very light (pseudo)scalars are boosted, leading to two fat jets. A more recent study [267] explores the $m_a > 15$ GeV regime. It focuses on the substructure of fat jets containing an entire boosted Higgs decay, and that could be two-, three-, or four-pronged. As before, Higgs production in association with vector bosons is considered. The authors include two cases depending on the mass of the scalar, s : (i) light scalar ($15 < m_s < 30$ GeV) and (ii) heavy scalar ($30 \text{ GeV} < m_s < m_h/2$). In the lighter regime, the

$h \rightarrow ss \rightarrow jjjj$ signature with 100% branching ratio can be observed at a significance of 3σ with 100 fb^{-1} of 14 TeV LHC luminosity, while for the heavy scalar case, the significance is too small to observe with the same amount of data. For a more realistic $\text{Br}(h \rightarrow 2a \rightarrow 4j) = 10\%$, 2σ exclusion for the light scalar case requires 1500 fb^{-1} . (Note the achievable limits become much stronger for $h \rightarrow 4b$ with b tags; see Sec. III.)

C. Existing experimental searches and limits

There are currently no existing experimental searches looking for a four-jet resonance in the low invariant mass region, which is understandable due to the large QCD background. Neither are there any existing searches that look for fat-jet resonances.

Overall, this is a highly challenging exotic Higgs decay channel. For $m_a \lesssim 5 \text{ GeV}$, 2σ exclusion of $\text{Br}(h \rightarrow 2a \rightarrow 4j) = 10\%$ requires 300 fb^{-1} of LHC14 data, while $m_a \gtrsim 5 \text{ GeV}$ requires more than 1000 fb^{-1} . This search should be undertaken at the 14 TeV LHC (especially for light m_a , where the decay is particularly motivated), but it is not plausibly part of the LHC7 or 8 physics program.

VIII. $h \rightarrow 2\gamma 2j$

A relatively clean exotic-decay mode of the Higgs boson is $h \rightarrow 2\gamma 2j$ [312]. The SM rate for this signature is negligible: decays into $2\gamma 2q$ are highly Yukawa suppressed while the $2\gamma 2g$ process is loop induced. However, going beyond the SM, more possibilities arise. In particular, here we consider Higgs boson decays to two scalars $ss^{(\prime)}$ which subsequently decay into photons and gluons or quarks. Below we outline some possible theoretical scenarios leading to such decays and briefly discuss their collider phenomenology.

A. Theoretical motivation

There are several ways in which a SM singlet scalar decays to photons, gluons or quarks. For example, it can do so via mixing with the Higgs boson, as in the singlet extensions discussed in Secs. IC 1 and IC 2. This will generally give a very suppressed rate to photons compared with that of quarks or gluons, due to the electromagnetic loop factor.

Alternatively, a singlet scalar s may couple to gluons and photons via a dimension-five operator $sF^{\mu\nu}F_{\mu\nu}$, which arises by introducing new colored and charged vectorlike states and coupling them to s . Such scenario can easily accommodate larger or even dominant $s \rightarrow 2\gamma$ branching ratios, depending on the color versus electric charge assignments of the new states. As a simple example, consider adding new heavy Dirac fermions ψ_i along with Yukawa couplings of the form $\lambda_i s \bar{\psi}_i \psi_i$. The fermions reside in a representation R_i under $SU(3)_C$ and have electric charge Q_i and mass m_i . The scalar s then decays to gluons

and photons via heavy fermion loops. The resulting branching ratios satisfy

$$\rho = \frac{\text{Br}(s \rightarrow 2\gamma)}{\text{Br}(s \rightarrow 2g)} = \frac{1}{8} \left(\frac{\alpha}{\alpha_s} \right)^2 \left[\frac{\sum \lambda_i Q_i^2 N(R_i)/m_i}{\sum \lambda_i C(R_i)/m_i} \right]^2, \quad (75)$$

where $N(R_i)$ and $C(R_i)$ are the dimension and normalization factor, respectively, of the representation R_i (the normalization factors of the lowest lying color representations $R = 3, 6, 8$ are $C = 1/2, 5/2, 3$). For example, one heavy down-type quark b' and one heavy charged lepton τ' [a combination which appears in a single “5” multiplet of $SU(5)$, along with a heavy neutrino], with masses m_2 and m_3 , and Yukawa couplings λ_2 and λ_3 , respectively, would result in

$$\begin{aligned} \rho &= \frac{1}{18} \left(\frac{\alpha}{\alpha_s} \right)^2 \left(1 + 3 \frac{\lambda_2 m_3}{\lambda_3 m_2} \right)^2 \\ &\simeq 0.02 \left(\frac{\lambda_2}{\lambda_3} \right)^2 \left(\frac{m_3}{30 \text{ TeV}} \right)^2 \left(\frac{10 \text{ TeV}}{m_2} \right)^2. \end{aligned} \quad (76)$$

Note that the heavy fermions need not be light in order to induce 2γ or $2g$ decays, as long as the singlet s does not mix with the Higgs boson.

In principle, the 4γ mode (Sec. IX) is much cleaner than $2\gamma 2j$, which is in turn much cleaner than the very difficult $4j$ (Sec. VII). However, since

$$\frac{\text{Br}(h \rightarrow 4\gamma)}{\text{Br}(h \rightarrow 2\gamma 2g)} \simeq \frac{1}{4} \frac{\text{Br}(h \rightarrow 2\gamma 2g)}{\text{Br}(h \rightarrow 4g)} \simeq \frac{1}{2} \frac{\text{Br}(s \rightarrow 2\gamma)}{\text{Br}(s \rightarrow 2g)} = \frac{\rho}{2}, \quad (77)$$

for small enough values of ρ , as defined in Eq. (75), the 4γ rate would be too small to be observable for a given integrated luminosity. In such a situation, which occurs if b' and τ' are degenerate in mass and couplings, the $2\gamma 2j$ signature may be competitive with 4γ .

Of course, the model described above is just one example of $h \rightarrow 2\gamma 2g$ decays. Other examples may feature two different states, s and s' , allowing for even more model-building freedom, or decays to quarks instead gluons. Since the main focus of this section is to explore the $2\gamma 2j$ signature and propose ways to discover it at the LHC, we content ourselves with the model described above and continue to discuss discovery reach and limits.

B. Existing collider studies

In [312], a search has been proposed for this channel, and the discovery (5σ) reach at the 14 TeV LHC with 300 fb^{-1} was derived as a function of the scalar mass m_s and Higgs mass m_h . Gluon fusion (ggF) and W -associated production (Wh) were considered. Here we only make use of the latter, both because it provides superior sensitivity in this analysis and because the ggF study, which was conducted before the

LHC came online, incorporated diphoton p_T thresholds which are much lower than current triggers.

The Wh analysis in [312] proceeds as follows: events are required to contain one lepton, two photons and two jets with $p_T > 20$ GeV and $|\eta| < 2.5$ for each of these objects. Moreover, each object pair $(jj, \gamma\gamma, j\gamma, j\ell, \ell\gamma)$ is subject to an angular isolation criterion of $\Delta R > 0.4$. The events are also required to have $E_T > 20$ GeV. Additional cuts made were $\Delta\phi_{\gamma\gamma} < 1.5$, $\Delta\phi_{jj} < 1.3$, and $|m_{jj} - m_{\gamma\gamma}| \leq 15$ GeV. The Higgs mass resolution was assumed to be ~ 8 – 10 GeV. The signal efficiency is claimed to be between 3% and 15% within the relevant mass range.

Rescaling the 5σ limit at 14 TeV with 300 fb^{-1} to 95% C.L. yields the sensitivity shown as the solid blue curve in Fig. 26. An estimate for the lower luminosity²⁸ of 100 fb^{-1} is shown as the blue dashed curve. At the 14 TeV LHC, a sensitivity to $\text{Br}(h \rightarrow 2\gamma 2j)$ below 0.01 is possible for part of the kinematically allowed s mass range. This study can also be used to obtain a *conservative* estimate of the sensitivity at the 8 TeV LHC. We scale the production cross section down appropriately without doing so for the background cross section. This will underestimate the strength of the limit (assuming the efficiencies do not change by a large amount at 8 versus 14 TeV). The resulting 95% C.L. sensitivity is shown as the green dash-dotted curve in Fig. 26. Run I data should be able to set a limit on $\text{Br}(h \rightarrow 2a \rightarrow 2\gamma 2j)$ as low as ~ 0.04 for some scalar masses, and likely better than that, given our pessimistic rescaling.

Two comments are in order.

- (1) Note that the angular isolation cuts reduce the background, but effectively eliminate sensitivity for $m_s \lesssim 20$ GeV. This weakness of the proposed search might be remedied by means of jet substructure-inspired techniques [313,314] (see also Sec. IX).
- (2) Since the best limits seem to be given by associated Wh production, we do not expect too much difficulty with triggering. However, since the threshold for the single lepton trigger will be raised for LHC14, it would be helpful to have a trigger that requires a lepton *and* a photon.

C. Existing experimental searches and limits

There are no limits from existing searches. Potentially relevant searches, such as supersymmetry searches and isolated photon-pair searches [315,316], are generally insensitive to $h \rightarrow 2\gamma 2j$, since (a) they employ relatively hard cuts and (b) without a cut on the total invariant mass, the QCD background is overwhelming.

The $h \rightarrow 2\gamma$ search in the VBF mode also cannot be used to place limits on $2\gamma 2j$, since the VBF dijet tag is targeted at

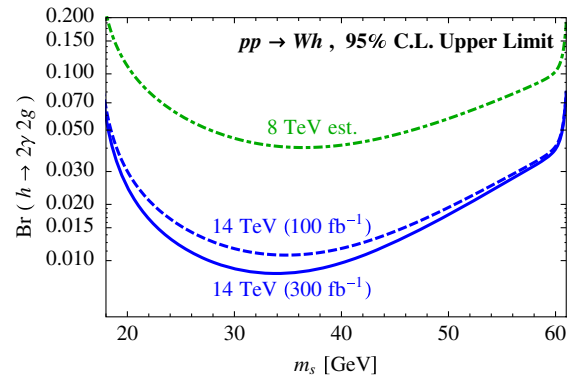


FIG. 26 (color online). Projected 95% C.L. limits on the branching fraction for $h \rightarrow 2\gamma 2g$ in associated production (Wh), as a function of m_s . The blue curves refer to 300 fb^{-1} (solid) and 100 fb^{-1} (dashed), both at the 14 TeV LHC. The dashed-dotted green curve shows a conservative estimate of the sensitivity for 20 fb^{-1} at 8 TeV. All three limits build on the proposed search in [312] (300 fb^{-1} at 14 TeV LHC), by scaling background with luminosity but not changing its cross section, while signal is rescaled according to both luminosity and cross section. This underestimates the achievable 8 TeV limit. See text for more details.

the forward and high rapidity gap region where a $2\gamma 2j$ signal is faint.

D. Proposals for future searches

Based on the results from [312], both the gluon fusion and the Vh associated production mode should be explored for $h \rightarrow 2j 2\gamma$ sensitivity at LHC runs I and II.

An interesting issue arises for very light intermediate resonances, which may result in unexpected signatures, as follows. As mentioned above, the previous search strategy involved an isolation cut on the photons. This spoils sensitivity for light s particles, since these would decay to a collimated pair of photons or gluons. One would therefore be missing an important portion of parameter space below $m_s \sim 20$ GeV. Using more sophisticated photon identification inspired by jet substructure techniques will improve the situation. However, for low enough $m_s \lesssim \text{GeV}$, the two jets cannot be resolved, resulting in a $j + 2\gamma$ signature.

Furthermore, in [317] it was shown that for very low $m_s \lesssim 100$ MeV the diphoton system is so collimated that a substantial fraction of the photon pairs would deposit their energy in a single electromagnetic calorimeter cell,²⁹ resulting in $h \rightarrow 4\gamma$ mimicking 2γ and 3γ signatures. While a scalar as light as to induce merged photons is generally not able to decay into gluons (namely, hadrons), having two different states with different masses may allow

²⁸Our rescalings include the assumed 10% systematic errors on the background rate [312].

²⁹The study in [317] was geared toward the ATLAS detector, but similar principles may be applied to CMS as well.

for merging both photons and gluons, resulting in signatures such as $2j + \gamma$ or $j + \gamma$.

It is therefore interesting to consider such topologies, although they are considered “impossible” for Higgs decays due to the “wrong” quantum numbers they seemingly possess. These subtleties should be taken into account when conducting a future $2\gamma 2j$ search. At the trigger level the two merged photons could pass as one single photon, necessitating the use of a single photon (possibly + jets) trigger.

IX. $h \rightarrow 4\gamma$

Here, we consider the decay of a Higgs to four photons. In the SM, the branching fraction for this decay is negligible, as it results from a dimension-nine operator and contains an additional factor of α in the amplitude relative to $h \rightarrow \gamma\gamma$. However, it can be important in certain new physics scenarios, as we now discuss.

A. Theoretical motivation

The basic decay chain that we consider is $h \rightarrow aa^{(\prime)}$, $a^{(\prime)} \rightarrow \gamma\gamma$. Enumerating the possible quantum numbers of the intermediate particles is simple if they decay into two photons and have spin less than two: they must be neutral and spin-0 by the Landau-Yang theorem [318,319]. The CP phase of the $a^{(\prime)}$ makes no difference phenomenologically as long as the photon polarizations are not measured.

There are a number of theoretically well-motivated candidates for a , among them the lighter pseudoscalar of the NMSSM, any pseudoscalar that mixes with the CP -odd Higgses of the (N)MSSM, or a generic SM-singlet boson whose coupling to photons is mediated by a renormalizable coupling to heavy vectorlike matter. In the first two cases, the coupling of a to light SM fermions can make the branching for $a \rightarrow \gamma\gamma$ subdominant, but the low backgrounds in 4γ can nonetheless make it an interesting final state. On the other hand, if a couples at the renormalizable level only to the Higgs and to heavy vectorlike uncolored matter, it may *only* be able to decay to $\gamma\gamma$, rendering the 4γ final state extremely important. If, alternatively, the vectorlike matter is colored and $a \rightarrow gg$ is allowed, $h \rightarrow gg\gamma\gamma$ can also be important (see Sec. VIII for details).

It is also worth noting that if $m_a < 2m_\mu$, only the $\gamma\gamma$ and e^+e^- final states may be kinematically allowed. The other final states in this case, $4e$ or $2e2\gamma$, are broadly similar phenomenologically to 4γ , since they involve electromagnetically interacting particles. We do not discuss them further here, leaving a detailed study for the future [320]. Furthermore, as we show below, for $m_a \lesssim 100$ MeV with a decaying only to photons, a is typically long lived on collider scales, potentially leading to displaced vertices or missing energy. Long lifetimes are also possible in certain hidden-valley models, even for much larger masses [32,224].

B. Existing collider studies

The $h \rightarrow aa \rightarrow 4\gamma$ decay chain was studied in [202], focusing on the Tevatron. In this paper, it was pointed out that for $m_a \lesssim 0.025m_h$ the a 's are boosted enough that photons coming from their decays are collimated to the extent that they will often deposit their energy in a single calorimeter cell, fail isolation cuts and potentially be reconstructed as a single photon. (We discuss some of the experimental issues regarding closely spaced photons below, focusing on the LHC.) This light a scenario is motivated if, e.g., a is the lightest pseudoscalar in the R -symmetric limit of the NMSSM (see Sec. I C 7). The results of the analysis of [202] imply that the full Tevatron data set is sensitive to branchings of $h \rightarrow aa$ at about the 0.5% level or larger, assuming $\text{Br}(a \rightarrow \gamma\gamma) = 1$.

In [311], a detailed study was performed of the $h \rightarrow aa \rightarrow 4\gamma$ decay at the LHC with $\sqrt{s} = 14$ TeV. The experimental cuts made in this study were that the transverse momenta of the photons were all greater than 20 GeV, the distance between the photons was $\Delta R > 0.4$, the photons had rapidity $|\eta| < 2.5$, and there were two separate pairs of photons that reconstructed the same invariant mass (the candidate a mass) to within 5 GeV. Finding backgrounds to be negligible with these cuts, this work indicated that for a Higgs at 125 GeV, 300 fb⁻¹ of data at the 14 TeV LHC would allow branchings $\text{Br}(h \rightarrow aa) \approx 5 \times 10^{-5}$ to be discovered at the 5σ level for $10 \text{ GeV} \lesssim m_a \lesssim m_h/2$, assuming that the a 's decay promptly to photons only. Rescaling this to 100 fb⁻¹ would indicate that $\text{Br}(h \rightarrow aa) \approx 9 \times 10^{-5}$ could be found at 5σ . The isolation cut of $\Delta R > 0.4$ is the reason for the lower bound on the a mass that can be accessed. A naive rescaling by the decreased luminosity and Higgs production cross section of the 7 and 8 TeV data sets, assuming that the dominant backgrounds' cross sections do not change appreciably, implies that the current data are sensitive to $\text{Br}(h \rightarrow aa) \sim \text{few} \times 10^{-4}$. As emphasized in [311], the reach is extremely sensitive to the value of the photon p_T cut, especially in the case of a relatively light Higgs with $m_h = 125$ GeV.

Closely spaced pairs of photons in $h \rightarrow aa \rightarrow 4\gamma$ at the LHC when $m_a \ll m_h = 125$ GeV were studied recently in [317], motivated by early hints at $\sqrt{s} = 7, 8$ TeV that the Higgs rate to diphotons could be larger than in the SM. However, photon pairs that fail mutual isolation criteria might or might not be detected as a single photon depending on the details of their geometric distribution, as we now explain in detail.

As mentioned above, it was noted in [202] that at the Tevatron, for sufficiently small m_a , the pairs of photons from each a decay could be collimated enough to appear as a single photon in the detector. If $m_a \lesssim 10$ GeV with the a 's produced in the decay of a 125 GeV Higgs, the photons that they decay into will fail the typical isolation cut of $\Delta R = 0.4$. However, their energy depositions in the

ECAL will normally be broader than that of a true single photon (whose electromagnetic shower has a typical width that is material dependent, called its Molière radius) and will not be tagged as a single photon. As the mass of the a is pushed down further, the decay photons do eventually become merged enough that their energy depositions are no longer much broader than a single photon's. The value of m_a where this becomes important depends on the spatial resolution of the ECAL in question. The increased granularity of the LHC detectors compared to those at the Tevatron means that m_a must be smaller at the LHC than at the Tevatron for this to be the case. At ATLAS, a single photon's electromagnetic shower deposits its energy in several neighboring cells in the innermost central portion of the ECAL where the cells have a width in the η direction of 0.0031 (corresponding to ~ 0.5 cm) because the Molière radius of the absorbing material, lead, is $\mathcal{O}(\text{cm})$ [321]. In Ref. [317], it was found that requiring $\Delta\eta < 0.0015$ (half the smallest cell size at ATLAS) between the two nearby photons from an a decay successfully reproduced the shower shape cuts used to distinguish single photons. For the photons to be this closely separated, $m_a \lesssim 100$ MeV.³⁰ In such a case, an apparent increase of $\sim 50\%$ in the apparent $h \rightarrow 2\gamma$ rate could be achieved for $\text{Br}(h \rightarrow aa) \approx 10^{-3} - 10^{-2}$. Other possible experimental consequences of this scenario mentioned in [317] are an increase in the number of events containing a converted photon, a mismatch between the momentum of charged tracks and the energy deposition in the calorimeter in conversions (when one of the two nearby photons converts), or the appearance of apparent $h \rightarrow \gamma + j$ events when one pair of photons is very collimated, faking a single photon, while the other is broader, failing isolation requirements for photons and looking like a jet (with large electromagnetic content).

Additionally, the usefulness of jet-substructure-motivated detector variables in distinguishing closely separated photons (termed photon jets generically in [322]) from single photons and their interplay in $h \rightarrow 4\gamma$ faking $h \rightarrow \gamma\gamma$ at the LHC was studied in detail in [313,314], dealing with both the case where the photons were merged enough to potentially fake a single photon and that in which they are less closely merged but do still fail isolation cuts, potentially looking like a jet. Examining $h \rightarrow 4\gamma$ with a Higgs mass of 120 GeV, they determined that the use of such variables could decrease the rate of photon jets faking single photons by a factor of over 10 while preserving at least 80% of the single photon signal.

Most of the literature assumes that the photon pairs necessarily reconstruct two equal-mass resonances; however, this will not be the case when two different particles a

³⁰This critical value of m_a makes sense since the LHC detectors were designed to be able to tell neutral pions apart from single photons.

and a' are introduced and the decay mode $h \rightarrow aa'$ is allowed. For an example of such a model which assumes $m_a \approx m_h$ and $m_{a'} \lesssim \text{GeV}$, which was originally designed to increase an observed $h \rightarrow \gamma\gamma$ rate, see [323]. In general, there are no direct constraints on $m_a, m_{a'}$.

We pause here to note that if a or a' is light, it is quite natural to get a decay length that is detector scale. For example, parametrizing the coupling of a pseudoscalar to photons as

$$\mathcal{L} = \frac{\pi\alpha}{M} a F_{\mu\nu} \tilde{F}^{\mu\nu} \quad (78)$$

one gets a decay length, if they are produced in the decay of h at rest, of

$$\gamma c\tau \approx 0.75 \text{ cm} \left(\frac{M}{5 \text{ TeV}} \right)^2 \left(\frac{1 \text{ GeV}}{m_a} \right)^4 \left(\frac{m_h}{125 \text{ GeV}} \right). \quad (79)$$

It is easy to see that for $m_a \lesssim 100$ MeV and $M \gtrsim 1$ TeV,³¹ a 's decay length could be of the order of several meters. Long decay lengths are therefore a generic feature of light pseudoscalars decaying to photons and should be kept in mind when contemplating such signals.³²

C. Existing experimental searches and limits

A search for $h \rightarrow aa \rightarrow 4\gamma$ in the case where $m_a \ll m_h$ leading to very collimated pairs of photons was performed by ATLAS on 4.9 fb^{-1} of 7 TeV data [324]. The search was very similar to the standard one for $h \rightarrow \gamma\gamma$ but shower shape variable cuts were relaxed to allow for increased acceptance of the 4γ signal. This resulted in a very good acceptance for events coming from the $h \rightarrow \gamma\gamma$ channel. Results were presented for $m_a = 100, 200, 400$ MeV, limiting $\text{Br}(h \rightarrow aa)\text{Br}(a \rightarrow \gamma\gamma)^2 \lesssim 0.01$ at $m_h = 125 \text{ GeV}$.³³ For larger a masses, there are no limits from collider searches.

Results from low energy experiments (see, e.g., Ref. [133]) are not constraining on this scenario for $m_a \gtrsim 10$ MeV so long as the a 's decay promptly at the LHC [317].

D. Proposals for new searches at the LHC

A search for $h \rightarrow 4\gamma$ using the full 7 and 8 TeV data set of both experiments would be highly desirable. Reference [311] indicates that 300 fb^{-1} of data at the 14 TeV LHC can access values of $\text{Br}(h \rightarrow aa)\text{Br}(a \rightarrow$

³¹We would expect such a scale if a 's coupling to photons came from integrating out charged matter above the electroweak scale.

³²This conclusion can be modified slightly when other decay channels for a are present or if the operator $aF_{\mu\nu}\tilde{F}^{\mu\nu}$ is generated below the electroweak scale. See [317] for details.

³³In the SM $\text{Br}(h \rightarrow \gamma\gamma) \sim 2 \times 10^{-3}$. Therefore the impact of the SM diphoton channel on this bound is still rather small.

$\gamma\gamma)^2 > 5 \times 10^{-5}$ at 5σ for $m_a \gtrsim 10$ GeV. For $m_a \lesssim 10$ GeV, the 4γ signal can be hard to disentangle from the large QCD dijet background and for $m_a \lesssim \text{few} \times 100$ MeV it can even look very similar to $h \rightarrow \gamma\gamma$. In these cases, as shown in [313,314], using detector variables from jet substructure can greatly reduce the QCD dijet backgrounds and help to distinguish these final states, greatly increasing the reach for $h \rightarrow 4\gamma$. Thus far, most work on this signal has concentrated on either the very light a regime where two photon pairs are very collimated or where $m_a > 10$ GeV and the four photons are well separated. The intermediate mass region is also well motivated and we encourage it to be studied as well.

The assumption that the two intermediate particles have the same mass cuts down on backgrounds but a more general search strategy looking for $\gamma\gamma$ bumps in $h \rightarrow 4\gamma$ could help to shed light on a scenario where this decay is dominantly mediated by two particles with distinct masses.

Lastly, macroscopic decay lengths for the particles mediating $h \rightarrow aa^{(\prime)} \rightarrow 4\gamma$ can be naturally realized in simple models, especially when they are light or if they are composites from a hidden valley, which motivates searches for 4γ events where two pairs of photons each resolve displaced vertices.

X. $h \rightarrow ZZ_D, Za \rightarrow 4\ell$

Below we discuss decays of the form $h \rightarrow Z + X$, where X denotes a non-SM light boson. We focus on two possibilities.

- (1) $X = Z_D$, a new gauge boson that acquires a mass and mixes with the SM gauge bosons; see Sec. IC 5.
- (2) $X = a$, a light pseudoscalar as in the 2HDM + S and the NMSSM [190]; see Secs. IC 2 and IC 7.

In both cases we are interested in a two-body decay of the Higgs boson, meaning we require $M_X \lesssim 34$ GeV. We outline the theoretical motivation to consider such decays and discuss the limits by LEP, Tevatron, and LHC.

A. Theoretical motivation

1. $h \rightarrow ZZ_D$

As discussed in Sec. IC 5, many theories feature a hidden $U(1)$ sector with small kinetic or mass mixing the SM photon and Z boson. This possibility often arises in connection to dark matter, but similar phenomenology can also arise in more general hidden-valley models; see Sec. IC 10. The minimal setup Eq. (38) to generate $h \rightarrow ZZ_D$ decay involves a kinetic mixing term between the hypercharge gauge boson and the dark $U(1)$ gauge boson

$$\mathcal{L}_{\text{gauge}} \supset \frac{1}{2} \frac{\epsilon}{\cos\theta_W} \hat{B}_{\mu\nu} \hat{Z}_D^{\mu\nu}, \quad (80)$$

where hatted quantities are fields before their kinetic terms are canonically renormalized by a shift of B_μ . In the

canonical basis, SM matter has a dark millicharge and there is mass mixing between the SM Z boson and Z_D . The dominantly dark vector mass eigenstate has photon-like couplings to SM fermions (proportional to the small mixing ϵ) up to $\mathcal{O}(m_{Z_D}^2/m_Z^2)$ corrections; see Eq. (47). If Z_D is the lightest state in the dark sector, it will decay to SM fermions via this coupling. Prompt decay requires $\epsilon \gtrsim 10^{-5}-10^{-3}$ (depending on m_{Z_D}), and the largest $\text{Br}(h \rightarrow ZZ_D)$ allowed from indirect constraints is $\sim 10^{-3}$; see Fig. 12.

It is also possible to have pure mass mixing after EWSB via operators of the form $hZ^\mu Z'_\mu$, but in this case additional constraints from parity violating interactions and rare meson decays apply, see [165,166,169]. Generically, new physics similar to that which generates kinetic mixing may also generate dimension-6 terms of the form $H^\dagger HB^{\mu\nu} Z_{D\mu\nu}/\Lambda^2$. Once the Higgs acquires a vacuum expectation value, this term yields the coupling in Eq. (80).

2. $h \rightarrow Za$

Next we consider the decay $h \rightarrow Za$. This is motivated by, for example, the 2HDM + S or the NMSSM, where one of the CP -odd Higgs masses can be small. The relevant interaction Lagrangian in terms of mass eigenstates h and a is given by Eq. (18) with an additional Yukawa term:

$$\mathcal{L}_{\text{int}} = g(a\partial^\mu h - h\partial^\mu a)Z_\mu - g_a \bar{f} i \gamma_5 f a \quad (81)$$

with $g = \sqrt{(g^2 + g'^2)}/2 \sin(\alpha - \beta) \sin\theta_a$. The parameter α is the mixing angle between the doublet scalars, $\tan\beta = v_u/v_d$, and θ_a is the mixing angle between the uneaten doublet pseudoscalar A and the singlet pseudoscalar. Since the Higgs coupling to ZZ and W^+W^- is also proportional to $\sin(\alpha - \beta)$, the SM-like rates in those channels (as well as the diphoton mode) favor the decoupling limit $\alpha = \pi/2 - \beta$. θ_a can be constrained by direct LEP and Tevatron searches for the CP -odd Higgs, but the SM-like Higgs could still have large branching fractions to Za [190]. The pseudoscalar coupling to fermions can be extracted from Table II:

$$g_a = \sin\theta_a \tan\beta \frac{m_f}{v}, \quad \text{for } b, \tau, \quad \text{and } \mu, \quad (82)$$

and the overall size of θ_a does not affect its branching ratios.

For the length of the LHC program it will likely be safe to take $\text{Br}(h \rightarrow Za) = 10\%$ as a benchmark point. In the next section, we discuss the experimental constraints on this mode. Depending on the mass of this pseudoscalar, the dominant decay mode could be $b\bar{b}$, $\tau^+\tau^-$, or $\mu^+\mu^- (s\bar{s})$. We consider all of these cases when proposing search strategies.

B. Existing collider studies

Up to different branching ratios and some angular correlations the final states for $h \rightarrow ZZ_D$ and $h \rightarrow Za$

are identical. As such, collider studies and experimental searches for one channel generally apply to both. The two relevant parameters to define a simplified model for this channel are

$$m_X \quad \text{and} \quad \text{Br}(h \rightarrow ZX \rightarrow Zyy) \quad (83)$$

for $X = a, Z_D$ and $y = \text{some SM particle}$, where the different a, Z_D branching ratios lend different importance to different choices of y .

There have not been many collider studies specifically performed for the $h \rightarrow Za$ mode. Reference [190] pointed out that this channel may be very large in the context of the NMSSM. References [325–327] discussed heavy non-SM-like Higgs decaying into Za .

More searches have been inspired by looking for a Z_D . The phenomenology of a Z_D with mass mixing to the Z has recently been discussed in [165,166,169,328] (see also, e.g., [31,167,177,329] for earlier work), including collider phenomenology of $h \rightarrow ZZ_D$, $h \rightarrow \gamma Z_D$, and $h \rightarrow Z_D Z_D$ decays, as well as low energy constraints from colliders and fixed-target experiments, $g-2$ of the muon and electron, rare meson decays, and electroweak precision observables (see Sec. XI for the $h \rightarrow Z_D Z_D$ mode).

In [166], the authors designed a search for $pp \rightarrow h \rightarrow ZZ_D \rightarrow e^+e^-\mu^+\mu^-$. The backgrounds considered are $Z(\rightarrow \ell^+\ell^-)jj$, j faking ℓ (probability $\sim 0.1\%$) and leptonic $t\bar{t}$ (reducible), as well as $h \rightarrow ZZ^*, Z\gamma^*, ZZ \rightarrow 4\ell$ (irreducible). The authors of [166] assumed only mass mixing of the form $\epsilon_Z m_Z^2 Z^\mu Z_{D\mu}$. For $m_{Z_D} \sim 5\text{--}10$ GeV, they find that the 14 TeV LHC has 2σ sensitivity to $\text{Br}(h \rightarrow ZZ_D \rightarrow Z\ell\ell) \sim \mathcal{O}(1) \times 10^{-4}$ with 30 fb^{-1} of luminosity.

C. Existing experimental searches and limits

A light pseudoscalar a can be searched for in Υ decays at BABAR [330], top decay at the Tevatron [331], and direct single production and decay to dimuons at the LHC [332,333]. These dedicated searches are discussed in other sections of this document, and their reach depends on many parameters of the theory. There are also many constraints (most of them not from high energy colliders) on the existence of a Z_D (see Fig. 12), but there are large regions of parameter space relevant for exotic Higgs decays that are not excluded.

Our focus is the hZX vertex ($X = a, Z_D$). No direct search for $h \rightarrow Za$ or ZZ_D has been performed to the best of our knowledge, but there are several channels and other searches at LEP, Tevatron, and LHC that are sensitive to this interaction term.

1. LEP

The hZX vertex not only gives rise to the $h \rightarrow ZX$ decay, but also opens the channel $e^+e^- \rightarrow Z^* \rightarrow hX$ at LEP. Related searches include $e^+e^- \rightarrow ha, ZZ' \rightarrow 4b$ [334],

4τ [334] and $2b2\tau$ [334]. For $\text{Br}(h \rightarrow Za) = 10\%$, these searches are not constraining because the cross section for $e^+e^- \rightarrow Z^* \rightarrow ha$ is at the subfemtobarn level. Even without considering any branching fraction suppression to the final states, LEP's integrated luminosity is still too small to be sensitive. One can also imagine more spectacular production modes such as $e^+e^- \rightarrow ha \rightarrow aaa \rightarrow 6b$ and $e^+e^- \rightarrow ha \rightarrow aaa \rightarrow 6\tau$, which can be recast into $e^+e^- \rightarrow ha \rightarrow Zaa \rightarrow 6b$ and $e^+e^- \rightarrow ha \rightarrow Zaa \rightarrow 6\tau$. These channels yield no constraints even before taking into account kinematic acceptances.

2. Tevatron and LHC

The most relevant existing search sensitive to $h \rightarrow ZZ_D$ and $h \rightarrow Za$ is $h \rightarrow ZZ^* \rightarrow 4\ell$ by CMS [175] and ATLAS [176], where 4ℓ stands for electrons and muons. The clean 4ℓ decay makes these existing searches very sensitive to ZZ_D or Za decaying into leptons.

The leptonic $h \rightarrow ZZ^*$ searches divide the four leptons of each event into two pairs, the ‘‘leading’’ pair (likely to have come from an on-shell Z) and the ‘‘subleading’’ pair (from the off-shell Z^* , denoted sometimes as ‘‘ Z_2 ’’ or m_{34}). The subleading dilepton mass distributions from ATLAS and CMS are shown in Fig. 23 of [176] and Fig. 9 of [175], respectively, using the full $20 + 5 \text{ fb}^{-1}$ data set of LHC7 + 8. With this information it is easy to estimate limits on $h \rightarrow ZX$ decay.³⁴ The new state X will contribute to $h \rightarrow Z\ell\ell$ events in two ways, firstly through resonant $h \rightarrow ZX$ production, and secondarily through interference with the SM amplitude $h \rightarrow ZZ^*$. Here we consider only resonant production, obtaining a conservative estimate on $\text{Br}(h \rightarrow ZX)$; a study incorporating the off-shell contributions will appear in future work.

A Z_D or a decaying through some small mixing to SM particles will have a much smaller width than $\Gamma_Z \approx 2.6$ GeV or $\Gamma_{h_{\text{SM}}} \approx 4.07$ MeV. Given the $\lesssim 3\%$ dilepton mass resolution of the experiments and the subleading dilepton mass (M_{Z_2}) binning of 1.25 (2.5) GeV by CMS (ATLAS) it is safe to assume that all of the leptonic $h \rightarrow ZX$ events land in a single bin $M_{Z_2} \approx m_X$. Defining the total expected number of produced $h \rightarrow ZZ^*$ events as

$$N_{\text{prod}}^{ZZ^*} = \sigma(pp \rightarrow h) \times L \times \text{Br}(h \rightarrow ZZ^* \rightarrow 4\ell), \quad (84)$$

the detector efficiency for dileptons from Z_D/a decay can be estimated as

$$\epsilon_{\ell\ell} \approx \frac{N_{\text{detect}}^{ZZ^*}}{N_{\text{prod}}^{ZZ^*}}, \quad (85)$$

³⁴The $\ell^+\ell^-$ distribution in $h \rightarrow Z\ell\ell$ events can also be used to search for indirect effects of new physics above the Higgs mass [335,336].

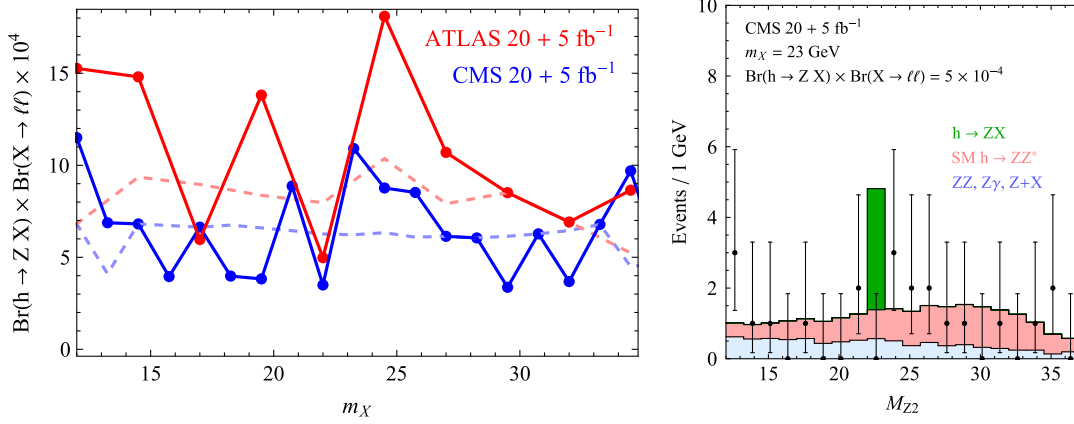


FIG. 27 (color online). Left: 95% C.L. exclusion limit on $\text{Br}(h \rightarrow ZX) \times \text{Br}(X \rightarrow \ell\ell)$ for $X = Z_D, a$, extracted from the SM $h \rightarrow 4\ell$ searches ($\ell = e, \mu$) assuming SM Higgs production rate and $\Gamma_X \ll 1$ GeV. (The lighter dashed lines indicate the expected limit. The large fluctuations in the observed limit are a consequence of low statistics in each bin.) Right: The CMS distribution of m_{Z_2} from [175], overlaid with a 23 GeV $h \rightarrow ZX \rightarrow 4\ell$ signal.

where $N_{\text{detect}}^{ZZ^*}$ is the total expected number of *detected* $h \rightarrow ZZ^*$ events as extracted from the plots of ATLAS and CMS.³⁵ Therefore, for a given exotic Higgs decay branching ratio, the expected number of events contributing to the m_{Z_2} distribution is

$$\begin{aligned}
 N_{\text{detect}}^{ZX} &= \epsilon_{\ell\ell} \times \sigma(pp \rightarrow h) \\
 &\quad \times L \times \text{Br}(h \rightarrow ZX \rightarrow 4\ell) \\
 &\approx N_{\text{detect}}^{ZZ^*} \times \frac{\text{Br}(Z \rightarrow \ell\ell)}{\text{Br}(h \rightarrow ZZ^* \rightarrow 4\ell)} \\
 &\quad \times [\text{Br}(h \rightarrow ZX) \times \text{Br}(X \rightarrow 2\ell)] \\
 &\approx N_{\text{detect}}^{ZZ^*} \times 450 \times [\text{Br}(h \rightarrow ZX) \\
 &\quad \times \text{Br}(X \rightarrow 2\ell)].
 \end{aligned}$$

By placing the above number of events in each m_{Z_2} bin we extract 95% C.L. bounds on the quantity in square brackets for different $m_X > 12$ GeV; see Fig. 27.

The bound on $\text{Br}(h \rightarrow ZX) \times \text{Br}(X \rightarrow \ell\ell)$ is $\lesssim 10^{-4} - 10^{-3}$ for $12 \text{ GeV} \lesssim m_X \lesssim 34 \text{ GeV}$ and $\ell = e, \mu$. Using Fig. 13 we see that this already corresponds to $\text{Br}(h \rightarrow ZZ_D) \lesssim 2 \times 10^{-3}$, which represents a new direct constraint on dark photons by the LHC; see Fig. 12. This limit can be optimized with a dedicated analysis, which would make LHC measurements the most sensitive probe of dark vector kinetic mixing in the mass range $10 \text{ GeV} \lesssim m_{Z_D} \lesssim m_h/2$.

³⁵Because of the $m_{Z_2} > 12$ GeV requirement this may slightly underestimate the efficiency. There may also be small differences in isolation for leptonic vector versus pseudoscalar decay. However, our method suffices for a conservative estimate of constraints.

The situation is more ambiguous for pseudoscalars. Their branching ratios are more model dependent in general, and their Yukawa couplings usually imply that $a \rightarrow \tau\tau$ is enormously preferred over e, μ . Typical branching ratios to 4ℓ ($\ell = e, \mu$) are $10^{-4} - 10^{-3}$, depending on the pseudoscalar mass. Bounds for $X \rightarrow \tau\tau$ could also be derived from the leptonic $h \rightarrow ZZ^*$ searches but would be much weaker. Nevertheless this may be the preferred discovery channel for 2HDM + S and NMSSM-type models, where $\text{Br}(h \rightarrow Za)$ could easily be 10% and $\text{Br}(a \rightarrow \tau\tau)$ is generally $\mathcal{O}(0.05 - 1)$; see Sec. IC 2.

D. Proposals for new searches at the LHC

For $m_{a, Z_D} > 12$ GeV it seems likely that LHC14 searches inspired by $h \rightarrow ZZ^*$ will constrain $h \rightarrow Za$ in the $a \rightarrow 2\tau$ modes, while LHC7 + 8 already gives significant *direct* bounds to $h \rightarrow ZZ_D \rightarrow 4\ell$. A Z + lepton-jet search would be able to set strong limits in particular for very light Z_D . Care must be taken to correctly account for challenging quarkonium backgrounds. Identifying promising search strategies will be the subject of future work.

XI. $h \rightarrow Z_D Z_D \rightarrow 4\ell$

A. Theoretical motivation

Similarly to the discussion in the previous section, two classes of models can give a Higgs to four-lepton signature, with two pairs of electrons and/or muons reconstructing the same resonance.

- (i) As discussed in Sec. IC 5, models with an additional $U(1)_D$ gauge group may lead to the $h \rightarrow Z_D Z_D$ decay, followed by $Z_D \rightarrow \ell^+ \ell^-$. In the minimal model, the dark $U(1)_D$ is broken by a dark scalar that does not mix with the SM Higgs. Then the

kinetic mixing operator involving the hypercharge gauge field B_μ and the Z_D^μ field leads to only a small branching ratio of the Higgs to two Z_D gauge bosons, since it is suppressed by the fourth power of the kinetic mixing parameter ϵ in Eq. (38). Much larger branching ratios can be obtained by introducing a mixing term between the scalar that breaks the $U(1)_D$ symmetry and the Higgs of the SM: $\zeta|S|^2|H|^2$. In these models, even $\zeta \sim 10^{-2}$ can lead to branching ratios for $h \rightarrow Z_D Z_D$ as large as $\sim 10\%$ in certain regions of parameter space (see left panel of Fig. 15). Furthermore, more extended Higgs sectors can also lead to sizable branching ratios. In particular, in [337] it has been shown that $\text{Br}(h \rightarrow Z_D Z_D) \sim 10\%$ is possible in 2HDM + S models where the SM singlet and one of the two Higgs doublets is charged under $U(1)_D$.

- (ii) Many hidden-valley models [32,135] (see Sec. IC 10), with either fundamental or composite spin-one bosons, can lead to the same final state.
- (iii) Models predicting a sizable branching ratio for $h \rightarrow aa$, where a is CP -odd scalar, can also lead to the 4ℓ signature. As presented in Sec. IC 2, such pseudoscalars can arise in 2HDM + S models, as for example in the approximately R -symmetric NMSSM scenarios (see Sec. IC 7). However, as shown in the figures of Sec. IC 2, if the pseudoscalar is above the tau threshold, it will preferentially decay into two taus, two gluons, or two quarks. More specifically, for $m_a > 2m_\tau$, $\text{Br}(a \rightarrow \ell^+ \ell^-) / \text{Br}(a \rightarrow \tau\tau) \sim m_\ell^2 / m_\tau^2 \sim 3 \times 10^{-3}$ (8×10^{-8}) for $\ell = \mu$ (e). For this reason, in the discussion of Sec. XIC below for the collider constraints on the 4ℓ signature, we will focus on models with dark gauge bosons. Searches that exploit the more dominant 4τ and $2\tau 2\mu$ decay modes of the pseudoscalar pair are discussed in Sec. VI.

B. Existing collider studies

The authors of [177] investigate the feasibility of probing $h \rightarrow Z_D Z_D \rightarrow 4\ell$ at Tevatron and at the LHC. In particular, they perform an estimation of the reach at the 14 TeV LHC for several benchmark scenarios: the most interesting for us are scenarios ‘‘A’’ and ‘‘B’’ with $m_h = 120$ GeV and $m_{Z_D} = 5(50)$ GeV, respectively. They show that there are very good prospects for detecting this Higgs decay mode, even for small Higgs branching ratios. In particular, they focus on a Higgs produced in gluon fusion followed by the decay $h \rightarrow Z_D Z_D \rightarrow e^+ e^- \mu^+ \mu^-$. For $\text{Br}(h \rightarrow Z_D Z_D) \sim \mathcal{O}(1)$, basic cuts on the p_T and η of the leptons, and the requirement that the four-lepton invariant mass is close to m_h , are sufficient to lead to $S/B \sim 10^4(10^3)$ [with $S \sim$ hundreds (tens) of fb in the case of $m_{Z_D} = 5(50)$ GeV]. Here B is simply given by the leading diboson background. Additionally, they comment on the

fact that the reach can be improved further by vetoing events with opposite sign, same-flavor (OSSF) lepton pairs reconstructing the Z resonance.

Furthermore, Ref. [338] shows that a light Higgs boson could have been discovered sooner in $h \rightarrow Z_D Z_D \rightarrow 4\ell$ than in the traditional decay modes, $\gamma\gamma$, $\tau\tau$, with the 7 TeV LHC data. In particular, the authors claim that, even for $\text{Br}(h \rightarrow Z_D Z_D) \sim \mathcal{O}(1\%)$, one could have expected five events with the first fb^{-1} of 7 TeV LHC data.

C. Existing experimental searches and limits

Searches for $h \rightarrow aa \rightarrow 4\mu$ were performed by the CMS Collaboration with 5 fb^{-1} of data at $\sqrt{s} = 7$ TeV [288] and 20 fb^{-1} at $\sqrt{s} = 8$ TeV [339]. For these searches, a refers to a spin-0 boson with a mass between 250 MeV and $2m_\tau$. Differences in the acceptance between this signal and $h \rightarrow Z_D Z_D \rightarrow 4\mu$ should be modest for this range of boson masses, and the limits from these searches at CMS are directly applicable. The 8 TeV search [339] is more sensitive and results in a limit $\text{Br}(h \rightarrow Z_D Z_D \rightarrow 4\mu) < 4.7 \times 10^{-5}$ for $m_h = 125$ GeV and $250 \text{ MeV} < m_{Z_D} < 2m_\tau$.

For the mass range $5 \text{ GeV} < m_{Z_D} < m_h/2$, limits can be obtained from SM Higgs searches as well as from a plot reported as part of a ZZ cross section measurement. To estimate limits on exotic Higgs decays to four leptons, we use MADGRAPH to generate Higgs decays to dark photons, $h \rightarrow Z_D Z_D$, followed by $Z_D \rightarrow \ell^+ \ell^-$, using FEYNRULES [340] to construct the dark photon model of Sec. IC 5. Gluon fusion signal events are generated in MADGRAPH 5 and matched up to one jet, with showering in PYTHIA.

We begin by considering the SM $h \rightarrow ZZ^*$ analyses, which are conducted with the full 7 + 8 TeV data sets in both experiments. The CMS search [175] requires four isolated leptons within kinematic acceptance, forming two OSSF pairs. The invariant mass of the OSSF pair that minimizes $|m_{\ell\ell} - m_Z|$ is denoted m_1 , while the remaining OSSF pair invariant mass is denoted m_2 . The pair invariant masses must satisfy

$$\begin{aligned} 40 \text{ GeV} < m_1 < 120 \text{ GeV}, \\ 12 \text{ GeV} < m_2 < 120 \text{ GeV}. \end{aligned} \quad (86)$$

Events in which any OSSF pair has invariant mass $m_{\ell\ell} < 4$ GeV are rejected, to suppress backgrounds from quarkonia. To compare to public data, we study the set of four-lepton events with four-lepton invariant mass in the range $m_{4\ell} \in (121.5, 130.5)$ GeV.

We estimate signal acceptance using the lepton efficiencies reported in [175]. Lepton energies are smeared according to the resolutions tabulated in the appendix of that work. Comparing our own event yield from SM $h \rightarrow ZZ^* \rightarrow 4\ell$ events to the experimental expectations in

Table 2 of [175] determines a final efficiency correction factor for electrons and muons separately.

The requirement that one OSSF pair of leptons lies within a Z window means that frequently $h \rightarrow Z_D Z_D$ events are not reconstructed as a pair of resonances: if $m_{Z_D} = 20$ GeV, for instance, a lepton pair with invariant mass near m_Z can only be obtained by taking one lepton from each Z_D decay. Since events with two electrons and two muons cannot be mispaired in this way, for $m_{Z_D} < 40$ GeV, $ee\mu\mu$ events cannot contribute to the reach at all. In Fig. 28 we show the signal $4e$ and 4μ events as they would appear in the m_1 - m_2 plane, both for $m_{Z_D} = 20$ GeV and $m_{Z_D} = 40$ GeV. As m_{Z_D} increases, the fraction of events which are reconstructed as a pair of resonances increases, so that when $m_{Z_D} = 60$ GeV, nearly all leptons are correctly paired.

To estimate limits resulting from this search, we perform a simple counting experiment. For signals with $m_{Z_D} < 40$ GeV, we define a signal region to be $m_1 < 80$ GeV, $m_2 > 30$ GeV, and set a 95% C.L. limit by treating all observed events in this region as signal. In this signal

region, there are one 4μ and one $2e2\mu$ event in the 7 TeV data set, and one 4μ and one $2e2\mu$ event in the 8 TeV data set. We consider six signal bins, one for each flavor combination in each CM energy, and define a joint likelihood function as the normalized product of Poisson likelihood functions $\mathcal{L}(\mu) = \text{Poisson}(N_{\text{obs}}|\mu N_{\text{sig}})$. When no signal is predicted, as for the $2e2\mu$ channel for masses $m_{Z_D} < 40$ GeV, we do not include the signal region in the likelihood function. The resulting 95% C.L. limits are shown in the red line in Fig. 30. For $m_{Z_D} \geq 40$ GeV, we define the signal region to be $m_{Z_D} - 5$ GeV $< m_1 < m_{Z_D} + 5$ GeV, $m_{Z_D} - 5$ GeV $< m_2 < m_{Z_D} + 5$ GeV. No observed events fall inside this signal region for any value of m_{Z_D} . To translate between limits on $h \rightarrow Z_D Z_D$ and $h \rightarrow Z_D Z_D \rightarrow 4\ell$ we point out that, as seen in Fig. 13 in Sec. 1C 5, for 10 GeV $\lesssim m_{Z_D} \lesssim 60$ GeV, $\text{Br}(Z_D \rightarrow \ell^+ \ell^-) \approx 0.3$. This implies that $\text{Br}(h \rightarrow Z_D Z_D \rightarrow 4\ell) \approx 0.09 \times \text{Br}(h \rightarrow Z_D Z_D)$.

We estimate limits on dark vectors of masses down to 5 GeV. For $m_{Z_D} = 5$ GeV, the daughter leptons are beginning to become collimated, with a typical

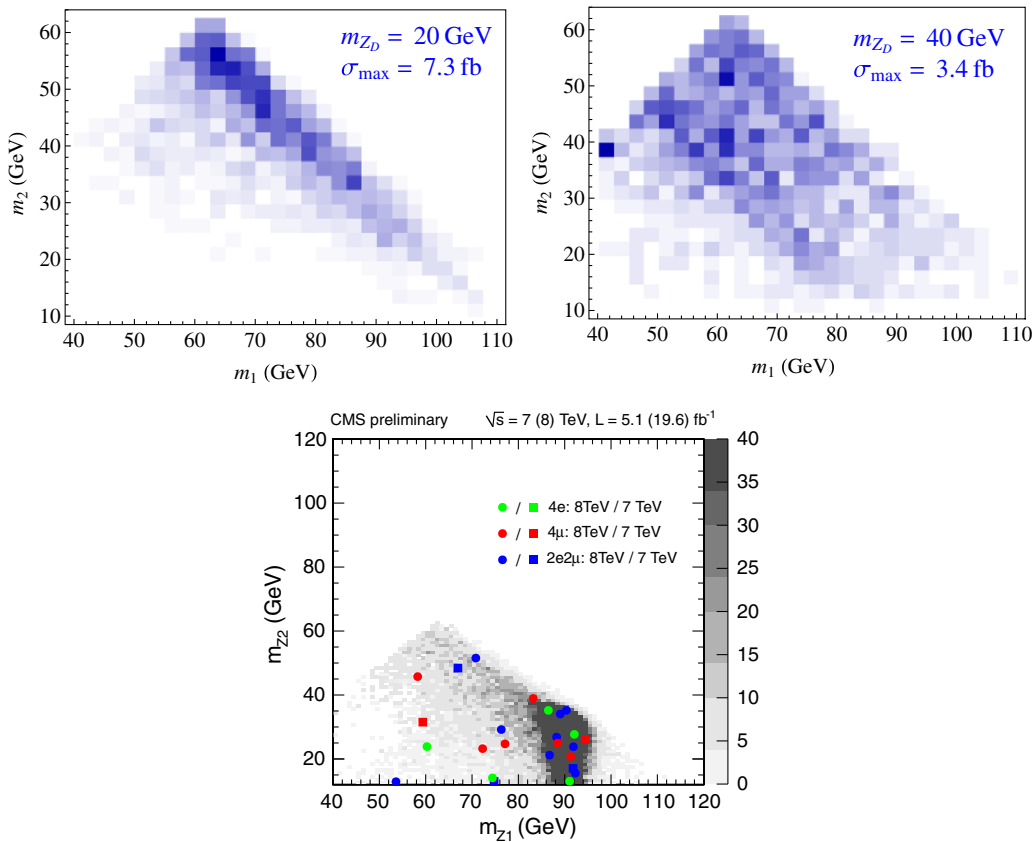


FIG. 28 (color online). Top left and right: Distribution of lepton pair invariant masses in $4e$ and 4μ events according to the event selection and reconstruction criteria of [175]. The maximum cross section [taking $\text{Br}(h \rightarrow Z_D Z_D) = 1$] in any 2.5×2.5 GeV square is indicated in each plot to establish a scale. Left: With $m_{Z_D} = 20$ GeV, only mispaired $4e$ and 4μ events pass the event selection criteria. Right: With $m_{Z_D} = 40$ GeV, both mispaired and correctly paired events are evident, with accumulation of events at the mass of the vector boson visible on the far left edge of the plot. (In this case, $2e2\mu$ events, not shown, also pass the selection criteria and accumulate at the mass of the vector boson.) Bottom: Expected distribution of lepton pair invariant masses for $h \rightarrow ZZ^* \rightarrow 4\ell$ with $m_{4\ell} \in (121.5, 130.5)$, overlaid with observed 7 and 8 TeV events, from [175].

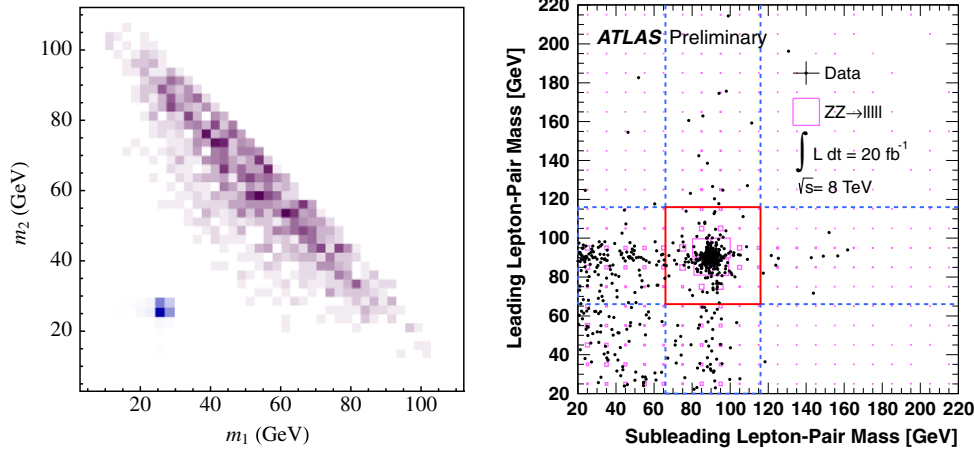


FIG. 29 (color online). Left: Distribution of lepton pair invariant masses for signal with $m_{Z_D} = 25$ GeV for all flavor combinations, according to the event selection and reconstruction criteria of [341]. Correctly paired events are shown in blue and make up 55% of the accepted events, while mispaired events, in purple, make up the remaining 45%. Right: Distribution of selected lepton pair invariant masses, from [341]. Note that the scales of the axes differ in the two plots.

$\Delta R_{\ell\ell} \sim 0.2$. Leptons are not allowed to spoil each other's isolation criteria in Ref. [175], and we have therefore applied the same identification efficiencies and smearings to these semicollimated leptons as we use for parameter points with better separated leptons. If this is a poor approximation, then the exclusion shown for the range $m_{Z_D} \sim 5$ GeV will prove to be optimistic. Nevertheless, reductions in electron efficiency of $\mathcal{O}(1)$ still result in interesting limits, and in the region $10 \text{ GeV} \lesssim m_{Z_D} \lesssim 20 \text{ GeV}$, the exclusions are robust.

The ATLAS SM $h \rightarrow ZZ^* \rightarrow 4\ell$ search [342] is similar in spirit to the CMS search. The major difference for our purposes is that the acceptance is tighter for the OSSF lepton pair minimizing $|m_{\ell\ell} - m_Z|$:

$$\begin{aligned} 50 \text{ GeV} < m_1 < 106 \text{ GeV}, \\ 12 \text{ GeV} < m_2 < 116 \text{ GeV}. \end{aligned} \quad (87)$$

This reduces the overall acceptance for the BSM signal, leading to weaker limits than those from CMS (as both experiments observed four total events in the signal region, and as ATLAS does not report flavor information for these events).

At low masses, the best limits are found from control regions in the ATLAS ZZ cross section measurement with 20 fb^{-1} of 8 TeV data [341]. Here, events are again required to have exactly four leptons, which can be paired into two OSSF pairs. Now when there is a choice of possible OSSF pairings, the assignment which minimizes $|m_1 - m_Z| + |m_2 - m_Z|$ is chosen. This still has some probability of mispairing $h \rightarrow Z_D Z_D$ events, as can be seen in Fig. 29. The invariant mass of the lepton pair with higher p_T is assigned to be m_1 . Note that, unlike the SM $h \rightarrow ZZ^*$ analyses, there is *no restriction* on the invariant mass of the four leptons.

We now set limits by defining a signal region for each mass, $m_{Z_D} - 2 \text{ GeV} < m_1 < m_{Z_D} + 2 \text{ GeV}$, $m_{Z_D} - 2 \text{ GeV} < m_2 < m_{Z_D} + 2 \text{ GeV}$. Lepton efficiencies are modeled with a p_T -dependent parameterization for electrons [343,344] and a flat efficiency for muons, and validated against the fiducial acceptances for ZZ events quoted in [341]. At most one event is observed in each $4 \text{ GeV} \times 4 \text{ GeV}$ signal bin. Treating any observed event in the signal region as signal, we obtain 95% C.L. limits as before.

Figure 30 shows the resulting limits (along with those from CMS's $h \rightarrow ZZ^*$ search), of order 10^{-3} , on Higgs branching fractions to dark vector bosons that further decay to lepton pairs. These limits, while impressive, are easy to improve at low masses by simply looking for OSSF pairs

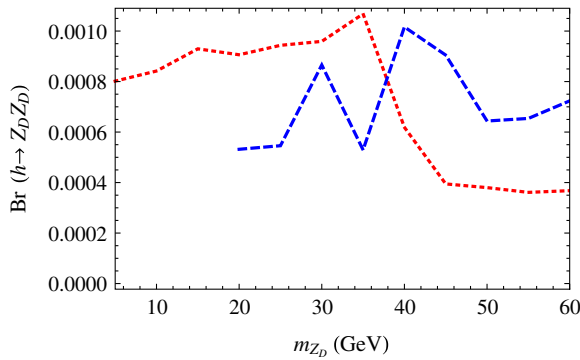


FIG. 30 (color online). Estimated 95% C.L. limits on the branching fraction $\text{Br}(h \rightarrow Z_D Z_D)$ coming from CMS $h \rightarrow ZZ^*$ [175] (red, dotted line) and ATLAS ZZ cross section [341] (blue, dashed line) measurements. Note that, as seen in Fig. 13 in Sec. IC 5, for this range of m_{Z_D} , $\text{Br}(Z_D \rightarrow \ell^+ \ell^-) \approx 0.3$ which implies that $\text{Br}(h \rightarrow Z_D Z_D \rightarrow 4\ell) \approx 0.09 \times \text{Br}(h \rightarrow Z_D Z_D)$.

which minimize $|m_1 - m_2|$, instead of a distance from the Z peak. As backgrounds are already zero for most bins, improving signal acceptance is the most likely to improve reach.

XII. $h \rightarrow \gamma + E_T$

We consider here the signature $h \rightarrow \gamma + E_T$. This signature can be usefully represented through the decay of the Higgs into two neutral fermions, $h \rightarrow \chi_1 \chi_2$, followed by the decay $\chi_2 \rightarrow \gamma \chi_1$.

A. Theoretical motivations

While our focus here is on decays to BSM particles, it is worthwhile to observe that the signature $h \rightarrow \gamma + E_T$ arises as a rare decay in the SM, through the loop-induced $h \rightarrow \gamma Z$, followed by $Z \rightarrow \nu \bar{\nu}$. The SM branching fraction is thus $\text{Br}(h \rightarrow \gamma + \nu \bar{\nu})|_{\text{SM}} = 1.54 \times 10^{-3} \times 0.20 = 3.08 \times 10^{-4}$ [345]. Searches for potential enhancements in $h \rightarrow \gamma Z$ are sensitive to the potential presence of new physics running in the loop, making this rare Higgs decay signature one of interest for several reasons. The decay $h \rightarrow \gamma Z$ implies specific kinematics for the photon and missing energy, however, which do not hold in more general models.

One class of models that gives rise to a $h \rightarrow \gamma + E_T$ signature are those with very low-scale supersymmetry breaking [346]. Here the Higgs decays into a gravitino and a neutralino that is dominantly bino, $h \rightarrow \tilde{G} \tilde{B}$, followed by the prompt decay $\tilde{B} \rightarrow \gamma \tilde{G}$ [51]. As the gravitino is effectively massless, this model is parameterized by one mass $m_{\tilde{B}}$. This mass should lie in the range $m_h/2 < m_{\tilde{B}} < m_h$ to obtain a large branching ratio to $h \rightarrow \gamma + E_T$, as for $m_h/2 > m_{\tilde{B}}$, the decay $h \rightarrow \tilde{B} \tilde{B}$ will dominate, leading to a $h \rightarrow 2\gamma + E_T$ signature.

This signature can also be realized in the PQ limit of the NMSSM (see Sec. IC 8). Here the lighter fermion χ_1 is dominantly singlino, and the heavier fermion is dominantly bino. The mass splitting between the two fermions is now much more free. However, in the PQ -symmetric limit, a light singlino is always accompanied by a light scalar s , and for the loop-induced branching fraction $\text{Br}(\chi_2 \rightarrow \chi_1 \gamma)$ to be sizable, the tree-level decays $\text{Br}(\chi_2 \rightarrow s^{(*)} \chi_1 \rightarrow f \bar{f} \chi_1)$ must be phase-space suppressed. Thus one generically expects mass splittings between the two neutralino species of no more than 10–20 GeV for the rate into $h \rightarrow \gamma + E_T$ to be appreciable. Outside the PQ -symmetric limit of the NMSSM, or in other extensions of the MSSM [347], special parameter cancellations are required to obtain substantial branching fraction for the radiative decay $\chi_2 \rightarrow \gamma \chi_1$.

A more bottom-up approach extends the SM by two Majorana fermions, χ_2 and χ_1 , with a dipole coupling

$$\delta \mathcal{L} = \frac{1}{\mu} \bar{\chi}_2 \sigma_{\mu\nu} B^{\mu\nu} \chi_1. \quad (88)$$

Note that the presence of the hypercharge field strength B would predict a $Z + E_T$ signal as well, if phase space allowed it; however, in many UV completions of the dipole operator, the mass splitting between the fermionic states arises due to some symmetry breaking which makes it challenging to realize $m_{\chi_2} - m_{\chi_1} \gtrsim m_Z$, and the Z mode will typically be highly suppressed. The simplified model is then characterized by two parameters m_1 and m_2 , where $m_1 < m_2$ and $m_1 + m_2 < m_h$.

Finally, the $\gamma + E_T$ signature also appears as a subleading decay mode in models of Higgs decay to right-handed neutrinos N [348]. Here the signature arises from $h \rightarrow NN$, followed by the decay of $N \rightarrow \gamma \nu$ on one side of the event and $N \rightarrow \nu \bar{\nu}$ on the other. In the realization of [348], both of these N decay modes are highly subdominant, and the photonic decay may be displaced.

B. Existing collider studies

A LHC study was carried out at parton level in [51]. This study targets Higgs bosons produced in gluon fusion and estimates that 20 fb^{-1} of 8 TeV data would allow 95% C.L. sensitivity to branching fractions ranging between $\text{Br}(h \rightarrow \gamma + E_T) < 0.002$ for $m_{\chi_2} = 120 \text{ GeV}$ and $\text{Br}(h \rightarrow \gamma + E_T) < 0.010$ for $m_{\chi_2} = 60 \text{ GeV}$. These results are based on selection criteria that are not obviously compatible with current LHC triggers, however, as the selection of Ref. [51] requires

$$45 \text{ GeV} < p_{T\gamma} < \frac{m_h}{2} \quad (89)$$

and no other triggerable objects. Current monophoton triggers require $p_{T,\gamma} > 80 \text{ GeV}$, although trigger cuts for CMS parked data are more relaxed, $p_{T,\gamma} > 30 \text{ GeV}$ and $E_T > 25 \text{ GeV}$ for central photons, and therefore could be relevant for this decay channel.

Replacing the cut on photon p_T with one on the transverse mass of the photon and the missing momentum gives a good separation between signal and backgrounds. Trigger thresholds ensure that the dominant contribution to the reach comes from the high- p_T tail of the Higgs production spectrum, where the Higgs recoils against one or more hard ISR jets. Depending on the mass difference between χ_1 and χ_2 and the analysis threshold achieved in parked monophoton + E_T triggers, the best signal acceptance may be achieved in monojet + E_T -triggered events rather than monophoton + E_T -triggered events.

C. Existing experimental searches and limits

In (N)MSSM realizations of the nonresonant signature, there are *indirect* limits on the Higgs branching fraction into neutralino-gravitino from electroweakino searches at Tevatron and at LHC (see also the nonresonant $2\gamma + E_T$ signature in Sec. XIII, where similar considerations apply).

In the case of the neutralino-gravitino realization, the lightest neutralino χ_1 must have some Higgsino component in order for the coupling $h\chi_1\tilde{G}$ to be present. In the neutralino-singlino realization, the heavier fermion χ_2 is typically dominantly \tilde{B} , with χ_1 dominantly singlino, and the vertex $h\chi_2\chi_1$ again proceeds through the Higgsino component of χ_2 . In both scenarios the nonzero Higgsino component implies the binolike state should be produced directly at hadron colliders via Drell-Yan [73], which may or may not lead to constraints depending on the ensuing decay modes of the bino. While it is of interest to work out these indirect limits, the surviving parameter space is multidimensional, and in more general models, where the coupling hn_2n_1 arises from a dimension-five Higgs portal coupling, the new neutral fermions do not need to have tree-level couplings to the Z boson, and no such indirect limit applies.

Very few existing collider searches place any limits on $\text{Br}(h \rightarrow \gamma + E_T)$. Searches for a hard photon plus E_T , designed to pick up invisible particles recoiling against a hard ISR photon [349–351], target very different kinematic configurations and are not constraining. Similar conclusions apply to the $Z\gamma$, $Z \rightarrow \nu\bar{\nu}$ cross-section measurements [352,353], which also target high- p_T photons recoiling against E_T .

Searches for supersymmetry in final states with $\gamma + \ell + E_T$ + jets at the LHC [354,355] and the Tevatron [356] can be sensitive to Wh associated production when the W decays leptonically. Acceptance for the Higgs signal in these supersymmetry searches is small, due to the hardness demanded of both the γ and the E_T . No limit is placed by the LHC Wh searches in any part of the m_1 - m_2 simplified model parameter space. The Tevatron searches likewise place no limits, partially due (particularly for large $m_2 - m_1$) to a 1σ excess of observed events relative to expectation. This quick limit check assumes 100% photon efficiency; incorporating realistic photon efficiency would further weaken the search. The general CDF search for anomalous $\gamma + E_T$ + at least one jet also does not constrain the Higgs branching fraction [357].

CMS's supersymmetry search in the $\gamma + E_T$ + jets final state [358] comes closer to being constraining; again, no limits are placed anywhere in the m_1 - m_2 simplified model parameter space, but as before this lack of constraint is partially due to a 1.3σ excess of events observed over background expectation (assuming 100% photon efficiency). An updated search in the same final state [359] with 4.04 fb^{-1} of 8 TeV data requires all events to have $H_T > 450 \text{ GeV}$, giving punishingly small signal efficiency. Despite the harshness of this cut, this analysis is beginning to gain sensitivity to the $\gamma + E_T$ decay mode, as shown in Fig. 31. The reported limits from [359] are difficult to recast due to the existence of signal contamination in a region $E_T < 100 \text{ GeV}$ used to model the dominant QCD background. The light 125 GeV Higgs contributes

proportionately more to the control region $E_T < 100 \text{ GeV}$ than do the pair-produced neutralinos with mass 375 GeV for which the background predictions are shown. The limits found by recasting the analysis for a light Higgs are likely overconservative to an extent that is difficult to estimate. In Fig. 31 we show the result of performing this simple recast. The signal region is divided into multiple exclusive bins in E_T , with background predictions as reported for the pair-produced neutralinos. We place limits by combining the limits from each individual bin using a Bayesian algorithm with flat priors and marginalize over background uncertainty according to a log-normal distribution. With perfect photon efficiency, the 95% C.L. limits obtained on $\text{Br}(h \rightarrow \gamma + E_T)$ is approximately unity in a large range of parameter space, suggesting that an analysis more tailored to the signal kinematics could place meaningful limits on the branching fraction for this channel.

As with all semi-invisible signals, collider reach could be extended by forming the transverse mass of the visible decay product(s), here the photon, with the missing transverse momentum vector, and requiring this to be bounded from above as consistent with production from an initial resonance. Much better sensitivity could be achieved if the prohibitively hard cut on H_T could be relaxed. This H_T cut is necessitated by the $\gamma + H_T$ trigger used to select the data in the current analysis and is not suited well to the study of the relatively low- p_T Higgs events. Somewhat better signal acceptance is realized for the monophoton + E_T triggers in current use for dark matter searches, though the degree of improvement depends on the spectrum; again, monojet + E_T triggers may provide better sensitivity.

XIII. $h \rightarrow 2\gamma + E_T$

In this section we consider the decay $h \rightarrow 2\gamma + E_T$. This signature can be realized in several ways.

- (i) First, consider the nonresonant signature where the photons come from opposite sides of the initial

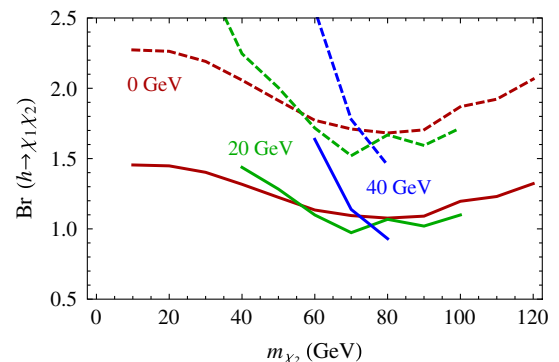


FIG. 31 (color online). Approximate 95% C.L. upper limit on $(\sigma/\sigma_{\text{SM}}) \times \text{Br}(h \rightarrow \chi_1\chi_2 \rightarrow \gamma + E_T)$ from the results of Ref. [359], for $m_{\chi_1} = (0, 20, 40 \text{ GeV}) < m_{\chi_2}$. Solid lines correspond to 100% photon efficiency, and dashed lines to a (flat) 80% photon efficiency.

two-body decay, $h \rightarrow XX$, followed by $X \rightarrow \gamma Y$ on each side of the event with Y a detector-stable, neutral particle.

- (ii) Second is the case where the photons reconstruct an intermediate resonance, $h \rightarrow XX$, with $X \rightarrow \gamma\gamma$ on one side and $X \rightarrow \text{invisible}$ on the other.
- (iii) The last decay topology we consider involves the initial decay $h \rightarrow XY$, followed by $X \rightarrow Y\phi$, $\phi \rightarrow \gamma\gamma$ with Y again appearing as missing energy in the detector.

These different cases may arise in different theoretical models and require related but distinct strategies to observe at colliders, as we discuss below.

A. Theoretical motivation

1. Nonresonant

The nonresonant decay of the Higgs boson to two photons and missing energy may be realized in several theoretical scenarios.

As a first example, consider gauge-mediated supersymmetry-breaking models. Here the lightest neutralino is mainly bino and decays via $\chi_1^0 \rightarrow \gamma\tilde{G}$. Minimal models of gauge mediation make it difficult to obtain a bino with $m_{\tilde{B}} < m_h/2$ while keeping winos sufficiently heavy to satisfy LEP bounds on the charginos as well as gluinos sufficiently heavy to avoid LHC constraints. However, more general models of gauge mediation [360] can allow this spectrum to be realized [73].

Another realization of the nonresonant $2\gamma + E_T$ signature may be obtained in the PQ limit of the NMSSM (see Secs. I C 7 and I C 8 for more details), where a light singlino \tilde{s} replaces the gravitino. In this case the photonic signature is realized through a loop-induced dipole coupling $\tilde{B}^\dagger \sigma^{\mu\nu} B_{\mu\nu} \tilde{s}$. There are typically several other decay modes available to the \tilde{B} in these NMSSM models, in particular

$$\tilde{B} \rightarrow Z^{(*)}\tilde{s}, \quad \tilde{B} \rightarrow a^{(*)}\tilde{s}, \quad \tilde{B} \rightarrow s^{(*)}\tilde{s}, \quad (90)$$

where a, s are light, dominantly singlet CP -odd and CP -even scalars. The radiative decay $\tilde{B} \rightarrow \gamma\tilde{s}$ is typically significantly subdominant to the tree-level decays. The $2\gamma + E_T$ signature is thus typically small compared to other exotic-decay modes in the PQ NMSSM.

More generally, this signature may be realized by having two new (Majorana) fermions χ_1 and χ_2 , with a dipole coupling

$$\delta\mathcal{L} = \frac{1}{\mu} \chi_2^\dagger \sigma_{\mu\nu} B^{\mu\nu} \chi_1 \quad (91)$$

and a dimension-five Higgs portal coupling $c_{22}|H|^2(\chi_2\chi_2 + \chi_2^\dagger\chi_2^\dagger)$. In this case, both m_{χ_1} and m_{χ_2} are parameters of the model. It is natural to extend this simple model to include in addition off-diagonal couplings $c_{12}|H|^2(\chi_2\chi_1 + \chi_2^\dagger\chi_1^\dagger)$ and couplings of the Higgs directly

to the lighter of the two new fermions, $c_{11}|H|^2(\chi_1\chi_1 + \chi_1^\dagger\chi_1^\dagger)$. This generic model would then also yield $h \rightarrow 1\gamma + E_T$ and $h \rightarrow E_T$ signatures with relative branching fractions uniquely determined by the c_{ij} . Previous study of this topology in the MSSM has been performed in [73] and, for the heavier MSSM Higgses, in [361]; see also [52].

2. Resonant

The $2\gamma + E_T$ final state can also occur for the decay chain $h \rightarrow aa$, with one intermediate state decaying to photons, $a \rightarrow \gamma\gamma$, and the other decaying invisibly, $a \rightarrow \text{inv}$. This can be simply realized in a bottom-up fashion by introducing a renormalizable Higgs portal interaction leading to a coupling of a to h , $\lambda|H|^2a^2$, and also coupling a to photons and to a neutral, detector-stable particle χ via, e.g.,

$$\frac{\alpha}{4\pi M} a F^{\mu\nu} \tilde{F}_{\mu\nu} + \frac{\partial_\mu a}{M'} \bar{\chi} \gamma^\mu \gamma^5 \chi. \quad (92)$$

M and M' are the scales of the two dimension-five operators, and we have assumed that a is a real pseudo-scalar and that χ is a Dirac fermion for definiteness. For some regions of parameter space, $a \rightarrow \gamma\gamma$ and $a \rightarrow \tilde{\chi}\chi$ can have comparable branching fractions, making $h \rightarrow 2\gamma + E_T$ an important final state. Another possibility arises from the decay chain $h \rightarrow \chi_1\chi_2 \rightarrow a\chi_1\chi_1$, where a decays via the first dimension-five operator and χ_1 is stable. Note, though these two decay topologies can be achieved in the R and PQ limits in the NMSSM (see Secs. I C 7 and I C 8), the branching fraction of $a \rightarrow \gamma\gamma$ tends to be small. Alternatively, a may be light enough so that $a \rightarrow ff$ is kinematically suppressed, in which case the lifetime is so long that a would decay outside the detector. More general models may give a larger $a \rightarrow \gamma\gamma$ coupling than the NMSSM.

Unlike the nonresonant case, the resonant signature has the useful additional handle that the two photons should reconstruct m_a , improving the search prospects. Additionally, as m_a is decreased and the intermediate particles become more boosted, a larger fraction of the photon pairs will fail isolation cuts. For $m_h = 125$ GeV, this becomes important for $m_a \lesssim$ few GeV. In this case, the signal would have some overlap with that from $h \rightarrow 2\gamma + E_T$ considered in Sec. XII [317].³⁶

This simplified model can be trivially generalized to the case that the Higgs decays to two distinct states, a_1 and a_2 , with $a_1 \rightarrow \gamma\gamma$ and $a_2 \rightarrow \text{inv}$. This can proceed through a dimension-four Higgs portal interaction, $\lambda_{12}|H|^2a_1a_2$, if a_1 couples to photons while a_2 decays invisibly. This decay mode can dominate over $h \rightarrow \text{inv}$ or $h \rightarrow 4\gamma$ if $\lambda_{12} \gg \lambda_{11,22}$

³⁶In the $m_a \ll m_h$ regime, the relationship between the $h \rightarrow 2\gamma + E_T$ and $h \rightarrow \gamma + E_T$ signals parallels that between $h \rightarrow 2\gamma$ and $h \rightarrow 4\gamma$. See Sec. IX for further details.

where $\lambda_{11,22}$ are the coupling constants of the other allowed Higgs portal interactions, $\lambda_{11}|H|^2 a_1^2 + \lambda_{22}|H|^2 a_2^2$. While, in this resonant case, we limit our study to the situation $m_{a_1} \simeq m_{a_2} \equiv m_a$, the two intermediate particles having different masses is a well-motivated possibility.

3. Cascade

The $h \rightarrow 2\gamma + E_T$ decay can proceed through $h \rightarrow \chi_1 \chi_2$, with $\chi_2 \rightarrow s \chi_1$, $s \rightarrow \gamma\gamma$ if χ_1 is neutral and stable on detector scales. It is easy to write down a simple model that gives rise to this decay chain. We can couple (Majorana) fermions χ_1 and χ_2 to the Higgs through a dimension-five Higgs portal coupling as in the nonresonant case above, $c_{12}|H|^2(\chi_2 \chi_1 + \chi_2^\dagger \chi_1^\dagger)$, as well as to the scalar s through a Yukawa interaction, $y_{12}s(\chi_2 \chi_1 + \chi_2^\dagger \chi_1^\dagger)$. Furthermore, s can decay to two photons through the dimension-five operator $sF_{\mu\nu}F^{\mu\nu}$.³⁷

B. Existing experimental searches and limits

In (N)MSSM realizations of the nonresonant signature, there are *indirect* limits on the Higgs branching fraction into neutralinos from general electroweakino searches at the Tevatron and at the LHC. These limits arise because the lightest neutralino χ_1^0 must have some Higgsino component in order for the coupling $h\chi_1^0\chi_1^0$ to be present. Because of this nonzero Higgsino component, the lightest neutralino couples to the Z and can be produced directly at hadron colliders via Drell-Yan. Model-dependent indirect limits on Higgs branching fractions arising from Drell-Yan direct production are nontrivial [73] and an interesting topic of study, but in the present work we confine ourselves to considering (model-independent) direct limits and make no assumptions about other production modes for the BSM states. In general (non-MSSM) models, where the coupling $h\chi_2\chi_2$ arises from a dimension-five Higgs portal coupling, the new neutral fermion χ_2 does not need to have tree-level couplings to the Z boson, and those indirect limits do not apply.

In gauge mediated supersymmetry breaking (GMSB) realizations of the nonresonant signal, sufficiently high SUSY-breaking scales lead to a macroscopic decay length for the neutralino. This can also occur in the general Higgs portal simplified model, for sufficiently large dipole suppression scales μ in the decay vertex of Eq. (91). In such cases, nonpointing photon searches may be motivated or necessary. Displaced signatures are beyond the scope of the present work but are an interesting and natural avenue for future exploration.

³⁷The $sF_{\mu\nu}F^{\mu\nu}$ operator could arise through mixing between s and h (see for example Sec. 1C 1), although that would lead to a very suppressed $h \rightarrow 2\gamma + E_T$ branching ratio compared to final states like $b\bar{b} + E_T$. For $2\gamma + E_T$ to be dominant, the $sF_{\mu\nu}F^{\mu\nu}$ operator would have to be generated by a direct coupling of s to electrically charged matter, e.g., (heavy) vectorlike leptons. For a similar model, see Sec. VIII.

GMSB searches at the LHC have good prospects for discovering or excluding exotic Higgs decays into $2\gamma + E_T$, in both the resonant and nonresonant scenarios. The ATLAS search for $2\gamma + E_T$ using 7 TeV data [362] has some sensitivity, setting limits of $\lesssim 15\%$ on the exotic Higgs branching fraction over much of the parameter space. The more recent CMS study using 4.04 fb^{-1} of 8 TeV data [359] sets the current best limits. This search selects events with at least two photons and at least one central jet and bins events in five exclusive E_T bins beginning from a minimum of 50 GeV. We show the reach of this search in the resonant and nonresonant cases in Figs. 32 and 33 (left), as a function of m_{χ_1} in the nonresonant topology and m_a in the resonant topology. In Fig. 33 (right), we show the reach in the case of the cascade topology as a function of m_s , setting $m_{\chi_1} = 0$ and $m_{\chi_2} = 60$ GeV. We find that the limit obtained in this case is not very sensitive to the value of $m_{\chi_2} = 60$ GeV chosen. In all three topologies the $\text{Br}(h \rightarrow 2\gamma + E_T)$ can be constrained at the level of a few percent over much of the parameter space. Higgs signal events are generated in MADGRAPH with showering in PYTHIA, and jet clustering is done with FASTJET. Gluon fusion is matched out to one jet, and cross sections for both gluon fusion and vector boson fusion processes are set to the values determined by the LHC Higgs Working Group [304]. VBF production is responsible for 20%–25% of the signal. To obtain limits we combine individual 95% C.L. limits from each of the five E_T bins according to a Bayesian algorithm with flat priors, marginalizing over the background uncertainty according to a log-normal distribution.

Since searches using only 4 fb^{-1} of 8 TeV data and optimized for other signatures are already able to place limits as stringent as $\mathcal{O}(5\%)$ on the Higgs branching fraction into this mode, $2\gamma + E_T$ is a good candidate for searches in the near future. The reach could be easily extended by requiring the transverse mass of the photons

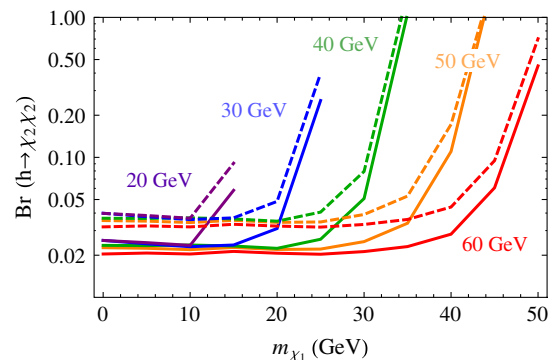


FIG. 32 (color online). Approximate 95% C.L. upper limit on $(\sigma/\sigma_{\text{SM}}) \times \text{Br}(h \rightarrow \chi_2\chi_2 \rightarrow 2\gamma + E_T)$ from the results of Ref. [359], for multiple values of m_{χ_2} as indicated by the text labeling the different curves. Solid lines correspond to 100% photon efficiency, and dashed lines to a (flat) 80% photon efficiency.

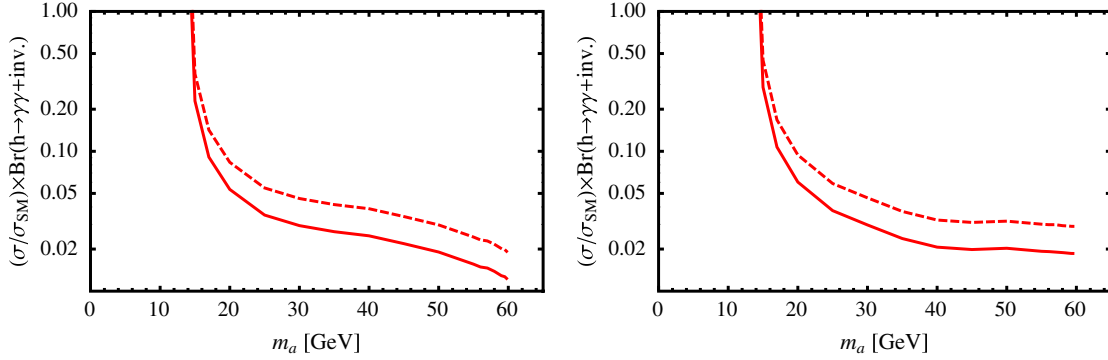


FIG. 33 (color online). Approximate 95% C.L. upper limit on $(\sigma/\sigma_{\text{SM}}) \times \text{Br}(h \rightarrow 2\gamma + E_T)$ from the $2\gamma + E_T$ search in [359]. The solid lines correspond to 100% photon efficiency, and the dashed lines to a (flat) 80% photon efficiency. Left: Resonant case, where $h \rightarrow aa$, one a decays to $\gamma\gamma$ and the other decays invisibly. Right: Cascade case, where $h \rightarrow \chi_1\chi_2$, $\chi_2 \rightarrow s\chi_1$, $s \rightarrow \gamma\gamma$. Here $m_{\chi_1} = 0$ and $m_{\chi_2} = 60$ GeV (although the limit is insensitive to the particular value of m_{χ_2} as long as it is kinematically allowed).

and E_T to be bounded from above, as consistent with resonant origin from the 125 GeV Higgs. In the resonant case, looking for a peak in the $\gamma\gamma$ spectrum could offer another useful handle.

XIV. $h \rightarrow 4$ ISOLATED LEPTONS + E_T

Exotic Higgs decays into multiple charged leptons together with missing energy are less frequently motivated by top-down model building than (e.g.) $h \rightarrow aa$ cascade decays, but on the other hand, they offer excellent discovery potential at the LHC, as we will demonstrate in this and following sections.

There is some overlap between the theoretical motivations and decay topologies for different $h \rightarrow \geq 2$ charged leptons + $E_T + X$ signatures. Here we briefly discuss all the cases we consider in this document before treating the $4\ell + E_T$ case in detail.

Depending on the specific model under consideration, the characteristic predictions for leptonic final states can be very different. Exotic Higgs decays $h \rightarrow X_1X_2$ (where $X_{1,2}$ may or may not be distinct species) can be divided into two main classes of topologies:

- (1) $\ell^+\ell^- + E_T$, which involves the topologies
 - (i) I: $X_1 \rightarrow \text{nonleptonic} + E_T$, $X_2 \rightarrow \ell^+\ell^- + E_T$;
 - (ii) II: $X_1 \rightarrow \text{nonleptonic} + E_T$, $X_2 \rightarrow \ell^+\ell^-$,
 where the nonleptonic part is typically either nothing (i.e., X_1 stable and invisible) or hadronic (i.e., $X_1 \rightarrow \text{soft jets} + E_T$)³⁸; and
- (2) $2 \times \ell^+\ell^- + E_T$, which can be achieved via the topology
 - (i) III: $X_1 \rightarrow \ell^+\ell^- + E_T$, $X_2 \rightarrow \ell^+\ell^- + E_T$;
 - (ii) IV: $X_1 \rightarrow \ell^+\ell^-$, $X_2 \rightarrow \ell^+\ell^- + E_T$.

Further, the cascade decays of X_2 in topologies I and III may either be three-body, or they may involve an on-shell intermediate state so that the leptons reconstruct a

³⁸Charged X 's each decaying to $\ell + E_T$ are highly constrained, and not considered here.

resonance. Depending on the mass of this resonance, and similarly on the mass of the X_2 resonance in topologies II and IV, the leptons may be either isolated or collimated.

This gives us a plethora of experimental signatures, all of which present interesting targets with the existing LHC data set. We discuss theoretical models and experimental prospects for these leptonic signatures here and in the following two sections. In the current section we discuss final states with four isolated leptons plus missing energy; in Sec. XV we discuss final states with two isolated leptons plus missing energy; in Secs. XVI and XVII we consider final states that include one or two lepton-jets, respectively; decays to leptons without E_T are discussed in Secs. X and XI.

A. Theoretical motivation

Several classes of models can give rise to Higgs decays to four isolated leptons + E_T . First, consider models with weak-scale neutral states that have nonvanishing couplings to the Z boson, such as exotic neutrinos or neutralinos. In this case, leptons can arise from the three-body decay of one neutral fermion χ_2 to a lighter one χ_1 through an off-shell Z boson, appearing as an opposite-sign, same flavor pair. The $4\ell + E_T$ signal then arises from cascades of the form $h \rightarrow \chi_2\chi_2 \rightarrow \chi_1Z^*\chi_1Z^*$ with both Z^* leptonic. In fourth-generation neutrino models, χ_2, χ_1 are the two Majorana-split halves of a Dirac neutrino state; in MSSM-like realizations, χ_2, χ_1 are neutralinos. The branching fraction into $4\ell + E_T$ is small compared to the total branching fraction into $\chi_2\chi_2$: $\text{Br}(h \rightarrow 4\ell + E_T)/\text{Br}(h \rightarrow \chi_2\chi_2) = \text{Br}(Z \rightarrow \ell\ell)^2 \approx 0.011$ (including τ 's). Despite the small relative branching fraction, we will see that the $4\ell + E_T$ final state is typically more constraining than final states with fewer leptons, due to the low backgrounds for multi-leptonic final states.

Hidden sectors with a kinetically mixed dark vector boson Z_D can also realize this decay chain [32,234]. For instance, a hidden sector with mesonlike pseudoscalar

states K_v , π_v , may have a spectrum such that the heavier meson may only decay via $K_v \rightarrow Z_D^* \pi_v \rightarrow f \bar{f} \pi_v$, and the lighter meson π_v is collider stable. The width for this K_v decay scales like

$$\Gamma_{K_v} \approx \alpha_D \alpha_{\text{EM}} \frac{\epsilon^2}{15 \cos^2 \theta_W} \frac{(m_{K_v} - m_{\pi_v})^5}{m_{Z_D}^4}, \quad (93)$$

where ϵ is the kinetic mixing between hypercharge and the dark vector boson (see Sec. IC 5). The K_v meson decay can be prompt provided the ratio of the dark meson mass splitting to the dark photon mass, $(m_{K_v} - m_{\pi_v})/m_{Z_D}$, is not particularly small. The branching fractions into leptonic final states are much larger here than in the case where the three-body decay is mediated by a virtual Z . For a dark vector with $m_{Z_D} > 2m_b \gtrsim 10$ GeV, the branching fraction into leptonic final states (including taus) is $\text{Br}(Z_D \rightarrow \text{leptonic}) \approx 45\%$, as discussed in Sec. IC 5.

Another realization of this type of decay chain with an off-shell kinetically mixed dark photon occurs in supersymmetric hidden sectors, with one or more hidden neutralinos. In this case the Higgs cascade decay could begin with a Higgs decay to binolike neutralinos \tilde{B} , which in turn decay via $\tilde{B} \rightarrow Z_D^* \chi_1^0$, where χ_1^0 is a hidden sector neutralino [52,149,363].

If the dark photon is sufficiently light, the decay $K_v \rightarrow Z_D \pi_v \rightarrow \ell \ell \pi_v$ can be allowed, and the leptons reconstruct a resonance at $m_{\ell \ell} = m_{Z_D}$. In the PQ -symmetric limit of the NMSSM, light (pseudo)scalars in the spectrum similarly enable the on-shell decay $\chi_2 \rightarrow s(a) \chi_1 \rightarrow \ell \ell \chi_1$. However, in the NMSSM, the branching fractions to light leptons are suppressed by small Yukawa couplings, and $\text{Br}(h \rightarrow 4\mu + E_T)$ is cripplingly small unless the scalar is below the τ threshold, $m_{s(a)} < 2m_\tau$. When the scalar is this light, it is often produced with $p_{T,s} \gg m_s$, leading to collimated muons, but this is spectrum dependent. Collimated lepton pairs (lepton-jets) are discussed in Secs. XVI and XVII.

In models with a nontrivial flavor structure, *flavor-violating* decays of the form $h \rightarrow \chi \chi \rightarrow 4\ell + 2\nu$ can occur. A familiar example is Higgs decay into R -parity-violating neutralinos χ_1 , where χ_1 decays through the leptonic $L_i L_j e_k$ operator. In this case the two charged leptons from the decay $\chi_1 \rightarrow \ell' \ell \nu$ need no longer necessarily form same-flavor pairs.

Finally, another realization of the same final state occurs when the Higgs decays into two heavy neutrinos N , which then each decay through $N \rightarrow W^* \ell \rightarrow \nu \ell' \ell$ [130]. Similar phenomena and final states can arise in scotogenic models [364,365].

B. Existing experimental searches and limits

Several LHC searches give interesting bounds on the exotic decay $h \rightarrow 4\ell + E_T$. The best bounds when the leptons are nonresonant come from 8 TeV LHC multilepton searches. In order to highlight the strong dependence on the

exotic spectrum, we will present bounds for two benchmark models where $h \rightarrow \chi_2 \chi_2$ and $\chi_2 \rightarrow \chi_1 Z^*$.

- (i) An ‘‘optimistic’’ benchmark scenario with relatively large mass splitting between χ_2 and χ_1 , with $M_2 = 55$ GeV and $M_1 = 20$ GeV. Generally, models of this type are allowed by the LEP precision measurement of the Z width, as long as the coupling of the Z boson to $\chi_1 \chi_2$ is smaller than ~ 0.05 .³⁹ Even for couplings $\mathcal{O}(0.01)$, the decay $\chi_2 \rightarrow \ell \ell \chi_1$ is prompt. In general the Drell-Yan production of $\chi_2 \chi_2$ will yield an additional and model-dependent contribution to the leptons + E_T signature. For simplicity, throughout our analysis, we will always assume that the Z coupling to $\chi_2 \chi_2$ is sufficiently small that the Drell-Yan contribution is much smaller than the contribution coming from Higgs decay.
- (ii) A ‘‘pessimistic’’ benchmark scenario with a smaller mass splitting, $M_2 = 55$ GeV and $M_1 = 35$ GeV. This particular parameter point is consistent with LEP data when χ_2, χ_1 have the Z couplings of fourth-generation neutrinos [128]. The relatively small mass difference between the exotic final states renders the final-state leptons softer and makes the benchmark more challenging at the LHC.

In both cases we take

$$\text{Br}(\chi_2 \rightarrow \ell^+ \ell^- \chi_1) = \text{Br}(Z^{(*)} \rightarrow \ell^+ \ell^-). \quad (94)$$

For Higgs bosons produced in gluon fusion and assuming a reference 10% branching ratio for $h \rightarrow \chi_2 \chi_2$, the initial signal cross section for

$$pp \rightarrow h \rightarrow \chi_2 \chi_2 \rightarrow 4\ell \chi_1 \chi_1 \quad (95)$$

is approximately 10 fb, giving already ~ 200 events in the present LHC data set. Below we will indicate the excellent potential of the LHC to set bounds on the optimistic benchmark by recasting existent searches in multileptons. To indicate the sensitivity of these searches to the mass splitting between χ_1, χ_2 we also show that the more pessimistic benchmark, with its much softer daughter leptons, is as yet unconstrained. Dark photon models, with larger branching fractions to leptonic final states, face more stringent limits.

The multilepton analysis strategy pursued by both ATLAS and CMS divides events into several exclusive bins depending on multiple variables. The variables most notable for our purposes are lepton counts N_ℓ ; OSSF lepton pair invariant masses; and either (i) the value of E_T and H_T (defined as the scalar sum of the transverse energies of all jets passing the preselection cuts) [298,366], (ii) the value

³⁹This number has been found under the assumption $g_V = g_A$, where g_V and g_A are the vector and axial-vector couplings $g_V Z^\mu \chi_2 \gamma_\mu \chi_1$ and $g_A Z^\mu \chi_2 \gamma_\mu \gamma_5 \chi_1$, respectively. Similar limits can be found for $g_V \neq g_A$.

of S_T (the scalar sum of E_T , H_T , and the p_T of all isolated leptons) [299,367], or (iii) the value of m_T in three-lepton searches [368]. A more inclusive strategy is pursued in [369], which uses only N_ℓ and lepton pair invariant masses to define the several signal regions, while [370] introduces more specialized kinematic constraints to target specific models of electroweak production. All of these analyses set limits on models beyond the SM by combining individual limits from all bins, both high background and low background. As reinterpreting multilepton searches is highly sensitive to the details of modeling lepton acceptance, our aim here is principally to demonstrate the interesting level of sensitivity already available to nonresonant multileptonic Higgs decay.

In order to estimate signal efficiency, we generate inclusive Higgs events with at least two leptons⁴⁰ in MADGRAPH 5, shower them in PYTHIA, and cluster them in FASTJET. We generate gluon fusion production matched to one jet, VBF, and Wh associated production. The signal production cross sections are normalized to the values reported by the LHC Higgs Working Group [13] (see Table I).

For CMS multilepton analyses, we are able to make a fairly precise approximation of the signal efficiency by passing signal events through the version of PGS tuned by the Rutgers theory group [113,371] to more exactly simulate the CMS detector. We employ in addition the modified b -tagging routines and the correction factors for electron, muon, and hadronic tau efficiencies as established in [372].

For the ATLAS multilepton analyses, we approximate signal acceptance using the p_T -dependent lepton identification efficiencies quoted in Refs. [343,344]. Since our signal is characterized by relatively soft leptons, it is important to note that the electron efficiency drops below 70% for $p_T^e \lesssim \mathcal{O}(10)$ GeV while the muon identification efficiency remains high even for very soft muons ($\sim 90\%$ for $p_T^\mu \gtrsim 7$ GeV).

To set limits we treat each bin as a single Poisson counting experiment, marginalizing over background uncertainty according to a log-normal distribution, and combine bins according to a Bayesian algorithm with flat priors on signal strength. We quote 95% C.L. upper bounds.

The best limits on the optimistic benchmark come from recasting the 19.6 fb^{-1} search performed by CMS in four-lepton final states [369]. This search requires exactly four light leptons in the final state, forming at least one OSSF pair. Denoting the invariant mass of the OSSF lepton pair with mass $m_{\ell\ell}$ closest to m_Z as $M_{\ell\ell 1}$ and the invariant mass of the remaining lepton pair as $M_{\ell\ell 2}$, the events are divided into nine exclusive categories depending on whether $M_{\ell\ell 1}$

and $M_{\ell\ell 2}$ are below, above, or inside the Z window 90 ± 15 GeV. The vast majority of exotic Higgs decays fall in the bin $M_{\ell\ell 1} < 75$ GeV, $M_{\ell\ell 2} < 75$ GeV. Indeed, this is the *only* bin populated by gluon fusion and VBF; Wh associated production is the only contributing process in the other bins. The combined limit from all populated bins is

$$\text{Br}(h \rightarrow \chi_2 \chi_2) < 11\%, \quad (96)$$

which is also the 95% C.L. limit set by the single dominant bin. This translates into the limit $\text{Br}(h \rightarrow 4\ell + E_T) < 1.2 \times 10^{-3}$, with $\ell = (e, \mu, \tau)$ ⁴¹ for dark vectors with $\text{Br}(Z_D \rightarrow \ell\ell) = 3 \times 0.15$, $\text{Br}(h \rightarrow K_\nu K_\nu) < 6.1 \times 10^{-3}$. We show predicted signal events for this bin together with the expected and observed number of events in Table VIII. To show the steep dropoff in signal acceptance when the mass splitting in the cascade decay becomes smaller, we also show signal predictions in the same bin for the pessimistic benchmark, where the acceptance in gluon fusion has almost entirely disappeared.

The CMS three- and four-lepton channel search of Ref. [299], done with 9.2 fb^{-1} of 8 TeV data, places a similar limit of

$$\text{Br}(h \rightarrow \chi_2 \chi_2) < 14\%. \quad (97)$$

The signal dominantly populates the lowest bin in S_T , namely $0 < S_T < 300$ GeV, for all lepton multiplicity channels; VBF production also contributes secondarily to the next-highest bin, $300 \text{ GeV} < S_T < 600$ GeV. The bin with the single greatest signal contribution is that with three identified leptons and one OSSF pair with mass below the Z window. However, the signal-to-background ratio is better in the bin with the second-largest number of signal events, namely the bin with four identified leptons and two OSSF pairs below the Z window, no b 's, and no hadronic taus. This bin dominates the limit combination.

For the pessimistic benchmark, Ref. [299] limits

$$\frac{\sigma(pp \rightarrow h)}{\sigma(pp \rightarrow h)|_{\text{SM}}} \text{Br}(h \rightarrow \chi_2 \chi_2) < 1.04, \quad (98)$$

or $\text{Br}(h \rightarrow 4\ell + E_T) < 0.011$. The reach is almost entirely from VBF production, with several bins contributing significantly to the limit.

The CMS search of Ref. [298] uses the same data set as Ref. [299] but bins events in E_T and H_T instead of in S_T , and sets comparable limits. Finally, the CMS searches performed in Ref. [370] use kinematic discriminants which are tailored to the electroweak production of heavy states and are not sensitive to the kinematics of our exotic Higgs decay signal.

⁴⁰We include taus in the generation of the events. Taus are decayed using the Tauola plug-in within PYTHIA.

⁴¹Note that this limit translates into $\text{Br}(h \rightarrow 4\ell + E_T) < 5.4 \times 10^{-4}$ considering simply $\ell = e, \mu$.

TABLE VIII. Benchmark predictions for the number of events in the dominant bin (see text) in the most constraining CMS multilepton search [369] (third column) and ATLAS three-lepton search [368] (fourth column), for the optimistic and pessimistic benchmarks defined in the text, with $\text{Br}(h \rightarrow \chi_2 \chi_2) = 1$ and $\text{Br}(\chi_2 \rightarrow \chi_1 \ell \ell) = \text{Br}(Z \rightarrow \ell \ell)$. In the CMS bin, 14 events are observed and 10.4 ± 2.0 are expected. In the ATLAS bin, 41.8 events are excluded at the 2σ level. Signal expectations are reported separately for gluon fusion, VBF, and associated Wh production.

Model	Mode	CMS bin prediction [369]	ATLAS bin prediction [368]
“Optimistic” ($M_1 = 20$ GeV, $M_2 = 55$ GeV)	Gluon fusion	50.4	2.4
	VBF	56.2	7.6
	Wh	2.1	14
	Total	109	24
“Pessimistic” ($M_1 = 35$ GeV, $M_2 = 55$ GeV)	Gluon fusion	...	0.6
	VBF	2.2	2.2
	Wh	0.2	3.6
	Total	2.4	6.4

ATLAS multilepton searches [367,368] are less sensitive than the CMS searches we have just discussed, mainly because of the missing energy requirement (at least 50 GeV in all the signal regions). In particular, the most sensitive search is the three-lepton search of [368] performed with 20.7 fb^{-1} of 8 TeV data. The most constraining bin is the so-called SRnoZa that requires $E_T > 50$ GeV and all OSSF lepton pairs to have an invariant mass below 60 GeV. As shown in Table VIII, the main contribution to this bin comes from a Higgs produced in association with a W boson. Assuming $\text{Br}(h \rightarrow \chi_2 \chi_2) = 1$, the optimistic benchmark model leads to only ~ 24 events, to be compared to the 41.8 events ATLAS can exclude in this bin.

We have checked that Zh associated production does not yield a sizable contribution to the CMS and ATLAS multilepton analyses. In particular, these events dominantly populate the CMS 4ℓ bin with $75 \text{ GeV} < M_{\ell\ell_1} < 105 \text{ GeV}$ and $M_{\ell\ell_2} < 75 \text{ GeV}$ [369], in which the signal would only be ~ 0.2 events.

The inclusive multilepton search strategy pursued by CMS does a reasonable job of constraining multileptonic Higgs decays when the mass splitting in the cascade decay is sufficiently large that all four leptons can be identified at a reasonable rate. However the rapid degradation of these limits as the mass splitting is squeezed suggests that further adapting multilepton searches to the kinematics of exotic Higgs decays would be beneficial in order to recover sensitivity to cascade decays with smaller mass splittings.

As the mass splitting is decreased, VBF and Wh associated production become more important relative to

gluon fusion. Although VBF production yields slightly higher- p_T final states than either gluon fusion or Wh , the Higgs exotic decay is still a lower- p_T signal than most BSM signals sought in multilepton searches. An analysis more tailored to the specific kinematics of a 125 GeV Higgs could improve the reach. Imposing cuts on the transverse mass of the leptons and the E_T could efficiently separate the Higgs signals from top and fake backgrounds, so long as VBF is more important than Wh ; it may also be beneficial to target VBF production directly, by requiring the presence of tagging jets. In the CMS multilepton searches, regardless of the mass splittings in the cascade, Wh production dominantly populates the bin with three identified leptons, one OSSF pair with invariant mass below the Z window, and zero τ 's and b jets, in the lowest S_T (H_T) bin. This is the same bin that receives the greatest single contribution from gluon fusion as well. The background composition in this bin contains a larger proportional contribution from fake leptons than in bins with higher S_T [299], suggesting tighter lepton ID may be beneficial in optimizing search strategies for the relatively low- p_T Higgs signal, as well as more aggressive b -jet rejection to suppress backgrounds from top pair production. Further, S_T regions designed for SM Higgs production mechanisms could help by concentrating the VBF signal in a single bin (as gluon fusion and Wh already are).

Finally, we comment on the case where the leptons form resonant pairs. In particular let us consider the decay chains $h \rightarrow K_v K_v \rightarrow 2Z_D 2\pi_v \rightarrow 4\ell + E_T$, so that $\text{Br}(h \rightarrow 4\ell + E_T)/\text{Br}(h \rightarrow \text{BSM}) = \text{Br}(Z_D \rightarrow \ell^+ \ell^-)^2$. In general, the signal acceptance in the above multilepton searches does not change substantially relative to the nonresonant signals. However, the presence of the leptonic resonances makes these decays much easier to constrain. Once again, limits will be highly sensitive to the BSM mass spectrum, which controls the lepton p_T 's. In spectra giving rise to decays with little to no E_T , exclusions on the parent exotic decay could approach the $\lesssim 10^{-3}$ level obtained for $h \rightarrow 4\ell$ decays with no E_T (see Sec. XI), with the sensitivity dropping rapidly as the spectrum is squeezed and the lepton acceptance drops.

XV. $h \rightarrow 2\ell + E_T$

In this section, we study exotic Higgs decays to final states that contain two isolated leptons and missing energy, where the leptons do not reconstruct a resonance (we also comment briefly on the case where they do). Models which realize these decays often also realize decays with four leptons and missing energy, covered in Sec. XIV.

A. Theoretical motivation

In Sec. XIV, we outlined many classes of theories where an initial decay $h \rightarrow XX$ is followed by the decay $X \rightarrow \ell \ell E_T$. One example, which produces an OSSF lepton

pair, is the decay of a neutralino χ_2 through an off-shell Z boson to $\ell\ell\chi_1$. Similarly, a hidden sector meson K_ν could decay through an off-shell dark vector boson Z_D into OSSF leptons plus a lighter, detector-stable hidden meson, $\ell\ell\pi_\nu$.

Decays where $h \rightarrow 2\ell + E_T + X$ can arise in these theories in two ways. First, in a decay that begins via $h \rightarrow \chi_2\chi_2$, one of the χ_2 's can decay to $2\ell + E_T$ while the other decays to $2j + E_T$ or $2\nu + E_T$. Second, the Higgs will frequently also have the off-diagonal decay $h \rightarrow \chi_2\chi_1$, giving $h \rightarrow 2\ell + E_T$. All of these decay chains result in an OSSF lepton pair together with missing energy and potentially extra soft jets [373].

Another realization of the signature $h \rightarrow 2\ell + E_T$ is found in theories with a light sterile neutrino, where the coupling $y_i N H L_i$ gives rise to the decays $h \rightarrow \nu N$, followed by both $N \rightarrow \ell_i W^{(*)} \rightarrow \ell_i \ell_j \nu$ and $N \rightarrow \nu Z^{(*)} \rightarrow \nu \ell \ell$ [55,373]. Decays through the (virtual) W could yield opposite-sign dileptons with no flavor correlation, unlike the OSSF pair of leptons generated through $Z^{(*)}$ and $Z_D^{(*)}$. These Higgs decays would also be accompanied by Drell-Yan production of $N\nu$, which yields a nonresonant contribution to the same final states.

As discussed in Sec. XIV, if there is a light bosonic state, the decay $\chi_2 \rightarrow \chi_1 \ell \ell$ can proceed via an intermediate on-shell state, $\chi_2 \rightarrow Z_D \chi_1, a \chi_1, s \chi_1$, such that the leptons reconstruct a resonance. For dark vector bosons, the branching ratio to light leptons is appreciable for any $m_{Z_D} < m_h/2$. For (pseudo)scalars with mass-weighted couplings, such as can appear in the PQ -NMSSM [54], we need $m_{(a,s)} \lesssim 2m_\tau$ for muonic branching fractions to be significant. This does not necessarily imply that the muons will be collimated, as the $a(s)$ is coming from a cascade decay, and depending on the particular values of m_2, m_1 , may be produced at relatively low p_T . Nevertheless the experimental searches for high- p_T isolated leptons almost invariably require $m_{\ell\ell} > (10-12)$ GeV for all OSSF pairs in order to suppress quarkonia backgrounds, making such searches insensitive to light bosons regardless of their p_T . We discuss the case of $h \rightarrow (\ell\ell) + E_T$ through a low-mass boson like a or s in Sec. XVI.

Finally, we also comment that flavor-violating decays $h \rightarrow \chi\chi$ followed by $\chi \rightarrow \ell q q'$ yield two leptons plus additional soft jets, albeit no missing energy. These decays can arise from Higgs decay to neutralinos, which decay through R -parity-violating operators such as $L_i Q_j d_k$. They also occur in models where the Higgs decays to two heavy right-handed neutrinos, followed by $N \rightarrow W^{(*)} \ell \rightarrow q q' \ell$ [130]. Similar final states can arise in scotogenic models [364,365]. When the neutrino or neutralino is Majorana, the leptons may have the same sign, yielding a distinctive signature.

B. Existing experimental searches and limits

The signature of ≥ 2 leptons together with missing energy occurs in the SM decays of a 125 GeV Higgs

boson: the decays of a Higgs into $WW^*, \tau\tau$ and ZZ^* , with subsequent decays of W/Z bosons and taus into leptons and neutrinos give rise to this final state. While the decay $h \rightarrow Z^{(*)}Z^* \rightarrow \ell\ell + \nu\nu$ suffers from a disadvantageous signal-to-background ratio, both $h \rightarrow WW^* \rightarrow 2\ell + E_T$ and $h \rightarrow \tau\tau \rightarrow 2\ell + E_T$ are standard SM Higgs search channels. These SM leptons + invisible Higgs decays can, depending on kinematics, present an important background for BSM Higgs searches in leptons plus missing energy final states. Conversely, existing SM Higgs searches have sensitivity to begin to constrain BSM leptons + invisible Higgs decays, though the tailoring of SM Higgs searches to SM decay kinematics reduces their reach for BSM multilepton + missing energy decays [374]. Associated Wh production also yields three-lepton final states, but at rates too small to be constrained by both ATLAS and CMS multilepton searches [298,299,367,368].

We will estimate the limits on a benchmark decay chain that begins with the off-diagonal decay $h \rightarrow \chi_1\chi_2$, followed by $\chi_2 \rightarrow \chi_1 + 2\ell$ through an off-shell Z :

$$h \rightarrow \chi_1\chi_2 \rightarrow 2\ell + 2\chi_1. \quad (99)$$

We will show results for the optimistic reference working point presented in the previous section, where $m_{\chi_1} = 20$ GeV, $m_{\chi_2} = 55$ GeV. Limits for $h \rightarrow \chi_2\chi_2 \rightarrow 2\ell + E_T + X$ cascade decays will be less constraining than those for the off-diagonal decay due to the reduced E_T .

For the decay $h \rightarrow \chi_2\chi_1$, depending on the masses m_2, m_1 , the kinematics of the daughter leptons and E_T are often broadly similar to the SM $h \rightarrow WW^*$ decay. Recalling that $\text{Br}(h \rightarrow WW^* \rightarrow 2\ell 2\nu) \approx 0.26 \times 0.103$ and that $\text{Br}(Z \rightarrow \ell\ell) \approx 0.102$ (we include τ 's), a Higgs with 10% branching fraction to $\chi_1\chi_2$ contributes roughly 40% the rate of the SM WW^* dileptonic decay mode before acceptance is taken into account.

Performing a careful recast of SM $h \rightarrow WW^*$ searches is challenging as the sensitivity to exotic signals is not straightforward to extract from the published experimental analyses. CMS's SM searches use multivariate discriminants to separate signal from background, rendering a careful recast challenging except in the earliest analyses (such as [375]), which are not constraining. Meanwhile, ATLAS's full 7 + 8 TeV results [376] extract the SM signal using a multichannel likelihood, and a recast would require use of the full likelihood function. Here our main aim is to estimate the BSM branching fraction into dileptonic modes that is allowed by SM Higgs searches. To this end we approximate the BSM acceptance to be equal to the SM acceptance in the multivariate discriminants. This is a conservative choice, but likely to be the correct order of magnitude for the particular benchmark model we consider. For more general choices of m_1, m_2 , the acceptance will often be significantly reduced relative to

this benchmark, as the daughter leptons may be much softer.

As in the previous section, to obtain these limits we use MADGRAPH 5 and PYTHIA 6 to generate gluon fusion Higgs signal events, matched out to one jet. For CMS searches, we employ a version of PGS tuned to CMS's operating parameters. For ATLAS searches, we use parameterized lepton efficiencies as reported in the searches under consideration, with jet clustering performed in FASTJET. We neglect VBF production, as well as the VBF-like event categories in the ATLAS and CMS searches.

The “cut-based” analysis of the full 7 + 8 TeV CMS 0j and 1j $h \rightarrow WW^*$ analysis [377] employs a multivariate discriminant in states with same-flavor leptons to separate $h \rightarrow WW^*$ signal from Drell-Yan pair production. Approximating the efficiency of this multivariate discriminant at the SM Higgs-like value $\epsilon \approx 0.5$ on the BSM decay mode $h \rightarrow \chi_2\chi_1 \rightarrow 2\ell + E_T$, and combining the effect of this multivariate cut with the rest of the analysis selection, we can estimate the ratio of the BSM signal to the SM signal. Using CMS's best fit for the SM signal strength μ in the $h \rightarrow WW^*$ mode in the 0 and 1 jet categories,

$$\mu|_{\text{fit}} = 0.79 \pm 0.38, \quad (100)$$

we estimate

$$\frac{\sigma(pp \rightarrow h)}{\sigma(pp \rightarrow h)|_{\text{SM}}} \text{Br}(h \rightarrow \chi_1\chi_2) \lesssim 1.0 \quad (101)$$

for the reference benchmark point. Again, this limit includes an assumed factor of $\text{Br}(Z \rightarrow \ell^+\ell^-) \sim 0.102$; decay chains with off-shell dark photons, which have leptonic branching fractions roughly 4 times larger, are subject to the tighter constraint $\text{Br}(h \rightarrow \chi_2\chi_1) \lesssim 0.24$.

Meanwhile, in the ATLAS analysis [376], the final step in the analysis is fitting SM signal and background distributions in the transverse mass variable $m_T(2\ell, E_T)$. ATLAS's background-subtracted predictions for the SM signal strength are shown in Fig. 34, together with the prediction from the BSM benchmark, to indicate the degree of similarity between the two signals in the final discriminating variable. The cuts employed in the ATLAS analysis give comparatively less sensitivity to the BSM signal than do the CMS cuts. As a consequence, under the simplifying assumption that the SM and BSM signals are extracted with similar efficiency in the final fit, no limit is placed on the branching fraction into the BSM final state.

Since the signal investigated in this section contributes almost entirely to same-flavor final states, better sensitivity could be obtained by considering different-flavor and same-flavor final states separately. As our recasting is highly approximate due to the lack of information about the multivariate discriminants employed in the same-flavor final states, we will simply mention this as one obvious

avenue for improving on the approximate bound shown in Eq. (101). In cases where the two leptons reconstruct a resonance, significantly better limits may be possible. Meanwhile the heavy neutrino decay through a (virtual) W , which does contribute to different-flavor final states, would show interesting departures from flavor universality depending on the flavor mixings in the neutrino sector; this heavy neutrino model should be looked for simultaneously in Drell-Yan and Higgs decays as the ratio of the two signals is fixed.

XVI. $h \rightarrow \text{ONE LEPTON-JET} + X$

In this and the following section, we study exotic Higgs decays to final states that contain one or two *low-mass* resonant lepton pairs. Higgs decays to collimated pairs of leptons (here $\ell = e, \mu$ but not τ) have been a focus of much experimental and theoretical work. Searches for collimated pairs of leptons are typically carried out inclusively; that is, no attempt to reconstruct the Higgs mass is made. Thus the same searches constrain decays both with and without the presence of E_T , although events with E_T (or other Higgs daughter products, such as soft jets) will typically have reduced acceptance. In this section, we consider Higgs decays to one lepton-jet + X , and in the following section we consider Higgs decays to two lepton-jets + X . For simplicity we focus on *simple* lepton-jets, consisting of a collimated pair of either electrons or muons; *complex* lepton-jets, which have a larger and more variable particle content that can involve hadrons and detector-stable states as well as leptons, are important and interesting signals, but less transparent to survey.

In the current section we study Higgs decays to one (simple) lepton-jet + X . Because experimental backgrounds for a single lepton-jet are higher than those for two, traditionally the focus has been on signals with two

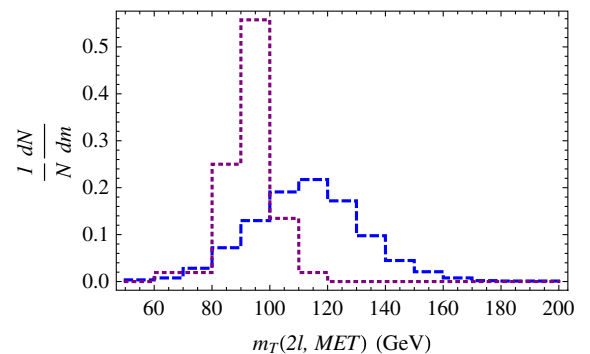


FIG. 34 (color online). Unit-normalized distributions of $m_T(2\ell, E_T)$. The blue dashed line shows the ATLAS prediction for SM $h \rightarrow WW^*$ events passing all selection criteria in both 7 and 8 TeV data sets [376]. The purple dotted line shows the distribution for the BSM $h \rightarrow 2\ell + E_T$ events arising from $h \rightarrow \chi_2\chi_1$ at the 8 TeV LHC in the benchmark model described in the text.

lepton-jets. In this section we emphasize, firstly, that there are well-motivated signals that produce a *single* lepton-jet only or dominantly, and secondly, that exclusive analyses targeting these states can yield meaningful sensitivity to these decays.

The opening angle of two partons coming from a parent particle X can be roughly estimated as $\Delta R \approx 2m_X/p_{T,X}$. We can estimate $p_{T,X} \sim 50$ GeV, for a particle X coming from the decay of a 125 GeV Higgs produced at rest. Partons from the X decay are then typically separated by $\Delta R < 0.2$ when $m_X \lesssim 5$ GeV. Therefore, we expect to have a Higgs decaying into collimated leptons that fail typical isolation cuts requiring $\Delta R > 0.4$ if the parent particle X has a mass of the order of 10 GeV or less. Meanwhile if the parent particle X is produced in a cascade decay instead of directly, it will be less boosted. Clearly the transition between having isolated leptons and collimated leptons happens smoothly as a function of the parent particle mass m_X . The reader may also be interested in Sec. XI, which considers isolated leptons with $m_{\ell\ell} > 4$ GeV.

A. Theoretical motivation

One theory that realizes the decay $h \rightarrow (\mu\mu) + E_T$ is the PQ -symmetric limit of the NMSSM [53,54]. In this limit, the degrees of freedom (s, a, χ_1) (scalar, pseudoscalar, and fermion, respectively) comprising the singlet multiplet are all light. Decays of the Higgs to $h \rightarrow \chi_1\chi_2$ or $h \rightarrow \chi_2\chi_2$, with subsequent decays $\chi_2 \rightarrow \chi_1 s, \chi_1 a$, give Higgs decay signatures with missing energy in the final state. In an appreciable portion of parameter space, these decays can dominate the exotic Higgs branching fraction, as detailed in Sec. IC 8 and Refs. [53,54]. If s (or a) is very light, with mass order $m \lesssim \mathcal{O}(1)$ GeV or below, phase space forbids decays to heavier fermions and the branching fraction into light leptons becomes appreciable [$\mathcal{O}(10\%)$; see, e.g., Fig. 7]. The resulting signatures are dileptons + E_T for $h \rightarrow \chi_1\chi_2$ and four leptons + E_T for $h \rightarrow \chi_2\chi_2$, which correspond to the type-I and type-III decay topologies presented in Sec. XIV. The $s(a)$ is produced with a p_T that is dependent on the masses of χ_2 and χ_1 , but in the regime where decays to muons dominate, typically we will have $p_{T(a,s)} \gg m_{a,s}$, and the daughter muons will be collimated: $\Delta R_{\ell\ell} \lesssim 0.1$.

Dark vector boson models can also realize the collimated leptons + E_T Higgs decay signature. In a supersymmetric context, χ_2 would now be mainly bino and χ_1 a dark photino, but in this case the off-diagonal $h \rightarrow \chi_2\chi_1$ decay can only be important if the decay $h \rightarrow \chi_2\chi_2$ is kinematically forbidden. In a more general hidden sector, the role of the neutralinos χ_i may be played instead by hidden sector mesons K_v, π_v or similar states; see Sec. IC 10. Dark photon models can also yield Higgs decays of type-II topology (see Sec. XIV). In this case, the Higgs decays directly to dark vectors, $h \rightarrow Z_D Z_D$, followed by $Z_D \rightarrow$

lepton jet on one side and $Z_D \rightarrow$ invisible on the other. Here the invisible states are detector-stable hidden sector states, perhaps dark photinos [52,149,363,378]; the relative branching fractions to leptons, E_T , and other SM partons are model dependent. Similar signatures can be obtained in the R -symmetric NMSSM if the light pseudoscalar is coupled to a hidden sector. Another possible realization of the type-II topology is provided by the decay $h \rightarrow ZZ_D$, followed by $Z \rightarrow \nu\nu$.

Also a possibility are decays $h \rightarrow (\mu\mu) + (jj)$, i.e., where the lepton-jet recoils against hadronic activity. This kind of decay arises in, e.g., the R -symmetric limit of the NMSSM, where $h \rightarrow aa$ is followed by $a \rightarrow \mu\mu$ on one side of the event and $a \rightarrow$ hadrons on the other. As $\text{Br}(a \rightarrow \mu\mu) \lesssim 0.1$ even below the τ threshold, $\text{Br}(h \rightarrow (\mu\mu)(jj)) > \text{Br}(h \rightarrow 2(\mu\mu))$; however the $2(\mu\mu)$ final state has notably lower background, as well as sharper resolution. Similarly, $h \rightarrow Z_D Z_D \rightarrow (\ell\ell)(jj)$ leads to a lepton-jet balanced against a “weird” hadronic jet.

Unlike the NMSSM (pseudo)scalars, dark photons have appreciable branching fractions to light leptons even for large masses m_{Z_D} . However, possible connections with cosmic ray anomalies [136,137] and the discrepancy between the measured and calculated muon anomalous magnetic moment [140] have stimulated interest in dark vectors with a mass at or below the GeV scale, thus involving collimated leptons in the final state. For discussion of dark vectors outside the collimated regime, see Secs. X and XI.

B. Existing collider studies

A dedicated analysis for $h \rightarrow \chi_1\chi_2 \rightarrow \ell^+\ell^- + E_T$ is presented in [54], which indicates that the 8 TeV LHC could have good sensitivity to this final state when a targeted search is performed that exploits the E_T in the final state from the Higgs decay. As an illustration, the analysis focuses on a benchmark inspired by the PQ -symmetric limit of the NMSSM, with a light scalar (pseudoscalar) resonance s (a) set to have a mass of 1 GeV (see Table IX).

The analysis focuses on the $W^\pm h$ production mode where the W decays leptonically. The resulting signature contains one hard lepton (e, μ) from the W decay, two collimated muons, and E_T . Since there are no jets in the hard scattering process, the W + jets, Z + jets, and $t\bar{t}$ backgrounds can be efficiently eliminated with a jet veto. The diboson WZ and ZZ backgrounds are removed by a dimuon mass window cut. A muon isolation cut is applied to remove the low-mass dimuon background from meson decays, which requires the transverse momentum sum of hadronic jets (excluding the contribution from any nearby muons) in a cone of $R = 0.4$ around each muon candidate to be less than 5 GeV. Then the light resonance can be reconstructed via the two nearby muons, and the main background is $W\gamma^*/Z$, with γ^*/Z decaying into $\mu^+\mu^-$. A trilepton trigger is assumed in the analysis, though

alternatively, one can trigger on the single lepton from the W decay. The analysis indicates that, with 20 fb^{-1} data, a sensitivity $S/\sqrt{B} > 6\sigma$ can be achieved at the 8 TeV LHC, with

$$c_{\text{eff}} = \frac{\sigma(h)}{\sigma(h_{\text{SM}})} \times \text{Br}(h \rightarrow \chi_1 \chi_2) \times \text{Br}(\chi_2 \rightarrow s \chi_1) \times \text{Br}(s \rightarrow \mu^+ \mu^-) = 0.1 \quad (102)$$

assumed. Details of the analysis can be found in [54].

This analysis for searching for a dimuon resonance with E_T can be easily generalized to other related possibilities. If the light resonance is a vector, then a wider range of masses should be considered, which would result in a larger average separation between the two daughter leptons. Another possibility arises from the decay chain $h \rightarrow \chi_2 \chi_2 \rightarrow (\mu\mu)(\tau\tau) + E_T$ or $(\mu\mu)(bb) + E_T$ (for details, see Sec. IC 8). Obviously such decay chains can be picked up also by the proposed collider search. Further, although in this analysis only Wh events are considered, it is straightforward to generalize the analysis to Zh events that trigger on the leptons from the Z decay. It is also of interest to consider gluon fusion and VBF production, where lepton-jet or even dilepton triggers may yield a reasonable acceptance for this decay mode. We leave this question for future work.

C. Existing experimental searches and limits

Leptons arising from very light parents will typically fail standard isolation requirements, and isolated leptons + E_T searches at LHC are not very sensitive to such scenarios. Even in searches where lepton isolation criteria are relaxed, typically a cut is placed on the invariant mass of any opposite-sign, same-flavor lepton pair in the event, usually $m_{\ell\ell} > 10\text{--}12 \text{ GeV}$ (in some cases $m_{\ell\ell} > 4 \text{ GeV}$), in order to suppress backgrounds from quarkonia. Thus even if a light boson were produced with moderate to low p_T , it would be missed by most searches in leptonic final states. The potentially significant bounds come from dedicated searches for lepton-jets, where modified lepton isolation criteria are applied, and low-mass ranges are considered. Searches for lepton-jets have been pursued by both CMS [379] and ATLAS [85,227,289].

In the ATLAS analyses, either a displaced vertex for the lepton-jets [85], or at least four muons within a single lepton-jet [289], or at least two lepton-jets are required [227,289]. All of these three features are absent in the scenario

TABLE IX. Mass parameters of the $h \rightarrow$ collimated leptons + E_T benchmark model.

m_s	m_h	m_{χ_1}	m_{χ_2}
1 GeV	125 GeV	10 GeV	80 GeV

$$h \rightarrow \chi_1 \chi_2 \rightarrow \ell^+ \ell^- + E_T. \quad (103)$$

The most relevant search is from the CMS search for light resonances decaying into pairs of muons [379], which sets an upper bound on the cross section for $pp \rightarrow (\phi \rightarrow \mu^+ \mu^-) + X$ for new bosons ϕ with masses below 5 GeV, using 35 pb^{-1} of data collected at the 7 TeV LHC. Selection cuts of $|\eta_{\mu\mu}| < 0.9$ and $p_{T,\mu\mu} > 80 \text{ GeV}$ are applied for the muon pair. As indicated by the study in [54], most events arising from the decay mode of Eq. (103) cannot pass the CMS selection cuts because the s -originating dimuon pairs are too soft, with an average $p_T \sim 40 \text{ GeV}$. The signal efficiency of the CMS selection cuts is $\epsilon \lesssim 0.7\%$ for the benchmark introduced below, and roughly of the same order for a lighter s . Then the signal cross section is given by $\sigma_{h_{\text{SM}}} \times c_{\text{eff}} \times \epsilon \sim (0.1 \text{ pb}) \times c_{\text{eff}}$, with $c_{\text{eff}} = \frac{\sigma(h)}{\sigma(h_{\text{SM}})} \times \text{Br}(h \rightarrow \chi_1 \chi_2) \times \text{Br}(\chi_2 \rightarrow s \chi_1) \times \text{Br}(s \rightarrow \mu^+ \mu^-)$, which well satisfies the 0.15–0.7 pb limit for masses $\lesssim 1 \text{ GeV}$ at 95% C.L. (at the mass point $m_{\ell\ell} \sim 1 \text{ GeV}$, the limit is $\sim 0.4 \text{ pb}$) obtained in [379]. This CMS analysis is not updated yet to use the full LHC run 1 data set. The experimental bounds obtained by the LHC searches therefore do not place any limits on the branching fraction $\text{Br}(h \rightarrow \mu^+ \mu^- + E_T)$ in the collimated/low-mass regime.

D. Proposals for new searches at the LHC

A search for $h \rightarrow$ one lepton-jet (or one light resonance) + E_T is highly motivated on both theoretical and experimental sides. Theoretically, such a decay topology can arise in a couple of well-motivated scenarios. Experimentally, E_T and the light resonance reconstruction bring new inputs for exploring new physics. Using the full 7 and 8 TeV data set of both experiments, strong constraints or discovery-level sensitivity might be achieved. As is illustrated in [54], for $h \rightarrow$ one lepton-jet($\mu\mu$) + E_T and $c_{\text{eff}} = 0.1$, a sensitivity $S/\sqrt{B} > 6\sigma$ can be achieved, using 20 fb^{-1} of data at the 8 TeV LHC. Though the light resonance is assumed to be $\sim 1 \text{ GeV}$, a good sensitivity for probing a wider range of masses should be expected.

XVII. $h \rightarrow$ TWO LEPTON-JETS + X

Here we consider Higgs decays to two lepton-jets + X ; see also the previous section for related signatures. Again, for simplicity we concentrate on simple lepton-jets, consisting of a single collimated electron or muon pair.

A. Theoretical motivation

As mentioned in the previous section, one well-studied model for a Higgs decaying to pairs of collimated muons is the NMSSM. Here the Higgs decays via $h \rightarrow aa$, with a subsequently decaying to pairs of SM partons according to the Yukawa couplings of a type-II 2HDM model plus a

singlet. The branching ratios of a to SM partons are shown in Fig. 7. Notably, in the NMSSM, branching fractions of a into a muon pair only reach the $\mathcal{O}(\text{few percent})$ level even below the mass threshold $m_a < 2m_\tau$. This necessarily places the pseudoscalar a in the mass range to produce collimated daughter muons. Another way to realize $h \rightarrow 2(\mu\mu) + X$ arises in the PQ -symmetric limit of the NMSSM (Sec. IC 8), where the initial Higgs decay is into neutralinos, producing light (pseudo)scalars in subsequent cascade decays, $h \rightarrow \chi_2\chi_2$, $\chi_2 \rightarrow (a)s\chi_1$ (see also Sec. XVI). In this case the light scalar will typically be less boosted, but in the mass range where decays to muons are relevant, the muons will generally still be collimated.

In any singlet-augmented 2HDM model, once $m_a > 2m_\tau$, the branching fraction for $a \rightarrow \mu\mu$ will always be suppressed by the small ratio $m_\mu^2/m_\tau^2 \sim 3.5 \times 10^{-3}$. As discussed in Sec. VI, the tiny branching fraction into $h \rightarrow 4\mu$ is not competitive with 4τ , $2\mu 2\tau$. Thus if a couples proportional to mass, only the range $2m_\mu < m_a < 2m_\tau$ is of interest for the decay $h \rightarrow 4\mu$. Decays to electron pairs are always negligible (unless $m_a \lesssim 2m_\mu$, which we do not consider comprehensively here).

Higgs decays to collimated lepton pairs may also arise in models with light vector bosons Z_D that mix with the SM hypercharge gauge boson (see Sec. IC 5). The motivation to consider $m_{Z_D} \ll m_h$ has been driven by dark matter models that require $m_{Z_D} \sim \text{GeV}$ or below [136,137]. In these models, the branching fractions of Z_D depend on the SM fermion gauge couplings, rather than on Yukawas, and therefore electron and muon pairs are produced with comparable branching fraction unless Z_D is extremely light, $m_{Z_D} \lesssim 2m_\mu$. Importantly [32], the branching fraction for $h \rightarrow 2(\ell\ell)$ remains large even when $m_{Z_D} > 2m_b$, motivating searches for both electrons and muons in this mass range.

Dark photon models can give $h \rightarrow 2$ lepton-jets directly, via an initial decay $h \rightarrow Z_D Z_D$, as well as $h \rightarrow 2$ lepton-jets + E_T . There are two distinct possibilities for obtaining E_T . One possibility is that nontrivial showering of the dark vector boson occurs, resulting in the production of detector-stable states in the dark sector together with leptons [32,149,378], yielding complex lepton-jets containing E_T . Another possibility is that the Higgs decays first to (e.g.) binolike neutralinos χ_2 , which then (similar to [52]) decay to a dark vector and a dark photino, $\chi_2 \rightarrow \chi_1 Z_D$. Since bino-dark photino mixing is proportional to the kinetic mixing parameter $\epsilon \ll 1$, off-diagonal decays $h \rightarrow \chi_2\chi_1 \rightarrow Z_D 2\chi_1$ are negligible in comparison to the unsuppressed $h \rightarrow \chi_2\chi_2 \rightarrow 2Z_D 2\chi_1$ as long as both decays are kinematically available. In a nonsupersymmetric case, the role of the neutralinos χ_i may be played instead by hidden sector mesons K_v , π_v or similar states [32], and the off-diagonal decays may not be suppressed; see Sec. IC 10.

B. Existing collider studies

A collider search for $h \rightarrow 2a \rightarrow 4\mu$ was first proposed in [380], which took $m_a \approx 215 \text{ MeV}$, as motivated by an excess in HyperCP measurements of $\Sigma^+ \rightarrow p\mu^+\mu^-$ decay [381]. This study pointed out that modifications of the (then-)standard muon isolation algorithms would be required to preserve the signal and concluded that as long as reasonable efficiencies for muon identification could be maintained, the signal had excellent prospects for detection. However the dominant QCD background to this signal was not identified. A more careful treatment of the dominant QCD backgrounds was carried out in [382], which concluded that the signal would still be nearly background-free, with excellent prospects for discovery in early 14 TeV LHC running (considering exotic branching fractions of tens of percent).

Reference [383] performed a collider study of the Higgs decaying to multiple electron jets plus E_T through a 100 MeV Z_D . Production in association with a leptonic W or Z was identified as the most promising channel, in which the dominant background is W or Z plus QCD jets. Reference [383] found that an analysis distinguishing electron jets from QCD jets using the electromagnetic fraction and charge ratio of the jet candidates could discover the Higgs with 1 fb^{-1} of 7 TeV LHC data at 95% C.L. with $\text{Br}(h \rightarrow \text{electron jets} + E_T) = 1$ for $m_h < 135 \text{ GeV}$.

C. Existing experimental searches and limits

The $h \rightarrow 2(\mu\mu)$ signature has become established in experimental programs, beginning with the D0 search [287]. The most stringent constraints on $h \rightarrow 2(\mu\mu) + X$ are set by the LHC, where several searches have been carried out, looking for Higgs decays to both prompt [288,339,379] and displaced [85] dimuon jets. As this final state is extremely clean, these searches are carried out inclusively, and in particular do not require $m_{4\mu} = m_h$. Thus these searches are sensitive to both the NMSSM-like $h \rightarrow aa \rightarrow 2(\mu\mu)$ decay topology and the SUSY-dark vectorlike topology $h \rightarrow \chi_2\chi_2 \rightarrow 2(\mu\mu)2\chi_1$, where the dimuon jets are accompanied by missing energy.

The best existing limits on prompt $h \rightarrow 2(\mu\mu) + X$ come from the recent CMS analysis [339], which was performed with the full 8 TeV data set. This search, like the previous CMS search [288], only covers the range $2m_\mu < m_a < 2m_\tau$.⁴² This search limits

$$\sigma(pp \rightarrow 2a + X)\text{Br}(a \rightarrow \mu\mu)^2\alpha_{\text{gen}} < 0.24 \text{ fb} \quad (104)$$

at 95% C.L. over almost all of the mass range in consideration, where α_{gen} is a (model-dependent) fiducial acceptance. This translates to a limit

⁴²It also requires the two lepton-jet masses to be within 0.1 GeV of each other, meaning it is insensitive to decays $h \rightarrow a_1 a_2$ with $a_1 \neq a_2$.

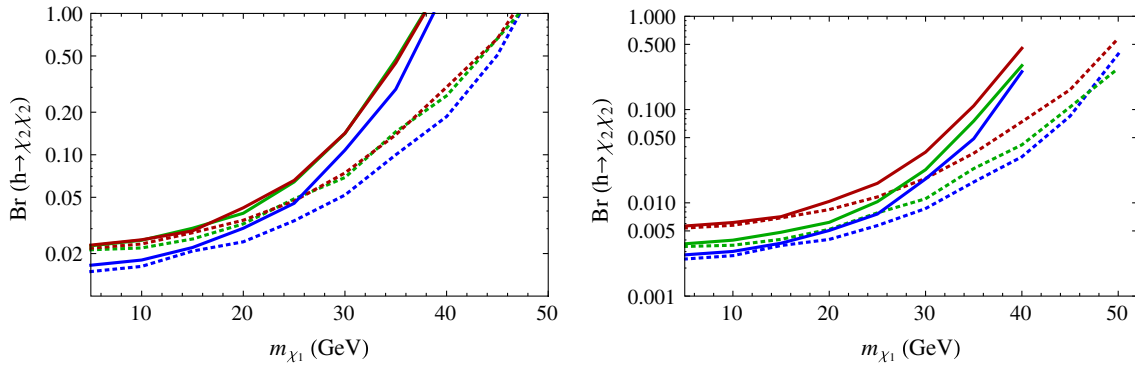


FIG. 35 (color online). Approximate bounds on the branching fraction for $h \rightarrow \chi_2 \chi_2$, assuming (left) $\text{Br}(\chi_2 \rightarrow a \chi_1) = 1$, and (right) $\text{Br}(\chi_2 \rightarrow Z_D \chi_1) = 1$, as a function of m_{χ_1} , from [339]. Here solid lines indicate $m_{\chi_2} = 50$ GeV and dotted lines $m_{\chi_2} = 60$ GeV, while red, green, and blue correspond to $m_{a,Z_D} = 3, 1$, and 0.4 GeV, respectively. We use tree-level results for $\text{Br}(Z_D \rightarrow \mu\mu)$ (see Fig. 13) and a reference $\text{Br}(a \rightarrow \mu\mu) = 0.1$ (which can occur in type-IV 2HDM + S models; see Fig. 9).

$$\text{Br}(h \rightarrow aa) \text{Br}(a \rightarrow \mu\mu)^2 \alpha_{\text{gen}} < 1.2 \times 10^{-5} \quad (105)$$

for $m_h = 125$ GeV. Outside this mass range, the 35 pb^{-1} search of Ref. [379] extends to 5 GeV, placing limits of $\sigma(pp \rightarrow 2a + X) \text{Br}(a \rightarrow \mu\mu)^2 \epsilon < 125 \text{ fb}$, where ϵ is again an acceptance.

The analysis of Ref. [339] has been presented in a way that is particularly easy to recast. Limits are shown as a function of the parameter α_{gen} , which represents the *generator level* efficiency for a given signal to have at least four muons satisfying $p_T > 8$ GeV, $|\eta| < 2.4$ and at least one muon to have $p_T > 17$ GeV, $|\eta| < 0.9$. Reference [339] estimates a systematic uncertainty on the relation of α_{gen} to the full efficiency of approximately 7.9%. We show some reinterpretations of the bound of Eq. (104) for the cascade decay $h \rightarrow \chi_2 \chi_2$, $\chi_2 \rightarrow a(Z_D) \chi_1$, $a(Z_D) \rightarrow \mu\mu$ in Fig. 35. Gluon fusion Higgs events are generated in MADGRAPH 5 and showered in PYTHIA 6, matched out to one jet. Our signal model contains no spin correlations; a proper treatment of spin would yield small corrections to the muon acceptance. We show results for masses $m_a(m_{Z_D}) = 0.4$ (blue), 1 (green), and 3 GeV (red). Dark vector branching fractions to muons are taken according to the tree-level computation of Sec. IC 5, while a reference branching fraction $\text{Br}(a \rightarrow \mu\mu) = 0.1$ is assumed. Caution should be used in interpreting the recast limits for the smallest values of $m_2 - m_1$, which is furthest from the spectra considered in Ref. [339], as in this region the linear relation between α_{gen} and the full experimental efficiency may no longer hold.

Searches in electron jets are more challenging, as backgrounds from QCD jets with a large electromagnetic fraction are significant, and as identifying collimated electrons from BSM physics is complicated by photon conversions. Nonetheless, searches for $h \rightarrow 2$ electron jets have been carried out, targeting Wh associated production first at CDF with 5.1 fb^{-1} data [228] and later at ATLAS

with 2.04 fb^{-1} of 7 TeV data [227] and inclusively for pairs of electron jets with 5 fb^{-1} of 7 TeV data [289]. It is challenging to reinterpret either of these searches as a limit on Higgs decays to simple electron jets, as both require > 2 tracks per electron jet, to better reject photon conversions.

XVIII. $h \rightarrow b\bar{b} + E_T$

Decays of the form $h \rightarrow b\bar{b} + E_T$ can be classified into two main types, assuming a primary two-body decay stage $h \rightarrow X_1 X_2$:

- (I) $X_1 \rightarrow E_T, X_2 \rightarrow b\bar{b} + E_T$;
- (II) $X_1 \rightarrow E_T, X_2 \rightarrow b\bar{b}$.

Here, $X_{1,2}$ are intermediate on-shell particles (possibly the same particle undergoing different decays), and X_1 is either stable and invisible or decays invisibly.⁴³ The $b\bar{b}$ pair may either be resonant or nonresonant in general for the first class of decays, though we will mainly assume that it is resonant. The second class is resonant by definition. Below, theoretical motivations and experimental search strategies will be discussed. As we will see, decays with a $b\bar{b}$ resonance might lead to an observable signal at the 14 TeV LHC.

A. Theoretical motivation

- (i) *NMSSM in PQ-symmetry limit: $h \rightarrow \chi_1 \chi_2$ (topology I, resonant); see also hidden valleys (Sec. IC 10).*— Here, X_1 and X_2 represent the lightest and the next-to-lightest neutralinos χ_1 and χ_2 , respectively, with χ_2 decaying to χ_1 plus a scalar or pseudoscalar of the extended Higgs sector. For details on the decay $h \rightarrow \chi_1 \chi_2$ (and $h \rightarrow \chi_2 \chi_2$) and example parameter points,

⁴³A logical third option that leads to this final state would be a decay into a pair of bottom partners, that each subsequently decay to $b + E_T$. However, this option is now almost entirely ruled out [45].

see Sec. IC 8 or [53,54]. If the scalar is heavier than $2m_b$, its decays are typically dominated by $b\bar{b}$. The signatures at colliders will then be one or two b jets + E_T , depending on how collimated the two b quarks are.

If $m_{\chi_2} - m_{\chi_1} > m_Z$, the decay $\chi_2 \rightarrow \chi_1 Z$ is open and the Z boson can further decay into a $b\bar{b}$ pair. However, this decay tends to be kinematically disfavored.

- (ii) ν SM: $h \rightarrow \nu N$ (topology I, resonant or nonresonant).—In the ν SM, the Higgs can decay into an active neutrino and a sterile neutrino via the neutrino portal Yukawa interaction, Eq. (25). In this case, we identify $X_1 = \nu$ and $X_2 = N$, and the topology is the same as in the PQ -symmetric NMSSM. The mass mixing between RH sterile neutrinos and LH active neutrinos allow the RH neutrinos to decay via $N \rightarrow \nu Z^{(*)} \rightarrow \nu b\bar{b}$. For more details, refer to Sec. IC 3.
- (iii) Other models: $h \rightarrow aa, Z_D Z_D, \phi_1 \phi_2$ (topology II).—In the PQ limit of the NMSSM (Sec. IC 7) it is possible for a to decay competitively into singlinos as well as bottom quarks. In that case, the decay $h \rightarrow 2a \rightarrow 2b + E_T$ may be realized. Dark vector extensions (Sec. IC 5) will usually have an invisible decay mode $Z_D \rightarrow \bar{\nu}\nu$, so the $2b + E_T$ final state can occur (even if it may not be the first discovery channel for such a model). Finally, it is of course possible to imagine a more complicated hidden sector (see, e.g., Sec. IC 10) where $h \rightarrow \eta_1 \eta_2$ and $\eta_1 \rightarrow b\bar{b}$ but η_2 is invisible or decays invisibly.

B. Existing collider studies

As the kinematics of $h \rightarrow b\bar{b} + E_T$ can be significantly different from the standard $h \rightarrow b\bar{b}$ decay, dedicated analyses are required to search for it. Inspired by the PQ limit of the NMSSM, a dedicated study of this process has recently been performed [54]. The signals from gluon fusion and vector boson fusion production would be overwhelmed by QCD backgrounds (similar to SM $h \rightarrow b\bar{b}$), even if they could be triggered on, so the analysis focuses on vector boson associated production, triggering on leptonic boson decays. As an illustration, Zh with $Z \rightarrow e^+e^-/\mu^+\mu^-$ is considered. In addition to two neutralinos χ_1, χ_2 , the final state includes a spin-0 state s (either scalar or pseudoscalar) that decays to $b\bar{b}$. The study is based on a benchmark model in the PQ limit of the NMSSM, with its parameters presented in Table X. The main backgrounds include $Zb\bar{b}, Zc\bar{c}, Zc + Z\bar{c}$ and $t\bar{t} + \text{jets}$. The analysis includes basic detector effects but no pile-up simulation. Jet substructure tools [384] are also applied to investigate b -tagged fat jets. The analysis indicates that $\sim 2\sigma$ sensitivity to $\text{Br}(h \rightarrow X_1 X_2 \rightarrow 2b + E_T) = 0.2$ may be possible at the 14 TeV LHC with

300 fb⁻¹, though it is very challenging, and more realistic studies are needed.

C. Existing experimental searches and limits

Although the signature $h \rightarrow b\bar{b} + E_T$ is well motivated, dedicated experimental searches have not yet been performed. There are similarities to the SM Higgs decay $h \rightarrow b\bar{b}$, but the generally softer bottom quarks and lower rate make this a more challenging signal to detect. The $h \rightarrow b\bar{b}$ searches from $(W \rightarrow \ell\nu)h$, $(Z \rightarrow \ell\ell)h$ and $(Z \rightarrow \nu\nu)h$ production by both the CMS and the ATLAS Collaborations [385,386] have only recently achieved SM sensitivity, yielding no constraints on the rarer $2b + E_T$ final state. The $(Z \rightarrow \nu\nu)h$ search could in principle be sensitive to this exotic Higgs decay from ggF and VBF production channels, with the orders-of-magnitude larger production rate offsetting the subdominant exotic Br. However, the jet p_T and E_T cuts in the standard Zh analysis are quite high and would likely eliminate almost all of the signal. This underlines the need for dedicated searches.

XIX. $h \rightarrow \tau^+\tau^- + E_T$

$h \rightarrow X_1 X_2 \rightarrow \tau^+\tau^- + E_T$ is another new class of exotic Higgs decays. As for the $2b + E_T$ final state of Sec. XVIII, the two most important nonexcluded topologies are

- (I) $X_1 \rightarrow E_T, X_2 \rightarrow \tau^+\tau^- + E_T$;
- (II) $X_1 \rightarrow E_T, X_2 \rightarrow \tau^+\tau^-$.

Here $X_{1,2}$ are intermediate particles, which can be either the same or different, and the $\tau^+\tau^-$ pair can be either resonant or nonresonant (though this resonance would be difficult to reconstruct with taus).

A. Theoretical motivation

- (i) The PQ limit of the NMSSM: $h \rightarrow \chi_1 \chi_2$ (topology I, resonant).—As discussed in detail in Sec. IC 8 (see also [52–54]), $X_{1,2}$ represent the lightest and next-to-lightest neutralinos in this limit, and we can get decay chains similar to those that lead to $h \rightarrow b\bar{b} + E_T$ (see Sec. XVIII A). The second neutralino χ_2 , which will often be mostly bino, decays into $\chi_1 s$ and/or $\chi_1 a$. If s or a have a mass $2m_\tau < m_{s/a} < 2m_b$, they dominantly decay into $\tau^+\tau^-$ via mixing with the MSSM Higgs doublets. In this case, the $\tau^+\tau^-$ pair is resonant.
- (ii) ν SM: $h \rightarrow \nu N$ (topology I, nonresonant).—Neutrino models can also give rise to this signature. For

TABLE X. Benchmark masses used for the $h \rightarrow b\bar{b} + E_T$ collider analysis of [54].

m_h	m_{χ_2}	m_{χ_1}	m_s
125 GeV	80 GeV	10 GeV	45 GeV

example, in the ν SM, the Higgs can decay into an active neutrino and a sterile neutrino via Yukawa interaction [55]. The mass mixing between RH sterile neutrinos and LH active neutrinos then make the RH neutrinos decay via $N \rightarrow \tau^+ W^{-(*)} \rightarrow \tau^+ \tau^- \bar{\nu}_\tau$ and its conjugate (given Majorana N), or/and $N \rightarrow \nu Z^{(*)} \rightarrow \nu \tau^+ \tau^-$. Here the $\tau^+ \tau^-$ are generally nonresonant, though in some cases they could sit on the Z resonance. For more details, see Sec. IC 3.

- (iii) *Other models: $h \rightarrow aa, Z_D Z_D, \phi_1 \phi_2$ (topology II).*— As explained in Sec. XVIII A, it is possible to realize topology II as a possibly subdominant mode in dark vector models (Sec. IC 5), in the PQ -NMSSM (Sec. IC 7) via a decaying to singlinos and taus if it satisfies $2m_\tau < m_a < 2m_b$, or in a more complicated hidden sector (Sec. IC 10).

B. Existing collider studies

A preliminary analysis for the type-I topology is in progress, based on a benchmark model inspired by the PQ limit of the NMSSM, which is presented in Table XI [387]. Given the large mass hierarchy between χ_2 and its decay products χ_1 and s (here a scalar or pseudoscalar), as well as the fact that $m_s/2m_\tau$ is only $\mathcal{O}(1)$, the $\tau^+ \tau^-$ pair produced in this decay tends to be highly collimated, forming a “ditau jet” (much like some of the cases discussed in Sec. VI and references therein). The study is focused on Higgs events from associated production with a leptonic Z boson ($Z \rightarrow e^+ e^-, \mu^+ \mu^-,$ and $\tau^+ \tau^-$), due to the very large expected QCD backgrounds for other production modes. The distinguishing features of this signal are therefore two leptons with their invariant mass falling in the Z mass window, one ditau jet, and a moderate amount of E_T . The dominant backgrounds in this analysis are $Z +$ jets, $t\bar{t} +$ jets, and diboson + jets. They can be greatly reduced by cutting on the number of tracks in the ditau-jet candidate (QCD jets have more tracks than ditaus) and requiring the reconstructed h to be back to back with the Z . This preliminary analysis suggests that extracting the $h \rightarrow X_1 X_2 \rightarrow 2\tau + E_T$ signal is extremely challenging at the 14 TeV LHC, although more study is in progress [387].

C. Existing experimental searches and limits

Though these decays are motivated in several theoretical contexts, there are no dedicated experimental searches yet, and the allowed parameter space is still mostly open. The main constraints could come from $h \rightarrow \tau^+ \tau^-$ searches [388,389], $h \rightarrow WW^*$ searches [376,390], and the $\tilde{\tau} \tilde{\tau}$ search by ATLAS [391]. However, in all of these analyses the selection cuts are too aggressive to pick up the exotic Higgs decay efficiently. Some LHC searches might partly pick up some special corners, though we will not attempt to delineate these regions here. Dedicated searches

are clearly needed, although, as mentioned above, very challenging.

XX. CONCLUSIONS AND OUTLOOK

We now summarize our results from various perspectives. Our main goals are to help experimentalists choose which analyses to undertake and to guide both theorists and experimentalists in understanding which feasibility studies would be well motivated but have not been done.

In Sec. IC, we considered various theories in which non-SM Higgs decays arise. Some of these are simplified models, others more fully established theoretical structures, such as the NMSSM. Within any one of these models, certain classes of decays tend to occur with definite relative probabilities. If we are in such a model, we may ask: which of the various decay modes offers the best sensitivity to the presence of the exotic decays? More precisely, given the limits on $\frac{\sigma}{\sigma_{\text{SM}}} \cdot \text{Br}(h \rightarrow \mathcal{F}_i)$ that can be obtained for the various exotic final states \mathcal{F}_i , which search gives us the strongest limit on $\frac{\sigma}{\sigma_{\text{SM}}} \cdot \text{Br}(h \rightarrow \text{non-SM decays}) = \frac{\sigma}{\sigma_{\text{SM}}} \cdot \sum_i \text{Br}(h \rightarrow \mathcal{F}_i)$?

For instance, as we will see in a moment, the case of $h \rightarrow Z_D Z_D$, where Z_D is a spin-one particle decaying to fermion pairs, leads to many final states, ranging from $jjjj$ to $b\bar{b}\ell^+\ell^-$ to $\ell^+\ell^-\ell^+\ell^-$. Not surprisingly, although $\ell^+\ell^-\ell^+\ell^-$ only appears in about 10% of $h \rightarrow Z_D Z_D$ decays, searches for it are so sensitive that it provides the best limit in $\frac{\sigma}{\sigma_{\text{SM}}} \cdot \text{Br}(h \rightarrow Z_D Z_D)$. As another example, if $h \rightarrow aa$, a a pseudoscalar decaying to $\tau^+ \tau^-, \mu^+ \mu^-$, the decay $\tau^+ \tau^- \mu^+ \mu^-$ provides the greatest sensitivity; a decay to four muons is too rare.

We now proceed to organize our results along these lines. Initially we will limit ourselves to cases without very low-mass particles that result in highly collimated pairs (or more) of jets, leptons, or photons. The collimated cases will be addressed separately.

At the end of this section we provide a final summary of our findings.

A. How to interpret the tables

Below we organize our results into tables to allow for certain comparisons to be made easily. These tables are presented to guide the reader but necessarily suppress many essential details, all of which are to be found in the main sections of our text. *It is important not to overinterpret the numbers presented in the tables*; the interested reader who is considering what searches or studies should be

TABLE XI. Mass parameters used for the $h \rightarrow \tau^+ \tau^- + E_T$ collider analysis.

m_h	m_{χ_2}	m_{χ_1}	m_s
125 GeV	80 GeV	10 GeV	8 GeV

undertaken must rely on the longer descriptions in the main text in order to obtain the full picture.

We consider a number of different “simplified model” scenarios below. For each one, we consider different final states \mathcal{F}_i to which the Higgs may decay. In the main text, we have obtained information from several different types of sources: from existing theoretical studies of a search for $h \rightarrow \mathcal{F}_i$ in the literature; from our own studies of this decay mode; from existing experimental searches for $h \rightarrow \mathcal{F}_i$; and from existing searches for other processes that we reinterpret as limits on $h \rightarrow \mathcal{F}_i$. Whichever of these gives the best *current or potential* limit is listed in the tables; we indicate with a comment whether the limit is current or potential and whether it arises from a theory study or from published LHC data. If no limit is known to us, we indicate it is “unknown” with the symbol “?”.

Importantly, *the numbers presented in the tables are merely representative*. The limits that can be obtained from any search depend on the masses of new particles to which the Higgs is decaying, and so in general they cover a range, sometimes a very wide one. Because our goal is to point out where searches may be worth performing, the tables present values at or near the *optimistic* end of the range. For example, if we show potential sensitivity at the 1% level, this means that there is a significant range of masses in which such a branching fraction would be experimentally accessible, though in other ranges sensitivity might be much less. Conversely our numbers are in many cases *conservative*, because they are often from theoretical studies that may not use optimal methods, or from reinterpreting experimental searches that were optimized for something other than Higgs decays. The reader is urged to look at the relevant sections in the main text to properly appreciate these subtleties.

B. Final states without E_T

1. $h \rightarrow aa \rightarrow$ fermions

In the simplified model of the SM coupled to a real or complex SM-singlet scalar (Sec. IC 1), in certain regimes of the two Higgs doublet model with an extra singlet (Sec. IC 2), and in regimes of the NMSSM (Sec. IC 7), Little Higgs models (Sec. IC 9), and hidden-valley models (Sec. IC 10), one often finds the phenomenon of a Higgs decaying to two particles that in turn decay to SM fermions *with couplings weighted by mass* (though sometimes separately for up-type quarks, down-type quarks, and leptons). We write this as $h \rightarrow aa$ for short.

We consider this situation in Table XII. For each decay mode \mathcal{F}_i that arises in this context, we list (second column) the best potential sensitivity to the particular mode, obtained either from existing papers in the literature, from our own studies, or from a reinterpretation of an existing ATLAS or CMS search for some other phenomenon. In later tables, we will also see *current limits* from ATLAS and

CMS searches for the mode $h \rightarrow \mathcal{F}_i$, where those exist. Where possible, we give estimates both for the existing run I data (LHC7 + 8) and for a certain amount of run II data (LHC14), taken to be 100 fb^{-1} except where indicated by an asterisk. In the third column, we indicate by G, V, W, Z whether the best known limit is obtained through $gg \rightarrow h$, vector boson fusion (VBF or $qq \rightarrow qqh$), Wh or Zh production.

We then try to put these results in a model-dependent but broad perspective. The relative branching fractions, i.e., the rates of particular final states relative to the total rate for all non-SM modes, are shown for two fiducial classes of models: one (fourth column) where a decays to both quarks and leptons with relative branching fractions representative of NMSSM-type models, and a second (sixth column) where quark decays are suppressed either by couplings (vanishing $aq\bar{q}$ couplings) or by kinematics ($m_a < 2m_b$). (In the latter case, our numbers are approximate because we ignore $a \rightarrow c\bar{c}$, etc.) Then, by dividing these relative branching fractions by the potential (or current) limit (second column), we obtain the sensitivity that this search provides for $\text{Br}(h \rightarrow aa)$, for the two fiducial models (fifth and seventh columns.) *We emphasize that some searches could be more constraining for other models* (e.g., for other types of 2HDM + S), as we describe below.

With $a \rightarrow q\bar{q}$ allowed and $a \rightarrow b\bar{b}$ dominant, it is notable that $h \rightarrow 4b$ and $h \rightarrow b\bar{b}\mu\mu$ are both potentially promising in run II. Furthermore, for this scenario $b\bar{b}\mu\mu$ is the only channel that may set marginally relevant limits with run I data. The $b\bar{b}\tau\tau$ mode suffers by comparison from the absence of a resonance and large $t\bar{t}$ backgrounds, and analysis improvements will be necessary if it is to be useful.

In the absence of $a \rightarrow$ quarks, or for $m_a < 10 \text{ GeV}$, the search for $h \rightarrow \tau^+\tau^-\mu^+\mu^-$ is more sensitive than that for $h \rightarrow \tau^+\tau^-\tau^+\tau^-$, but sufficiently close that both should be investigated further. It is worth considering both modes in searches within run I data.

In some models the ratio of $a \rightarrow bb$ to $a \rightarrow \tau\tau$ can change continuously as a function of parameters. Since the achievable limits on $\text{Br}(h \rightarrow 2a \rightarrow 2b2\mu)$ and $\text{Br}(h \rightarrow 2a \rightarrow 2\tau2\mu)$ are very similar, the former will set a better limit on overall exotic branching fraction if $\text{Br}(a \rightarrow 2b) \gtrsim \text{Br}(a \rightarrow 2\tau)$, and vice versa. At least one of these two channels should approach a sensitivity of $\text{Br}(h \rightarrow aa) \sim 0.1$. Investigating both is therefore vital to achieve “full coverage” of this scenario.

Our suggestion is that the searches for $b\bar{b}\mu^+\mu^-$ and $\tau^+\tau^-\mu^+\mu^-$, assuming a $\mu^+\mu^-$ resonance at the a mass, should be undertaken, even with run I data. We note that both triggering and analysis are far easier for $b\bar{b}\mu^+\mu^-$ and $\tau^+\tau^-\mu^+\mu^-$ than for other modes, due to the higher- p_T muons and the narrow peak in the dimuon mass. We also emphasize that these searches should be carried out *with minimal prejudice as to the range of m_a* . For $\tau^+\tau^-\mu^+\mu^-$, the common assumption $m_a < 2m_b$ is unnecessary; as we have

TABLE XII. Estimates for current or projected limits on various processes in $h \rightarrow aa$, if a couplings are proportional to masses, and either $a \rightarrow$ quarks is allowed as in an NMSSM-type model (center columns) or $a \rightarrow$ quarks is suppressed relative to $a \rightarrow$ leptons (right columns). If no relevant estimate is known, we indicate this with a “?”. The source of each estimate is listed in the “Comments” column. Production modes: G for $gg \rightarrow h$, V for vector boson fusion, W, Z for Wh and Zh . For 14 TeV, estimates require 100 fb^{-1} . See Sec. XX A for additional information and cautionary remarks.

Decay mode \mathcal{F}_i	Projected/ current 2σ limit on $\text{Br}(\mathcal{F}_i)$ 7 + 8 [14] TeV	Production mode	Quarks allowed		Quarks suppressed		Comments
			$\frac{\text{Br}(\mathcal{F}_i)}{\text{Br}(\text{non-SM})}$	Limit on $\frac{\sigma}{\sigma_{\text{SM}}} \cdot \text{Br}(\text{non-SM})$ 7 + 8 [14] TeV	$\frac{\text{Br}(\mathcal{F}_i)}{\text{Br}(\text{non-SM})}$	Limit on $\frac{\sigma}{\sigma_{\text{SM}}} \cdot \text{Br}(\text{non-SM})$ 7 + 8 [14] TeV	
$b\bar{b}b\bar{b}$	0.7 [0.2]	W	0.8	0.9 [0.2]	0	– [–]	Recast of expt. result [276], Sec. III Theory study [192,267], Sec. III
$b\bar{b}\tau\tau$	> 1 [0.15]	V	0.1	> 1 [1]	0	– [–]	Theory study [278], Sec. IV
$b\bar{b}\mu\mu$	$(2-7) \times 10^{-4}$ [[0.6-2) $\times 10^{-4}$]	G	3×10^{-4}	0.5-1 [0.2-0.8]	0	– [–]	Our study, Sec. V Our study, Sec. V
$\tau\tau\tau\tau$	0.2-0.4 [?]	G	0.005	40-80 [?]	1	0.2-0.4 [?]	Recast of expt. result [298,300], Sec. VI
$\tau\tau\mu\mu$	$(3-7) \times 10^{-4}$ [?]	G	3×10^{-5}	10-20 [?]	0.007	0.04-0.1 [?]	Our study, Sec. VI
$\mu\mu\mu\mu$	1×10^{-4} [?]	G	1×10^{-7}	1000 [?]	1×10^{-5}	10 [?]	Recast of expt. result [175,341], Sec. XI

noted in Sec. IC 2, there are many models in which $a \rightarrow b\bar{b}$ is suppressed not by kinematics but by coupling constants. Meanwhile, for $b\bar{b}\mu^+\mu^-$, the assumption that both fermion-antifermion pairs come from the same type of particle implies that $m_{\mu\mu} = m_a > 2m_b$, but the decay $h \rightarrow aa'$ can occur in some nonminimal models, in which case $m_{a'} = m_{\mu\mu} < 2m_b < m_a$ may occur, possibly with an increased rate.

2. $h \rightarrow aa \rightarrow$ SM gauge bosons

Next we turn to a case where the a does not couple strongly to fermions and instead decays mainly to gluon pairs and photon pairs through loops of heavy particles. Such couplings are commonly proportional to gauge couplings squared (i.e., to α_i), in which case $\text{Br}(a \rightarrow \gamma\gamma) \sim 0.004 \times \text{Br}(a \rightarrow gg)$ for a degenerate $SU(5)$ multiplet of fermions coupling equally to a (see Sec. VIII). But if the masses M of the heavy colored particles in the loops are larger than the masses m of the colorless ones, the rate for photon production may be enhanced by at least a factor of $(M/m)^2$.

Estimated limits for this case are shown in Table XIII. If the heavy particles are degenerate and in complete $SU(5)$ multiplets, then the center columns show that only the four-jet search has any reach, with

phenomenologically relevant sensitivity possible for $m_a \lesssim 5 \text{ GeV}$ with 300 fb^{-1} of data. If the branching fraction $a \rightarrow \gamma\gamma$ is enhanced by a factor of 10, as would happen if the colored particles appearing in the loop graph were about 3 times heavier than the colorless particles, then the situation is given in the right columns. In this case, the four-photon search is clearly superior.

We should of course note that it is possible to have a particle that dominantly decays to $\gamma\gamma$. This could occur for a pseudoscalar a if it couples to the visible sector only through loops of heavy colorless charged particles. In this case there would be only 4γ decays and no $4j$ or $2j2\gamma$ decays.

With these considerations in mind, it would seem four-jet, four-photon, and mixed searches are all well motivated in run II. However, for run I data, a four-jet search is hopeless, while a four-photon search is already sensitive to models where a has enhanced decays to photons. We therefore suggest a search for $h \rightarrow 4\gamma$ even in the existing run I data. We also suggest that triggers for multiple photons be set so as to retain this signal in run II.

3. $h \rightarrow Z_D Z_D, ZZ_D, Za$

Now we consider the possibility that the Higgs decays either to two dark vector bosons Z_D or to one Z_D and one

TABLE XIII. As in Table XII, estimates for various processes in $h \rightarrow aa$ if a decays only to SM gauge bosons through loops. The central columns show the case where the couplings are generated by initially degenerate $SU(5)$ multiplets; the right columns show the case where the $a \rightarrow \gamma\gamma$ rate is enhanced by a factor of 10. An asterisk denotes that all 14 TeV estimates shown require 300 fb^{-1} of data.

Decay mode \mathcal{F}_i	Projected/current 2σ limit on $\text{Br}(\mathcal{F}_i)$ 7 + 8 [14] TeV	Production mode	$\text{Br}(a \rightarrow \gamma\gamma) \approx 0.004$		$\text{Br}(a \rightarrow \gamma\gamma) \approx 0.04$		Comments
			$\frac{\text{Br}(\mathcal{F}_i)}{\text{Br}(\text{non-SM})}$	Limit on	$\frac{\text{Br}(\mathcal{F}_i)}{\text{Br}(\text{non-SM})}$	Limit on	
				$\frac{\sigma}{\sigma_{\text{SM}}} \cdot \text{Br}(\text{non-SM})$ 7 + 8 [14] TeV		$\frac{\sigma}{\sigma_{\text{SM}}} \cdot \text{Br}(\text{non-SM})$ 7 + 8 [14] TeV	
$jjjj$	> 1 [0.1*]	W	0.99	> 1 [0.1*]	0.92	> 1 [0.1*]	Theory study [220,269], Sec. VII
$\gamma\gamma jj$	0.04 [0.01*]	W	0.008	5 [1*]	0.08	0.5 [0.1*]	Theory study [312], Sec. VIII
$\gamma\gamma\gamma\gamma$	2×10^{-4} [3×10^{-5} *]	G	1×10^{-5}	20 [1*]	0.001	0.2 [0.03*]	Our study, Sec. IX Theory study [311], Sec. IX

SM Z . This can occur in dark vector scenarios (Sec. IC 5) and more general hidden valleys (Sec. IC 10). The main difference compared to $h \rightarrow aa$ is that Z_D branching ratios are ordered by SM gauge charge instead of mass, which leads to large leptonic branching fractions.

The $h \rightarrow ZZ_D$ search can also set limits on the $h \rightarrow Za$ scenario, where a is a pseudoscalar which decays to fermions in proportion to their masses. If decays to $b\bar{b}$ are suppressed or forbidden, the limits can already be appreciable.

A useful fiducial model is to take Z_D to couple to SM fermions proportional to their electric charge. This is the case if decays occur via kinetic $\gamma - Z_D$ mixing, and if $m_{Z_D} \ll m_Z$ so that photon- Z mixing is unimportant (see Fig. 13 in Sec. IC 5), but also gives the qualitatively correct picture for more general dark vector scenarios.

We first treat the $h \rightarrow Z_D Z_D$ decay; see Table XIV. Not surprisingly, the search for $h \rightarrow (\ell^+ \ell^-)(\ell^+ \ell^-)$, which allows full reconstruction at high resolution, is the most powerful. The published data on four-lepton events used in the Higgs search and in $Z^{(*)}Z^{(*)}$ studies put tremendous constraints on this decay, already, according to our reinterpretation of the published data, reaching $\text{Br}(h \rightarrow Z_D Z_D) < 4 \times 10^{-4}$. It is important to improve on the constraints we found on this well-motivated model; specifically, our reinterpretation did not allow for an optimal constraint, since it does not make full use of the three available mass resonances.

Limits on $\text{Br}(h \rightarrow Z_D Z_D)$ from dilepton plus jets searches are probably in the few times 10^{-2} range; see Sec. V. As the table indicates, our studies suggest that $j j \mu^+ \mu^-$ and $b \bar{b} \mu^+ \mu^-$ would have comparable sensitivity, and this might also be true for electron final states, though triggering and reconstruction efficiencies will be lower than for muons in many cases. But even combining all of these together, it appears that dilepton plus jets final states would only be competitive in models where the branching

fractions for leptons is significantly reduced compared to the case we consider in Table XIV.

The constraints on $h \rightarrow ZZ_D$ and Za are shown in Table XV. The $h \rightarrow Z^* Z$ search sets powerful constraints. In the case of ZZ_D , they are still one order of magnitude weaker than indirect constraints from electroweak precision measurements for $m_{Z_D} \gtrsim 10 \text{ GeV}$ (see Fig. 12). (For $m_{Z_D} \lesssim 10 \text{ GeV}$, the constraints are even stronger.) A more optimized search with sufficient luminosity at the 14 TeV LHC will yield competitive or even eventually superior limits for $m_{Z_D} \gtrsim 10 \text{ GeV}$. The bounds on $h \rightarrow Za$ from four-lepton final states are rather weak due to Yukawa suppression. The decay $h \rightarrow Za$ is an example of an asymmetric $h \rightarrow 2 \rightarrow 4$ decay, and other search channels such as $h \rightarrow Za \rightarrow (\ell^+ \ell^-)(b\bar{b})$ may provide better sensitivity in the long run.

We therefore find that searches for four-lepton final states in $h \rightarrow (\ell^+ \ell^-)(\ell^+ \ell^-)$ via non-SM channels are extremely well motivated in run I. As we have noted earlier, the available data as published in the search for the SM $h \rightarrow ZZ^*$ mode are not ideal for the $Z_D Z_D$ or ZZ_D searches, since neither the selection cuts nor the analysis approach are appropriate to the signal, with some events unnecessarily discarded and with leptons often systematically misassigned. The analysis for ZZ_D in particular (but also $Z_D Z_D$ in general) should preferably also extend to very low Z_D mass ranges, where isolation cuts and quarkonium backgrounds are an issue.

Triggering is not a problem for these final states because the leptons have relatively high p_T . Multilepton triggers where two or three leptons are soft may contribute to sensitivity, a point that deserves further exploration.

C. Final states with E_T

In the $h \rightarrow 2 \rightarrow 4$ final states we discussed above, only one unknown particle need appear, and its decays are often controlled by a single type of coupling. By contrast, final

TABLE XIV. As in Table XII, estimates for various processes in $h \rightarrow Z_D Z_D$ if $m_{Z_D} > 2m_b$ and couplings are proportional to electric charges. $\ell = e, \mu$ and all numbers represent the *sum* of processes involving e and μ ; j represents all jets except b quarks. An asterisk indicates that 300 fb^{-1} was assumed; otherwise all estimates for 14 TeV assume 100 fb^{-1} .

Decay mode \mathcal{F}_i	Projected/current 2σ limit on $\text{Br}(\mathcal{F}_i)$ 7 + 8 [14] TeV	Production mode	$\frac{\text{Br}(\mathcal{F}_i)}{\text{Br}(\text{non-SM})}$	Limit on $\frac{\sigma}{\sigma_{\text{SM}}} \cdot \text{Br}(\text{non-SM})$ 7 + 8 [14] TeV	Comments
$jjjj$	> 1 [0.1*]	W	0.25	> 1 [0.4*]	Theory study [220,269], Sec. VII
$\ell\ell\ell\ell$	4×10^{-5} [?]	G	0.09	4×10^{-4} [?]	Recast of expt. result [175,341], Sec. XI
$jj\mu\mu$	0.002–0.008 [(5–20) $\times 10^{-4}$]	G	0.15	0.01–0.06 [0.003–0.01]	Our study, Sec. V Our study, Sec. V
$b\bar{b}\mu\mu$	$(2-7) \times 10^{-4}$ [(0.6–2) $\times 10^{-4}$]	G	0.015	0.01–0.05 [0.003–0.01]	Our study, Sec. V Our study, Sec. V

states with E_T can arise from multiple decay topologies (see Fig. 2), and the type of search required may depend on whether the energy carried by invisible particles is large (in the Higgs rest frame) relative to m_h .

1. Larger E_T , without resonances

First we consider cases where the E_T in the h rest frame is a significant fraction of its mass, and the invariant mass of the visible objects in the Higgs decay lies well below 125 GeV and may be highly variable. In general, there may be no resonances among the visible particles in the non-SM Higgs decay modes. Fermion-antifermion pairs may be produced in three-body decays such as $\psi \rightarrow f\bar{f}\psi'$; in this case there will be kinematic end points, but statistics may be too small to use them. Branching fractions are very model dependent but tend to be similar either to the heavy-flavor-weighted or the flavor-democratic cases associated

with (pseudo)scalars a or vectors Z_D discussed above. Tables XVI and XVII show that cases with leptons are promising, but with $b\bar{b}$ or $\tau\tau$ the situation is difficult even if, as in the studies we refer to in the main text, the $2b$ and 2τ are assumed to be on resonance. More study of the difficult cases is warranted.

In particular, for $b\bar{b}E_T$, $\tau\tau E_T$, and even $\mu\mu E_T$ where the muons are too soft to pass dimuon trigger thresholds, it may become important to consider VBF production. Triggering in this case might require combining a VBF dijet requirement, a E_T requirement, and a requirement of b , τ , or μ candidates. This requires further investigation.

Photons, by contrast, may be produced singly, as in $\psi \rightarrow \gamma\psi'$, and thus nonresonant $\gamma + E_T$ and $\gamma\gamma + E_T$ final states are possible. We show results in Table XVIII. There is no preferred pattern of branching fractions here; the decay $\psi \rightarrow \gamma\psi'$ may have a branching fraction of 100% or

TABLE XV. As in Table XII, estimates for all-leptonic processes in $h \rightarrow ZZ_D$ and $h \rightarrow Za \rightarrow \ell\ell\ell\ell$; other processes were not studied. For Z_D we assume couplings are proportional to electric charges; for a we assume all couplings are proportional to masses, and either that $a \rightarrow b\bar{b}$ is dominant or highly suppressed (as in certain type-III 2HDM + S models described in Sec. I C 2). Here $\ell = e, \mu$ and all numbers represent the *sum* of processes involving e and μ . An asterisk indicates that 300 fb^{-1} was assumed; otherwise all estimates for 14 TeV assume 100 fb^{-1} .

Decay mode \mathcal{F}_i	Projected/current 2σ limit on $\text{Br}(\mathcal{F}_i)$ 7 + 8 [14] TeV	Production mode	$\frac{\text{Br}(\mathcal{F}_i)}{\text{Br}(\text{non-SM})}$	Limit on $\frac{\sigma}{\sigma_{\text{SM}}} \cdot \text{Br}(\text{non-SM})$ 7 + 8 [14] TeV	Comments
$ZZ_D \rightarrow \ell\ell\ell\ell$	4×10^{-5} [?]	G	0.02	0.002 [?]	Recast of expt. result [175,176], Sec. X
$Za \rightarrow \ell\ell\mu\mu$ $\text{Br}(a \rightarrow b\bar{b}) \sim 0.9$	4×10^{-5} [?]	G	2×10^{-5}	2 [?]	Recast of expt. result [175,176], Sec. X
$Za \rightarrow \ell\ell\mu\mu$ $\text{Br}(a \rightarrow b\bar{b}) = 0$	4×10^{-5} [?]	G	2×10^{-4}	0.2 [?]	Recast of expt. result [175,176], Sec. X

TABLE XVI. As in Table XII, estimates for various processes $h \rightarrow \psi\psi'$, where ψ' is invisible and $\psi \rightarrow \psi' + \bar{f}f$ via an intermediate a coupling to fermions proportional to their masses. In the two cases shown, either $\text{Br}(a \rightarrow b\bar{b})$ dominates (center columns) or quarks are suppressed relative to leptons (right columns). The limits for $b\bar{b}$ and $\tau\tau$ assume an intermediate resonance (indicated with parentheses), while the $\mu\mu$ limits do *not* assume a resonance and are artificially weak. An asterisk indicates that all 14 TeV estimates shown require 300 fb^{-1} of data.

Decay mode \mathcal{F}_i	Projected/ current 2σ limit on $\text{Br}(\mathcal{F}_i)$ 7 + 8 [14] TeV	Production mode	Quarks allowed		Quarks suppressed		Comments
			$\frac{\text{Br}(\mathcal{F}_i)}{\text{Br}(\text{non-SM})}$	Limit on $\frac{\sigma}{\sigma_{\text{SM}}} \cdot \text{Br}(\text{non-SM})$ 7 + 8 [14] TeV	$\frac{\text{Br}(\mathcal{F}_i)}{\text{Br}(\text{non-SM})}$	Limit on $\frac{\sigma}{\sigma_{\text{SM}}} \cdot \text{Br}(\text{non-SM})$ 7 + 8 [14] TeV	
$(b\bar{b})E_T$	> 1 [0.2*]	Z	0.9	> 1 [0.2*]	0	– [–]	Our study, Sec. XVIII Theory study [53,54], Sec. IC 8
$(\tau\tau) E_T$	> 1 [> 1*]	Z	0.1	> 1 [> 1*]	1	> 1 [> 1*]	Our study, Sec. XIX Theory study [53,54], Sec. IC 8
$\mu\mu E_T$	0.07 [?]	G	0.003	40 [?]	0.03	4 [?]	Recast of expt. result [376,377], Sec. XV

may be diluted by other final states, such as $\psi \rightarrow Z^*\psi'$ or $\psi \rightarrow Z_D\psi'$. Existing searches involving $\gamma + E_T$ have a high H_T cut and are very inefficient for a Higgs signal of this type; see Sec. XII. Because we do not know the size of fake E_T backgrounds in $\gamma + \text{jet}$ events at low photon p_T and especially low E_T , we cannot determine whether a single photon search is well justified; experimental studies would be required on this point. We note that data from a parked data trigger for $\gamma + E_T$, available at least for CMS [34], may allow for an interesting search.

In any case, a $\gamma\gamma E_T$ search in run I data is certainly justified. It is quite reasonable theoretically to have $\text{Br}(h \rightarrow \chi_2\chi_2) \sim 0.1$ and $\text{Br}(\chi_2 \rightarrow \gamma\chi_1) = 1$, and (see Fig. 32) a nonoptimized GMSB search already reaches the level of $\text{Br}(h \rightarrow \gamma\gamma + E_T) \sim 0.05$. A search more optimized for a Higgs signal should do considerably better.

2. Larger E_T , with resonances

If the objects in the final states are produced in resonances, and the resonances in question are from scalar or vector particles, then as in the previous section there are preferred scenarios for their branching fractions. In these cases, the limits will obviously be stronger than in the nonresonant cases, especially for photons and leptons. On the other hand, the numbers we have presented in this document are obtained by reinterpreting ATLAS and CMS searches which do *not* seek resonances and are therefore unnecessarily pessimistic.

For instance, in a decay $h \rightarrow \psi\psi'$ where $\psi \rightarrow a\psi'$, ψ' is invisible, and a decays to gluon and photon pairs, we will potentially have $h \rightarrow jj + E_T$ and $h \rightarrow \gamma\gamma + E_T$; see Table XIX. The dijet signal has not been studied, and given the difficulty of the search for $h \rightarrow b\bar{b} + E_T$ it is not likely to be useful. We therefore show only the $2\gamma + E_T$ case. Note these numbers are obtained from searches that

do not require a diphoton resonance, so the true sensitivity may be significantly higher in a resonance search. Even so there may only be sensitivity in this channel at present with some enhancement of $\text{Br}(a \rightarrow \gamma\gamma)$, but since this is a reasonable possibility, we view a dedicated search in run I data as well motivated. Even though we have not done so in this document, one could also investigate $h \rightarrow \psi\psi' \rightarrow 4\gamma + E_T$ via two intermediate pseudoscalars. Aside from a direct search for the final state, perhaps a ≥ 3 -photon search, where one looks for a resonance in nearby photon pairs, is warranted.

Meanwhile, in a decay $h \rightarrow \psi\psi'$ where $\psi \rightarrow a\psi'$, ψ' is invisible, and a decays to fermions with couplings proportional to masses, we will potentially have $h \rightarrow b\bar{b} + E_T$, $jj + E_T$, $\tau^+\tau^- + E_T$, $\mu^+\mu^- + E_T$ final states. We already showed results for this case in Table XVI. Only the $\mu^+\mu^-$ search will be sensitive in the next few years, and the rate for this final state may be quite low if $m_a \gg 2m_\tau$, but importantly the search may be quite a bit more sensitive than shown when one requires a resonance. Admittedly we are quoting numbers for optimistic scenarios; as the E_T increases and the p_T of the visible objects decreases, efficiencies and sensitivities may drop rapidly. Also shown are the numbers if the decay of the a to $b\bar{b}$ is suppressed by kinematics or by coupling constants. Even in this case the decay to $\mu^+\mu^-$ appears too small, but it important to note that the numbers for $\mu^+\mu^- + E_T$ are obtained assuming no resonances (see Sec. XIV). Therefore, in this case a search in the 7 + 8 TeV data is probably merited.

Note that if $m_h - 2m_\psi$ is small, the leptons will have low p_T . Then the search strategy we refer to in Table XVI, which relies on $gg \rightarrow h$, will not work, because the leptons will lie below dilepton trigger thresholds. This is unfortunate, because despite their low p_T the leptons may form a resonance that makes off-line backgrounds small. So as not to lose the possibility of discovery, it may be essential to

TABLE XVII. As in Table XII, estimates for various processes $h \rightarrow \psi\psi'$ (middle column) and $h \rightarrow \psi\psi$ (right column), where ψ' is invisible and $\psi \rightarrow \psi' + \bar{f}f$ via an intermediate (possibly off-shell) vector boson, which couples to fermions proportionally to electric charges. The limits for $\bar{b}b$ and $\tau\tau$ assume an intermediate resonance (indicated with parentheses), while the $2\ell, 4\ell$ limits do not, making the limits artificially weak. For $h \rightarrow \psi\psi$ (rightmost columns), there are four fermions in the final state; we assume here that the limits obtained for $\bar{f}f + E_T$ are not much changed by the presence of the two additional fermions. An asterisk denotes that all 14 TeV estimates shown require 300 fb⁻¹ of data.

Decay mode \mathcal{F}_i	Projected/ current 2σ limit on $\text{Br}(\mathcal{F}_i)$ 7 + 8 [14] TeV	Production mode	$h \rightarrow \psi\psi' \rightarrow \bar{f}f + E_T$		$h \rightarrow \psi\psi \rightarrow \bar{f}_1f_1 + \bar{f}_2f_2 + E_T$		Comments
			$\frac{\text{Br}(\mathcal{F}_i)}{\text{Br}(\text{non-SM})}$	Limit on $\frac{\sigma}{\sigma_{\text{SM}}} \cdot \text{Br}(\text{non-SM})$ 7 + 8 [14] TeV	$\frac{\text{Br}(\mathcal{F}_i)}{\text{Br}(\text{non-SM})}$	Limit on $\frac{\sigma}{\sigma_{\text{SM}}} \cdot \text{Br}(\text{non-SM})$ 7 + 8 [14] TeV	
$(\bar{b}b) E_T$	> 1 [0.2*]	Z	0.05	> 1 [4*]	0.1	> 1 [2*]	Our study, Sec. XVIII Theory study [52], Sec. IC 10
$(\tau\tau) E_T$	> 1 [> 1*]	Z	0.15	> 1 [> 1*]	0.28	> 1 [> 1*]	Our study, Sec. XIX Theory study [52], Sec. IC 10
$\ell\ell E_T$	0.07 [?]	G	0.30	0.2 [?]	0.51	0.1 [?]	Recast of expt. result [376,377], Sec. XV
$\ell\ell\ell\ell E_T$	5×10^{-4} [?]	G, V	–	– [–]	0.09	0.005 [?]	Recast of expt. result [369], Sec. XIV

trigger on such events produced via VBF, where the trigger combines the jets from VBF with E_T and the soft leptons.

Note that if instead of $h \rightarrow a + E_T$ the decay is to $h \rightarrow aa + E_T$, via $h \rightarrow \psi\psi$ and $\psi \rightarrow a\psi'$, the situation is quite similar. Aside from $\mu^+\mu^- + E_T$ inclusive, which has twice as large a branching fraction as in Table XVI, no other searches may be sensitive in the near term. However, some advantage can be obtained from $\tau^+\tau^-\mu^+\mu^- E_T$ events, via multilepton searches.

Next we turn to the case where a is replaced by Z_D . We already showed both the cases where $h \rightarrow Z_D + E_T$ and $h \rightarrow Z_D Z_D + E_T$ in Table XVII. Again we emphasize that no resonances are assumed in the leptonic searches, so true sensitivities should be better than shown. Clearly searches in the dilepton and four-lepton mode are well motivated by these models.

3. Small E_T

If the amount of E_T is always small, modes with E_T may be probed in searches that assume no E_T , as long as kinematic requirements are loosened appropriately. These

include both searches for SM decay modes and for non-SM $h \rightarrow 2 \rightarrow 4$ modes discussed above.

Small E_T arises naturally when the invisible particles are emitted in two-body decays that constrain their p_T to be small, for instance in $h \rightarrow aa'$ where a' is invisible and $m_h \sim m_a \gg m_h - m_a \sim m_{a'}$. It is common for the other particle in the two-body decay to then produce an observable resonance; in the previous example we might have $a \rightarrow b\bar{b}$ resonantly. In addition to this $h \rightarrow 2 \rightarrow 3$ decay, similar features may arise in a $h \rightarrow 2 \rightarrow 4 \rightarrow 6$ decay, such as $h \rightarrow \psi\psi$ and $\psi \rightarrow Y\psi'$, where $m_{\psi'} < m_\psi - m_Y \ll m_h$ and Y decays visibly; in this case there are two Y resonances, plus small E_T . Another possibility is for a $h \rightarrow 2 \rightarrow 3 \rightarrow 4$ decay, for instance if $h \rightarrow \psi\psi'$, $\psi \rightarrow Y\psi'$, if $m_Y \sim m_{\psi'} \sim m_h$.

For an $h \rightarrow 2 \rightarrow 3$ (or $h \rightarrow 2 \rightarrow 3 \rightarrow 4$) decay with one (or two) low- p_T invisible particles, SM searches are often sensitive, as long as cuts do not exclude resonances below 125 GeV. For example, the decay $h \rightarrow \psi'\psi \rightarrow \psi'\psi'Y \rightarrow \psi'\psi'(f\bar{f})$, where f is a SM fermion, closely resembles the decay $h \rightarrow f\bar{f}$, except that the mass of the $f\bar{f}$

TABLE XVIII. As in Table XII, estimates for $h \rightarrow \psi\psi$ or $\psi\psi'$, where $\psi \rightarrow \psi' + \gamma$ and ψ' is invisible. Note the limits we have obtained do not require a $\gamma\gamma$ resonance.

Decay mode \mathcal{F}_i	Projected/current 2σ limit Limit on $\text{Br}(\mathcal{F}_i)$ 7 + 8 [14] TeV	Production mode	Comments
γE_T	> 1 [?]	G	Recast of expt. result [359], Sec. XII
$\gamma\gamma E_T$	0.04 [?]	G	Recast of expt. result [359], Sec. XIII

TABLE XIX. As in Table XII, estimates for $h \rightarrow a + E_T$ with $a \rightarrow \gamma\gamma$ if a couplings to gluons and photons are proportional to gauge couplings (center columns), or with $\text{Br}(a \rightarrow \gamma\gamma)$ enhanced by a factor of 10 (right columns). Note the limits we have obtained do not require a $\gamma\gamma$ resonance.

Decay mode \mathcal{F}_i	Projected/ current 2σ limit on $\text{Br}(\mathcal{F}_i)$ 7 + 8 [14] TeV	Production mode	$\text{Br}(a \rightarrow \gamma\gamma) \approx 0.004$		$\text{Br}(a \rightarrow \gamma\gamma) \approx 0.04$		Comments
			$\frac{\text{Br}(\mathcal{F}_i)}{\text{Br}(\text{non-SM})}$	Limit on $\frac{\sigma}{\sigma_{\text{SM}}} \cdot \text{Br}(\text{non-SM})$ 7 + 8 [14] TeV	$\frac{\text{Br}(\mathcal{F}_i)}{\text{Br}(\text{non-SM})}$	Limit on $\frac{\sigma}{\sigma_{\text{SM}}} \cdot \text{Br}(\text{non-SM})$ 7 + 8 [14] TeV	
$\gamma\gamma E_T$	0.04 [?]	G	0.004	10 [?]	0.04	1 [?]	Recast of expt. result [359], Sec. XIII

lies at m_Y , slightly below m_h . The same applies for a decay to photons.

For a $h \rightarrow 2 \rightarrow 4 \rightarrow 6$ decay, with two low- p_T invisible particles, the final state of the Higgs resembles an $h \rightarrow 2 \rightarrow 4$ decay, such as we have already discussed extensively in the preceding subsection. The only new requirement is to allow for the total invariant mass of the two Y resonances to lie between $2m_Y$ and m_h .

There are other cases to consider, such as $h \rightarrow ZZ_D$, $Z_D \rightarrow a_1 s_1$ where a_1 decays outside the detector and $s_1 \rightarrow \mu^+ \mu^-$. The general lesson is the same, however: if the E_T is small and the final states are resonant, as is commonly the case, the only necessary change between standard and exotic searches is to relax the requirement, as appropriate, that the invariant mass of the visible objects is 125 GeV. This loosening of cuts is only relevant in channels where the invariant mass reconstruction has excellent resolution, i.e., final states containing electrons, muons, or photons.

We therefore find that

- (i) the four-lepton and four-photon searches mentioned in the previous section, aimed at $h \rightarrow 2 \rightarrow 4$ decays, should also be performed so that limits can be obtained on scenarios where the invariant mass of the observed objects lies somewhat below m_h , whether or not the leptons or photons form resonances in pairs;
- (ii) it is useful to study the data from the SM diphoton search for resonances below 125 GeV and for continua that extend from a lower mass limit up to m_h .

We emphasize that in these cases, a premature invariant-mass requirement in event preselection could eliminate a signal. (This same concern applies to these searches for another reason: the possibility of a second Higgs with a different mass, a low cross section, and unknown branching fractions to SM-like and non-SM-like decays.)

4. Summary

Summarizing the situation for final states with invisible non-SM particles, we suggest searches already in run I for $\gamma\gamma + E_T$, $\ell^+ \ell^- + E_T$, and $\ell^+ \ell^- \ell^+ \ell^- + E_T$, both with and

without requiring pairwise resonances. Multiphoton searches may also be warranted, now or in run II. If possible, various possible simplified models generating these final states should be considered for each search, including ones that have very different kinematics for the observed particles and for the E_T . Experimental studies of the $\gamma + E_T$ final state are warranted. Study of the final states with pairwise resonances is lacking and may be useful.

D. Collimated objects in pairs

Kinematics may force pairs or groups of visible particles to be produced with large p_T compared to their invariant mass, such that they emerge collimated. In such situations, special search strategies are necessary, since the collimated particles must often be treated as a single special object in order that they be distinguished from a single QCD jet, or be viewed as a pair of objects with special isolation criteria, such that each does not ruin the isolation of the other. We have briefly discussed a few cases and summarize them below and in Table XX. In contrast to other tables, we do not attempt to interpret the results in terms of models, because for particles of mass $\ll 5$ GeV, branching fractions to specific final states often vary rapidly as a function of mass.

In this document, collimated leptons are considered in Secs. XVI (one lepton jet) and XVII (two lepton jets). We concentrate on simple lepton-jets, consisting of a single lepton-antilepton pair that are collimated, yet isolated from other particles. Complex lepton-jets, which may contain multiple lepton-antilepton pairs and possibly hadron pairs as well, are not studied here. Simple lepton-jets may involve both muons and electrons (for a vector Z_D), muons almost always (for a scalar or pseudoscalar a with $m_a > 2m_\mu$), or electrons only (for $m_a < 2m_\mu$) though we have not considered the latter case.

There have been no searches using more than 35 pb^{-1} of LHC data for final states with a single lepton jet. However, the study conducted by [54] (see Sec. XVI) indicates that exotic branching fractions $\sim 10^{-2}$ can be probed if there is additional E_T from the Higgs decay.

Searches for two dilepton jets have been carried out at both the Tevatron and the LHC, as shown in Table XX, but there has not been systematic coverage, and existing LHC searches have in some cases been done with only a small fraction of the existing data set. There are specifically searches for Higgs decays to two dimuon jets $\{\mu^+\mu^-\}\{\mu^+\mu^-\}$ (here curly brackets denote collimation) without reconstructing the h resonance, so we can use these searches to constrain the cases with and without E_T . There have been searches for lepton jets with > 2 muons but we do not consider them in our table. Meanwhile, although there are searches for two electronic lepton-jets, the one search [227] for $h \rightarrow$ electron jets looks for two $\{e^+e^-e^+e^-\}$ jets, while the only search for two dielectron jets $\{e^+e^-\}\{e^+e^-\}$ [289] assumes a large supersymmetric production cross section. We have not attempted to reinterpret either search as a limit on $h \rightarrow$ two $\{e^+e^-\}$ -jets, and so leave these cases blank in our table. To our knowledge there are no searches for two lepton-jets of different types.

Section VI considered collimated τ pairs in $h \rightarrow \{\tau^+\tau^-\}\{\tau^+\tau^-\}$ decays, as well as $\{\tau^+\tau^-\}\{\mu^+\mu^-\}$. We found that a search for the latter is more powerful, since the collimated muons have higher p_T than any daughters of τ decays and have a fixed invariant mass. Our study suggested limits even at run 1 in the $(3-7) \times 10^{-4}$ range might be possible. This is much stronger than the previous measurement from D0 [287] and would put limits on $\text{Br}(h \rightarrow aa)$, assuming $a \rightarrow \tau\tau, \mu\mu$ with couplings weighted by mass, in the range of 5%–10%. States such as $b\bar{b}\tau\tau$ and $b\bar{b}\mu\mu$ will not have collimated leptons or taus if the b pair and lepton pair come from two particles of the

same mass $> 2m_b$; only in more complex models will this arise (though for $m_a \lesssim 25$ GeV, the $2b$'s can merge into a single jet; see below). For this reason, along with the fact that there are no strong experimental limits on these cases, we have not listed them in our table.

A more complete search program is highly warranted in run I data looking for simple lepton-jets, both within Higgs searches and beyond. For reasons that we have outlined, no mass restrictions should be placed on these searches, except those absolutely required by kinematics. For instance, even if a model has $a \rightarrow \mu^+\mu^-$ as motivation, it should not be restricted to $m_a < 2m_\tau$ or $m_a < 2m_b$, both because such a search has sensitivity to a vector Z_D , with substantial leptonic branching fractions at all masses, and because if a couples weakly to b quarks, then the $b\bar{b}$ threshold will have almost no effect on its branching fractions. Similarly, models with a Z_D vector boson may have electron-positron lepton-jets with arbitrary invariant mass, so such a search should not be limited to extremely low masses. The range between the obviously collimated region ($m_{\ell\ell} < 5$ GeV) and the obviously uncollimated one ($m_{\ell\ell} > 20$ GeV) remains almost completely unexplored, and efforts to close this gap would be well motivated. Once the simple lepton-jets are fully covered, a program to study more complex lepton-jets will also be a high priority.

Collimated photons can arise if a scalar or pseudoscalar with a substantial coupling to photons has a low mass. A search for $h \rightarrow \{\gamma\gamma\}\{\gamma\gamma\}$ where the photon pairs are very highly collimated, loosely reconstructed as a single photon, has already been done. A search for $h \rightarrow \{\gamma\gamma\}\{\gamma\gamma\}$ with

TABLE XX. Estimates for sensitivity of certain searches for collimated pairs of objects; collimation is denoted by curly brackets. See Table XII for notation and text for more details. An asterisk indicates that 300 fb^{-1} was assumed; otherwise all estimates for 14 TeV assume 100 fb^{-1} .

Decay mode \mathcal{F}_i	Projected/current 2σ limit on $\text{Br}(\mathcal{F}_i)$ 7 + 8 [14] TeV	Production mode	Comments
$\{\mu\mu\}\{\mu\mu\}$	1×10^{-5} (5×10^{-3}) [?]	G	CMS [339], $2m_\mu < m_a < 2m_\tau$ (CMS [379] $m_a < 5$ GeV)
$\{ee\}\{ee\}$	Limit unclear [?]	W, G	Reinterpretation of [227,289] needed
$\{\mu\mu\}X$	1 [?]	G	CMS, [379], $2m_\mu < m_a < 5$ GeV
$\{\mu\mu\} E_T$	0.03 [?]	W	Theory study [53,54], Sec. IC 8 and Appendix B; our study, Sec. XVI
$\{\mu\mu\}\{\mu\mu\} E_T$	1×10^{-5} (5×10^{-3}) [?]	G	CMS [339], $2m_\mu < m_a < 2m_\tau$ (CMS [379] $m_a < 5$ GeV) however, see Sec. XVII for important details
$\{ee\}\{ee\} E_T$	Limit unclear [?]	W, G	Reinterpretation of [227,289] needed
$\{\tau\tau\}\{\mu\mu\}$	$(3-7) \times 10^{-4}$ [?]	G	This work, see Sec. VIB
$\{\gamma\gamma\}\{\gamma\gamma\}$	0.01 [?]	G	ATLAS [324], $m_a < 400$ MeV
$\{\gamma\gamma\} E_T$? [?]		no studies
$\{gg\}\{gg\}$	> 1 [0.7]	W	Boosted Wh [267], $m_a < 30$ GeV
$\{b\bar{b}\}\{b\bar{b}\}$	0.7 [0.2]	W	Boosted Wh [267], $m_a \sim 15$ GeV

less collimated photon pairs, recognizable as two separate but closely spaced photons that are isolated from other particles, is also well motivated. The ability to identify just one such object with low backgrounds is critical for any search for $h \rightarrow \{\gamma\gamma\} + E_T$; see Sec. XIII. Whether these searches are well motivated in run I data needs further study.

For completeness, we include $4b$ and $4j$ final states in our table. These cases, which are important if $h \rightarrow aa$ and then $a \rightarrow b\bar{b}$ or $a \rightarrow gg$ are dominant, are effectively collimated if $m_{jj}, m_{bb} < 20$ GeV or so, since the jets will typically merge. Moreover, searches for these modes almost certainly require a boosted h , so in the end there will potentially be further merging.

E. For further study

We note a number of important possible decays that we have not considered in this work and that merit study. First, we did not study two-body decays such as $h \rightarrow \tau\mu$ or $h \rightarrow Z\gamma$, but these have been studied extensively in the literature. More exotic decays that have received varying degrees of attention include

- (i) $h \rightarrow 2 \rightarrow 6$, e.g., decays of the Higgs to neutralinos that decay via R -parity violation to three jets, etc.;
- (ii) h to > 4 leptons, τ 's, b 's; decays such as $h \rightarrow 6\tau$ or $8b$ have been suggested in the literature [264] (see also Secs. IC 5 and IC 10), but both theoretical and experimental study has been limited, though CDF has looked for decays of the Higgs to many soft leptons [228];
- (iii) h to complex lepton jets (i.e., with > 2 tracks), including both purely electronic, purely muonic, purely leptonic with a mix of muons and electrons, and mixed leptonic and hadronic jets (see for example [383]);
- (iv) decays to one or more photonic jets (consisting of ≥ 2 collimated photons) need more experimental study; theory studies include [313,314,322];
- (v) h decaying to long-lived particles with decays in flight [32,76,77]. There have been a number of searches for specific final states at particular decay lifetimes, but not a coherent program that covers all cases.

This is certainly not the complete list; for example one should not forget $h \rightarrow 3 \rightarrow n$, with a three-body decay $h \rightarrow Z_D Z_D^*$ or $h \rightarrow aa^*$ (for $m_{Z_D}, m_a \geq m_h/2$), though, with the exception of all-leptonic modes, sensitivity to such decay modes needs further study.

- (i) Further studies in more difficult channels, such as $b\bar{b}\tau\tau$, $b\bar{b}E_T$, $\tau\tau E_T$, $jj\gamma\gamma$, are needed particularly in the context of VBF production. If such studies reveal VBF can yield significant improvements in sensitivity, then developing triggers for 2015 aimed at these final states may offer a significant advantage.

- (ii) Also well motivated are studies of exotic decays in the tth associated production channel, which can be competitive with Wh , Zh for non-SM Higgs decays. The combinatoric backgrounds that make this channel difficult for a SM Higgs may be significantly reduced for certain non-SM decay modes [220], and the hard leptons and b jets from the t decays offer another inclusive trigger pathway.

F. Summary of suggestions

Based on our results so far, we find that the following searches are highly motivated within the 7 and 8 TeV data set as well as within future data sets. In some cases, especially in regimes where the objects are collimated, searches have already been done by ATLAS and/or CMS, though not always with the full data set.

- (i) Search for $h \rightarrow Z_D Z_D \rightarrow (\ell^+ \ell^-)(\ell^+ \ell^-)$ across the full range of kinematically allowed Z_D masses, including regimes where the leptons are collimated (forming simple lepton-jets). This could also be interpreted as a search for $h \rightarrow Z_D Z_D'$ if the dilepton pairs have different masses, or as $h \rightarrow Z_D Z_D + E_T$, for small E_T , if the condition $m_{A\ell} = m_h$ is relaxed.
- (ii) Search for $h \rightarrow ZZ_D \rightarrow (\ell^+ \ell^-)(\ell^+ \ell^-)$ across the full range of kinematically allowed Z_D masses, including regimes where the leptons are collimated (forming a simple lepton-jet). This search should also be interpreted as a search for $h \rightarrow Za \rightarrow (\ell^+ \ell^-)(\mu^+ \mu^-)$.
- (iii) Search for $h \rightarrow \ell^+ \ell^- + E_T$, including regimes where the leptons are collimated, and including the cases where there is a resonance in $m_{\ell\ell}$. Benchmark models include $h \rightarrow XY \rightarrow Z_D YY$ or aYY , $h \rightarrow XX \rightarrow aa^{(\prime)}YY$ for $m_a < 2m_\tau$, $h \rightarrow XX \rightarrow Z^* Z^* YY$, where Y is invisible and Z^* is an off-shell Z boson.
- (iv) Search for $h \rightarrow \ell^+ \ell^- \ell^+ \ell^- + E_T$, including regimes where the leptons are collimated, and including the cases where there is a resonance in $m_{\ell\ell}$. Benchmark models include $h \rightarrow XX \rightarrow Z_D Z_D YY$, $h \rightarrow XX \rightarrow aa^{(\prime)}YY$ for $m_a < 2m_\tau$, $h \rightarrow XX \rightarrow Z^* Z^* YY$, where Y is invisible and Z^* is an off-shell Z .
- (v) Search for $h \rightarrow aa \rightarrow (b\bar{b})(\mu^+ \mu^-)$ across the full range of kinematically allowed a masses, including regimes where the $b\bar{b}$ pair tend to merge. If possible, searches for $h \rightarrow aa'$, where $m_a > 2m_b > m_{a'}$, could be considered, in which case the leptons may be collimated.
- (vi) Search for $h \rightarrow aa \rightarrow (\tau^+ \tau^-)(\mu^+ \mu^-)$ across the full range of kinematically allowed a masses, including regimes where the leptons are collimated. A search for $h \rightarrow aa \rightarrow (\tau^+ \tau^-)(\tau^+ \tau^-)$ may not be as powerful but deserves to be investigated further.
- (vii) Search for $h \rightarrow aa \rightarrow (\gamma\gamma)(\gamma\gamma)$, including regimes where the photons are collimated. This could also be

interpreted as a search for $h \rightarrow aa'$ if the diphoton pairs have different masses, or as $h \rightarrow aa + E_T$, for small E_T , if the condition $m_{4\gamma} = m_h$ is relaxed.

- (viii) Search for $h \rightarrow \gamma\gamma + E_T$, including the cases where there is a resonance in $m_{\gamma\gamma}$. Benchmark models include $h \rightarrow XY \rightarrow aYY$, $h \rightarrow XX \rightarrow aa^{(\prime)}YY$, $h \rightarrow XX \rightarrow (\gamma Y)(\gamma Y)$, where Y is invisible.

Additional theoretical and experimental studies relevant for 14 TeV and up to 100 fb^{-1} appear warranted for

- (i) $h \rightarrow XY \rightarrow \gamma YY$ where Y is invisible, giving $\gamma + E_T$;
- (ii) $h \rightarrow aa \rightarrow (b\bar{b})(b\bar{b})$;
- (iii) $h \rightarrow aa \rightarrow (b\bar{b})(\tau^+\tau^-)$, perhaps in VBF production.

Note also the other suggestions in Sec. XX E.

It is important to reemphasize that searches should look for a reconstructed ‘‘Higgs’’ resonance at mass *not* equal to 125 GeV. This is because new Higgs bosons, produced with lower rates and unknown branching fractions, may lie hidden in the data, either at higher or lower masses than the known Higgs. Also, h decays involving low E_T may show up in searches for SM or non-SM decay modes as bumps or broad features below 125 GeV.

We conclude by noting the implications of our study for triggering in run II.

- (i) For several searches, boosted h recoiling against a leptonically decaying W or Z is expected to be necessary. Presumably even the higher lepton p_T thresholds required at run II will not much affect these searches.
- (ii) However, many searches that we have not studied directly (high multiplicity of soft particles, long-lived particles, etc.) will require as many events as possible be retained under triggers on the lepton in Wh (and $t\bar{t}h$) and on the jets in VBF. Keeping the one-lepton trigger thresholds low, or combining one lepton or VBF dijet triggers with signatures of unusual Higgs decay final states, is critically important for achieving high sensitivity.
- (iii) Many of our searches involve triggering on two or more leptons, possibly soft and possibly collimated; these issues have been well explored already in run I and should remain a priority.
- (iv) For $h \rightarrow \ell^+\ell^-E_T$, if the leptons are soft and the E_T is substantial, then a VBF-based search may be essential, in which triggering off a combination of the VBF jets, the E_T , and the soft leptons may be needed.
- (v) The same issues apply to photons; triggering on multiple photons, possibly collimated, and on softer photons in combination with VBF jets and E_T may be important.
- (vi) We have not studied them here, but final states with leptons and at least one photon are possible; this may have trigger implications for any combined lepton and photon trigger pathway.

- (vii) Triggering in the VBF context is also potentially important for other difficult modes, such as $b\bar{b}\tau\tau$, $b\bar{b}E_T$, etc., but more theory studies are needed.
- (viii) Although the search at CMS for $\gamma + E_T$ is expected to benefit from a data parking trigger in the 2012 data, the trigger challenge for this final state in run II is very severe, and a thorough study is needed to determine if it is both feasible and worth the bandwidth. The VBF channel may be helpful here.

To conclude, exotic decays of the Higgs represent a unique opportunity to discover new physics. A large number of experimental searches and additional theoretical and experimental studies are highly motivated in order to realize the full and exciting physics potential of the LHC.

ACKNOWLEDGMENTS

We thank Joseph Boudreau, Neil Christensen, Hooman Davoudiasl, Sally Dawson, Albert de Roeck, Yuri Gershtein, Andy Haas, Tao Han, John Hobbs, Jinrui Huang, Philip Ilten, Greg Landsberg, Hye-Sung Lee, Ian Lewis, Patrick Meade, Maurizio Pierini, George Redlinger, Pedro Schwaller, Robert Shrock, George Sterman, Shufang Su, Scott Thomas, Dmitri Tsybychev, Tomer Volansky, Lian-Tao Wang, and Felix Yu for useful conversations. We thank Adam Falkowski for useful correspondence on the electroweak precision bounds shown in the green EWPM region in Fig. 12. We thank Philip Ilten for help tracking down and fixing a bug in PYTHIA’s 2τ spin correlation code. Thanks in particular to M. Park and S. Thomas for providing a modified version of PGS. D. C. and Z. S. are supported in part by the National Science Foundation (NSF) under Grant No. PHY-0969739. R. E. is supported in part by the Department of Energy (DoE) Early Career research program DESC0008061 and by a Sloan Foundation Research fellowship. S. G. is supported in part by Perimeter Institute for Theoretical Physics. Research at Perimeter Institute is supported by the Government of Canada through Industry Canada and by the Province of Ontario through the Ministry of Research and Innovation. P. J. is supported in part by the DoE under Grant No. DE-FG02-97ER41022. A. K. is supported in part by the NSF under Grant No. PHY-0855591. T. L. is supported in part by his start-up fund at the Hong Kong University of Science and Technology. Z. L. is supported in part by the DoE under Grant No. DE-FG02-95ER40896, by the NSF under Grant No. PHY-0969510 (LHC Theory Initiative), the Andrew Mellon Predoctoral Fellowship from Dietrich School of Art and Science, University of Pittsburgh, and by the PITT PACC. D. M. is supported in part by NSERC, Canada and the U.S. Department of Energy under Grant No. DE-FG02-96ER40956. J. S. is supported in part by NSF Grant No. PHY-1067976 with additional support for this work provided by the LHC Theory Initiative under Grant No. NSF-PHY-0969510. M. S. is supported in part

by the DOE under Grants No. DE-FG02-96ER40959 and No. DE-SC00391 and by the NSF under Grant No. PHY-0904069. B.T. is supported in part by the DoE under Grants No. DE-FG-02-91ER40676 and No. DE-FG-02-95ER40896, by the NSF under Grant No. PHY-0969510 (LHC Theory Initiative), and by the PITT PACC. Y.Z. is supported in part by the DoE under Grant No. DESC0008061. We thank variously the SEARCH Workshop; the Aspen Center for Physics under Grant No. NSF 1066293; the KITP and the National Science Foundation under Grant No. PHY05-25915; the Galileo Galilei Institute for Theoretical Physics and the INFN; and Kavli Institute for Theoretical Physics China for hospitality during the completion of this work.

APPENDIX A: DECAY RATE COMPUTATION FOR 2HDM + S LIGHT SCALAR AND PSEUDOSCALAR

We will now outline how the branching ratios in Secs. I C 1 (SM + S) and I C 2 (2HDM + S) are calculated. We mostly follow [98,99], neglecting hadronization effects. This is sufficient for our purposes of demonstrating the range of possible exotic Higgs decay phenomenologies in 2HDM + S.

The relevant part of the Lagrangian is

$$\mathcal{L} \supset -\sum_f \frac{m_f}{v} [\bar{f}f(H_1^0 g_{H_1^0 f\bar{f}} + H_2^0 g_{H_2^0 f\bar{f}}) - i\bar{f}\gamma_5 f A^0 g_{A^0 f\bar{f}}], \quad (\text{A1})$$

where f stands for SM charged fermions. Higgs-vector boson interactions are obtained from the kinematic terms of the vector bosons. The relevant terms are

$$\begin{aligned} \mathcal{L} \supset & -\sum_V \frac{2m_V^2}{v} [V_\mu V^\mu (H_1^0 g_{H_1^0 VV} + H_2^0 g_{H_2^0 VV})] \\ & + \sum_{i=1,2} i \frac{m_Z}{v} g_{ZH_i^0 A^0} \partial_\mu Z^\mu H_i^0 A^0. \end{aligned} \quad (\text{A2})$$

Given the $A^0, H_{1,2}^0$ content of the singletlike scalar s and pseudoscalar a in Eqs. (17) and (24), and the couplings in Table II, the couplings $g_{sf\bar{f}}$, $g_{af\bar{f}}$, and g_{sVV} can be derived.

The approach for calculating branching ratios is different for light Higgs mass above or below $\sim \text{GeV}$. The theoretical uncertainties in the hadronic region of the latter case are very large, and an effective theory computation must be used.

1. Light singlet mass above 1 GeV

According to the discussion in Sec. I C 2, the relevant decay channel for the lightest Higgs scalar or pseudoscalar are $a/s \rightarrow f\bar{f}$, $a/s \rightarrow \gamma\gamma$, and $a/s \rightarrow gg$. Reference [98]

contains the decay widths for the MSSM Higgs at tree level and higher orders. We include the relevant formulas here, which are valid for the 2HDM + S and SM + S case after rescaling the Yukawa and gauge couplings by the small singlet mixing angle.

- (i) *Decays to light SM fermion pairs $a/s \rightarrow f\bar{f}$.*—The tree-level decay width of $\phi = a, s$ into fermion pairs is given by

$$\Gamma(\phi \rightarrow f\bar{f}) = \frac{N_c G_F}{4\sqrt{2}\pi} g_{\phi f\bar{f}}^2 m_\phi m_f^2 \beta_f^p, \quad (\text{A3})$$

where the phase volume β is

$$\beta_f = 1 - \frac{4m_f^2}{m_\phi^2} \quad (\text{A4})$$

with $p = 1$ (3) for $\phi =$ pseudoscalar a (scalar s). For quarks, additional $\mathcal{O}(\alpha_s^2)$ and $\mathcal{O}(\alpha_s^3)$ QCD radiative corrections are taken into consideration:

$$\begin{aligned} \Gamma(\phi \rightarrow q\bar{q}) \\ = \frac{3G_F}{4\sqrt{2}\pi} g_{\phi q\bar{q}}^2 m_\phi \bar{m}_q^2 \beta_q^p (1 + \Delta_{qq} + \Delta_\phi^2). \end{aligned} \quad (\text{A5})$$

Here \bar{m}_q stands for the running of the quark mass in the $\overline{\text{MS}}$ scheme with the renormalization scale $\mu = m_\phi$. This redefinition absorbs logarithms of masses of quarks from NLO QCD. The QCD correction factor Δ_{qq} for $\overline{\text{MS}}$ scheme is given by

$$\Delta_{qq} = 5.67 \frac{\bar{\alpha}_s}{\pi} + (35.94 - 1.35N_f) \left(\frac{\bar{\alpha}_s}{\pi} \right)^2, \quad (\text{A6})$$

where N_f is the number of active light quarks. $\bar{\alpha}_s$ stands for the running of strong coupling up to three-loop order in QCD. Again we choose the renormalization scale $\mu = m_\phi$. Above $\sim \text{GeV}$, α_s is small enough that perturbative QCD can give accurate results. Δ_ϕ^2 accounts for additional $\mathcal{O}(\alpha_s^2)$ corrections for a and h :

$$\Delta_a^2 = \frac{\bar{\alpha}_s^2}{\pi^2} \left(3.83 - \log \frac{m_a^2}{m_t^2} + \frac{1}{6} \log^2 \frac{\bar{m}_q^2}{m_a^2} \right), \quad (\text{A7})$$

$$\Delta_s^2 = \frac{\bar{\alpha}_s^2}{\pi^2} \left(1.57 - \frac{2}{3} \log \frac{m_s^2}{m_t^2} + \frac{1}{9} \log^2 \frac{\bar{m}_q^2}{m_s^2} \right). \quad (\text{A8})$$

- (ii) *Loop-induced decays to photon pairs $a/s \rightarrow \gamma\gamma$.*—The couplings between Higgs scalars and $\gamma\gamma$ are induced by charged particle loops. The decay widths can be written as

$$\Gamma(a \rightarrow \gamma\gamma) = \frac{G_F \alpha^2 m_a^3}{128\sqrt{2}\pi^3} \left| \sum_f N_c Q_f^2 g_{af\bar{f}} A_{1/2}^a \left(\frac{m_a^2}{4m_f^2} \right) \right|^2, \quad (\text{A9})$$

$$\Gamma(s \rightarrow \gamma\gamma) = \frac{G_F \alpha^2 m_s^3}{128\sqrt{2}\pi^3} \left| \sum_f N_c Q_f^2 g_{sf\bar{f}} A_{1/2}^s \left(\frac{m_s^2}{4m_f^2} \right) + g_{svV} A_1^s \left(\frac{m_s^2}{4m_W^2} \right) \right|^2, \quad (\text{A10})$$

where Q_f 's are electric charges in units of e . The form factors for spin half and one particles, $A_{1/2}$ and A_1 , are given by

$$A_{1/2}^a(x) = 2x^{-1}f(x), \quad (\text{A11})$$

$$A_{1/2}^s(x) = 2[x + (x-1)f(x)]x^{-2}, \quad (\text{A12})$$

$$A_1^s(x) = -[2x^2 + 3x + 3(2x-1)f(x)]x^{-2} \quad (\text{A13})$$

with

$$f(x) = \begin{cases} \arcsin^2 \sqrt{x} & x \leq 1, \\ -\frac{1}{4} \left[\log \frac{1+\sqrt{1-1/x}}{1-\sqrt{1-1/x}} - i\pi \right]^2 & x > 1. \end{cases} \quad (\text{A14})$$

In the limit $x \rightarrow 0$

$$A_{1/2}^a \rightarrow 2, \quad (\text{A15})$$

$$A_{1/2}^s \rightarrow 4/3, \quad (\text{A16})$$

$$A_1^s \rightarrow -7. \quad (\text{A17})$$

We neglect the contributions of possible heavy BSM charged particles, which are generically highly suppressed.

Equation (A10) shows that the dominant contribution to $s \rightarrow \gamma\gamma$ for SM-like fermion couplings comes from W and t loops. The top loop also dominates $a \rightarrow \gamma\gamma$ but there is no W contribution. However, α' - and β -dependent factors in the couplings can also make the b loop important. This

occurs in type-II and type-IV models when $\tan \beta \times \tan \alpha'$ or $\tan \alpha$ is large for s or a , respectively.

For the purposes of computing QCD correction we can treat t in the heavy quark limit ($m_t \rightarrow \infty$). The QCD corrections on $A_{1/2}(x)$ are then

$$A_{1/2}^a(x) \rightarrow A_{1/2}^a(x) \quad (\text{no NLO correction}), \quad (\text{A18})$$

$$A_{1/2}^s(x) \rightarrow \left(1 - \frac{\bar{\alpha}_s(m_s/2)}{\pi} \right) A_{1/2}^s(x). \quad (\text{A19})$$

Here the renormalization scale $\bar{\alpha}_s$ is chosen to be $\mu = m_s/2$. The above expressions are also valid for the scalar mass in the range $m_\phi < 2m_b$, but QCD corrections become more complicated near the b threshold $m_\phi \gtrsim 2m_b$ [392,393].

(iii) *Loop-induced decays to gluon pairs* $a, s \rightarrow gg$.—Gluons are massless particles that couple to the Higgs dominantly via heavy quark loops, $Q = t, b, c$. The decay widths are given by

$$\Gamma(\phi \rightarrow gg) = \frac{G_F \bar{\alpha}_s^2 m_\phi^3}{36\sqrt{2}\pi^3} \left| \frac{3}{4} \sum_{Q=t,b,c} g_{\phi Q\bar{Q}} A_{1/2}^\phi \left(\frac{m_\phi^2}{4m_Q^2} \right) \right|^2. \quad (\text{A20})$$

Other potential heavy particle contributions are neglected. Adding NLO QCD corrections yields the decay width

$$\Gamma(a \rightarrow gg) = \frac{G_F \bar{\alpha}_s^2 m_a^3}{36\sqrt{2}\pi^3} \left| \frac{3}{4} \sum_{Q=t,b,c} g_{aQ\bar{Q}} A_{1/2}^a \left(\frac{m_a^2}{4m_Q^2} \right) \right|^2 \left(1 + \left(\frac{97}{4} - \frac{7}{6} N_f \right) \frac{\bar{\alpha}_s}{\pi} \right), \quad (\text{A21})$$

$$\Gamma(h \rightarrow gg) = \frac{G_F \bar{\alpha}_s^2 m_h^3}{36\sqrt{2}\pi^3} \left| \frac{3}{4} \sum_{Q=t,b,c} g_{hQ\bar{Q}} A_{1/2}^h \left(\frac{m_h^2}{4m_Q^2} \right) \right|^2 \left(1 + \left(\frac{95}{4} - \frac{7}{6} N_f \right) \frac{\bar{\alpha}_s}{\pi} \right), \quad (\text{A22})$$

where the renormalization scale of $\bar{\alpha}_s$ is $\mu = m_\phi$.

(iv) *Other decay channels of the lightest Higgs*.—Decays to γ + quarkonium final states are enhanced for pseudoscalar masses near the $2c, 2b$ thresholds.

These are challenging to calculate [124], and we neglect them along with hadronization effects, which likely invalidates our quantitative results near the B/D -meson and quarkonia thresholds.

2. Light singlet mass below 1 GeV

For a sub-GeV (pseudo)scalar Higgs, hadronization effects dominate and the perturbative analysis is not valid above the pion threshold. The calculation of decay widths in this region is extremely difficult due to the QCD uncertainties in the hadronic final states. Light (pseudo) scalars that decay to two (three) pions would look similar to hadronic taus in an experimental analysis, and care would have to be taken not to reject them based on track quality requirements.

We now outline our methods for estimating the branching ratios in this low-mass regime.

- (i) *Singletlike scalar s* .—For $m_s < 2m_e \approx 1.02$ MeV, $\gamma\gamma$ decay is the only available channel. In the region $2m_e \leq m_s < 2m_\mu \approx 211$ MeV, e^+e^- rises and competes with $\gamma\gamma$. Br's of $\gamma\gamma$ may be enhanced in type II, III, and IV by appropriate choice of $\tan\beta$ and α' . In the region $2m_\mu \leq m_s < 2m_{\pi^0} \approx 270$ MeV, $\mu^+\mu^-$ decay appears and replaces e^+e^- to compete with $\gamma\gamma$.

Branching ratios are most difficult to estimate accurately in the mass window from the $\pi\pi$ threshold to about 1 GeV. $\mu^+\mu^-$ competes with $\gamma\gamma$, $\pi\pi$, $K\bar{K}$, and $\eta\eta$. Several methods are available for the estimation in

this region, such as soft pion theory and the chiral Lagrangian method. All suffer from significant final-state uncertainties. According to Ref. [41], the perturbative spectator approximation gives a reasonable and relatively simple approximation of decay widths. They are given by⁴⁴

$$\begin{aligned} \Gamma(s \rightarrow \gamma\gamma) &= \frac{G_F \alpha^2 m_s^3}{128\sqrt{2}\pi^3} \left| \sum_f N_c Q_f^2 g_{sf\bar{f}} A_{1/2}^s \left(\frac{m_s^2}{4m_f^2} \right) - 7g_{sVV} \right|^2, \end{aligned} \quad (\text{A23})$$

$$\Gamma(s \rightarrow \mu\bar{\mu}, e\bar{e}) = \frac{G_F}{4\sqrt{2}\pi} m_s g_{s\mu\bar{\mu}, e\bar{e}}^2 m_{\mu, e}^2 \beta_\mu^3, \quad (\text{A24})$$

$$\Gamma(s \rightarrow u\bar{u}, d\bar{d}) = \frac{3G_F}{4\sqrt{2}\pi} m_s g_{su\bar{u}, d\bar{d}}^2 m_{u, d}^2 \beta_\pi^3, \quad (\text{A25})$$

$$\Gamma(s \rightarrow s\bar{s}) = \frac{3G_F}{4\sqrt{2}\pi} m_s g_{ss\bar{s}}^2 m_s^2 \beta_K^3, \quad (\text{A26})$$

$$\Gamma(s \rightarrow gg) = \frac{G_F \alpha_s^2 m_s^3}{36\sqrt{2}\pi^3} \left(\sum_q g_{sq\bar{q}} - (g_{su\bar{u}} + g_{sd\bar{d}}) \beta_\pi^3 - g_{ss\bar{s}} \beta_K^3 \right)^2, \quad (\text{A27})$$

and we define the non-charm hadron decay width as

$$\begin{aligned} \Gamma(s \rightarrow \text{had}) &= \Gamma(s \rightarrow u\bar{u}) + \Gamma(s \rightarrow d\bar{d}) + \Gamma(s \rightarrow s\bar{s}) \\ &+ \Gamma(s \rightarrow gg). \end{aligned} \quad (\text{A28})$$

Another source of uncertainty in the Br estimation lies in the definition of the light quark mass. Different definitions render different Br's, especially to $\gamma\gamma$. For our computation, we use $m_u = m_d = 40$ MeV, $m_s = 450$ MeV, and $\alpha_s/\pi = 0.15$ as [41]. The values are chosen such that results from the spectator approximation method match results from the chiral Lagrangian method, but we emphasize that the uncertainties remain very large above the pion threshold.

- (ii) *Singletlike pseudoscalar a* .—Below the 3π threshold ($m_a < 3m_{\pi^0} \approx 405$ MeV), Br's of a are similar to Br's of h and dictated mostly by thresholds (and possibly a competitive decay to $\gamma\gamma$). Above the 3π threshold, decays of a to 3π , $\rho^0\gamma$, $\omega\gamma$, $\theta\pi\pi$ arise as m_a increases and competes with $\mu^+\mu^-$ and $\gamma\gamma$ decays.

We apply a similar spectator approximation as for the scalar case, with a threshold of twice the Kaon mass, $2m_K$, for strange quark final states [394]:

$$\Gamma(a \rightarrow \gamma\gamma) = \frac{G_F \alpha^2 m_a^3}{128\sqrt{2}\pi^3} \left| \sum_f N_c Q_f^2 g_{af\bar{f}} A_{1/2}^a \left(\frac{m_a^2}{4m_f^2} \right) \right|^2, \quad (\text{A29})$$

$$\Gamma(a \rightarrow \mu\bar{\mu}, e\bar{e}) = \frac{G_F}{4\sqrt{2}\pi} m_a g_{a\mu\bar{\mu}, e\bar{e}}^2 m_{\mu, e}^2 \beta_\mu, \quad (\text{A30})$$

$$\Gamma(a \rightarrow u\bar{u}, d\bar{d}) = \frac{3G_F}{4\sqrt{2}\pi} m_a g_{au\bar{u}, d\bar{d}}^2 m_{u, d}^2 \beta_\pi, \quad (\text{A31})$$

$$\Gamma(a \rightarrow s\bar{s}) = \frac{3G_F}{4\sqrt{2}\pi} m_a g_{as\bar{s}}^2 m_s^2 \beta_K, \quad (\text{A32})$$

$$\Gamma(a \rightarrow gg) = \frac{G_F \alpha_s^2 m_a^3}{16\sqrt{2}\pi^3} \left(\sum_q g_{aq\bar{q}} - (g_{au\bar{u}} + g_{ad\bar{d}}) \beta_\pi - g_{as\bar{s}} \beta_K \right)^2, \quad (\text{A33})$$

$$\Gamma(a \rightarrow \text{had}) \equiv \Gamma(a \rightarrow u\bar{u}) + \Gamma(a \rightarrow d\bar{d}) + \Gamma(a \rightarrow s\bar{s}) + \Gamma(a \rightarrow gg). \quad (\text{A34})$$

⁴⁴Here “s” stands for the strange quark in order to differentiate with the singletlike scalar s .

APPENDIX B: SURVEYING HIGGS PHENOMENOLOGY IN THE PQ -NMSSM

As the exotic Higgs decay phenomenology of the PQ limit of the NMSSM may not be as well known as the $h \rightarrow aa$ decays familiar from the NMSSM in the R -symmetric limit, we provide in this Appendix some quantitative illustrations of the phenomenology discussed in Sec. IC 8 (also see [53,54]).

Figure 36 shows the results of parameter scans run with the package NMSSMTOOLS [205–208]. All points in this scan are required to have a SM-like Higgs in the mass window $m_h \in (124, 126)$ GeV. We assumed soft squark masses of 2 TeV, slepton masses of 200 GeV, $A_{u,d,e} = -3.5$ TeV, and bino, wino and gluino masses of 30–120, 150–500 and 2000 GeV, respectively. Scans are

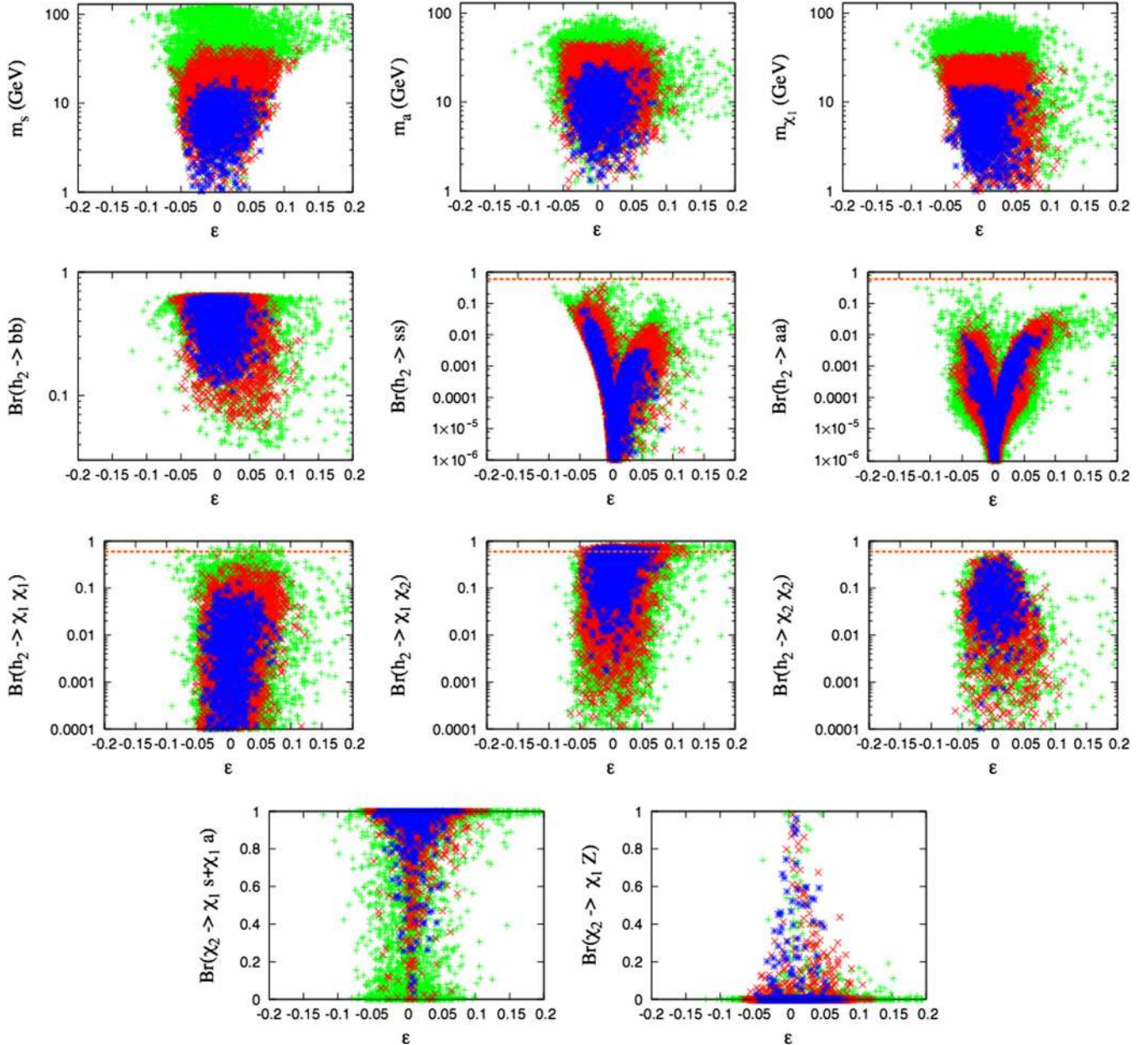


FIG. 36 (color online). Higgs phenomenology in the PQ -symmetry limit of the NMSSM, as discussed in Sec. IC 8 [54]. Top row: Masses of s , a , and χ_1 , respectively. Second and third rows: Branching ratios of the SM-like Higgs h (denoted here as h_2) to $b\bar{b}$, $s\bar{s}$, aa , $\chi_1\chi_1$, $\chi_1\chi_2$, and $\chi_2\chi_2$, respectively. Bottom row: Branching ratios of the next-to-lightest neutralino χ_2 to on-shell $\chi_1 s + \chi_1 a$ and $\chi_1 Z$, respectively. All points are required to have a mass 124–126 GeV for their SM-like Higgs boson. Green (light gray) points are sampled in the ranges $3 \leq \tan\beta \leq 30$, $0.015 \leq \lambda \leq 0.5$, $0.0005 \leq \kappa \leq 0.05$, $-0.8 \leq \epsilon' \leq 0.8$, $-50 \text{ GeV} \leq A_\kappa \leq 0$, and $0.1 \text{ TeV} \leq \lambda v_s \leq 1 \text{ TeV}$, green (light gray) points cover the whole scan range, red (medium gray) points correspond to the subset satisfying $\lambda < 0.30$, $\kappa/\lambda < 0.05$ and $\lambda v_s < 350 \text{ GeV}$, while blue (dark gray) points satisfy $\lambda < 0.15$, $\kappa/\lambda < 0.03$ and $\lambda v_s < 250 \text{ GeV}$.

TABLE XXI. Example models illustrating the main exotic-decay modes of the SM-like Higgs boson in the PQ -symmetry limit of the NMSSM [54]. Here soft squark masses of 2 TeV, slepton masses of 200 GeV, $A_{u,d,e} = -3.5$ TeV, and wino and gluino soft masses 250 and 2000 GeV are universally assumed.

Examples	$h \rightarrow \chi_1 \chi_2$	$h \rightarrow \chi_1 \chi_2$	$h \rightarrow \chi_2 \chi_2$
λ	0.18	0.064	0.02
κ	3.4×10^{-3}	9.0×10^{-3}	1.2×10^{-3}
$\tan \beta$	9.0	12.5	10
λ_s (GeV)	326	138	160
A_λ (GeV)	2960	1700	1800
A_κ (GeV)	-43.5	-17	-7
M_1 (GeV)	85	80	55
m_s (GeV)	23.0	34.6	17.4
m_h (GeV)	124.7	125.3	124.9
m_a (GeV)	28.7	31.6	14.2
m_{χ_1} (GeV)	12.7	39.1	19.7
m_{χ_2} (GeV)	80.8	66.4	47.3
$\text{BR}(h \rightarrow aa)$	< 0.01	< 0.01	< 0.01
$\text{BR}(h \rightarrow \chi_1 \chi_1)$	< 0.01	0.04	< 0.01
$\text{BR}(h \rightarrow \chi_1 \chi_2)$	0.28	0.27	0.05
$\text{BR}(h \rightarrow \chi_2 \chi_2)$	< 0.01	< 0.01	0.31
$\text{BR}(\chi_2 \rightarrow \chi_1(a, s))$	$0.92 + 0.08$	< 0.01	$0.09 + 0.60$
$\text{BR}(\chi_2 \rightarrow \chi_1(a, s)^*)$	< 0.01	0.96	0.30
$\text{BR}(\chi_2 \rightarrow \chi_1 \gamma)$	< 0.01	0.04	0.01

done over the parameter $\varepsilon \equiv \lambda \mu_{\text{eff}} / m_Z \times \varepsilon'$, with ε' given by Eq. (63) and $\mu_{\text{eff}} \equiv \lambda v_s$.

The simultaneous smallness of the s , a , and χ_1 masses and the generic suppression of $\text{Br}(h \rightarrow aa, ss)$ are shown in the first and the second rows of Fig. 36. The branching ratios of h into $\chi_1 \chi_1$, $\chi_1 \chi_2$, and $\chi_2 \chi_2$ as well as the branching ratios of χ_2 into $\chi_1 s + \chi_1 a$ (on shell) and $\chi_1 Z$ (on shell) are presented in the third row. These plots clearly indicate that, although $h \rightarrow \chi_1 \chi_1$ has a larger available phase space, that branching fraction tends to be suppressed compared to $h \rightarrow \chi_2 \chi_2$ and especially $h \rightarrow \chi_1 \chi_2$. Almost all points in the blue region have $m_{\chi_2} - m_{\chi_1} > \min\{m_s, m_a\}$. Thus χ_2 overwhelmingly decays

into on-shell s or a and χ_1 , while both $\chi_2 \rightarrow \chi_1 Z$ and three-body decays are suppressed. In the red and green regions, the $\min\{m_s, m_a\}$ values increase. Some points (mainly green ones) have $m_{\chi_2} - m_{\chi_1} < \min\{m_s, m_a\}$, so that $\chi_2 \rightarrow \chi_1 \gamma$ may become significant. On-shell $\chi_2 \rightarrow \chi_1 Z$ can occur in a small sliver of the m_1, m_2 plane.

We present three example model points in Table XXI, which represent the main exotic Higgs decay modes in this limit: (i) $h \rightarrow \chi_1 \chi_2$, with $\chi_2 \rightarrow \chi_1 a, \chi_1 s$; (ii) $h \rightarrow \chi_1 \chi_2$, with χ_2 mainly decaying to $\chi_1 a^*$ or $\chi_1 s^*$ with $a^* \rightarrow \text{SM}$ and $s^* \rightarrow \text{SM}$; (iii) $h \rightarrow \chi_2 \chi_2$, with χ_2 decaying to $\chi_1 a, \chi_1 s$.

-
- [1] ATLAS Collaboration, *Phys. Lett. B* **716**, 1 (2012).
[2] CMS Collaboration, *Phys. Lett. B* **716**, 30 (2012).
[3] F. Englert and R. Brout, *Phys. Rev. Lett.* **13**, 321 (1964).
[4] P. W. Higgs, *Phys. Lett.* **12**, 132 (1964).
[5] P. W. Higgs, *Phys. Rev. Lett.* **13**, 508 (1964).
[6] G. Guralnik, C. Hagen, and T. Kibble, *Phys. Rev. Lett.* **13**, 585 (1964).
[7] P. W. Higgs, *Phys. Rev.* **145**, 1156 (1966).
[8] T. Kibble, *Phys. Rev.* **155**, 1554 (1967).
[9] S. Glashow, *Nucl. Phys.* **22**, 579 (1961).
[10] S. Weinberg, *Phys. Rev. Lett.* **19**, 1264 (1967).
[11] A. Salam, in *Proceedings of the Eighth Nobel Symposium* (Almqvist & Wiksell, Stockholm, 1968).
[12] <http://exotichiggs.physics.sunysb.edu>.
[13] S. Dittmaier *et al.* (LHC Higgs Cross Section Working Group Collaboration), [arXiv:1101.0593](https://arxiv.org/abs/1101.0593).
[14] G. Belanger, B. Dumont, U. Ellwanger, J. Gunion, and S. Kraml, *Phys. Lett. B* **723**, 340 (2013).
[15] P. P. Giardino, K. Kannike, I. Masina, M. Raidal, and A. Strumia, *J. High Energy Phys.* **05** (2014) 046.
[16] J. Ellis and T. You, *J. High Energy Phys.* **06** (2013) 103.
[17] K. Cheung, J. S. Lee, and P.-Y. Tseng, *J. High Energy Phys.* **05** (2013) 134.
[18] A. Djouadi and G. Moreau, *Eur. Phys. J. C* **73**, 2512 (2013).
[19] CMS Collaboration, Report No. CMS-PAS-HIG-12-045.
[20] ATLAS Collaboration, Reports No. ATLAS-CONF-2013-034, No. ATLAS-COM-CONF-2013-035.

- [21] B. A. Dobrescu and J. D. Lykken, *J. High Energy Phys.* **02** (2013) 073.
- [22] M. E. Peskin, [arXiv:1207.2516](https://arxiv.org/abs/1207.2516).
- [23] CMS Collaboration, [arXiv:1307.7135](https://arxiv.org/abs/1307.7135).
- [24] ATLAS Collaboration, [arXiv:1307.7292](https://arxiv.org/abs/1307.7292).
- [25] R. E. Shrock and M. Suzuki, *Phys. Lett.* **110B**, 250 (1982).
- [26] J. Gunion and H. E. Haber, *Nucl. Phys.* **B272**, 1 (1986).
- [27] L.-F. Li, Y. Liu, and L. Wolfenstein, *Phys. Lett.* **159B**, 45 (1985).
- [28] J. Gunion and H. E. Haber, *Nucl. Phys.* **B278**, 449 (1986).
- [29] V. Silveira and A. Zee, *Phys. Lett.* **161B**, 136 (1985).
- [30] T. Binoth and J. van der Bij, *Z. Phys. C* **75**, 17 (1997).
- [31] R. Schabinger and J. D. Wells, *Phys. Rev. D* **72**, 093007 (2005).
- [32] M. J. Strassler and K. M. Zurek, *Phys. Lett. B* **651**, 374 (2007).
- [33] B. Patt and F. Wilczek, [arXiv:hep-ph/0605188](https://arxiv.org/abs/hep-ph/0605188).
- [34] CMS Collaboration, Report No. CMS DP-2012/022, 2012.
- [35] B. A. Petersen, Technical Report No. ATL-DAQ-PROC-2012-071, CERN, Geneva, 2012.
- [36] S. Chang, R. Dermisek, J. F. Gunion, and N. Weiner, *Annu. Rev. Nucl. Part. Sci.* **58**, 75 (2008).
- [37] G. Belanger, U. Ellwanger, J. Gunion, Y. Jiang, and S. Kraml, [arXiv:1208.4952](https://arxiv.org/abs/1208.4952).
- [38] P. Bechtle, S. Heinemeyer, O. Stål, T. Stefaniak, G. Weiglein, and L. Zeune, *Eur. Phys. J. C* **73**, 2354 (2013).
- [39] R. Barbieri, D. Buttazzo, K. Kannike, F. Sala, and A. Tesi, *Phys. Rev. D* **88**, 055011 (2013).
- [40] T. Han, T. Li, S. Su, and L.-T. Wang, *J. High Energy Phys.* **11** (2013) 053.
- [41] J. Gunion, H. Haber, G. Kane, and S. Dawson, *The Higgs Hunter's Guide*, Frontiers in Physics Vol. 80 (Perseus, New York, 2000).
- [42] G. Blankenburg, J. Ellis, and G. Isidori, *Phys. Lett. B* **712**, 386 (2012).
- [43] R. Harnik, J. Kopp, and J. Zupan, *J. High Energy Phys.* **03** (2013) 026.
- [44] L3 Collaboration, [arXiv:hep-ex/0310007](https://arxiv.org/abs/hep-ex/0310007).
- [45] B. Batell, C. E. M. Wagner, and L.-T. Wang, *J. High Energy Phys.* **05** (2014) 002.
- [46] S. B. Giddings, T. Liu, I. Low, and E. Mintun, *Phys. Rev. D* **88**, 095003 (2013).
- [47] O. J. Eboli and D. Zeppenfeld, *Phys. Lett. B* **495**, 147 (2000).
- [48] Y. Bai, P. Draper, and J. Shelton, *J. High Energy Phys.* **07** (2012) 192.
- [49] F. Riva, C. Biggio, and A. Pomarol, *J. High Energy Phys.* **02** (2013) 081.
- [50] A. Azatov, R. Contino, A. Di Iura, and J. Galloway, *Phys. Rev. D* **88**, 075019 (2013).
- [51] C. Petersson, A. Romagnoni, and R. Torre, *J. High Energy Phys.* **10** (2012) 016.
- [52] M. J. Strassler, [arXiv:hep-ph/0607160](https://arxiv.org/abs/hep-ph/0607160).
- [53] P. Draper, T. Liu, C. E. Wagner, L.-T. Wang, and H. Zhang, *Phys. Rev. Lett.* **106**, 121805 (2011).
- [54] J. Huang, T. Liu, L.-T. Wang, and F. Yu, *Phys. Rev. Lett.* **112**, 221803 (2014).
- [55] A. de Gouvea, [arXiv:0706.1732](https://arxiv.org/abs/0706.1732).
- [56] M. L. Graesser, [arXiv:0705.2190](https://arxiv.org/abs/0705.2190).
- [57] M. L. Graesser, *Phys. Rev. D* **76**, 075006 (2007).
- [58] S. Chang and N. Weiner, *J. High Energy Phys.* **05** (2008) 074.
- [59] U. Ellwanger, J. F. Gunion, C. Hugonie, and S. Moretti, [arXiv:hep-ph/0305109](https://arxiv.org/abs/hep-ph/0305109).
- [60] U. Ellwanger, J. F. Gunion, and C. Hugonie, *J. High Energy Phys.* **07** (2005) 041.
- [61] M. Almarashi and S. Moretti, *Phys. Rev. D* **84**, 015014 (2011).
- [62] U. Ellwanger, J. Gunion, C. Hugonie, and S. Moretti, [arXiv:hep-ph/0401228](https://arxiv.org/abs/hep-ph/0401228).
- [63] W. Kilian, D. Rainwater, and J. Reuter, *Phys. Rev. D* **71**, 015008 (2005).
- [64] K. Cheung and J. Song, *Phys. Rev. D* **76**, 035007 (2007).
- [65] C. Csaki, J. Hubisz, G. D. Kribs, P. Meade, and J. Terning, *Phys. Rev. D* **68**, 035009 (2003).
- [66] H.-C. Cheng, B. A. Dobrescu, and C. T. Hill, *Nucl. Phys.* **B589**, 249 (2000).
- [67] M. Cvetič, D. A. Demir, J. Espinosa, L. Everett, and P. Langacker, *Phys. Rev. D* **56**, 2861 (1997).
- [68] J. Erler, P. Langacker, and T.-J. Li, *Phys. Rev. D* **66**, 015002 (2002).
- [69] C. Panagiotakopoulos and K. Tamvakis, *Phys. Lett. B* **469**, 145 (1999).
- [70] C. Panagiotakopoulos and A. Pilaftsis, *Phys. Rev. D* **63**, 055003 (2001).
- [71] B. A. Dobrescu and K. T. Matchev, *J. High Energy Phys.* **09** (2000) 031.
- [72] V. Barger, P. Langacker, and G. Shaughnessy, *AIP Conf. Proc.* **903**, 32 (2007).
- [73] J. D. Mason, D. E. Morrissey, and D. Poland, *Phys. Rev. D* **80**, 115015 (2009).
- [74] C. Englert, M. Spannowsky, and C. Wymant, *Phys. Lett. B* **718**, 538 (2012).
- [75] B. Batell, J. Pradler, and M. Spannowsky, *J. High Energy Phys.* **08** (2011) 038.
- [76] M. J. Strassler and K. M. Zurek, *Phys. Lett. B* **661**, 263 (2008).
- [77] L. M. Carpenter, D. E. Kaplan, and E.-J. Rhee, *Phys. Rev. Lett.* **99**, 211801 (2007).
- [78] V. Abazov *et al.* (D0 Collaboration), *Phys. Rev. Lett.* **97**, 161802 (2006).
- [79] A. Abulencia *et al.* (CDF Collaboration), *Phys. Rev. Lett.* **99**, 121801 (2007).
- [80] T. Aaltonen *et al.* (CDF Collaboration), *Phys. Rev. D* **78**, 032015 (2008).
- [81] V. Abazov *et al.* (D0 Collaboration), *Phys. Rev. Lett.* **101**, 111802 (2008).
- [82] V. Abazov *et al.* (D0 Collaboration), *Phys. Rev. Lett.* **103**, 071801 (2009).
- [83] CMS Collaboration, Reports No. CMS-EXO-11-067, No. CERN-PH-EP-2012-164.
- [84] CMS Collaboration, Report No. CMS-PAS-EXO-11-004.
- [85] ATLAS Collaboration, *Phys. Lett. B* **721**, 32 (2013).
- [86] ATLAS Collaboration, *Phys. Rev. Lett.* **108**, 251801 (2012).
- [87] CMS Collaboration, *J. High Energy Phys.* **11** (2012) 172.
- [88] LHCb Collaboration, Reports No. LHCb-CONF-2012-014, No. CERN-LHCb-CONF-2012-014.
- [89] CMS Collaboration, Report No. CMS-EXO-11-101.
- [90] CMS Collaboration, Report No. CMS-PAS-EXO-11-035.

- [91] CMS Collaboration, *Phys. Lett. B* **722**, 273 (2013).
- [92] CMS Collaboration, *J. High Energy Phys.* 02 (2013) 085.
- [93] ATLAS Collaboration, *Phys. Lett. B* **719**, 280 (2013).
- [94] ATLAS Collaboration, Report No. CERN-PH-EP-2012-241.
- [95] CMS Collaboration, Report No. CMS-PAS-EXO-12-038.
- [96] D. Alves *et al.* (LHC New Physics Working Group Collaboration), *J. Phys. G* **39**, 105005 (2012).
- [97] D. E. Morrissey and M. J. Ramsey-Musolf, *New J. Phys.* **14**, 125003 (2012).
- [98] A. Djouadi, *Phys. Rep.* **459**, 1 (2008).
- [99] A. Djouadi, *Phys. Rep.* **457**, 1 (2008).
- [100] R. Dermisek and J. F. Gunion, *Phys. Rev. D* **81**, 075003 (2010).
- [101] B. Echenard, *Adv. High Energy Phys.* **2012**, 514014 (2012).
- [102] J. Lees *et al.* (BABAR Collaboration), *Phys. Rev. D* **88**, 071102 (2013).
- [103] D. McKeen, *Phys. Rev. D* **79**, 015007 (2009).
- [104] M. Lisanti and J. G. Wacker, *Phys. Rev. D* **79**, 115006 (2009).
- [105] H. E. Haber and G. L. Kane, *Phys. Rep.* **117**, 75 (1985).
- [106] J. E. Kim, *Phys. Rep.* **150**, 1 (1987).
- [107] R. Peccei and H. R. Quinn, *Phys. Rev. Lett.* **38**, 1440 (1977).
- [108] M. Trodden, [arXiv:hep-ph/9805252](https://arxiv.org/abs/hep-ph/9805252).
- [109] G. C. Branco, P. M. Ferreira, L. Lavoura, M. N. Rebelo, M. Sher, and J. P. Silva, *Phys. Rep.* **516**, 1 (2012).
- [110] C.-Y. Chen, M. Freid, and M. Sher, *Phys. Rev. D* **89**, 075009 (2014).
- [111] A. Dery, A. Efrati, G. Hiller, Y. Hochberg, and Y. Nir, *J. High Energy Phys.* 08 (2013) 006.
- [112] W. Altmannshofer, S. Gori, and G. D. Kribs, *Phys. Rev. D* **86**, 115009 (2012).
- [113] N. Craig, J. A. Evans, R. Gray, C. Kilic, M. Park, S. Somalwar, and S. Thomas, *J. High Energy Phys.* 02 (2013) 033.
- [114] J. Gunion, B. Grzadkowski, H. Haber, and J. Kalinowski, *Phys. Rev. Lett.* **79**, 982 (1997).
- [115] G. Belanger, B. Dumont, U. Ellwanger, J. Gunion, and S. Kraml, *Phys. Rev. D* **88**, 075008 (2013).
- [116] P. Ferreira, R. Santos, M. Sher, and J. P. Silva, *Phys. Rev. D* **85**, 035020 (2012).
- [117] D. S. Alves, P. J. Fox, and N. J. Weiner, [arXiv:1207.5499](https://arxiv.org/abs/1207.5499).
- [118] P. M. Ferreira, R. Santos, M. Sher, and J. P. Silva, *Phys. Rev. D* **85**, 077703 (2012).
- [119] N. Craig and S. Thomas, *J. High Energy Phys.* 11 (2012) 083.
- [120] N. Craig and A. Katz, *J. High Energy Phys.* 05 (2013) 015.
- [121] Y. Bai, V. Barger, L. L. Everett, and G. Shaughnessy, *Phys. Rev. D* **87**, 115013 (2013).
- [122] A. Azatov and J. Galloway, *Int. J. Mod. Phys. A* **28**, 1330004 (2013).
- [123] C.-Y. Chen and S. Dawson, *Phys. Rev. D* **87**, 055016 (2013).
- [124] M. Baumgart and A. Katz, *J. High Energy Phys.* 08 (2012) 133.
- [125] R. Essig, R. Harnik, J. Kaplan, and N. Toro, *Phys. Rev. D* **82**, 113008 (2010).
- [126] J. Kersten and A. Y. Smirnov, *Phys. Rev. D* **76**, 073005 (2007).
- [127] C. Csaki, E. Kuflik, and T. Volansky, *Phys. Rev. Lett.* **112**, 131801 (2014).
- [128] L. M. Carpenter, [arXiv:1010.5502](https://arxiv.org/abs/1010.5502).
- [129] W.-Y. Keung and P. Schwaller, *J. High Energy Phys.* 06 (2011) 054.
- [130] L. M. Carpenter and D. Whiteson, [arXiv:1107.2123](https://arxiv.org/abs/1107.2123).
- [131] P. Langacker, *Rev. Mod. Phys.* **81**, 1199 (2009).
- [132] J. Jaeckel and A. Ringwald, *Annu. Rev. Nucl. Part. Sci.* **60**, 405 (2010).
- [133] J. Hewett *et al.*, [arXiv:1205.2671](https://arxiv.org/abs/1205.2671).
- [134] R. Essig *et al.*, [arXiv:1311.0029](https://arxiv.org/abs/1311.0029).
- [135] M. J. Strassler, [arXiv:0801.0629](https://arxiv.org/abs/0801.0629).
- [136] N. Arkani-Hamed, D. P. Finkbeiner, T. R. Slatyer, and N. Weiner, *Phys. Rev. D* **79**, 015014 (2009).
- [137] M. Pospelov and A. Ritz, *Phys. Lett. B* **671**, 391 (2009).
- [138] D. P. Finkbeiner and N. Weiner, *Phys. Rev. D* **76**, 083519 (2007).
- [139] P. Fayet, *Phys. Rev. D* **70**, 023514 (2004).
- [140] M. Pospelov, *Phys. Rev. D* **80**, 095002 (2009).
- [141] B. Holdom, *Phys. Lett.* **166B**, 196 (1986).
- [142] P. Galison and A. Manohar, *Phys. Lett.* **136B**, 279 (1984).
- [143] K. R. Dienes, C. F. Kolda, and J. March-Russell, *Nucl. Phys.* **B492**, 104 (1997).
- [144] S. Abel and B. Schofield, *Nucl. Phys.* **B685**, 150 (2004).
- [145] S. Abel, M. Goodsell, J. Jaeckel, V. Khoze, and A. Ringwald, *J. High Energy Phys.* 07 (2008) 124.
- [146] M. Goodsell, J. Jaeckel, J. Redondo, and A. Ringwald, *J. High Energy Phys.* 11 (2009) 027.
- [147] M. Cicoli, M. Goodsell, J. Jaeckel, and A. Ringwald, *J. High Energy Phys.* 07 (2011) 114.
- [148] M. Goodsell, S. Ramos-Sanchez, and A. Ringwald, *J. High Energy Phys.* 01 (2012) 021.
- [149] M. Baumgart, C. Cheung, J. T. Ruderman, L.-T. Wang, and I. Yavin, *J. High Energy Phys.* 04 (2009) 014.
- [150] N. Arkani-Hamed and N. Weiner, *J. High Energy Phys.* 12 (2008) 104.
- [151] R. Essig, P. Schuster, and N. Toro, *Phys. Rev. D* **80**, 015003 (2009).
- [152] J. D. Bjorken, R. Essig, P. Schuster, and N. Toro, *Phys. Rev. D* **80**, 075018 (2009).
- [153] J. Bjorken, S. Eklund, W. Nelson, A. Abashian, C. Church, B. Lu, L. Mo, T. Nunamaker, and P. Rassmann, *Phys. Rev. D* **38**, 3375 (1988).
- [154] E. M. Riordan *et al.*, *Phys. Rev. Lett.* **59**, 755 (1987).
- [155] A. Bross, M. Crisler, S. Pordes, J. Volk, S. Errede, and J. Wrbanek, *Phys. Rev. Lett.* **67**, 2942 (1991).
- [156] B. Batell, M. Pospelov, and A. Ritz, *Phys. Rev. D* **79**, 115008 (2009).
- [157] J. Blumlein and J. Brunner, *Phys. Lett. B* **701**, 155 (2011).
- [158] S. Andreas, C. Niebuhr, and A. Ringwald, *Phys. Rev. D* **86**, 095019 (2012).
- [159] M. Reece and L.-T. Wang, *J. High Energy Phys.* 07 (2009) 051.
- [160] B. Aubert *et al.* (BABAR Collaboration), *Phys. Rev. Lett.* **103**, 081803 (2009).
- [161] F. Archilli *et al.*, *Phys. Lett. B* **706**, 251 (2012).
- [162] S. Abrahamyan *et al.* (APEX Collaboration), *Phys. Rev. Lett.* **107**, 191804 (2011).
- [163] H. Merkel *et al.* (A1 Collaboration), *Phys. Rev. Lett.* **106**, 251802 (2011).

- [164] J. B. Dent, F. Ferrer, and L. M. Krauss, [arXiv:1201.2683](#).
- [165] H. Davoudiasl, H.-S. Lee, and W. J. Marciano, *Phys. Rev. D* **85**, 115019 (2012).
- [166] H. Davoudiasl, H.-S. Lee, I. Lewis, and W. J. Marciano, *Phys. Rev. D* **88**, 015022 (2013).
- [167] A. Hook, E. Izaguirre, and J. G. Wacker, *Adv. High Energy Phys.* **2011**, 859762 (2011).
- [168] D. Babusci *et al.* (KLOE-2 Collaboration), *Phys. Lett. B* **720**, 111 (2013).
- [169] H. Davoudiasl, H.-S. Lee, and W. J. Marciano, *Phys. Rev. D* **86**, 095009 (2012).
- [170] M. Endo, K. Hamaguchi, and G. Mishima, *Phys. Rev. D* **86**, 095029 (2012).
- [171] P. Adlarson *et al.* (WASA-at-COSY Collaboration), *Phys. Lett. B* **726**, 187 (2013).
- [172] G. Agakishiev *et al.* (HADES Collaboration), *Phys. Lett. B* **731**, 265 (2014).
- [173] H. Merkel *et al.*, *Phys. Rev. Lett.* **112**, 221802 (2014).
- [174] J. Lees *et al.* (BABAR Collaboration), [arXiv:1406.2980](#).
- [175] CMS Collaboration, Technical Report No. CMS-PAS-HIG-13-002, CERN, Geneva, 2013.
- [176] ATLAS Collaboration, Report No. ATLAS-CONF-2013-013.
- [177] S. Gopalakrishna, S. Jung, and J. D. Wells, *Phys. Rev. D* **78**, 055002 (2008).
- [178] C.-F. Chang, E. Ma, and T.-C. Yuan, *J. High Energy Phys.* **03** (2014) 054.
- [179] J. Beringer *et al.* (Particle Data Group Collaboration), *Phys. Rev. D* **86**, 010001 (2012).
- [180] K. Hagiwara, J. S. Lee, and J. Nakamura, *J. High Energy Phys.* **10** (2012) 002.
- [181] M. Drees, *Phys. Rev. D* **86**, 115018 (2012).
- [182] G. Barenboim, C. Bosch, M. Lpez-Ibaez, and O. Vives, *J. High Energy Phys.* **11** (2013) 051.
- [183] J. F. Gunion and H. E. Haber, *Nucl. Phys.* **B307**, 445 (1988).
- [184] D. Albornoz Vasquez, G. Belanger, R. Godbole, and A. Pukhov, *Phys. Rev. D* **85**, 115013 (2012).
- [185] N. Desai, B. Mukhopadhyaya, and S. Niyogi, [arXiv:1202.5190](#).
- [186] H. K. Dreiner, J. S. Kim, and O. Lebedev, *Phys. Lett. B* **715**, 199 (2012).
- [187] T. Han, Z. Liu, and A. Natarajan, *J. High Energy Phys.* **11** (2013) 008.
- [188] B. Ananthanarayan, J. Lahiri, P. Pandita, and M. Patra, *Phys. Rev. D* **87**, 115021 (2013).
- [189] U. Ellwanger, C. Hugonie, and A. M. Teixeira, *Phys. Rep.* **496**, 1 (2010).
- [190] N. D. Christensen, T. Han, Z. Liu, and S. Su, *J. High Energy Phys.* **08** (2013) 019.
- [191] J. Cao, F. Ding, C. Han, J. M. Yang, and J. Zhu, *J. High Energy Phys.* **11** (2013) 018.
- [192] R. Dermisek and J. F. Gunion, *Phys. Rev. D* **75**, 075019 (2007).
- [193] D. E. Morrissey and A. Pierce, *Phys. Rev. D* **78**, 075029 (2008).
- [194] R. Peccei and H. R. Quinn, *Phys. Rev. D* **16**, 1791 (1977).
- [195] E. Chun, *Phys. Lett. B* **348**, 111 (1995).
- [196] P. Ciafaloni and A. Pomarol, *Phys. Lett. B* **404**, 83 (1997).
- [197] L. J. Hall and T. Watari, *Phys. Rev. D* **70**, 115001 (2004).
- [198] B. Feldstein, L. J. Hall, and T. Watari, *Phys. Lett. B* **607**, 155 (2005).
- [199] D. Miller and R. Nevzorov, [arXiv:hep-ph/0309143](#).
- [200] R. Barbieri, L. J. Hall, A. Y. Papaioannou, D. Pappadopulo, and V. S. Rychkov, *J. High Energy Phys.* **03** (2008) 005.
- [201] O. Lebedev and S. Ramos-Sanchez, *Phys. Lett. B* **684**, 48 (2010).
- [202] B. A. Dobrescu, G. L. Landsberg, and K. T. Matchev, *Phys. Rev. D* **63**, 075003 (2001).
- [203] C. Panagiotakopoulos and K. Tamvakis, *Phys. Lett. B* **469**, 145 (1999).
- [204] D. Miller, S. Moretti, and R. Nevzorov, [arXiv:hep-ph/0501139](#).
- [205] <http://www.th.u-psud.fr/NMHDECAY/nmssmtools.html>.
- [206] U. Ellwanger and C. Hugonie, *Comput. Phys. Commun.* **177**, 399 (2007).
- [207] M. Muhlleitner, A. Djouadi, and Y. Mambrini, *Comput. Phys. Commun.* **168**, 46 (2005).
- [208] D. Das, U. Ellwanger, and A. M. Teixeira, *Comput. Phys. Commun.* **183**, 774 (2012).
- [209] J. Cao, K.-i. Hikasa, W. Wang, and J. M. Yang, *Phys. Lett. B* **703**, 292 (2011).
- [210] N. Arkani-Hamed, A. G. Cohen, and H. Georgi, *Phys. Lett. B* **513**, 232 (2001).
- [211] N. Arkani-Hamed, A. G. Cohen, E. Katz, A. E. Nelson, T. Gregoire, and J. G. Wacker, *J. High Energy Phys.* **08** (2002) 021.
- [212] M. Perelstein, *Prog. Part. Nucl. Phys.* **58**, 247 (2007).
- [213] M. Perelstein, M. E. Peskin, and A. Pierce, *Phys. Rev. D* **69**, 075002 (2004).
- [214] Z. Surujon and P. Uttayarat, *Phys. Rev. D* **83**, 076010 (2011).
- [215] G. D'Ambrosio, G. Giudice, G. Isidori, and A. Strumia, *Nucl. Phys.* **B645**, 155 (2002).
- [216] R. S. Chivukula and H. Georgi, *Phys. Lett. B* **188**, 99 (1987).
- [217] L. Hall and L. Randall, *Phys. Rev. Lett.* **65**, 2939 (1990).
- [218] A. Buras, P. Gambino, M. Gorbahn, S. Jager, and L. Silvestrini, *Phys. Lett. B* **500**, 161 (2001).
- [219] B. Bellazzini, C. Csaki, A. Falkowski, and A. Weiler, *Phys. Rev. D* **80**, 075008 (2009).
- [220] A. Falkowski, D. Krohn, L.-T. Wang, J. Shelton, and A. Thalappillil, *Phys. Rev. D* **84**, 074022 (2011).
- [221] B. Bellazzini, C. Csaki, A. Falkowski, and A. Weiler, *Phys. Rev. D* **81**, 075017 (2010).
- [222] I. Lewis and J. Schmitthener, *J. High Energy Phys.* **06** (2012) 072.
- [223] J. E. Juknevich, D. Melnikov, and M. J. Strassler, *J. High Energy Phys.* **07** (2009) 055.
- [224] J. E. Juknevich, *J. High Energy Phys.* **08** (2010) 121.
- [225] J. L. Feng and J. Kumar, *Phys. Rev. Lett.* **101**, 231301 (2008).
- [226] Z. Chacko, H.-S. Goh, and R. Hamik, *Phys. Rev. Lett.* **96**, 231802 (2006).
- [227] ATLAS Collaboration, *New J. Phys.* **15**, 043009 (2013).
- [228] T. Aaltonen *et al.* (CDF Collaboration), *Phys. Rev. D* **85**, 092001 (2012).
- [229] F. Abe *et al.* (CDF Collaboration), *Phys. Rev. D* **58**, 051102 (1998).

- [230] A. L. Scott (CDF Collaboration), *Int. J. Mod. Phys. A* **20**, 3263 (2005).
- [231] J. McDonald, *Phys. Rev. D* **50**, 3637 (1994).
- [232] C. Burgess, M. Pospelov, and T. ter Veldhuis, *Nucl. Phys. B* **619**, 709 (2001).
- [233] Y. Mambrini, *Phys. Rev. D* **84**, 115017 (2011).
- [234] B. Batell, *Phys. Rev. D* **83**, 035006 (2011).
- [235] M. Pospelov and A. Ritz, *Phys. Rev. D* **84**, 113001 (2011).
- [236] S. Weinberg, *Phys. Rev. Lett.* **110**, 241301 (2013).
- [237] S. P. Martin and J. D. Wells, *Phys. Rev. D* **60**, 035006 (1999).
- [238] T. Han, P. Langacker, and B. McElrath, *Phys. Rev. D* **70**, 115006 (2004).
- [239] V. Barger, P. Langacker, H.-S. Lee, and G. Shaughnessy, *Phys. Rev. D* **73**, 115010 (2006).
- [240] L. J. Hall, D. Pinner, and J. T. Ruderman, *J. High Energy Phys.* **04** (2012) 131.
- [241] J. Kozaczuk and S. Profumo, *Phys. Rev. D* **89**, 095012 (2014).
- [242] D. Bertolini, K. Rehermann, and J. Thaler, *J. High Energy Phys.* **04** (2012) 130.
- [243] A. S. Joshipura and S. D. Rindani, *Phys. Rev. Lett.* **69**, 3269 (1992).
- [244] A. Dedes, T. Figy, S. Hoche, F. Krauss, and T. E. Underwood, *J. High Energy Phys.* **11** (2008) 036.
- [245] A. Delgado, J. R. Espinosa, and M. Quiros, *J. High Energy Phys.* **10** (2007) 094.
- [246] N. Craig and K. Howe, *J. High Energy Phys.* **03** (2014) 140.
- [247] A. Rozanov and M. Vysotsky, *Phys. Lett. B* **700**, 313 (2011).
- [248] W.-Y. Keung and P. Schwaller, *J. High Energy Phys.* **06** (2011) 054.
- [249] M. L. Graesser, *Phys. Rev. D* **76**, 075006 (2007).
- [250] S. Banerjee, P. S. B. Dev, S. Mondal, B. Mukhopadhyaya, and S. Roy, *J. High Energy Phys.* **10** (2013) 221.
- [251] J. Gunion, *Phys. Rev. Lett.* **72**, 199 (1994).
- [252] B. P. Kersevan, M. Malawski, and E. Richter-Was, *Eur. Phys. J. C* **29**, 541 (2003).
- [253] A. Djouadi, A. Falkowski, Y. Mambrini, and J. Quevillon, *Eur. Phys. J. C* **73**, 2455 (2013).
- [254] D. Cavalli *et al.* (Higgs Working Group Collaboration), [arXiv:hep-ph/0203056](https://arxiv.org/abs/hep-ph/0203056).
- [255] R. Godbole, M. Guchait, K. Mazumdar, S. Moretti, and D. Roy, *Phys. Lett. B* **571**, 184 (2003).
- [256] ATLAS Collaboration, Technical Reports Nos. ATL-PHYS-PUB-2009-061 and ATL-COM-PHYS-2009-220, CERN, Geneva, 2009.
- [257] H. Davoudiasl, T. Han, and H. E. Logan, *Phys. Rev. D* **71**, 115007 (2005).
- [258] D. Ghosh, R. Godbole, M. Guchait, K. Mohan, and D. Sengupta, *Phys. Lett. B* **725**, 344 (2013).
- [259] S. Frederiksen, N. Johnson, G. L. Kane, and J. Reid, *Phys. Rev. D* **50**, R4244 (1994).
- [260] ATLAS Collaboration, Report No. CERN-PH-EP-2013-210.
- [261] ATLAS Collaboration, Technical Report No. CMS-PAS-HIG-13-018, CERN, Geneva, 2013.
- [262] ATLAS Collaboration, Technical Report No. CMS-PAS-HIG-13-013, CERN, Geneva, 2013.
- [263] K. Cheung, J. Song, and Q.-S. Yan, *Phys. Rev. Lett.* **99**, 031801 (2007).
- [264] S. Chang, P. J. Fox, and N. Weiner, *J. High Energy Phys.* **08** (2006) 068.
- [265] T. Stelzer, S. Wiesenfeldt, and S. Willenbrock, *Phys. Rev. D* **75**, 077701 (2007).
- [266] M. Carena, T. Han, G.-Y. Huang, and C. E. Wagner, *J. High Energy Phys.* **04** (2008) 092.
- [267] D. E. Kaplan and M. McEvoy, *Phys. Rev. D* **83**, 115004 (2011).
- [268] B. Bellazzini, C. Csaki, J. Hubisz, and J. Shao, *Phys. Rev. D* **83**, 095018 (2011).
- [269] C.-R. Chen, M. M. Nojiri, and W. Sreethawong, *J. High Energy Phys.* **11** (2010) 012.
- [270] M. A. Luty, D. J. Phalen, and A. Pierce, *Phys. Rev. D* **83**, 075015 (2011).
- [271] CMS Collaboration, Technical Report No. CMS-PAS-HIG-11-031, CERN, Geneva, 2011.
- [272] ATLAS Collaboration, Report No. ATLAS-CONF-2012-161.
- [273] S. Chatrchyan *et al.* (CMS Collaboration), *Phys. Lett. B* **722**, 207 (2013).
- [274] ATLAS Collaboration, *Phys. Lett. B* **718**, 369 (2012).
- [275] ATLAS Collaboration, *Eur. Phys. J. C* **72**, 2174 (2012).
- [276] CMS Collaboration, *Phys. Rev. D* **89**, 012003 (2014).
- [277] U. Aglietti *et al.*, [arXiv:hep-ph/0612172](https://arxiv.org/abs/hep-ph/0612172).
- [278] N. Adam *et al.*, [arXiv:0803.1154](https://arxiv.org/abs/0803.1154).
- [279] CMS Collaboration, Technical Report No. CMS-PAS-HIG-12-050, CERN, Geneva, 2012.
- [280] ATLAS Collaboration, *J. High Energy Phys.* **02** (2013) 095.
- [281] C. Englert, J. Jaeckel, E. Re, and M. Spannowsky, *Phys. Rev. D* **85**, 035008 (2012).
- [282] D. Curtin, R. Essig, Z. Surujon, and Y.-M. Zhong (to be published).
- [283] CMS Collaboration, *J. High Energy Phys.* **10** (2011) 007.
- [284] S. Gonzalez, E. Ros, and M. Vos, Report No. ATL-PHYS-2002-021.
- [285] J. Alwall, M. Herquet, F. Maltoni, O. Mattelaer, and T. Stelzer, *J. High Energy Phys.* **06** (2011) 128.
- [286] ATLAS Collaboration, Technical Report No. ATLAS-CONF-2012-097, CERN, Geneva, 2012.
- [287] V. Abazov *et al.* (D0 Collaboration), *Phys. Rev. Lett.* **103**, 061801 (2009).
- [288] CMS Collaboration, *Phys. Lett. B* **726**, 564 (2013).
- [289] ATLAS Collaboration, *Phys. Lett. B* **719**, 299 (2013).
- [290] R. Dermisek and J. F. Gunion, *Phys. Rev. D* **73**, 111701 (2006).
- [291] G. Abbiendi *et al.* (OPAL Collaboration), *Eur. Phys. J. C* **27**, 483 (2003).
- [292] P. W. Graham, A. Pierce, and J. G. Wacker, [arXiv:hep-ph/0605162](https://arxiv.org/abs/hep-ph/0605162).
- [293] A. Belyaev *et al.*, [arXiv:0805.3505](https://arxiv.org/abs/0805.3505).
- [294] C. Englert, T. S. Roy, and M. Spannowsky, *Phys. Rev. D* **84**, 075026 (2011).
- [295] A. Katz, M. Son, and B. Tweedie, *Phys. Rev. D* **83**, 114033 (2011).
- [296] S. Schael *et al.* (ALEPH Collaboration), *J. High Energy Phys.* **05** (2010) 049.

- [297] CMS Collaboration, *J. High Energy Phys.* **06** (2012) 169.
- [298] CMS Collaboration, Report No. CMS PAS SUS-12-026, 2012.
- [299] CMS Collaboration, Report No. CMS PAS SUS-12-027.
- [300] CMS Collaboration, Report No. CMS PAS SUS-13-10, 2013.
- [301] ATLAS Collaboration, *Phys. Rev. D* **87**, 052002 (2013).
- [302] ATLAS Collaboration, *J. High Energy Phys.* **12** (2012) 007.
- [303] T. Sjostrand, S. Mrenna, and P. Z. Skands, *Comput. Phys. Commun.* **178**, 852 (2008).
- [304] LHC Higgs Cross Section Working Group, in *Handbook of LHC Higgs Cross Sections: I. Inclusive Observables*, edited by S. Dittmaier, C. Mariotti, G. Passarino, and R. Tanaka (CERN, Geneva, 2011).
- [305] G. Bozzi, S. Catani, D. de Florian, and M. Grazzini, *Nucl. Phys.* **B737**, 73 (2006).
- [306] D. de Florian, G. Ferrera, M. Grazzini, and D. Tommasini, *J. High Energy Phys.* **11** (2011) 064.
- [307] S. Kanemura, K. Tsumura, and H. Yokoya, *Phys. Rev. D* **85**, 095001 (2012).
- [308] A. Birkedal, Z. Chacko, and M. K. Gaillard, *J. High Energy Phys.* **10** (2004) 036.
- [309] Z. Berezhiani, P. H. Chankowski, A. Falkowski, and S. Pokorski, *Phys. Rev. Lett.* **96**, 031801 (2006).
- [310] C. Csaki, G. Marandella, Y. Shirman, and A. Strumia, *Phys. Rev. D* **73**, 035006 (2006).
- [311] S. Chang, P. J. Fox, and N. Weiner, *Phys. Rev. Lett.* **98**, 111802 (2007).
- [312] A. Martin, [arXiv:hep-ph/0703247](https://arxiv.org/abs/hep-ph/0703247).
- [313] S. D. Ellis, T. S. Roy, and J. Scholtz, *Phys. Rev. Lett.* **110**, 122003 (2013).
- [314] S. D. Ellis, T. S. Roy, and J. Scholtz, *Phys. Rev. D* **87**, 014015 (2013).
- [315] ATLAS Collaboration, *J. High Energy Phys.* **01** (2013) 086.
- [316] CMS Collaboration, *J. High Energy Phys.* **01** (2012) 133.
- [317] P. Draper and D. McKeen, *Phys. Rev. D* **85**, 115023 (2012).
- [318] L. D. Landau, *Dokl. Akad. Nauk Ser. Fiz.* **60**, 207 (1948).
- [319] C.-N. Yang, *Phys. Rev.* **77**, 242 (1950).
- [320] D. McKeen and J. Scholtz (to be published).
- [321] ATLAS Collaboration, Technical Report No. ATL-PHYS-PUB-2011-007, CERN, Geneva, 2011.
- [322] N. Toro and I. Yavin, *Phys. Rev. D* **86**, 055005 (2012).
- [323] B. Batell, D. McKeen, and M. Pospelov, *J. High Energy Phys.* **10** (2012) 104.
- [324] ATLAS Collaboration, Technical Report No. ATLAS-CONF-2012-079, CERN, Geneva, 2012.
- [325] G. Mahlon and S. J. Parke, *Phys. Rev. D* **74**, 073001 (2006).
- [326] S. Chang and A. Menon, *J. High Energy Phys.* **02** (2013) 152.
- [327] M. M. Almarashi and S. Moretti, *Phys. Rev. D* **85**, 017701 (2012).
- [328] H. Davoudiasl, H.-S. Lee, and W. J. Marciano, *Phys. Rev. Lett.* **109**, 031802 (2012).
- [329] K. Babu, C. F. Kolda, and J. March-Russell, *Phys. Rev. D* **57**, 6788 (1998).
- [330] F. Domingo, *J. High Energy Phys.* **04** (2011) 016.
- [331] T. Aaltonen *et al.* (CDF Collaboration), *Phys. Rev. Lett.* **107**, 031801 (2011).
- [332] ATLAS Collaboration, Technical Report No. ATLAS-CONF-2011-020, CERN, Geneva, 2011.
- [333] CMS Collaboration, *Phys. Rev. Lett.* **109**, 121801 (2012).
- [334] S. Schael *et al.* (ALEPH, DELPHI, L3, OPAL, LEP Working Group for Higgs Boson Searches Collaboration), *Eur. Phys. J. C* **47**, 547 (2006).
- [335] B. Grinstein, C. W. Murphy, and D. Pirtskhalava, *J. High Energy Phys.* **10** (2013) 077.
- [336] G. Isidori, A. V. Manohar, and M. Trott, *Phys. Lett. B* **728**, 131 (2014).
- [337] H.-S. Lee and M. Sher, *Phys. Rev. D* **87**, 115009 (2013).
- [338] A. Martin and T. S. Roy, [arXiv:1103.3504](https://arxiv.org/abs/1103.3504).
- [339] CMS Collaboration, Technical Report No. CMS-PAS-HIG-13-010, CERN, Geneva, 2013.
- [340] N. D. Christensen and C. Duhr, *Comput. Phys. Commun.* **180**, 1614 (2009).
- [341] ATLAS Collaboration, Technical Report No. ATLAS-CONF-2013-020, CERN, Geneva, 2013.
- [342] ATLAS Collaboration, Technical Report No. ATLAS-CONF-2013-013, CERN, Geneva, 2013.
- [343] ATLAS Collaboration, [arXiv:0901.0512](https://arxiv.org/abs/0901.0512).
- [344] ATLAS Collaboration, *Eur. Phys. J. C* **72**, 1909 (2012).
- [345] S. Heinemeyer *et al.* (LHC Higgs Cross Section Working Group Collaboration), [arXiv:1307.1347](https://arxiv.org/abs/1307.1347).
- [346] A. Djouadi and M. Drees, *Phys. Lett. B* **407**, 243 (1997).
- [347] D. Suematsu, *Phys. Rev. D* **57**, 1738 (1998).
- [348] M. L. Graesser, [arXiv:0705.2190](https://arxiv.org/abs/0705.2190).
- [349] G. Aad *et al.* (ATLAS Collaboration), *Phys. Rev. Lett.* **110**, 011802 (2013).
- [350] ATLAS Collaboration, Technical Report No. ATLAS-CONF-2012-085, CERN, Geneva, 2012.
- [351] CMS Collaboration, *Phys. Rev. Lett.* **108**, 261803 (2012).
- [352] ATLAS Collaboration, *Phys. Rev. D* **87**, 112003 (2013).
- [353] CMS Collaboration, *J. High Energy Phys.* **10** (2013) 164.
- [354] ATLAS Collaboration, Technical Report No. ATLAS-CONF-2012-144, CERN, Geneva, 2012.
- [355] CMS Collaboration, *J. High Energy Phys.* **06** (2011) 093.
- [356] A. Abulencia *et al.* (CDF Collaboration), *Phys. Rev. D* **75**, 112001 (2007).
- [357] CDF Collaboration, Report No. FERMILAB-PUB-09-221-E.
- [358] CMS Collaboration, Report No. CMS-PAS-SUS-12-013.
- [359] CMS Collaboration, Report No. CMS-PAS-SUS-12-018.
- [360] P. Meade, N. Seiberg, and D. Shih, *Prog. Theor. Phys. Suppl.* **177**, 143 (2009).
- [361] J. L. Diaz-Cruz, D. K. Ghosh, and S. Moretti, *Phys. Rev. D* **68**, 014019 (2003).
- [362] ATLAS Collaboration, *Phys. Lett. B* **718**, 411 (2012).
- [363] Y. F. Chan, M. Low, D. E. Morrissey, and A. P. Spray, *J. High Energy Phys.* **05** (2012) 155.
- [364] S.-Y. Ho and J. Tandean, *Phys. Rev. D* **87**, 095015 (2013).
- [365] S.-Y. Ho and J. Tandean, *Phys. Rev. D* **89**, 114025 (2014).

- [366] CMS Collaboration, Report No. CMS PAS SUS-12-022, 2012.
- [367] ATLAS Collaboration, Report No. ATLAS-CONF-2013-036.
- [368] ATLAS Collaboration, Report No. ATLAS-CONF-2013-035, 2013.
- [369] CMS Collaboration, Technical Report No. CMS-PAS-SUS-13-010, CERN, Geneva, 2013.
- [370] CMS Collaboration, Technical Report No. CMS-PAS-SUS-13-006, CERN, Geneva, 2013.
- [371] E. Contreras-Campana, N. Craig, R. Gray, C. Kilic, M. Park, S. Somalwar, and S. Thomas, *J. High Energy Phys.* **04** (2012) 112.
- [372] N. Craig, M. Park, and J. Shelton, [arXiv:1308.0845](https://arxiv.org/abs/1308.0845).
- [373] S. Chang and N. Weiner, *J. High Energy Phys.* **05** (2008) 074.
- [374] S. Chang and T. Gregoire, [arXiv:0903.0403](https://arxiv.org/abs/0903.0403).
- [375] CMS Collaboration, Technical Report No. CMS-PAS-HIG-13-022, CERN, Geneva, 2013.
- [376] ATLAS Collaboration, ATLAS Public Note No. ATLAS-CONF-2013-030, 2013.
- [377] CMS Collaboration, Technical Report No. CMS-PAS-HIG-13-003, CERN, Geneva, 2013.
- [378] A. Falkowski, J. T. Ruderman, T. Volansky, and J. Zupan, *J. High Energy Phys.* **05** (2010) 077.
- [379] CMS Collaboration, *J. High Energy Phys.* **07** (2011) 098.
- [380] S.-h. Zhu, [arXiv:hep-ph/0611270](https://arxiv.org/abs/hep-ph/0611270).
- [381] H. Park *et al.* (HyperCP Collaboration), *Phys. Rev. Lett.* **94**, 021801 (2005).
- [382] A. Belyaev, J. Pivarski, A. Safonov, S. Senkin, and A. Tatarinov, *Phys. Rev. D* **81**, 075021 (2010).
- [383] A. Falkowski, J. T. Ruderman, T. Volansky, and J. Zupan, *Phys. Rev. Lett.* **105**, 241801 (2010).
- [384] J. M. Butterworth, A. R. Davison, M. Rubin, and G. P. Salam, *Phys. Rev. Lett.* **100**, 242001 (2008).
- [385] CMS Collaboration, Report No. CMS PAS HIG-13-012, 2013.
- [386] ATLAS Collaboration, Report No. ATLAS-CONF-2013-079, 2013.
- [387] J. Huang, T. Liu, L.-T. Wang, and F. Yu, [arXiv:1407.0038](https://arxiv.org/abs/1407.0038).
- [388] CMS Collaboration, CMS Public Note No. CMS-PAS-HIG-13-004, 2013.
- [389] ATLAS Collaboration, *J. High Energy Phys.* **09** (2012) 070.
- [390] CMS Collaboration, CMS Public Note No. CMS-PAS-HIG-13-003, 2013.
- [391] ATLAS Collaboration, ATLAS Public Note No. ATLAS-CONF-2013-028, 2013.
- [392] M. Spira, A. Djouadi, D. Graudenz, and P. M. Zerwas, *Nucl. Phys.* **B453**, 17 (1995).
- [393] J. Fleischer, O. V. Tarasov, and V. O. Tarasov, *Phys. Lett. B* **584**, 294 (2004).
- [394] R. Dermisek and J. F. Gunion, [arXiv:1002.1971](https://arxiv.org/abs/1002.1971).